I. Copper-Catalyzed Arylation of 1,2-Amino Alcohols
II. Synthesis of N-Terminal, Peptide Helix Initiators, and Characterization of Highly Helical, Capped Polyalanine Peptides

by

Gabriel E. Job

B.S. Chemistry, University of Illinois-Champaign, Urbana, 2000

Submitted to the Department of Chemistry in partial fulfillment of the requirements for the degree of

Doctor of Philosophy

at the

Massachusetts Institute of Technology

May 2005 [June 2005]

Signature of Author _____

Department of Chemistry
May 24, 2005

Certified by _____

Daniel S. Kemp
Professor of Chemistry
Thesis Supervisor

Accepted by _____

Robert W. Field
Professor of Chemistry
Chairman, Departmental Committee on Graduate Students

This doctoral thesis has been examined by a Committee of the Department of Chemistry as follows:

Professor Timothy M. Swager _____
Chair

Professor Daniel S. Kemp _____
Thesis Supervisor

Professor Stephen L. Buchwald _____

I. Copper-Catalyzed Arylation of 1,2-Amino Alcohols
II. Synthesis of N-Terminal, Peptide Helix Initiators, and Characterization of Highly Helical, Capped Polyalanine Peptides

by
Gabriel E. Job

Submitted to the Department of Chemistry at
the Massachusetts Institute of Technology on May 24, 2005 in partial fulfillment of the requirements for the degree of
Doctor of Philosophy in Chemistry

Abstract

I. An improved Ullmann reaction for *N*- or *O*-arylation of 1,2-aminoalcohols with aryl iodides is described. The procedures enjoy several advantages over traditional methods: a substoichiometric amount of copper catalyst is employed, the reactions take place in low boiling and non-toxic solvents such as isopropanol, the reactions occur at relatively low temperatures, and a variety of non-activated aryl iodide substrates may be used.

II. Recent advances in solubilization of polyalanine and helix stabilization by end capping were combined to synthesize a series of highly helical, water-soluble polyalanine peptides permitting straightforward context-free investigation of this most common helix-forming α-amino acid. Three types of peptides incorporating this helical polyalanine region were made, each for a specific purpose: structure determination by NMR; fractional helicity measurement by amide NH→ND exchange in D_2O, observed by NMR; and CD analysis. CD spectra of these helical peptides were used to directly verify an equation used for peptide structural analysis.

The helix-initiating N-terminal cap (Hel) used to create the highly helical polyalanines is a synthetically modified Pro-Pro dipeptide. Hel was developed in the Kemp group a decade ago, and peptides created with it have been extensively studied in this group. However, the 18-step synthesis of Hel has hindered its use by others. Therefore, simpler analogs of Hel have been made and preliminary studies have been conducted. The simpler N-caps were synthesized in twelve steps or fewer and proved effective at helix initiation, as judged by CD spectroscopy. The studies reported herein have also identified an even simpler helix initiator: the dipeptide sequence $^{\beta}$DPro. Further evaluation of these new N-caps under conditions that are not ideal for helix formation awaits.

Thesis Supervisor: Professor Daniel S. Kemp
Title: Professor of Chemistry

Acknowledgments

I am indebted to my mentors and colleagues who have taught, encouraged, and supported me over the last seven years. At the University of Illinois, Prof. Bill Pirkle's unfailing good nature and kind mentoring fostered my interest in chemistry. Doc never missed an opportunity to laugh or teach. Working in the Pirkle group was a pleasure, owing considerably to my lab mates—Seth Snyder, Cody Cole, Dawn Bounds, and especially my closest collaborator, Alex Shvets, whose talent and unassuming confidence were greatly appreciated.

At MIT, I have been fortunate to work for two renown chemists—Prof. Steve Buchwald and Prof. Dan Kemp. It has been a privilege to learn from Steve and Dan, and I have benefited greatly from their knowledge and wisdom. I wish my classmates in the Buchwald group—Eric Streiter, Ed Hennessy, Matt Rainka, and Russ Driver—all the best. I also thank the members of the Kemp group—Bob Kennedy, Sharon Walker, and Björn Heitmann. I thank Bob for his innumerable and selfless contributions to the group and my research. Bob also deserves mention for his uncanny ability to keep track of Prof. Kemp's (worthwhile) nested digressions. I am indebted to Björn for his NMR expertise and scientific ability; also, his inexhaustible good cheer made the basement brighter. Without Bob and Björn, this thesis would not have been possible.

In closing, I thank my family for their steadfast support and encouragement. This thesis is for all of you: for my mom whose correspondence brightened my days, for my dad who would have been proud beyond words, for my in-laws who made Boston their vacation destination, for my brother and sister who patiently listened to my complaints, for my wife's family for making me one of their own, and for the many nieces and nephews who warm our hearts. As for the one who has endured the most over these three, I mean four—well, maybe seven years, ok? She gets her own page.

For Susan

Table of Abbreviations

CD	circular dichroism
ORD	optical rotary dispersion
cpl	circularly polarized light
PLBG	poly-γ-benzyl-L-glutamate
θ_λ	CD ellipticity at an undefined wavelength
$[\theta]_\lambda$	molar CD ellipticity at an undefined wavelength
$[\theta_n]_\lambda$	per-residue molar CD ellipticity at an undefined wavelength
$[\theta_\infty]_\lambda$	per-residue molar CD ellipticity of an infinite helix at an undefined wavelength
X	end-residue parameter for length correction calculation of $[\theta_n]_\lambda$
FH	fractional helicity: number of helical residues / total residues
w	helical propensity for an amino acid residue
v^2	Lifson–Roig helix initiation constant
Ala (A)	alanine
Lys (K)	lysine, a solubilizing residue
tert-Leu (^{t}L)	*tert*-leucine, a spacing residue
Trp (W)	tryptophan, a UV reporting residue
Inp	isonipecotic acid, a spacing residue
Hel	constrained, modified diproline peptide; N-terminal helix initiating cap
$^\beta$Asp ($^\beta$D)	β-linked aspartate, residue added to Hel to increase capping efficacy
beta	β-amino alanine; C-terminal helix-stabilizing and helix-terminating cap
HATU	[*O*-(7-azabenzotriazol-1-yl)-1,1,3,3-tetramethyluronium hexafluorophosphate, carboxyl activating reagent for solid phase peptide synthesis
TFA	trifluoroacetic acid
DIEA	diisopropylethylamine
DMSO	dimethyl sulfoxide
Fmoc	9-fluorenylcarboxymethyl amine protecting group
Cbz	Benzyloxycarbonyl amine protecting group

Boc	*tert*-butyloxycabonyl amine protecting group
Acc	*trans*-4-aminocyclohexane carboxylic acid, a spacing residue
TOCSY	TOtal Correlation SpectroscopY
ROESY	Rotational nuclear Overhauser Effect SpectroscopY
NOESY	Nuclear Overhauser Effect SpectroscopY
PDB	X-ray crystallographic protein structure database
^{U}Ala	uniformly ^{13}C, ^{15}N-labeled alanine
^{1}Ala	1-^{13}CO-labeled alanine
PF_{NHi}	protection factor of the alanine amide at site *i*
k_{StdNH}	reference rate of exchange for an unprotected alanine amide proton
$k_{PeptideNH}$	measured rate of exchange for an alanine amide proton
FH_{NHi}	fractional helicity of alanine amide *i*
FH_i	fractional helicity at alanine site *i*
$[\theta]_{\lambda, Core}$	molar ellipticity attributable to central alanine residues unaffected by caps
$[\theta]_{\lambda, SS-Caps}$	molar ellipticity attributable to terminal alanine residues affected by end caps and solubilizing residues
k	parameter for length correction calculation of $[\theta_n]_\lambda$ that accounts for the number of alanine residues affected by the caps
AUC	analytical ultracentrifugation
HPLC	high pressure liquid chromatography
Arg(R)	arginine
Aib	aminoisobutyric acid
D-Ala	unnatural configuration of alanine
Hyp	(4*R*)-4-hydroxyproline, a naturally occurring derivative of proline
Pro(P)	proline
ES-MS	electrospray mass spectroscopy
DBU	1,8-diazabicyclo[5.4.0]undec-7-ene
TCEP·HCl	hydrochloride salt of tris(carboxyethyl)phosphine
Xaa	indeterminate amino acid
Ala-n	denotes alanine site, reading from N-terminus to C-terminus
Ala_n	denotes number of alanine residues in a row

Chapter I: Copper(I)-Catalyzed Arylation of 1,2-Amino Alcohols

1. Background

The research in the Buchwald group since 1994 has been predominantly directed towards the development of efficient and general metal-catalyzed cross-coupling reactions between aryl halides and a variety of nucleophiles, resulting in substituted anilines and phenols. Initially the research centered on palladium catalysis—specifically, the Pd-catalyzed arylation of primary amines with unactivated aryl bromides. Starting from Migita's method employing a tributyltin amide and bromobenzene to form substituted anilines,[1] the Buchwald group quickly made the reaction more general by introducing a method for *in situ* generation of the tributyltin amide.[2] However, the greatest advance occurred shortly thereafter—in both the Buchwald and Hartwig groups—with the elimination of tin from the reaction.[3,4] In the ensuing years, the development of bulky monodentate phosphine ligands for palladium further enhanced the practicality of what has become known as the Buchwald–Hartwig reaction (Figure 1).[5]

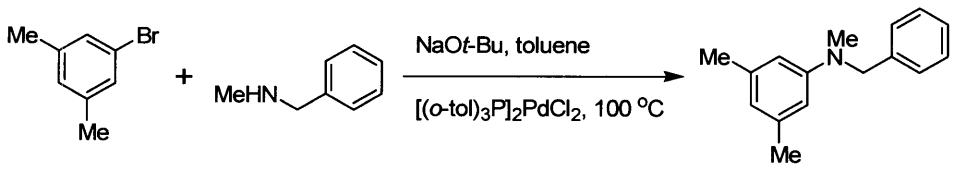

Figure 1: Early example of the Buchwald–Hartwig reaction.

When work on the palladium-catalyzed formation of anilines was begun in the Buchwald and Hartwig groups, a Cu-catalyzed alternative known as the Ullmann

---

[1] Kosugi, M.; Kameyama, M.; Sano, H.; Migita, T. "Palladium-Catalyzed Aromatic Amination of Aryl Bromides with *N,N*-Diethylamino-tributyltin" *Chem. Lett.* **1983**, 927–928.

[2] Guram, A.S.; Buchwald, S.L. "Palladium-Catalyzed Aromatic Aminations with in Situ Generated Aminostannanes" *J. Am. Chem. Soc.* **1994**, *116*, 7901–7902.

[3] Guram, A.S.; Rennels, R.A.; Buchwald, S.L. "A Simple Method for the Conversion of Aryl Bromides to Arylamines" *Angew. Chem., Int. Ed. Engl.* **1995**, *34*, 1348–1350.

[4] Louie, J.; Hartwig, J.F. "Palladium-Catalyzed Synthesis of Arylamines from Aryl Halides. Mechanistic Studies Lead to Coupling in the Absence of Tin Reagents" *Tetrahedron Lett.* **1995**, *36*, 3609–3612.

[5] Muci, A.R.; Buchwald, S.L. "Practical Palladium Catalysts for C–N and C–O Bond Formation" *Top. Curr. Chem.*, Vol. 219, Springer-Verlag, Berlin **2002**, p. 131–209.

condensation had been known for nearly 100 years (Figure 2).[6] Although the Ullmann condensation[7] is catalytic, the poor solubility of the catalyst requires high catalyst loading. This is one of the limitations of the Ullmann reactions that prompted development of the palladium-catalyzed methods. Other commonly cited shortcomings of the Ullmann condensation are its capricious nature, the requirement for high temperatures (> 150 °C), and the use of toxic and high boiling solvents.[8] These qualities overshadow the otherwise economically favorable copper catalyst.

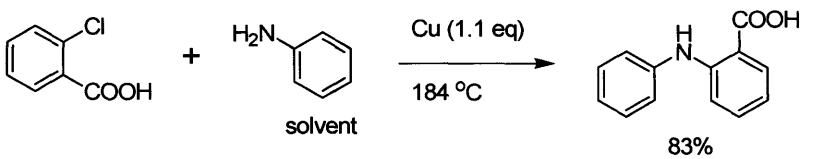

Figure 2: First published example of the Ullmann condensation.

Recently, Cu-mediated arylation reactions experienced a renaissance as several groups sought to eliminate the associated handicaps; two disparate approaches emerged. One approach, introduced by groups at Merck[9] and Dupont, [10] was the mild, cupric acetate-mediated reaction of aryl boronic acids and various nucleophiles—amines, anilines, amides, imides, sulfonamides, ureas, and carbamates. Related methods using arylstannanes[11] or triarylbismuth[12] reagents were known, but the use of an aryl boronic acid as the aryl donor was superior. The requirement for one to two equivalents of the

---

[6] Ullmann, F. "Ueber eine neue Bildungsweise von Diphenyl-aminderivaten" *Chem. Ber.* **1903**, *36*, 2382–2384.

[7] This nomenclature is used to distinguish the C–N bond forming reaction from the Ullmann biaryl synthesis, referred to simply as the Ullmann reaction in Ley's review. Ley, S.V.; Thomas, A.W. "Modern Synthetic Methods for Copper-Mediated C(aryl)–O, C(aryl)–N, and C(aryl)–S Bond Formation" *Angew. Chem., Intl. Ed. Eng.* **2003**, *42*, 5400–5449.

[8] Lindley, J. "Copper Assisted Nucleophilic Substitution of Aryl Halogen" *Tetrahedron Lett.* **1984**, *40*, 1433–1456.

[9] Lam, P.Y.S.; Clark, C.G.; Saubern, S.; Adams, J.; Winters, M.P.; Chan, D.M.T.; Combs, A. "New Aryl/Heteroaryl C–N Bond Cross-coupling Reactions via Arylboronic Acid/Cupric Acetate Arylation" *Tetrahedron Lett.* **1998**, *39*, 2941–2944.

[10] Chan, D.M.T.; Monaco, K.L.; Wang, R.-P.; Winters, M.P. "New *N*- and *O*-Arylations with Phenylboronic acids and Cupric Acetate" *Tetrahedron Lett.* **1998**, *39*, 2933–2936.

[11] López-Alvarado, P.; Avedaño, C.; Menéndez, J.C. "New Synthetic Applications of Aryllead Triacetates. *N*-Arylation of Azoles" *J. Org. Chem.* **1995**, *60*, 5678–5682.

[12] (a) Chan, D.M.T. "Promotion of Reaction of N-H Bonds with Triarylbismuth and Cupric Acetate" *Tetrahedron Lett.* **1996**, *37*, 9013–9016. (b) Finet, J.-P. "Arylation Reactions with Organobismuth Reagents" *Chem. Rev.* **1989**, *89*, 1487–1501.

copper reagent, the need for as many as three equivalents of the aryl donor, long reaction times, and the often moderate yields all detract from this method. However, cupric acetate is cheap and the ability to conduct Ullmann reactions at room temperature is remarkable. Naturally, a catalytic version has been sought; these efforts have met with some success.[13]

The other approach was to use ligands to solubilize the copper catalyst used in Ullmann reactions. In an early report of an additive-accelerated Ullmann reaction, Weingarten proposed that the additive ethylene diacetate solubilized the copper catalyst, thereby facilitating the reaction.[14] Consistent with this idea was the later discovery that the traditional Ullmann reaction is catalyzed by a soluble copper(I) species.[15] More examples of ligand-facilitated Ullmann reactions followed.[16]

An early example of the ligand-acceleration strategy from the Buchwald group was a $Cu(OTf)_2$·phenanthroline catalyst for the arylation of phenols and imidazoles.[17] Whereas the use of a soluble Cu-phenanthroline complex was a significant improvement on the standard Ullmann diphenyl ether synthesis, the need for Schlenck tube manipulations was a drawback. A breakthrough in the elimination of such precautions came from the efforts of Dr. Artis Klapars, Xiaohua Huang, and Dr. Jon Antilla[18] who found that the Goldberg reaction—the Ullmann condensation of amides with aryl

---

[13] (a) Collman, J.P.; Zhong, M. "An Efficient Diamine•Copper Complex-Catalyzed Coupling of Arylboronic Acids with Imidazoles" *Org. Lett.* **2000**, *2*, 1233–1236. (b) Antilla, J.C.; Buchwald, S.L. "Copper-Catalyzed Coupling of Arylboronic Acids and Amines" *Org. Lett.* **2001**, *3*, 2077–2079.

[14] Weingarten, H. "Mechanism of the Ullmann Condensation" *J. Org. Chem.* **1964**, *29*, 3624–3626.

[15] Paine, A.J. "Mechanisms and Models for Copper Mediated Nucleophilic Aromatic Substitution. 2. A Single Catalytic Species from Three Different Oxidation States of Copper in an Ullmann Synthesis of Triarylamines" *J. Am. Chem. Soc.* **1987**, *109*, 1496–1502.

[16] (a) Goodbrand, H.B.; Hu, N.-X. "Ligand-Accelerated Catalysis of the Ullmann Condensation: Application to Hole Conducting Triarylamines" *J. Org. Chem.* **1999**, *64*, 670–674. (b) Fagan, P.J.; Hauptman, E.; Shapiro, R.; Casalnuovo, A. "Using Intelligent/Random Library Screening to Design Focused Libraries for the Optimization of Homogeneous Catalysts: Ullmann Ether Formation" *J. Am. Chem. Soc.* **2000**, *122*, 5043–5051. (c) Gujadhur, R.K.; Bates, C.G.; Venkataraman, D. "Formation of Aryl–Nitrogen, Aryl–Oxygen, and Aryl–Carbon Bonds Using Well-Defined Copper(I)-Based Catalysts" *Org. Lett.* **2001**, *3*, 4315–4317.

[17] (a) Marcoux, J.-F.; Doye, S.; Buchwald, S.L. "A General Copper-Catalyzed Synthesis of Diaryl Ethers" *J. Am. Chem. Soc.* **1997**, *119*, 10539–10540. (b) Kiyomori, A.; Marcoux, J.-F.; Buchwald, S.L. "An Efficient Copper-Catalyzed Coupling of Aryl Halides with Imidazoles" *Tetrahedron Lett.* **1999**, *40*, 2657–2660.

[18] Klapars, A.; Antilla, J.C.; Huang, X.; Buchwald, S.L. "A General and Efficient Copper Catalyst for the Amidation of Aryl Halides and the *N*-Arylation of Nitrogen Heterocycles" *J. Am. Chem. Soc.* **2001**, *123*, 7727–7729.

bromides—could be improved by use of the bidentate additive *trans*-cyclohexanediamine, as shown in Figure 3. This system, using catalytic amounts of CuI and ligand with the mild base potassium phosphate, proved general for the arylation of formamides of primary amines, lactams, and primary amides. Moreover, the reactions could be carried out without rigorous exclusion of air and water. Flush with the success of this mild, Cu-catalyzed C–N bond formation method, the group quickly turned its attention to other reactions in the Ullmann family.

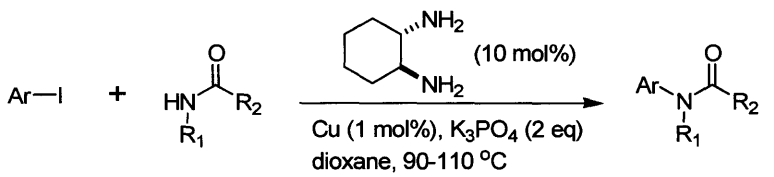

Figure 3: Improved Golderg reaction.

2. *N*-Arylation of 1,2-Amino Alcohols

2.1. *N*-Arylation: Strong Base Method

The impetus for investigation of the title transformation was the copper-catalyzed *N*-arylation of α-amino acids (Figure 4) reported by Ma in 1998.[19] Ma proposed that α-amino acids act as their own bidentate ligands, thereby solubilizing the Cu(I) ion that catalyzes the transformation. Although the method was quite successful for the *N*-arylation of amino acids, an attempt at *N*-arylation of valinol was low yielding (5%). The ability to use a reaction substrate as its own ligand and the prevalence of the 1,2-amino alcohol motif in pharmacologically important molecules[20] provided the rationale for exploring the arylation of these compounds.

---

[19] Ma, D.; Zhang, Y.; Yao, J.; Wu, S.; Tao, F. "Accelerating Effect Induced by the Structure of α-Amino Acid in the Copper-Catalyzed Coupling Reaction of Aryl Halides with α-Amino Acids. Synthesis of Benzolactam V-8" *J. Am. Chem. Soc.* **1998**, *120*, 12459–12467.

[20] For example: β-blockers, ephedrine, tuloberol, mefloquine.

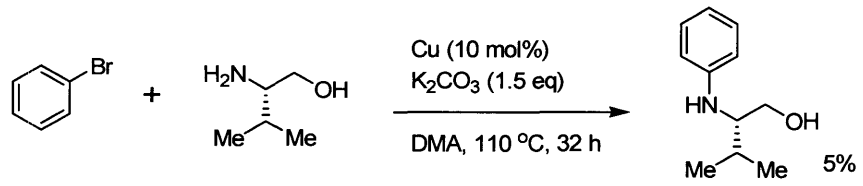

Figure 4: Ma's procedure for the *N*-arylation of valinol.

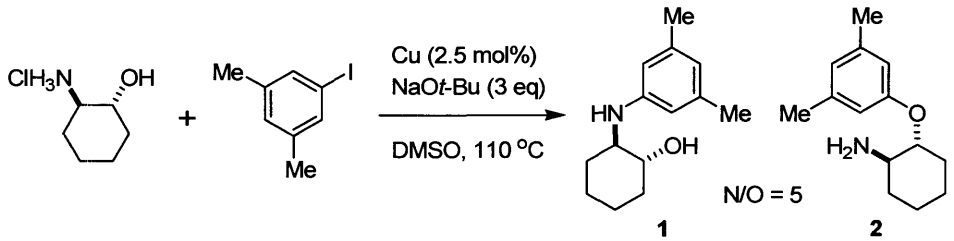

Figure 5: Preliminary strong base *N*-arylation protocol.

In an initial survey of conditions, solvent polarity and base strength were varied for the reaction of *trans*-2-amino-cyclohexanol with 3,5-dimethyl-bromobenzene. The *N*-arylation product was readily obtained in good yield with the DMSO/NaO^{t}Bu system shown in Figure 5. The conversion of the starting amino alcohol was nearly complete within six hours and two products with identical mass were present in a 5:1 ratio, corresponding to the *N*-aryl and *O*-aryl products. The identities of the two products were assigned by running the reaction again with bromobenzene in lieu of 3,5-dimethyl-bromobenzene since the two resulting mono-phenylated products had been previously synthesized and characterized. The *N*-aryl product had been synthesized by the tin(II) triflate-catalyzed reaction of cyclohexene oxide with aniline.[21] The *O*-aryl product had been synthesized by the reaction of potassium phenoxide and *N*-phthalamido cyclohexane aziridine, followed by hydrazinolysis of the phthalamide group and Raney Ni reduction.[22] Comparison of the spectra for compounds **1** and **2** with the published ^{1}H NMR data demonstrated that the *N*-aryl product was favored by the conditions shown in Figure 5

[21] Singh, V.K. and Sekar, G. "An Efficient Method for Cleavage of Epoxides with Aromatic Amines" *J. Org. Chem.* **1999**, *64*, 287–289.

[22] von Egli, M.; Hoesch, L.; Dreiding, A.S. "β-Funktionalisierte Hydrazine aus *N*-Phthalimidoaziridinen und ihre hydrogenolytische N,N-Spaltung zu Aminen" *Helv. Chim. Acta* **1985**, *68*, 220–230.

(N/O = 5). Further evidence for *N*-arylation regioselectivity was required since most compounds in Table 1 were not known previously. Because *O*-arylation leaves only exchangeable amine protons, one piece of evidence for *N*-arylation was the presence of two broad peaks in the ^{1}H NMR spectrum corresponding to the two exchangeable protons—N*H* and O*H*.[23] Although the exchangeable protons of compound **1** are coincident in its ^{1}H NMR spectrum, the two exchangeable protons in an *N*-aryl compound were frequently resolved in the ^{1}H NMR spectra. Furthermore, the TLC retention factors of the two regioisomers differed greatly; functionalized anilines such as **1** have greater R_f values than alkyl amines such as **2**, doubtlessly owing to the greater basicity of the alkyl amines.

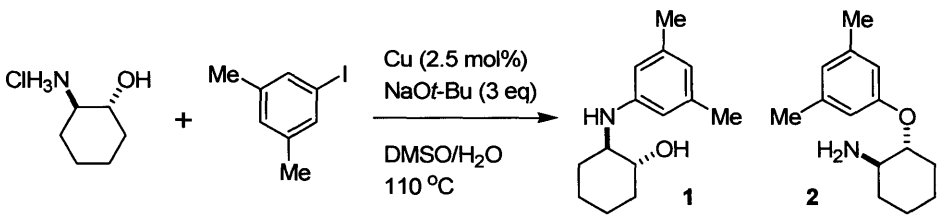

vol % H_2O	N/O
1.25	8
5	32
25	130

Figure 6: An improved aqueous system for *N*-arylation.

One humid day, the sodium *tert*-butoxide being weighed out for an *N*-arylation reaction absorbed water. The reaction was run anyway to test if water would be tolerated in the reaction. Upon GC analysis of the reaction mixture, the N/O ratio was found to have improved slightly. To determine if the water contamination caused this change, a series of reactions with dry NaO^{t}Bu were prepared and increasing amounts of water were deliberately added to the reactions. As shown in Figure 6, the addition of water did indeed improve the N/O ratio, with subsequent improvement in the GC yield of the *N*-aryl species. The optimal combination of DMSO and water was found to be two parts

[23] In cases where a secondary amino alcohol was arylated, acetylation of the product revealed the position of the aryl group: if amide rotamers were observed, *O*-arylation had taken place.

DMSO and one part water; additionally, NaO^{t}Bu was replaced with NaOH. Eventually, isopropanol was found to work as well as the DMSO/water solvent. It is noteworthy that the two solvent systems yield essentially the same results even though the sodium hydroxide base is poorly soluble in isopropanol and completely soluble in the DMSO–water solvent. Thus, the final systems shown in Table 1 were devised; several *N*-aryl products synthesized by these methods with hydroxide base are given.[24]

Most examples in Table 1 are reactions run using the amino alcohol as the limiting reagent. This is a reasonable choice because the amino alcohol may often be the more elaborate and costly reaction partner, especially since synthesis of this component is more likely to demand consideration of stereoselectivity. However, one can imagine cases in which the aryl iodide would be the more precious commodity; as entry 4b (Table 1) demonstrates, a slightly lower yield can be anticipated if the aryl iodide is used as the limiting reagent. A significant side reaction for the strong base *N*-arylation procedure is the conversion of aryl iodide to the corresponding phenol; therefore, using the aryl iodide as the limiting reagent reduces the yield. For reactions in which the amino alcohol is the limiting reagent, the use of 1.2 equivalents of aryl iodide allows for this degradation of starting material. Even so, in some cases a trace amount (generally < 3%) of amino alcohol could be detected in the reaction after 16 h. These reactions could usually be forced to completion by the use of 1.4 equivalents of aryl iodide or the use of 10 mol % of CuI. However, the very minor increases in yield did not justify these measures. A further consideration that weighed against such actions was the ease with which the starting amino alcohol was separated from its *N*-aryl derivative. Flash chromatography readily separated the compounds, and even when extraction was used to isolate the product (compound **4**) no trace of the amino alcohol in the product was observed by ^{1}H NMR. For any reaction, the choice of reagent quantity depends on numerous variables such as the cost of materials, time constraints, and purification method; each reaction must be optimized accordingly, and the examples in Table 1 provide a guideline.

---

[24] Job, G.E.; Buchwald, S.L. "Copper-Catalyzed Arylation of *β*-Amino Alcohols" *Org. Lett.* **2002**, *4*, 3703–3706.

Table 1: Hydroxide Base Procedure for *N*-arylation of 1,2-Amino Alcohols.

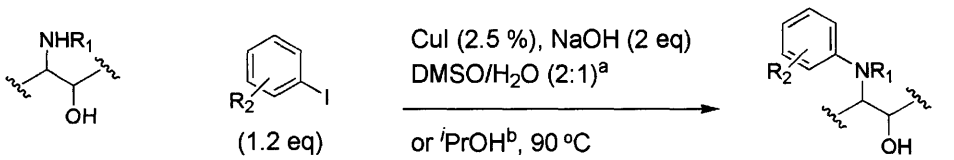

entry	product		time (h)	% yield[c]
1[d]	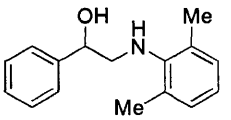	**3**	17	86
2[e]	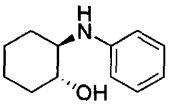	**4**	15	87
3	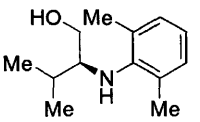	**5**	17	88
4a b[f]	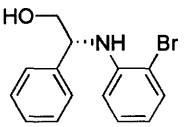	**6**	16	84 76
5a b[e]	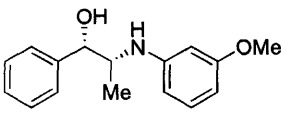	**7**	17	84 77
6a[g] b[h]	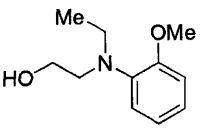	**8**	17	77 89
7	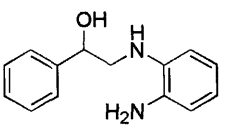	**9**	15	63

Conditions: 1 mL of ^{i}PrOH or DMSO/$H_2$0 under N_2 in a sealed tube. [a] Reactions 1-3. [b] Reactions 4-7. [c] Average of two isolated yields; satisfactory combustion analyses were obtained for all products. [d] 100 °C. [e] Amino alcohol used as the HCl salt, requiring 3 mmol base. [f] Stoichiometries of the two reactants were reversed. [g] Three equivalents of amino alcohol and 0.8 mL ^{i}PrOH were used. [h] Reaction run in neat amino alcohol.

The procedure for *N*-arylation using NaOH as base typically gave N/O > 50. Lower values were found for products which have a sterically hindered nitrogen atom (compound **8**), and for products derived from hindered aryl iodides (compound **3**). Attempts at arylating ephedrine failed; the principal outcome of the reaction between ephedrine and iodobenzene was the conversion of iodobenzene to phenol at comparable rates to the arylation of ephedrine. Increasing the equivalents of aryl iodide and the amount of catalyst did not overcome this limitation. Presumably, the combination of branching alpha to the nitrogen and the secondary amine renders ephedrine an unfavorable reactant.

Control reactions lacking the CuI catalyst were run for each example in Table 1; in all cases, the amount of product formed was negligible (< 5%). Another set of control reactions in which simple amines were subjected to the *N*-arylation conditions produced no arylated amines, conclusively demonstrating that the bidentate arrangement of heteroatoms is important for the success of the reaction. Although aryl iodides worked well for the reaction, aryl bromides did not as shown by the high selectivity for arylation using 2-bromo-iodobenzene (compound **6**). Attempts at using aryl bromides as reagents for the *N*-arylation reaction gave slow reactions and poor N/O selectivity. In addition to bromides, aromatic amino groups were tolerated (compound **9**).

A large number of naturally occurring, enantiopure 1,2-amino alcohols exist, and many stereoselective routes to these compounds have been discovered.[25] On the other hand, few stereoselective syntheses of *N*-aryl-1,2-amino alcohols have been reported.[26] Our methods for arylation of 1,2-amino alcohols make use of the ready supply of enantio- and diastereopure amino alcohols. All arylation reactions reported herein proceeded with

---

[25] (a) Chang, H.-T.; Sharpless, K.B. "A Practical Route to Enantiopure 1,2-Aminoalcohols" *Tetrahedron Lett.* **1996**, *37*, 3219.3222–. (b) Martinez, L.E.; Leighton, J.L.; Carsten, D.H.; Jacobsen, E.N. "Highly Enantioselective Ring Opening of Epoxides Catalyzed by (salen)Cr(III) Complexes" *J. Am Chem. Soc.* **1995**, *117*, 5897–5898. (c) Reddy, K.C.; Sharpless, K.B. "From Styrenes to Enantiopure α-Arylglycines in Two Steps" *J. Am. Chem. Soc.* **1998**, *120*, 1207–1217. (d) Hoffman, R.V.; Maslouh, N.; Cervantes-Lee, F. "Highly Stereoselective Syntheses of *syn*- and *anti*-1,2-Amino Alcohols" *J. Org. Chem.* **2002**, *67*, 1045–1056.

[26] (a) Fu, X.-L.; Wu, S.-H. "A Regio- and Stereoselective Synthesis of β-Amino Alcohols" *Synth. Commun.* **1997**, *27*, 1677–1683. (b) Hou, X.-L.; Wu, J.; Dai, L.-X.; Xia, L.-J.; Tang, M.-H. "Desymmetric Ring-opening of *meso*-Epoxides with Anilines: A Simple Way to Chiral β-Amino Alcohols" *Tetrahedron: Asymmetry* **1998**, *9*, 1747–1752. (c) Lautens, M.; Fagnou, K. "Effects of Halide Ligands and Protic Additives on Enantioselectivity and Reactivity in Rhodium-Catalyzed Asymmetric Ring-Opening Reactions" *J. Am. Chem. Soc.* **2001**, *123*, 7170–7171.

complete retention of stereochemistry at chiral centers in the amino alcohol. For those products bearing a single stereocenter, comparison of the product with its racemate or antipode by chiral HPLC demonstrated complete retention of stereochemistry in the coupling reactions. Retention of stereochemistry for products bearing two stereocenters was demonstrated by the absence of diastereomers, as evidenced by ^{1}H NMR analysis.

2.2 *N*-Arylation: Mild Base Method

Because the use of hydroxide base limits the scope of the arylation procedure, a method using a mild base was sought. A survey of mild bases—Cs_2CO_3, K_2CO_3, Na_2CO_3, K_3PO_4, DBU—in a variety of solvents failed to identify a procedure for the selective *N*-arylation of amino alcohols; very slow reaction rates accompanied their use. The selectivities ranged between 0.5 and 2.0; although a selectivity of two could be useful, no reaction with a mild base went to completion with reasonable amounts of reagents in an acceptable amount of time. Fortunately, the project benefited from the concurrent work of Dr. Michael Kwong who discovered that simple primary amines could be efficiently arylated with aryl iodides by using two equivalents of ethylene glycol as a ligand; the reactions were run in isopropanol with K_3PO_4 base.[27]

I reasoned that, instead of using the amino alcohols as their own ligand, the amino alcohols could be treated as a simple amine and arylated using Dr. Kwong's system. The use of one equivalent of ethylene glycol as a ligand did indeed over-ride the undesirable tendencies of the mild base reactions for 1,2-amino alcohols observed earlier; N/O selectivities were typically less than ten, but still quite useful. The mild base procedure is given in Table 2 along with examples illustrating the functional group compatibility of the method. As with the strong base method, control reactions lacking copper were run, and no significant product formation was noted. Similarly, no epimerization was evident by ^{1}H NMR or HPLC.

[27] Kwong, F.Y.; Klapars, A.; Buchwald, S.L "Copper-Catalyzed Coupling of Alkyamines and Aryl Iodides: An Efficient System Even in an Air Atmosphere" *Org. Lett.* **2002**, *4*, 581–584.

Table 2: Mild base method for the *N*-arylation of 1,2-amino alcohols.

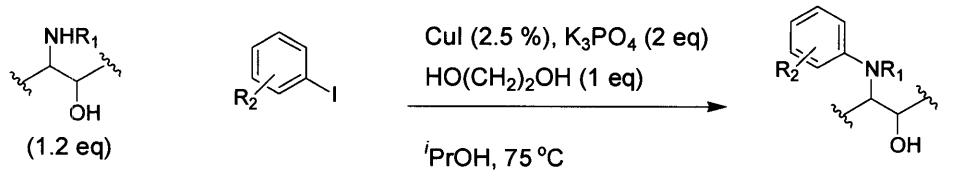

entry	product		time (h)	% yield[a]
1a	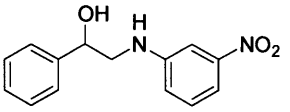	**10**	16	73
b[b]				66
2[b,c]	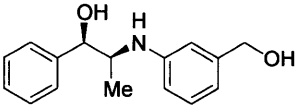	**11**	17	76
3	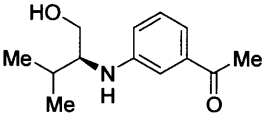	**12**	17	75

Conditions: 1.1 mL of ^{i}PrOH under N_2 in a sealed tube. [a] Average of two isolated yields; satisfactory combustion analyses were obtained for all products. [b] Stoichiometries of the two reactants were reversed. [c] 80 °C.

3. Arylation of Simple Alcohols

During a discussion with Dr. Kwong on the by-products formed in our respective mild base arylation reactions, I realized that 1,2-amino alcohols could be used as ligands for the arylation of simple alcohols. In our reactions, arylation of ethylene glycol was always observed, as was conversion of the aryl iodide to the corresponding phenol. I had also identified by GC/MS small amounts of aryl isopropyl ethers in my reactions, whereas Michael had not. Because the only difference between our reactions was the nature of the nitrogen nucleophile, it seemed reasonable to explore the use of a 1,2-amino alcohol as a ligand for the arylation of simple alcohols. The reaction shown in Figure 7 was run; gratifyingly, the amino alcohol and amino acid ligands produced phenyl hexyl

ether as shown.[28] Reactions run in the absence of the putative ligands gave only traces of the aryl alkyl ether.

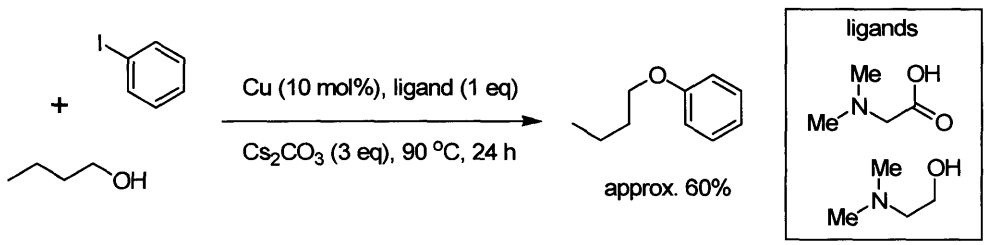

Figure 7: Method for the arylation of simple aliphatic alcohols.

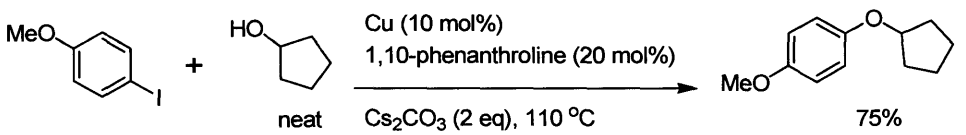

Figure 8: Initial *O*-arylation reaction for a simple alcohol.

The idea of arylating simple alcohols had been considered previously, of course. In fact, Whitesides and Sadowski demonstrated that copper(I) alkoxides could be arylated in good yield by reaction with aryl halides in pyridine. However, the use of air- and water-sensitive copper(I) alkoxides is inconvenient.[29] Furthermore, some prospecting for *O*-arylation techniques had been done in the Buchwald group, but no yields as promising as that in Figure 7 had been encountered. The details of this lead reaction were given to Dr. Gero Nordmann who quickly found that 1,10-phenanthroline was a better ligand for the arylation of simple alcohols. Figure 8 gives a typical procedure for the formation of aryl alkyl ethers taken from the communication of this work.[30] Incidentally, the *N,N*-

[28] Although the Williamson ether synthesis could be used to generate this simple compound, similar reactions involving tertiary alcohols or deactivated phenols would fail.

[29] Whitesides, G.M.; Sadowski, J.S.; Lilburn, J. "Copper(I) alkoxides. Synthesis, reactions, and thermal decompositions." *J. Am. Chem. Soc.* **1974**, *96*, 2829–2835.

[30] Wolter, M.; Nordmann, G.; Job, G.E.; Buchwald, S.L. "Copper-Catalyzed Coupling of Aryl Iodides with Aliphatic Alcohols" *Org. Lett.* **2002**, *4*, 973–976.

dimethylglycine ligand in Figure 7 later appeared in methods for the arylation of phenols[31] and amines[32] published by Ma in 2003.

4. *O*-arylation of 1,2-Amino Alcohols

The low *N*-aryl selectivity—and in some cases moderate *O*-aryl selectivity—observed for the mild base protocols raised the question whether 1,2-amino alcohols could be selectively *O*-arylated. The answer was affirmative; however, the best results were obtained for 1,2-amino alcohols bearing a secondary amino group.[24] Entries **1** and **2** in Table 3 demonstrate this difference in reactivity. Typically, O/N selectivities for the arylation of secondary amino alcohols were less than five, and lower for primary amino alcohols. The use of cesium carbonate as base for this transformation was critical; no other mild base gave useful rates with comparable selectivity, consistent with experience in our group on related methods for Cu-mediated C–O bond formation.[17,30] The final scheme for *O*-selective arylation of 1,2-amino alcohols is shown in Table 3, along with examples illustrating the scope of the reaction.

Even fewer synthetic routes are available for *O*-aryl-1,2-amino alcohols than for *N*-aryl-1,2-amino alcohols, and all are moderate yielding at best. The S_NAr displacement of fluoride from arene·$Cr(CO)_3$ complexes has been used to make a series of mexiletine analogs similar to compound **17** in Table 3;[33] the best yield was less than 50%. The Mitsunobu and Williamson reactions have both been applied to the synthesis of mexiletine analogs as well.[34] Additionally, the previously mentioned method involving the opening of *N*-phthalimido aziridines with phenols does provide the *O*-aryl amino alcohols, albeit under harsh conditions with multiple manipulations.[22]

Our single-step arylation methods are easy to perform and provide routes to arylated 1,2-amino alcohols that compliment or supersede the existing methodology.

---

[31] Ma, D.; Cai, Q. "*N,N*-Dimethyl Glycine-Promoted Ullmann Coupling Reaction of Phenols and Aryl Halides" *Org. Lett.* **2003**, *5*, 3799–3802.

[32] Ma, D.; Cai, Q.; Zhang, H. "A Mild Method for Ullmann Coupling Reaction of Amines and Aryl Halides" *Org. Lett.* **2003**, *5*, 2453–2455.

[33] Loughhead, D.G.; Flippin, L.A.; Weikert, R.J. "Synthesis of Mexiletine Stereoisomers and Related Compounds via S_NAr Nucleophilic Substitution of a $Cr(CO)_3$-Complexed Aromatic Fluoride" *J. Org. Chem.* **1999**, *64*, 3373–3375.

[34] Carocci, A.; Catalano, A.; Corbo, F.; Duranti, A.; Amoroso, R.; Franchini, C.; Lentini, G.; Tortorella, V. "Stereospecific Synthesis of Mexiletine and Related Compounds: Mitsunobu versus Mitsunobu Reaction" *Tetrahedron: Asymmetry* **2000**, *11*, 3619–3634.

Although no single method is likely to be ideal for the synthesis of every member of a class of compounds, the direct arylation technology provides a simple alternative to many existing routes, thus providing greater flexibility in planning synthetic routes.

Table 3: *O*-selective arylation of 1,2-amino alcohols.

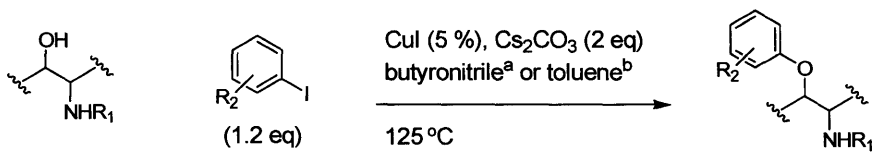

entry	product[c]		time (h)	% yield[d]
1[e]	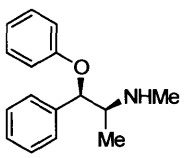	**13**	25	74
2	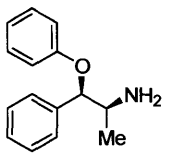	**14**	14	53
3	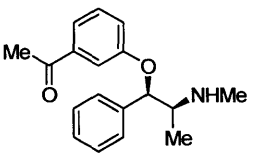	**15**	21	52
4	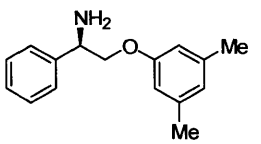	**16**	14	47
5[f]	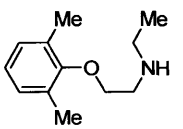	**17**	30	72
6[f,g]	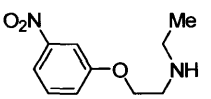	**18**	21	54

Conditions: 1 mL of solvent under N_2 in a sealed tube. [a] Entries 1-5. [b] Entry 6. [c] Isolated as the HCl salt. [d] Average of two isolated yields. Entries 2 and 4 were determined as >95% pure by ^{1}H NMR; water was the chief impurity. All other products gave satisfactory elemental analyses. [e] 1.5 eq. of aryl iodide. [f] 2 eq. amino alcohol, 1 eq. aryl iodide. [g] 115 °C.

5. Experimental Procedures

5.1 General Considerations

Copper(I) iodide (98%) and cesium carbonate were purchased from Strem Chemical Company. Potassium phosphate was manufactured by Riedel-de Haen and was purchased from Fluka; this finely granulated form has proven to be better than other forms. All other reagents are available commercially and were used without further purification. All reagents were weighed and handled in air. Flash column chromatography was performed with Silicycle ultra pure silica gel (230 - 400 mesh). Melting points were recorded on a Mel-Temp II, Laboratory Devices, Inc. IR spectra were recorded on an ASI ReactIRTM 1000 and were obtained by placing samples directly on the DiComp probe. Elemental analyses were performed by Atlantic Microlabs, Inc., Norcross, GA. ^{1}H and ^{13}C NMR were obtained on a Varian 300 or 500 MHz instrument with chemical shifts reported relative to tetramethyl silane using residual solvent signals or TMS as an internal standard. High resolution mass spectra were obtained on a Bruker ESP-300 EPR spectrometer. Gas chromatographic analyses were performed on a Hewlett Packard 5890 instrument with a FID detector and a Hewlett Packard 30 m x 0.25 mm i.d. HP-5 capillary column. Chiral HPLC analyses were performed on a Hewlett-Packard 1100 system with an HP 1100 Diode Array Detector (monitoring at 254 nm) using an analytical (*R*,*R*)-Whelk-O1 column (25 cm x 4.6 mm i.d., 5 micron 100 Å spherical silica) purchased from Regis Technologies Inc., Morton Grove, IL. Samples were compared with their identically prepared racemates or were chromatographed in various ratios with their antipodes, likewise prepared identically. Control reactions without CuI were performed for all compounds; the amount of product observed by gas chromatography for the control reactions was 0 – 8%. Although satisfactory elemental analyses were obtained for all *N*-aryl products, the ^{1}H NMR of the products obtained as oils sometimes indicated the presence of trace amounts of chromatography solvent.

5.2 Characterization Data

2-(2,6-Dimethyl-phenylamino)-1-phenyl-ethanol (3)

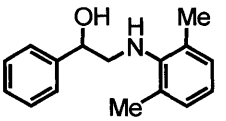

A screw-cap test tube was charged with CuI (5.0 mg, 0.025 mmol, 2.5 mol%), sodium hydroxide (80.0 mg, 2.0 mmol), 2-amino-1-phenyl ethanol (137 mg, 1.0 mmol), and 2,6-dimethyl iodobenzene (169 μL, 1.2mmol). The test tube was fitted with a septum and purged with nitrogen before addition of DMSO (0.67 mL) and H_2O (0.33 mL). The test tube was then capped and stirred in an oil bath at 90 °C for 16.5 h. The resulting mixture was cooled to room temperature and diluted with water (4 mL) before extraction with methylene chloride (3 x 5 mL). The combined organic layers were washed with 0.1 M NaOH (1 x 5 mL), washed with brine (1 x 5 mL), dried over $MgSO_4$, and concentrated in vacuo. Flash chromatography of the crude product (CH_2Cl_2:Et_2O, 90:10) provided 206.4 mg (86%) of the title compound as a pale yellow oil. ^1H NMR (300 MHz, $CDCl_3$): δ 2.20 (s, 3H), 3.04 (dd, J = 12.6, 8.5 Hz, 1H), 3.17 (dd, J = 12.9, 3.9 Hz, 1H), 3.41 (broad s, 2H), 4.69 (dd, J = 8.5, 3.6 Hz, 1H), 6.81 (dd, J = 8.2, 6.2 Hz, 1H), 6.94 (d, J = 8.1 Hz, 2H), 7.26 (m, 5H). ^{13}C NMR (75 MHz, $CDCl_3$): δ 17.3, 51.3, 72.0, 110.2, 117.5, 122.6, 125.7, 127.0, 127.8, 128.4, 130.1, 142.0, 145.5. IR ($CDCl_3$, cm^{-1}): 3599, 3379, 3033, 2917, 1594, 1503, 1474, 1059. Anal. Calcd. for $C_{16}H_{19}NO$: C, 79.63; H, 7.94. Found: C, 79.64; H, 8.00.

trans-2-phenylamino-cyclohexanol (4)

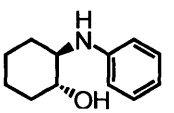

A screw-cap test tube was charged with CuI (5.0 mg, 0.025 mmol, 2.5 mol%), sodium hydroxide (120.0 mg, 3.0 mmol), *trans*-2-amino-1-cyclohexanol hydrochloride (152 mg, 1.0 mmol), and iodobenzene (134 μL, 1.2 mmol). The test tube was fitted with a septum and purged with nitrogen before addition of DMSO (0.67mL) and H_2O (0.33 mL). The test tube was then capped and stirred in an oil bath at 90 °C for 15h. The resulting mixture was cooled to room temperature and diluted with water (4 mL) before extraction with methylene chloride (3 x 5 mL). The combined organic layers were washed with 3 M HCl (3 x 5 mL). The acid extracts were cooled on ice and a saturated NaOH solution

was added until the mixture became cloudy (pH~12). The solution was then washed with methylene chloride (3 x 10 mL). The combined organic layers were washed with brine (1 x 10 mL), dried over $MgSO_4$ and concentrated in vacuo to yield 165.8 mg (87%) of the title compound as an off-white solid. ^1H NMR (500 MHz, $CDCl_3$): δ 0.96 (m, 1H), 1.29 (m, 3H), 1.68 (m, 2H), 2.05 (m,2H), 3.06 (ddd, J = 13.1, 9.2, 4.0 Hz, 1H), 3.12 (broad s, 1H), 3.27 (ddd, J = 10.1, 9.2, 4.3 Hz, 1H), 3.42 (broad s, 1H), 6.66 (dd, J = 8.6, 1.2 Hz, 2H), 6.71 (tt, J = 7.3, 0.9 Hz, 1H), 7.14 (dt, J = 7.8, 1.2 Hz, 2H). ^{13}C NMR (125 MHz, $CDCl_3$): δ 24.1, 24.7, 31.3, 33.1, 59.7, 74.0, 114.0, 117.9, 129.1, 147.7. IR ($CDCl_3$, cm^{-1}): 3525, 3390, 2937, 2860, 1602, 1501, 1065, 1040. Melting point: 57 – 58 °C. Anal. Calcd. for $C_{12}H_{17}NO$: C, 75.35; H, 8.96. Found: C, 75.25; H, 8.90.

(*S*)-2-(3,5-Dimethyl-phenylamino)-3-methyl-butan-1-ol (5)

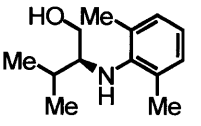

A screw-cap test tube was charged with CuI (5.0 mg, 0.025 mmol, 2.5 mol%), sodium hydroxide (80.0 mg, 2.0mmol), (*S*)-valinol (111 μL, 1.0 mmol), and 3,5 dimethyl-iodobenzene (173 μL, 1.2 mmol). The test tube was fitted with a septum and purged with nitrogen before adding DMSO (0.67 mL) and H_2O (0.33 mL). The test tube was then capped and stirred in an oil bath at 90 °C for 16.5 h. The resulting mixture was cooled to room temperature and diluted with water (4 mL) before extraction with methylene chloride (3 x 5 mL). The combined organic layers were washed with 0.1 M NaOH (1 x 5 mL), washed with brine (1 x 5 mL), dried over $MgSO_4$, and concentrated in vacuo. Flash chromatography of the crude product (CH_2Cl_2:EtOAc, 90:10) provided 183.1 mg (88%) of the title compound as a pale yellow oil that solidified into an off-white solid under high vacuum. ^1H NMR (500 MHz, $CDCl_3$): δ 0.91 (d, J = 6.9 Hz, 3H), 0.94 (d, J = 6.9 Hz, 3H), 1.83 (dsept, J = 6.8, 6.7 Hz, 1H), 2.22 (s, 6H), 2.55 (broad s, 1H), 3.23 (dd, J =6.5, 6.4 Hz, 1H), 3.44 (broad s, 1H), 3.46 (dd, J = 11.0, 7.0 Hz, 1H), 3.69 (d, J = 10.1 Hz, 1H), 6.28 (s, 2H), 6.36 (s, 1H). ^{13}C NMR (125 MHz, $CDCl_3$): δ 18.9, 19.0, 21.3, 30.0, 60.7, 62.4, 111.5, 119.5, 138.8, 148.4. IR ($CDCl_3$, cm^{-1}): 3614, 3415, 3025, 2962, 1600, 1468, 1337, 1185. Melting point: 44 – 45 °C. Anal. Calcd. for $C_{13}H_{21}NO$: C, 75.32; H, 10.21. Found: C, 75.19; H, 10.31. Chiral chromatography: ambient

temperature, hexanes:*i*-PrOH (98.5:1.5), 1.75 mL/min, t_1 (*S*) = 13.3 min, t_2 (*R*) = 25.8 min. $[\alpha]^{20}_D = -33.5$ ($CHCl_3$, c 0.23).

(*R*)-2-(2-Bromo-phenylamino)-2-phenyl-ethanol (6)

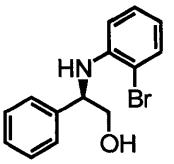

A screw-cap test tube was charged with CuI (5.0 mg, 0.025 mmol, 2.5 mol%), sodium hydroxide (80.0 mg, 2.0 mmol), (*R*)-phenylglycinol (137 mg, 1.0 mmol), and 2-bromo-iodobenzene (154 μL, 1.2 mmol). The test tube was fitted with a septum and purged with nitrogen before adding isopropanol (1.0 mL). The test tube was then capped and stirred in an oil bath at 90 °C for 16.5 h. The resulting mixture was cooled to room temperature and diluted with water (4 mL) before extraction with methylene chloride (3 x 5 mL). The combined organic layers were washed with 0.1 M NaOH (1 x 5 mL), washed with brine (1 x 5 mL), dried over $MgSO_4$, and concentrated in vacuo. Flash chromatography of the crude product (CH_2Cl_2) provided 246.9 mg (84%) of the title compound as a yellow oil. For reaction 4b, the conditions above were modified as follows: (*R*)-phenylglycinol (165 mg, 1.2 mmol), and 2-bromo iodobenzene (128 μL, 1.0 mmol). ^{1}H NMR (300 MHz, $CDCl_3$): δ 2.21 (broad s, 1H), 3.72 (dd, J = 11.3, 7.0 Hz, 1H), 3.88 (dd, J = 11.3, 4.3 Hz, 1H), 4.47 (ddd, J = 6.4, 5.8, 4.3 Hz, 1H), 5.15 (d, J = 5.8 Hz, 1H), 6.37 (dd, J = 7.9, 1.2 Hz, 1H), 6.50 (dt, J = 7.5, 1.2 Hz, 1H), 6.94 (dt, J = 7.7, 1.5 Hz, 1H), 7.26 (m, 5H), 6.94 (dd, J = 7.9, 1.5 Hz, 1H). ^{13}C NMR (75 MHz, $CDCl_3$): δ 59.6, 67.1, 110.2, 112.9, 118.2, 126.5, 127.6, 128.2, 128.8, 132.2, 139.3, 143.8. IR ($CDCl_3$, cm^{-1}): 3575, 3400, 3029, 2879, 1596, 1503, 1453, 1322, 1021. Anal. Calcd. for $C_{14}H_{14}NOBr$: C, 57.55; H, 4.83. Found: C, 57.60; H, 4.90. Chiral chromatography: 0 °C, hexanes:*i*-PrOH (98.5:1.5), 1.75 mL/min, $t_{(R)}$ = 17.6 min, $t_{(S)}$ = 20.4 min. $[\alpha]^{20}_D$ –22.9 ($CHCl_3$, c 1.97).

(*1S,2R*)-2-(3-Methoxy-phenylamino)-1-phenyl-propan-1-ol (7)

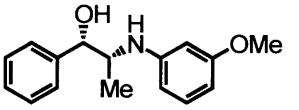

A screw-cap test tube was charged with CuI (5.0 mg, 0.025 mmol, 2.5 mol%), sodium hydroxide (80.0 mg, 2.0 mmol), (1*S*,2*R*)-norephedrine (151 mg, 1.0 mmol), and 3-iodo-anisole (143 μL, 1.2 mmol). The test tube was fitted with a septum and purged with nitrogen before adding isopropanol (1.0 mL). The test tube was then capped and stirred in an oil bath at 90 °C for 16 h. The resulting mixture was cooled to room temperature and diluted with water (4 mL) before extraction with methylene chloride (3 x 5 mL). The combined organic layers were washed with 0.1 M NaOH (1 x 5 mL), washed with brine (1 x 5 mL), dried over $MgSO_4$, and concentrated in vacuo. Flash chromatography of the crude product (CH_2Cl_2:EtOAc, 95:5) provided 216.1 mg (84%) of the title compound as a yellow oil. For reaction 5b, the conditions above were modified as follows: (*1S,2R*)-norephedrine hydrochloride (188 mg, 1.0 mmol) and sodium hydroxide (120 mg, 3.0 mmol). ^{1}H NMR (300 MHz, $CDCl_3$): δ 0.95 (d, J = 6.6 Hz, 3H), 2.80 (broad s, 1 H), 3.67 (m, 1H), 3.70 (s, 3H), 3.82 (broad s, 1H), 4.88 (d, J = 2.5 Hz, 1H), 6.18 (t, J = 2.2 Hz, 1H), 6.25 (ddd, J = 7.8, 5.4, 2.2 Hz, 2H), 7.04 (t, J = 8.3 Hz, 1H), 7.26 (m, 5H). ^{13}C NMR (75 MHz, $CDCl_3$): δ 13.9, 54.3, 55.1, 74.2, 99.8, 102.8, 106.7, 125.7, 127.2, 128.1, 130.0, 141.2, 148.2, 160.6. IR ($CDCl_3$, cm^{-1}): 3612, 3413, 2975, 1615, 1600, 1509, 1212, 1164. Anal. Calcd. for $C_{16}H_{19}NO_2$: C, 74.68; H, 7.44. Found: C, 74.48; H, 7.41. $[\alpha]^{20}_D$ – 74.4 ($CHCl_3$, c 1.53).

2-[ethyl-(2-methoxyphenyl)-amino]-ethanol (8)

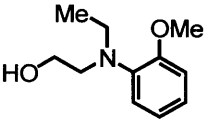

A screw-cap test tube was charged with CuI (5.0 mg, 0.025 mmol, 2.5 mol%), sodium hydroxide (80.0 mg, 2.0 mmol), 2-(aminoethyl)ethanol (294 μL, 3.0 mmol), and 2-iodo-anisole (130 μL, 1.0 mmol). The test tube was fitted with a septum and purged with nitrogen before adding isopropanol (0.8 mL). The test tube was then capped and stirred in an oil bath at 90 °C for 17 h. The resulting mixture was cooled to room temperature

and diluted with water (4 mL) before extraction with methylene chloride (3 x 5 mL). The combined organic layers were washed with 0.1 M NaOH (1 x 5 mL), washed with brine (1 x 5 mL), dried over $MgSO_4$, and concentrated in vacuo. Flash chromatography of the crude product (CH_2Cl_2:EtOAc, 80:20) provided 151.2 mg (77%) of the title compound as a pale yellow oil. For the reaction in 6b, the solvent was neat amino alcohol (1.0 mL, 10.2 mmol). ^1H NMR (300 MHz, $CDCl_3$): δ 0.99 (t, J = 7.0 Hz, 1H), 3.12 (q, J = 7.0 Hz, 2H), 3.14 (t, J = 5.5 Hz, 3H), 3.37 (broad s, 1H), 3.56 (t, J = 5.2 Hz, 2H), 3.82 (s, 3H), 6.87 (dd, J = 7.9, 1.2 Hz, 1H), 6.90 (dt, J = 7.6, 1.2 Hz, 1H), 7.05 (dt, J = 7.7, 1.8 Hz, 1H), 7.07 (dd, J = 7.6, 1.5 Hz, 1H). ^{13}C NMR (75 MHz, $CDCl_3$): δ 12.5, 47.0, 55.2, 55.6, 59.1, 111.4, 120.6, 123.4, 124.3, 138.6, 154.7. IR ($CDCl_3$, cm^{-1}): 3429, 2968, 2836, 1594, 1499, 1235, 1027. Anal. Calcd. for $C_{11}H_{17}NO_2$: C, 67.66; H, 8.78. Found: C, 67.47; H, 8.96.

2-(2-amino-phenylamino)-1-phenyl-ethanol (9)

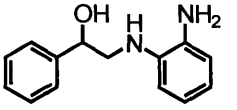

A screw-cap test tube was charged with CuI (5.0 mg, 0.025 mmol, 2.5 mol%), sodium hydroxide (80.0 mg, 2.0 mmol), 2-amino-1-phenylethanol (137 mg, 1.0 mmol), and 2-iodoaniline (263 mg, 1.2 mmol). The test tube was fitted with a septum and purged with nitrogen before adding isopropanol (1.0 mL). The test tube was then capped and stirred in an oil bath at 90 °C for 14.5 h. The resulting mixture was cooled to room temperature and diluted with EtOAc (10 mL). This mixture was washed with water (2 x 5 mL), dried over $MgSO_4$, and concentrated in vacuo. Flash chromatography of the crude product (CH_2Cl_2:EtOAc, 75:25) provided a dark yellow solid that was recrystallized from hexanes/EtOAc to yield 143.7 mg (63%) of the title compound as fibrous, light brown crystals. ^1H NMR (300 MHz, $CDCl_3$): δ 3.19 (broad s, 4H), 3.30 (dd, J = 12.9, 8.8 Hz, 1H), 3.41 (dd, J = 12.4, 3.3 Hz, 1H), 4.95 (dd, J = 8.8, 3.6 Hz, 1H), 6.71 (m, 3H), 6.79 (m, 1H), 7.36 (m, 5H). ^{13}C NMR (125 MHz, $CDCl_3$): δ 52.0, 72.3, 112.6, 116.7, 119.4, 120.6, 125.8, 127.9, 128.6, 134.7, 136.9, 142.0. IR ($CDCl_3$, cm^{-1}): 3415, 3053, 1625, 1598, 1509, 1455, 1059. Anal. Calcd. for $C_{14}H_{16}N_2O$: C, 73.66; H, 7.06. Found: C, 73.55; H, 6.93.

2-(3-nitro-phenylamino)-1-phenyl-ethanol (10)

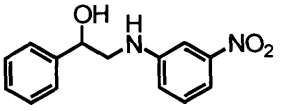

A screw-cap test tube was charged with CuI (5.0 mg, 0.025 mmol, 2.5 mol%), potassium phosphate (425.0 mg, 2.0 mmol), 2-amino-1-phenylethanol (165 mg, 1.2 mmol), ethylene glycol (56 μL, 1.0 mmol), and 3-nitro-1-iodobenzene (249 mg, 1.0 mmol). The test tube was fitted with a septum and purged with nitrogen before adding isopropanol (1.1 mL). Next, the test tube was capped and stirred in an oil bath at 75 °C for 16 h. The resulting mixture was cooled to room temperature and diluted with H_2O (10 mL). The reaction mixture was then extracted with methylene chloride (3 x 10 mL). The organic layers were washed with brine (1 x 10 mL), dried over $MgSO_4$, and concentrated in vacuo. Flash chromatography of the crude product (CH_2Cl_2:EtOAc, 95:5) provided 188.1 mg (73%) of the title compound as an orange oil. For reaction 1b, the conditions above were modified as follows: 2-amino-1-phenylethanol (137 mg, 1.0 mmol) and 3-nitro-1-iodobenzene (299 mg, 1.2 mmol). ^1H NMR (300 MHz, $CDCl_3$): δ 2.95 (broad s, 1H), 3.28 (ddd, J = 13.1, 8.5, 4.9 Hz, 1H), 3.38 (ddd, J = 12.8, 7.0, 4.0 Hz, 1H), 4.52 (dd, J = 6.6, 4.9 Hz, 1H), 4.88 (dd, J = 8.6, 4.0 Hz), 6.85 (ddd, J = 8.0, 2.2, 0.5 Hz, 1H), 7.22 (t, J = 8.0 Hz, 1H), 7.31 (m, 1H), 7.34 (m, 1H), 7.36 (m, 4H), 7.47 (app ddd, J = 8.0, 2.2, 0.8 Hz, 1H). ^{13}C NMR (125 MHz, $CDCl_3$): δ 52.0, 72.3, 112.6, 116.7, 119.4, 120.6, 125.8, 127.9, 128.6, 134.7, 136.9, 142.0. IR ($CDCl_3$, cm^{-1}): 3415, 3053, 1625, 1598, 1509, 1455, 1059. Anal. Calcd. for $C_{14}H_{14}N_2O_3$: C, 73.66; H, 7.06. Found: C, 73.55; H, 6.93.

(*1R,2S*)-2-(3-Hydroxymethyl-phenylamino)-1-phenyl-propan-1-ol (11)

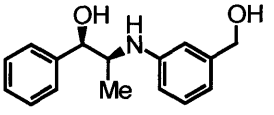

A screw-cap test tube was charged with CuI (5.0 mg, 0.025 mmol, 2.5 mol%), potassium phosphate (425.0 mg, 2.0 mmol), (*1R, 2S*)-norephedrine (151 mg, 1.0 mmol), ethylene glycol (56 μL, 1.0 mmol), and 3-iodobenzyl alcohol (152 μL, 1.2 mmol). The test tube was fitted with a septum and purged with nitrogen before adding isopropanol (1.1 mL). Next, the test tube was capped and stirred in an oil bath at 80 °C for 16.5 h. The resulting mixture was cooled to room temperature and diluted with H_2O (10 mL). The reaction mixture was then extracted with methylene chloride (3 x 10 mL). The organic layers

were washed with brine (1 x 10 mL), dried over $MgSO_4$, and concentrated in vacuo. Flash chromatography of the crude product (CH_2Cl_2:EtOAc, 60:40) provided 195.6 mg (76 %) of the title compound as a clear oil. ^1H NMR (300 MHz, $CDCl_3$): δ 0.98 (d, J = 6.6 Hz, 3H), 3.20 (broad s, 1H), 3.50 (broad s, 2H), 3.74 (dq, J = 6.6, 3.0 Hz, 1H), 4.55 (s, 2H), 4.94 (d, J = 2.8 Hz, 1H), 6.56 (ddd, J = 8.0, 2.4, 0.8 Hz, 1H), 6.64 (m, 2H), 7.14 (t, J = 8.0 Hz, 1H), 7.28 (m, 5H). ^{13}C NMR (75 MHz, $CDCl_3$): δ 13.6, 55.1, 65.2, 73.9, 113.2, 113.6, 117.2, 125.7, 127.2, 128.1, 129.4, 141.1, 142.2, 146.1. IR ($CDCl_3$, cm^{-1}): 3589, 3396, 3054, 2979, 2877, 1607, 1488, 1266. Anal. Calcd. for $C_{16}H_{19}NO_2$: C, 74.68; H, 7.44. Found: C, 74.80; H, 7.29. $[\alpha]^{20}_D$ +69.2 ($CHCl_3$, c 1.15).

(*S*)-1-[3-(1-hydroxymethyl-2-methyl-propylamino)-phenyl]-ethanone (12)

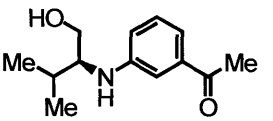

A screw-cap test tube was charged with CuI (5.0 mg, 0.025 mmol, 2.5 mol%), potassium phosphate (425.0 mg, 2.0 mmol), (*S*)-valinol (134 μL, 1.2 mmol), ethylene glycol (56 μL, 1.0 mmol), and 3-iodobenzophenone (246 mg, 1.0 mmol). The test tube was fitted with a septum and purged with nitrogen before adding isopropanol (1.1 mL). Next, the test tube was capped and stirred in an oil bath at 75 °C for 16.5 h. The resulting mixture was cooled to room temperature and diluted with H_2O (2 mL) and methylene chloride (5 mL). The organic layer was washed with brine (1 x 5 mL), dried over $MgSO_4$, and concentrated in vacuo. Flash chromatography of the crude product (CH_2Cl_2:EtOAc, 80:20) provided 165.0 mg (75%) of the title compound as a yellow oil. ^1H NMR (300 MHz, $CDCl_3$): δ 0.96 (d, J = 6.9 Hz, 3H), 0.98 (d, J = 6.9 Hz, 3H), 1.83 (dsept, J = 6.9, 6.8 Hz, 1H), 2.39 (dd, J = 6.9, 4.5 Hz, 1H), 2.50 (s, 3H), 3.22 (m, 1H), 3.57 (ddd, J = 10.1, 6.3, 3.9 Hz, 1H), 3.74 (ddd, J = 11.0, 6.9, 4.1 Hz, 1H), 3.89 (d, J = 6.6 Hz, 1H), 6.83 (m, 1H), 7.21 (m, 3H). ^{13}C NMR (75 MHz, $CDCl_3$): δ 19.1, 19.3, 26.8, 30.1, 60.6, 62.5, 112.0, 117.7, 118.0, 129.3, 137.9, 148.5, 198.6. IR ($CDCl_3$, cm^{-1}): 3427, 2964, 2877, 1677, 1602, 1358. Anal. Calcd. for $C_{13}H_{19}NO_2$: C, 70.56; H, 8.65. Found: C, 70.28; H, 8.50. Chiral chromatography: ambient temperature, hexanes:*i*-PrOH (98.5:1.5), 1.75 mL/min, $t_{(S)}$ = 18.7 min, $t_{(R)}$ = 25.7 min. $[\alpha]^{20}_D$ –44.7 ($CHCl_3$, c 1.48).

(*1S,2R*)-methyl-(1-methyl-2-phenoxy-2-phenyl-ethyl)-amine (13)

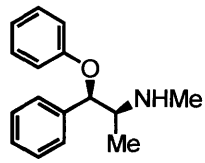

A screwcap test tube was charged with CuI (10.0 mg, 0.05 mmol, 5 mol%), cesium carbonate (652.0 mg, 2.0 mmol), (*1R, 2S*)-ephedrine (165 mg, 1.0 mmol), and iodobenzene (168 μL, 1.5 mmol). The test tube was fitted with a septum and purged with nitrogen before adding butyronitrile (1.0 mL). Next, the test tube was capped and stirred in an oil bath at 125 °C for 25 h. The reaction mixture was cooled to room temperature and filtered, washing well with EtOAc. The filtrate was concentrated to yield a yellow oil that was taken up in a few drops of Et_2O and added to 5 mL of 0.24 M HCl contained in a fritted glass Buchner funnel. A solid immediately precipitated and the aqueous solution was removed by vacuum filtration. The filter cake was washed with water (5 mL) and then hexanes. The title compound was obtained as a white solid (206.1 mg, 74%). The ^{13}C NMR spectrum was obtained using the free base. ^1H NMR (300 MHz, d_6-DMSO): δ 1.16 (d, J = 6.7 Hz, 3H), 2.63 (s, 3H), 3.58 (m, 1H), 5.91 (d, J = 2.2 Hz, 1H), 6.91 (m, 3H), 7.23 (m, 2H), 7.34 (m, 5H), 9.27 (broad s, 2H). ^{13}C NMR (75 MHz, $CDCl_3$): δ 14.8, 34.0, 60.3, 81.3, 115.6, 120.6, 126.4, 127.4, 128.3, 129.1, 139.2, 158.0. IR (solid HCl salt, cm^{-1}): 2983, 2836, 2765, 2721, 1596, 1495, 1241, 1179, 1005, 747, 704. Melting point > 260 °C. Anal. Calcd. for $C_{16}H_{20}NO_2Cl$: C, 69.18; H, 7.26. Found: C, 68.99; H, 7.34. $[\alpha]^{20}_D$ +21.4 (DMSO, c 0.35).

(*1S,2R*)-1-methyl-2-phenoxy-2-phenyl-ethylamine (14)

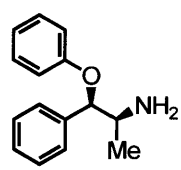

A screw-cap test tube was charged with CuI (10.0 mg, 0.05 mmol, 5 mol%), cesium carbonate (652.0 mg, 2.0 mmol), (*1R, 2S*)-norephedrine (151 mg, 1.0 mmol), and iodobenzene (134 μL, 1.2 mmol). The test tube was fitted with a septum and purged with nitrogen before adding butyronitrile (1.0 mL). Next, the test tube was capped and stirred in an oil bath at 125 °C for 14 h. The reaction mixture was cooled to room temperature and filtered. The filtrate was concentrated and the resulting oil was taken up in 10 mL of methylene chloride. A solution of HCl in Et_2O (1.0 M, 1 mL) was

added and the resulting precipitate was collected by filtration to yield 140.1 mg (53%) of the title compound as a white solid. NMR spectra were taken using the HCl salt. ^{1}H NMR (300 MHz, d_6-DMSO): δ 1.14 (d, J = 6.7 Hz, 3H), 3.61 (broad s, 1H), 5.73 (d, J = 3.1 Hz, 1H), 6.91 (t, J = 8.2 Hz, 1H), 6.91 (dd, J = 8.4 Hz, 2H), 7.22 (dd, J = 8.4, 7.3 Hz, 2H), 7.34 (m, 5H), 8.50 (broad s, 3H). ^{13}C NMR (75 MHz, d_6-DMSO): δ 12.0, 51.1, 78.1, 116.1, 121.4, 126.4, 128.2, 128.7, 136.6, 157.0. IR (solid HCl salt, cm^{-1}): 3033, 2939, 2827, 1598, 1492, 1237, 1036, 980, 745, 700, 691. Melting point: 248 – 250 °C. High resolution mass spectrum: 227.1309 (M+), 183.0807, 134.0966, 115.0543. $[\alpha]^{20}_D$ – 34.4 (H_2O, c 0.47).

(*1R,2S*)-1-[3-(2-methylamino-1-phenyl-propoxy)-phenyl]-ethanone (15)

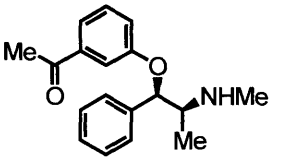

A screw-cap test tube was charged with CuI (10.0 mg, 0.05 mmol, 5 mol%), cesium carbonate (652.0 mg, 2.0 mmol), (*1R, 2S*)-ephedrine (165 mg, 1.0 mmol), and 3-iodoacetophenone (295 mg, 1.2 mmol). The test tube was fitted with a septum and purged with nitrogen before adding butyronitrile (1.0 mL). Next, the test tube was capped and stirred in an oil bath at 125 °C for 21 h. The reaction mixture was cooled to room temperature and filtered, washing well with ethyl acetate. The filtrate (25 mL) was washed with 3 M HCl (3 x 10 mL) and the acid extracts were washed with CH_2Cl_2 (4 x 10 mL). The organic layers were dried over $MgSO_4$, filtered, and concentrated to provide a yellow solid that was triturated in Et_2O. The yellow solid was collected by vacuum filtration and the filter cake was washed with ethyl acetate (1 x 3 mL) and Et_2O to provide 167.7 mg (52 %) of the title compound as an off-white solid. NMR spectra were taken using the HCl salt. ^{1}H NMR (300 MHz, $CDCl_3$): δ 1.33 (d, J = 6.8 Hz, 3H), 2.50 (s, 3H), 2.52 (s, 3H), 3.41 (m, 1H), 5.92 (d, J = 2.4 Hz, 1H), 7.09 (ddd, J = 8.2, 2.5, 1.0 Hz, 2H), 7.18 (t, J = 8.1 Hz, 1H), 7.32 (m, 5H), 7.43 (dt, J = 7.5, 1.2 Hz, 1H), 7.58 (t, J = 2.1 Hz, 1H). ^{13}C NMR (75 MHz, $CDCl_3$): δ 9.5, 26.9, 30.1, 31.0, 59.4, 116.2, 120.2, 121.3, 126.0, 128.5, 128.9, 129.5, 135.4, 138.1, 156.5, 197.5. IR (solid HCl salt, cm^{-1}): 2964, 2715, 1679, 1578, 1445, 1270, 1208, 1007, 745, 702. Melting point: 178 – 179 °C.

Anal. Calcd for $C_{18}H_{22}NO_2Cl$: C, 67.60, H, 6.93. Found: C, 67.36, H, 6.78. $[\alpha]^{20}_D$ +58.1 ($CHCl_3$, c 0.43).

(*R*)-2-(3,5-dimethyl-phenoxy)-1-phenylethylamine (16)

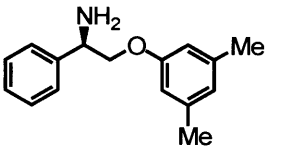

A screw-cap test tube was charged with CuI (10.0 mg, 0.05 mmol, 5 mol%), cesium carbonate (652.0 mg, 2.0 mmol), (*R*)-phenylglycinol (137 mg, 1.0 mmol), and 3,5-dimethyl-1-iodobenzene (173 μL, 1.2 mmol). The test tube was fitted with a septum and purged with nitrogen before adding butyronitrile (1.0 mL). Next, the test tube was capped and stirred in an oil bath at 125 °C for 14 h. The reaction mixture was cooled and filtered. The filtrate was concentrated in vacuo and the oil obtained was taken up in ethyl acetate (8 mL). To this solution was added 1 mL of HCl in Et_2O (1.0 M). The white precipitate that formed was collected by filtration and the filter cake was washed with hexanes. A volume of hexanes (15 mL) was added to the mother liquor and the solution was allowed to stand overnight. A second crop of white precipitate formed and was added to the first crop. The title compound was obtained as a white solid (130.0 mg, 47%). NMR spectra were taken using the HCl salt. ^{1}H NMR (500 MHz, $CDCl_3$): δ 2.22 (s, 3H), 4.06 (dd, J = 9.8, 4.1 Hz, 1H), 4.15 (broad s, 1H), 4.38 (t, J = 8.9 Hz, 1H), 6.62 (s, 1H), 6.68 (s, 2H), 7.19 (t, J = 7.0 Hz, 2H), 7.26 (t, J = 7.6, 1H), 7.36 (d, J = 7.3 Hz, 2H). ^{13}C NMR (125 MHz, $CDCl_3$): δ 21.4, 55.0, 68.0, 112.5, 123.2, 127.5, 129.0, 129.1, 133.0, 139.3, 157.8. IR (solid HCl salt, cm^{-1}): 3033, 2941, 2838, 1598, 1492, 1237, 1036, 980, 745, 700, 691. Melting point: 229 – 230 °C. High resolution mass spectrum: 241.1462 (M+), 120.0808, 106.0648. $[\alpha]^{20}_D$ –42.0 (H_2O, c 0.49). Chiral chromatography: ambient temperature, hexanes:EtOAc (75:25), 1.75 mL/min, $t_{(R)}$ = 8.75 min, $t_{(R)}$ = 17.4 min.

[2-(2,6-dimethylphenoxy)-ethyl]-ethylamine (17)

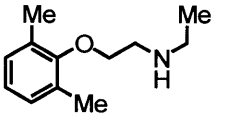

A screw-cap test tube was charged with CuI (10.0 mg, 0.05 mmol, 5 mol%), cesium carbonate (652.0 mg, 2.0 mmol), 2-(ethylamino)ethanol (195 μL, 2.0 mmol), and 2,6-dimethyl-1-iodobenzene (140 μL, 1.0 mmol). The test tube was fitted with a septum and

purged with nitrogen before adding butyronitrile (1.0 mL). Next, the test tube was capped and stirred in an oil bath at 125 °C for 30 h. The reaction mixture was cooled to room temperature, transferred to a separatory funnel, and diluted with ethyl acetate to a volume of approximately 25 mL. The mixture was washed with water (2 x 5 mL), dried over $MgSO_4$, filtered, and concentrated. The oil obtained was taken up in 8 mL Et_2O and 1 mL of HCl in Et_2O (1.0 M) was added. The resulting precipitate was collected by filtration, washed with 16 mL Et_2O, washed with 3 mL acetone, and washed again with 16 mL Et_2O. Approximately 15 mL of Et_2O were then added to the mother liquor and a second crop of white precipitate formed upon standing. The two crops were combined to provide 163.6 mg (72%) of the title compound as a white solid. NMR spectra were taken using the free base. ^{1}H NMR (300 MHz, $CDCl_3$): δ 1.18, (t, J = 7.2 Hz, 3H), 1.85 (broad s, 1H), 2.28 (s, 3H), 2.76 (q, J = 7.2 Hz, 2H), 3.01 (t, J = 5.2 Hz, 2H), 3.89 (t, J = 5.2 Hz, 2H), 6.89 (dd, J = 8.3, 6.3 Hz, 1H), 6.98 (d, J = 7.1 Hz, 2H). ^{13}C NMR (75 MHz, $CDCl_3$): δ 15.4, 16.3, 44.2, 49.8, 71.1, 123.8, 128.6, 130.7, 155.4. IR (solid HCl salt, cm^{-1}): 2943, 2786, 2750, 2726, 2472, 1457, 1262, 1204, 1030, 760. Melting point: 170 – 171 °C. Anal. Calcd for $C_{12}H_{20}NOCl$: C, 62.73, H, 8.77. Found: C, 62.73, H, 9.01.

Ethyl-[2-(3-nitrophenoxy)-ethyl]-amine (18)

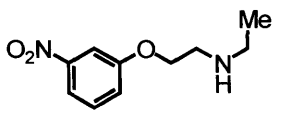

A screw-cap test tube was charged with CuI (10.0 mg, 0.05 mmol, 5 mol%), cesium carbonate (652.0 mg, 2.0 mmol), 2-(ethylamino)ethanol (195 μL, 2.0 mmol), and 3-nitro-1-iodobenzene (249 mg, 1.0 mmol). The test tube was fitted with a septum and purged with nitrogen before adding butyronitrile (1.0 mL). Next, the test tube was capped and stirred in an oil bath at 125 °C for 21 h. The reaction mixture was cooled to room temperature, filtered, and concentrated. The concentrate was taken up in 10 mL of methylene chloride and washed with water (2 x 5 mL). The organic layers were dried over $MgSO_4$, filtered, and concentrated to yield dark oil. The oil was taken up in acetone and 1 mL of HCl in Et_2O (1.0 M) was added. The resulting precipitate was collected by filtration and washed well with Et_2O, EtOAc (5 mL), and Et_2O again. The title compound was obtained as a brown solid (132.7 mg, 54%). NMR spectra were taken using the HCl salt. ^{1}H NMR (300 MHz, $CDCl_3$): δ 1.45 (t, J = 7.2 Hz, 3H), 3.15 (q, J =

5.5 Hz, 2H), 3.38 (t, J = 5.1 Hz, 2H), 4.46 (t, J = 5.1 Hz, 2H), 7.34 (ddd, J = 8.4, 2.2, 1.1 Hz, 1 H), 7.41 (t, J = 8.0 Hz, 1H), 7.72 (t, J = 2.2 Hz, 1H), 7.82 (ddd, J = 8.0, 1.9, 1.0 Hz, 1H). ^{13}C NMR (75 MHz, $CDCl_3$): δ 11.3, 43.3, 45.6, 63.5, 108.9, 116.7, 121.8, 130.1, 148.8, 157.7. IR (solid HCl salt, cm^{-1}): 2954, 2794, 2738, 2686, 2503, 1526, 1355, 1258, 1038, 799, 735, 675. Melting point: 155 – 156 °C. Anal. Calcd. for $C_{10}H_{15}N_2O_3Cl$: C, 48.69, H, 6.13. Found: C, 48.45, H, 6.09.

Synthesis of the acetyl derivative of 2-(3,5-dimethyl-phenoxy)-1-phenyl-ethylamine.

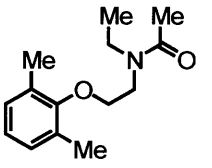

A round bottom flask was charged with the hydrochloride salt of 2-(3,5-dimethyl phenoxy)-1-phenyl-ethylamine and dissolved in methylene chloride. Excess triethylamine and acetic anhydride were added and the reaction was stirred at room temperature overnight. The reaction was quenched by addition of a solution of saturated bicarbonate equal to the reaction volume. After stirring for a half hour the contents of the flask were transferred to a separatory funnel and the organic layer was washed with equal volumes of a saturated sodium bicarbonate solution (2×) and then with equal volumes of water (2x). The organic layer was dried over $MgSO_4$, filtered, and concentrated to yield a white solid that was recrystallized from hexanes and ethyl acetate. ^1H NMR (500 MHz, $CDCl_3$): δ 2.03 (s, 3H), 2.26 (s, 6H), 4.18 (dd, J = 9.5, 4.3 Hz, 1H), 4.22 (dd, J = 9.6, 4.6 Hz, 1H), 5.37 (dt, J = 7.9, 3.9 Hz, 1H), 6.25 (d, J = 7.9 Hz, 1H), 6.51 (s, 2H), 6.60 (s, 1H), 7.27 (tt, J = 7.2, 1.4 Hz, 1H), 7.33 (t, J = 7.2 Hz, 2H), 7.38 (d, J = 7.3 Hz, 2H). ^{13}C NMR (125 MHz, $CDCl_3$): δ 21.4, 23.4, 52.3, 69.7, 112.2, 123.0, 127.0, 127.7, 128.1, 139.3, 139.4, 158.3, 169.5. IR (solid, cm^{-1}): 3284, 3068, 2923, 1632, 1542, 1297, 1169, 1075, 832, 695. Melting point: 120 – 122 °C. Anal. Calcd. for $C_{18}H_{21}NO_2$: C, 76.30; H, 7.47. Found: C, 76.34; H, 7.44.

5.3 Selected ^{1}H NMR Spectra

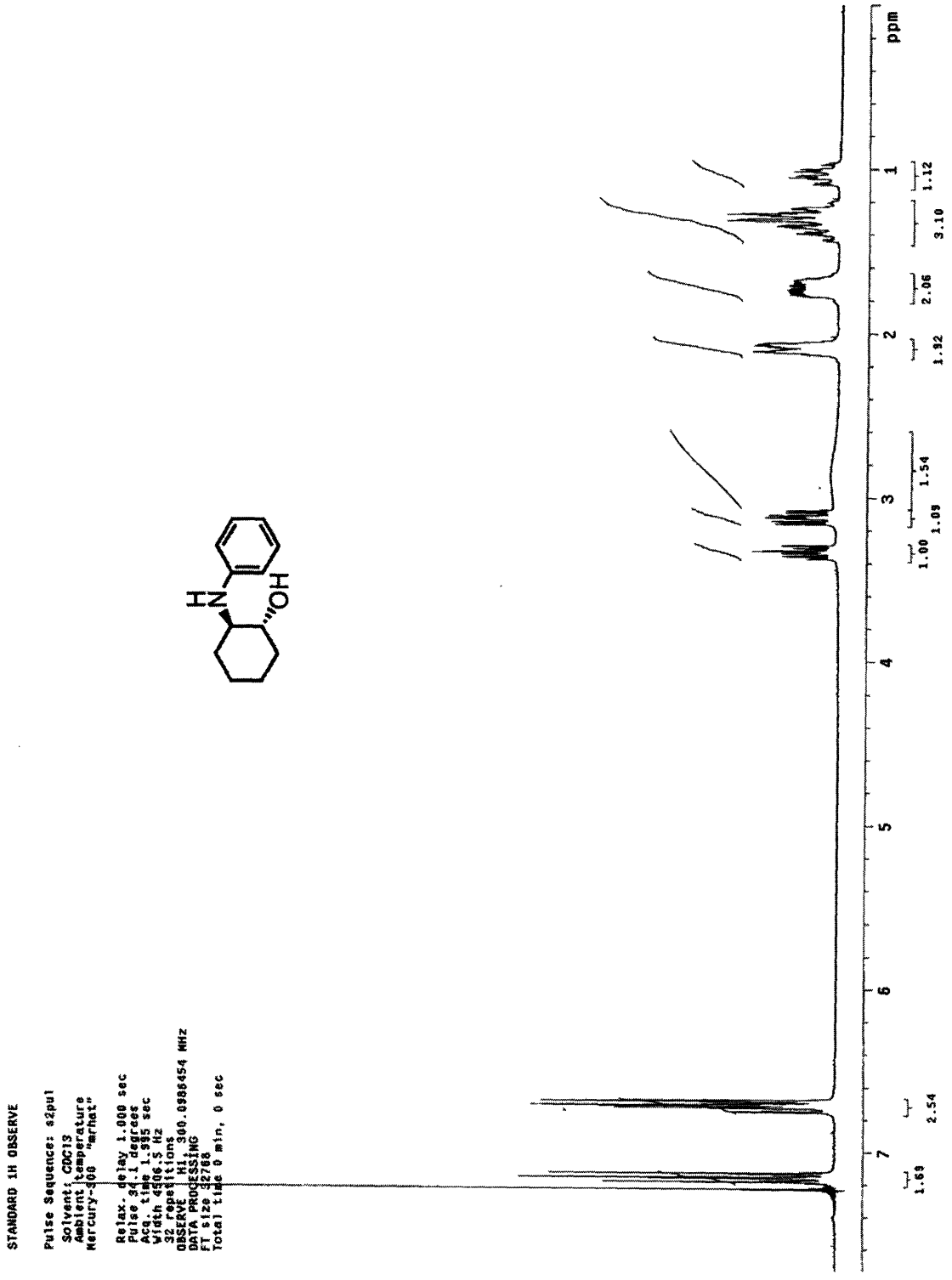

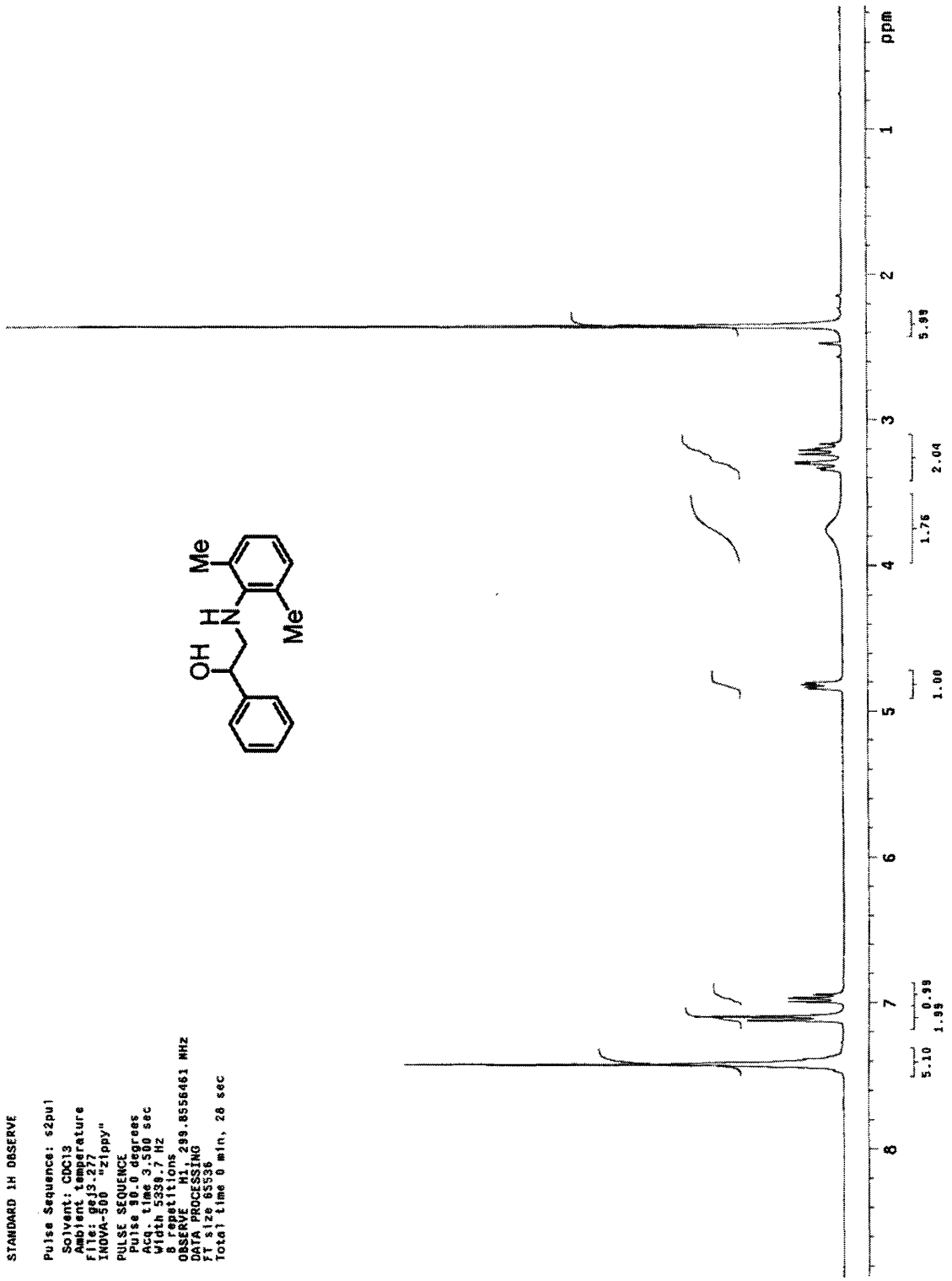
STANDARD 1H OBSERVE
Pulse Sequence: s2pul
Solvent: CDCl3
Ambient temperature
File: gej3-277
INOVA-500 "zippy"
PULSE SEQUENCE
Pulse 90.0 degrees
Acq. time 3.500 sec
Width 5330.7 Hz
8 repetitions
OBSERVE H1, 299.8556461 MHz
DATA PROCESSING
FT size 65536
Total time 0 min, 28 sec
Me
H
N
OH
Me
ppm
1
2
3
4
5
6
7
8
5.99
2.04
1.76
1.00
0.99
1.99
5.10

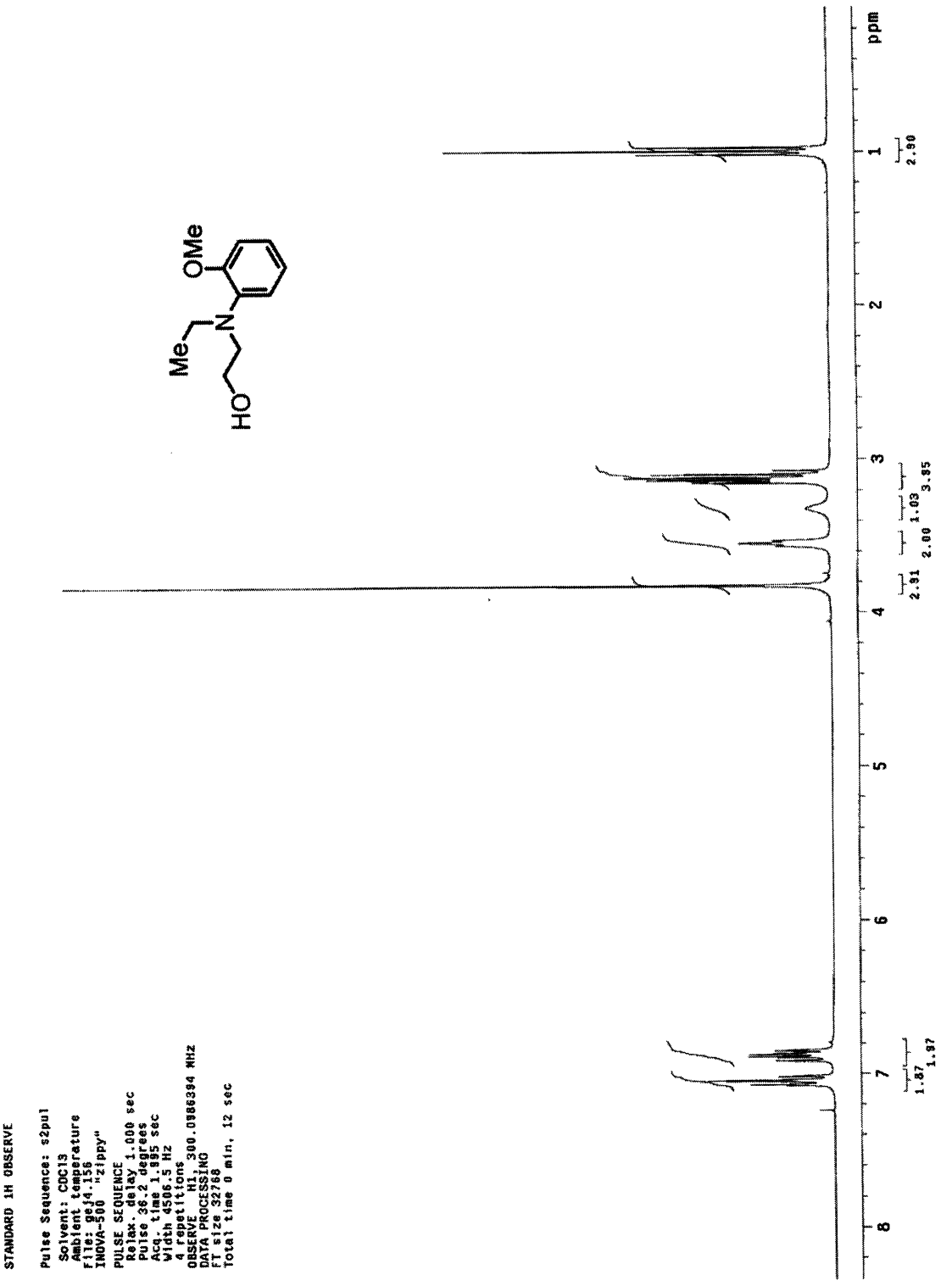
STANDARD 1H OBSERVE
Pulse Sequence: s2pul
Solvent: CDCl3
Ambient temperature
File: gej4.156
INOVA-500 "zippy"
PULSE SEQUENCE
Relax. delay 1.000 sec
Pulse 30.2 degrees
Acq. time 1.895 sec
Width 4506.5 Hz
4 repetitions
OBSERVE H1, 300.0886394 MHz
DATA PROCESSING
FT size 32768
Total time 0 min, 12 sec
OMe
Me
N
HO
ppm
1
2
3
4
5
6
7
8
2.90
2.91
2.00
1.03
3.05
1.87
1.97

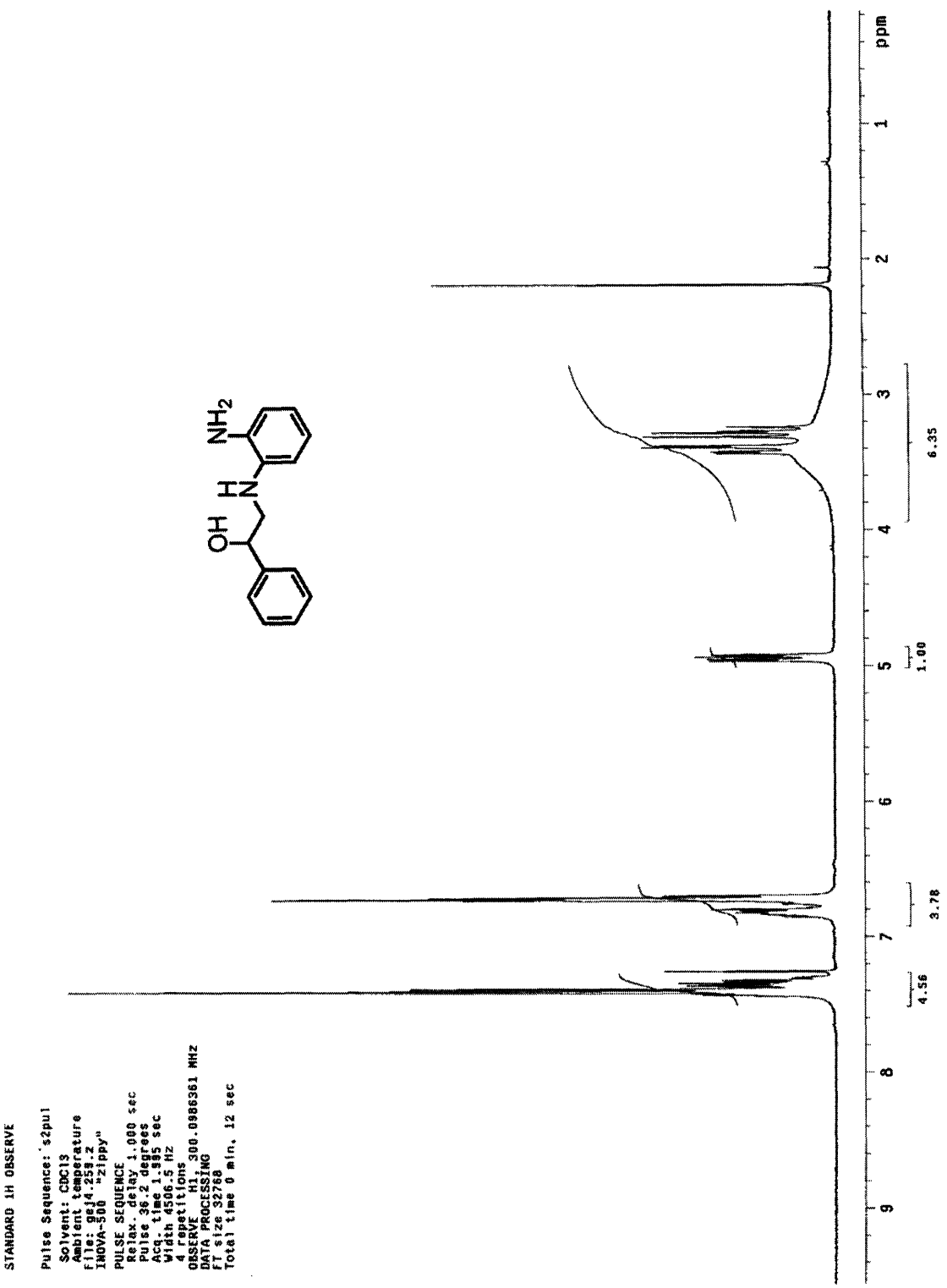
STANDARD 1H OBSERVE
Pulse Sequence: s2pul
Solvent: CDCl3
Ambient temperature
File: gaj4.25a.z
INOVA-500 "zippy"
PULSE SEQUENCE
Relax. delay 1.000 sec
Pulse 36.2 degrees
Acq. time 1.995 sec
Width 4506.5 Hz
4 repetitions
OBSERVE H1, 300.0986361 MHz
DATA PROCESSING
FT size 32768
Total time 0 min, 12 sec
NH2
H N
OH
ppm
1
2
3
4
5
6
7
8
9
6.35
1.00
3.78
4.56

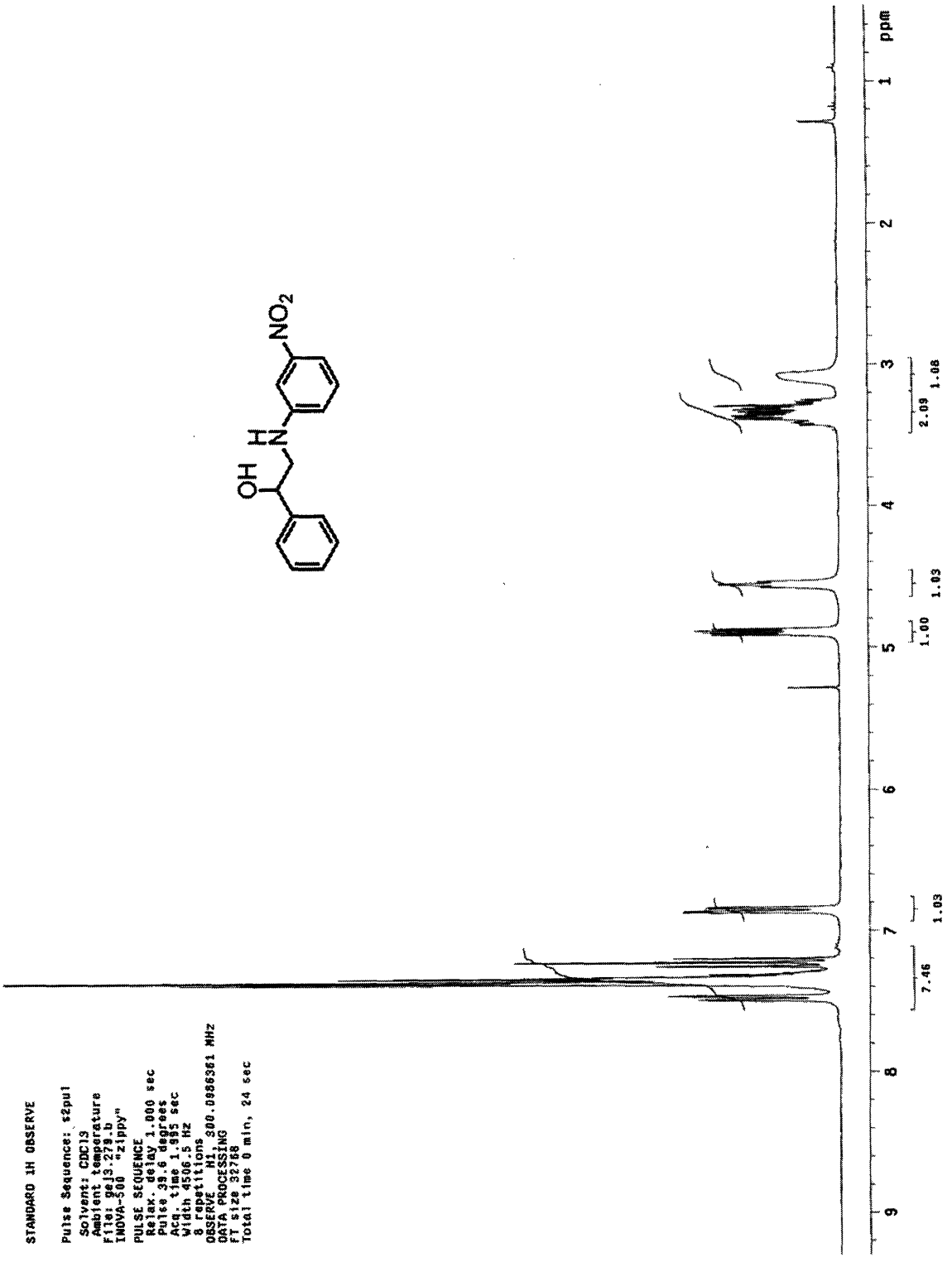
STANDARD 1H OBSERVE
Pulse Sequence: s2pul
Solvent: CDCl3
Ambient temperature
File: gej3.27a.b
INOVA-500 "zippy"
PULSE SEQUENCE
Relax. delay 1.000 sec
Pulse 38.6 degrees
Acq. time 1.995 sec
Width 4506.5 Hz
8 repetitions
OBSERVE H1, 500.0986361 MHz
DATA PROCESSING
FT size 32768
Total time 0 min, 24 sec
NO2
H
N
OH
ppm
7.46
1.03
1.00
1.03
2.09
1.08

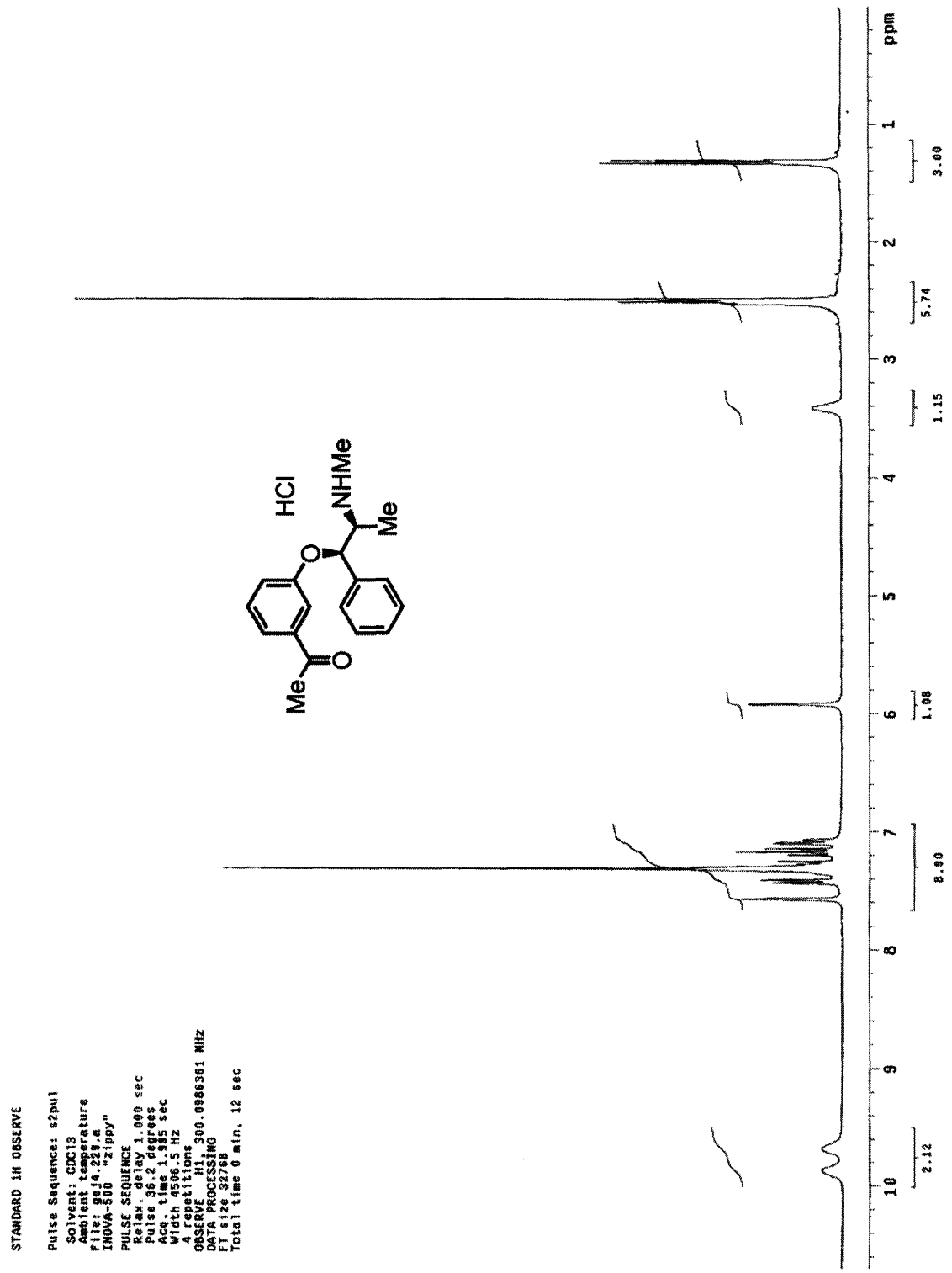
STANDARD 1H OBSERVE
Pulse Sequence: s2pul
Solvent: CDCl3
Ambient temperature
File: gaj4.228.a
INOVA-500 "zippy"
PULSE SEQUENCE
Relax. delay 1.000 sec
Pulse 36.2 degrees
Acq. time 1.385 sec
Width 4506.5 Hz
4 repetitions
OBSERVE H1, 300.0986361 MHz
DATA PROCESSING
FT size 32768
Total time 0 min, 12 sec
HCl
NHMe
Me
Me
O
O
ppm
2.12
8.90
1.08
1.15
5.74
3.00

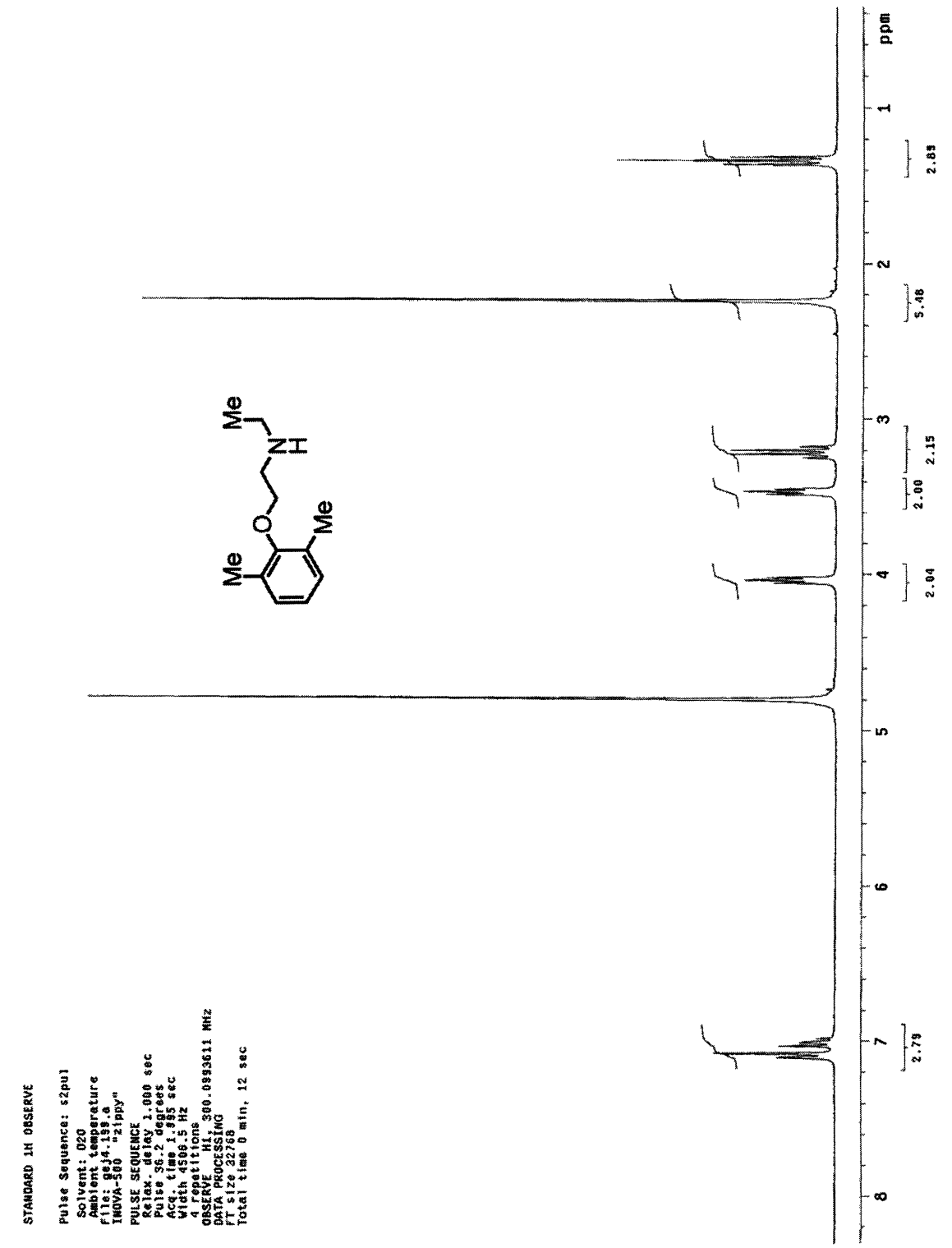
STANDARD 1H OBSERVE
Pulse Sequence: s2pul
Solvent: CDCl3
Ambient temperature
File: gaj4.139.a
INOVA-500 "zippy"
PULSE SEQUENCE
Relax. delay 1.000 sec
Pulse 36.2 degrees
Acq. time 1.995 sec
Width 4509.5 Hz
4 repetitions
OBSERVE H1, 300.0993611 MHz
DATA PROCESSING
FT size 32768
Total time 0 min, 12 sec
Me
N
H
O
Me
Me
ppm
2.79
2.04
2.00
2.15
5.48
2.89

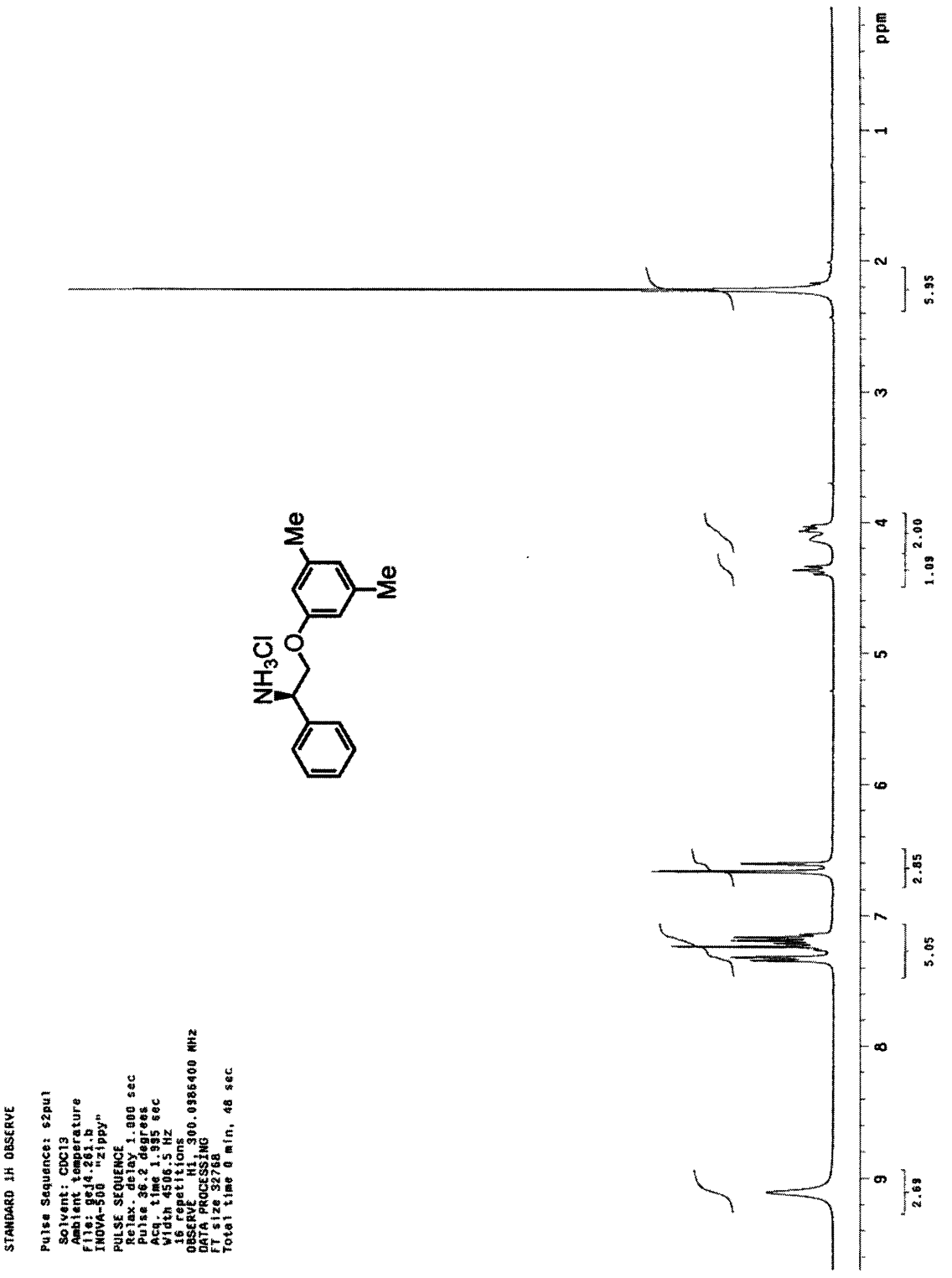
STANDARD 1H OBSERVE
Pulse Sequence: s2pul
Solvent: CDCl3
Ambient temperature
File: gej4.261.b
INOVA-500 "zippy"
PULSE SEQUENCE
Relax. delay 1.000 sec
Pulse 36.2 degrees
Acq. time 1.995 sec
Width 4506.5 Hz
16 repetitions
OBSERVE H1, 300.0386400 MHz
DATA PROCESSING
FT size 32768
Total time 0 min, 48 sec
NH3Cl
O
Me
Me
ppm
2.69
5.05
2.85
1.09
2.00
5.95

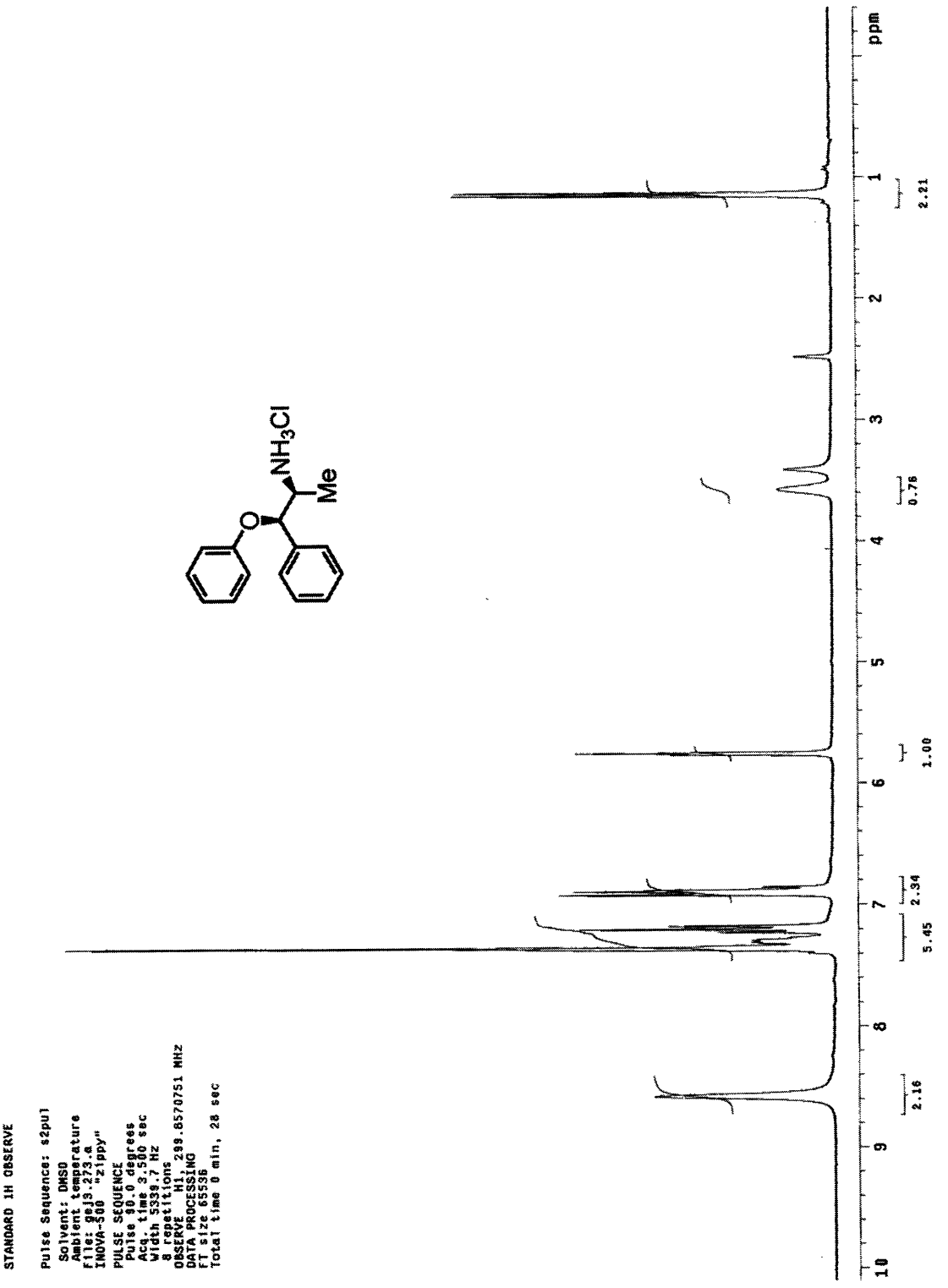
STANDARD 1H OBSERVE
Pulse Sequence: s2pul
Solvent: DMSO
Ambient temperature
File: gej3.273.a
INOVA-500 "zippy"
PULSE SEQUENCE
Pulse 90.0 degrees
Acq. time 3.500 sec
Width 5339.7 Hz
8 repetitions
OBSERVE H1, 299.8570751 MHz
DATA PROCESSING
FT size 65536
Total time 0 min, 28 sec
NH3Cl
Me
O
ppm
10
9
8
7
6
5
4
3
2
1
2.16
5.45
2.34
1.00
0.76
2.21

Chapter II. Helical Polyalanine Standards for CD Calibration

1. Introduction

1.1 Historical Overview

Proteins, composed mainly of twenty naturally occurring α-amino carboxylic acids, fulfill numerous disparate roles in a living body, ranging from structural elements to intercellular messengers to catalysts. Their construction from amino acids was demonstrated in the early nineteenth century by Braconnot who isolated glycine from gelatin hydrolysates.[1] That the individual amino acids in a protein are connected by amide bonds was not formally proposed until the beginning of the twentieth century by Fischer and Hofmeister.[2] Although Fischer correctly deduced the amide linkages, he held the conventional view of the time that proteins were variable collections of short polypeptides lacking uniform structure, similar to colloids. However, this notion was challenged by Svedberg's centrifugation experiments that demonstrated consistent particle sizes in native soluble protein extracts.[3]

Another method for structural analysis gaining popularity in the 1930's—X-ray diffraction—also provided evidence of protein structure. The diffraction pattern of keratin revealed a regular, periodic arrangement of atoms along the axis of this insoluble protein fiber. As the field of X-ray structure analysis grew, attention turned to crystalline proteins. Two ambitious practitioners, Bernal and Crowfoot, obtained a sharp diffraction pattern from crystalline pepsin, contrary to expectations.[4] At the time, the 3-dimensional diffraction data were too complex to be solved, and the simpler patterns from keratin would be interpreted first, thus providing a foothold for understanding the structure of proteins.

1.2. The α-Helix

An early study of wool keratin revealed two types of regular structures with

---

[1] Greenstein, J.P.; Winitz, M. *Chemistry of the Amino Acids*; Robert E. Krieger Publishing Co.: Malabar, FL, 1984; Vol.3, p. 1955.
[2] Greenstein, J.P.; Winitz, M. *Chemistry of the Amino Acids*; Robert E. Krieger Publishing Co.: Malabar, FL, 1984; Vol.2, p. 765.
[3] Svedberg, T. "A Discussion on the Protein Molecule" *Proc. R. Soc London.* **1939**, *A170*, 40–56.
[4] Bernal, J.D.; Crowfoot, D. "X-ray Photographs of Crystalline Pepsin" *Nature* **1934**, *794*, 133–34.

characteristic diffraction patterns.[5] The pattern obtained from natural wool fiber differed from the pattern obtained from the same fiber stretched under steam heat. These two forms were named α-keratin and β-keratin, respectively. The diffraction pattern of β-keratin was ascribed to alignment of the polypeptide chains in the fully extended conformation, thus forming hydrogen-bonded sheets.[6] In one of a series of landmark papers, Pauling provided an important revision, called the pleated β-sheet, which eliminated steric interference between residue side chains of adjacent strands.[7] However, Pauling's greatest contribution to protein chemistry—presented in the same series of papers—was the elucidation of a fundamental repeating structure for the poly-amino acids consistent with the diffraction pattern of α-keratin.

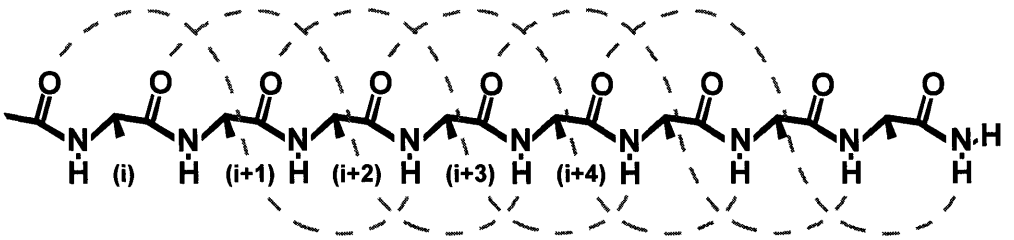

Figure 1: Hydrogen bonding pattern of the α-helix. The carbonyl oxygen of the *i*th residue forms a hydrogen bond with the amide proton of the (*i*+4)th residue.

What came to be known as the α-helix, corresponding to α-keratin, was conceived using simple hand-made models of amino acids.[8] The α-helix is characterized by an $i \rightarrow (i+4)$ hydrogen bond pattern (Figure 1); formation of each hydrogen bond creates a 13-member ring (Figure 2). An impediment to the discovery of the α-helix was the non-integral repeating unit of the helix. Previously, repeating structures with fundamental units containing integral numbers of amino acids had been sought,[9] owing to

[5] Astbury, W.T.; Woods, H.J. "The X-ray Interpretation of the Structure and Elastic Properties of Hair Keratin" *Nature* **1930**, *126*, 913.
[6] Huggins, M. L. "The Structure of Fibrous Proteins" *Chem. Rev.* **1943**, *32*, 195–218.
[7] Pauling, L.; Corey, R. B. "The Pleated Sheet, a New Layer Configuration of Polypeptide Chains" *Proc. Natl. Acad. Sci. USA.* **1951**, *37*, 251–256.
[8] Pauling, L.; Corey, R. B. "Atomic Coordinates and Structure Factors for Two Helical Configurations of Polypeptide Chains" *Proc. Natl. Acad. Sci. USA* **1951**, *37*, 235–240.
[9] Schulz, G.E.; Schirmer, R.H. *Principles of Protein Structure*; Springer-Verlag: New York, **1979**; p.69.

earlier work with X-ray crystallography of salts, the unit cells of which contain an integral number of the fundament unit. Pauling realized that the fundamental unit of the α-helix could be larger than a single helical turn; in his helix, a realignment of frame occurs every three turns, comprising 11 residues—in other words, 3.67 residues per turn.

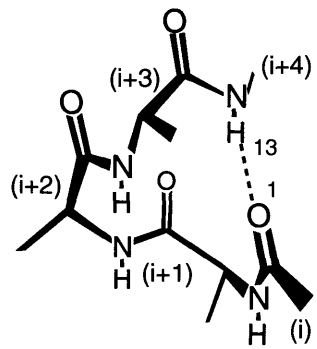

Figure 2: A single turn of an α-helix. Formation of the hydrogen bond creates a 13-member ring encompassing three residues between the two hydrogen bonded residues.

Although others had proposed helical structures for α-keratin,[10] Pauling rightly took into account the planar conformation of the amide group, which others had previously ignored, and used bond lengths calculated from X-ray diffraction studies of simple amino acid derivatives.[11] Additionally, Pauling was aware of intra-residue steric constraints. Some conformations of an amino acid residue are untenable because of steric strain, and any rationalization of secondary structure must account for the two rotational degrees of freedom in the backbone of each residue, the ϕ and ψ dihedral angles (Figure 3a). For Pauling's helix, these angles are $\phi = -47°$ and $\psi = -57°$ (Figure 3b). Ramachandran's diagram[12] (Figure 4) provides a way to visualize the available conformational space for an amino acid residue in a peptide chain. The large region in

[10] Bragg, L.; Kendrew, J.C.; Perutz, M.F. "Polypeptide Chain Configurations in Crystalline Proteins" *Proc. R. Soc. London, Ser. A.* **1950**, *203*, 321–357.
[11] Corey, R.B.; Donohue, J. "Interatomic Distances and Bond Angles in the Polypeptide Chain of Proteins" *J. Am. Chem. Soc.* **1950**, *72*, 2899–2900.
[12] Ramachandran, G.N.; Ramkrishnan, C.; Sasisekharan, V. "Stereochemistry of Polypeptide Chain Configurations" *J. Mol. Biol.* **1963**, *7*, 95–99.

the upper left quadrant contains ϕ,ψ combinations of extended and β-sheet conformations. The shaded ellipse in the third quadrant contains ϕ,ψ pairs near the ideal Corey–Pauling helical values, constrained by the relation $\phi + \psi = -103°$.[13]

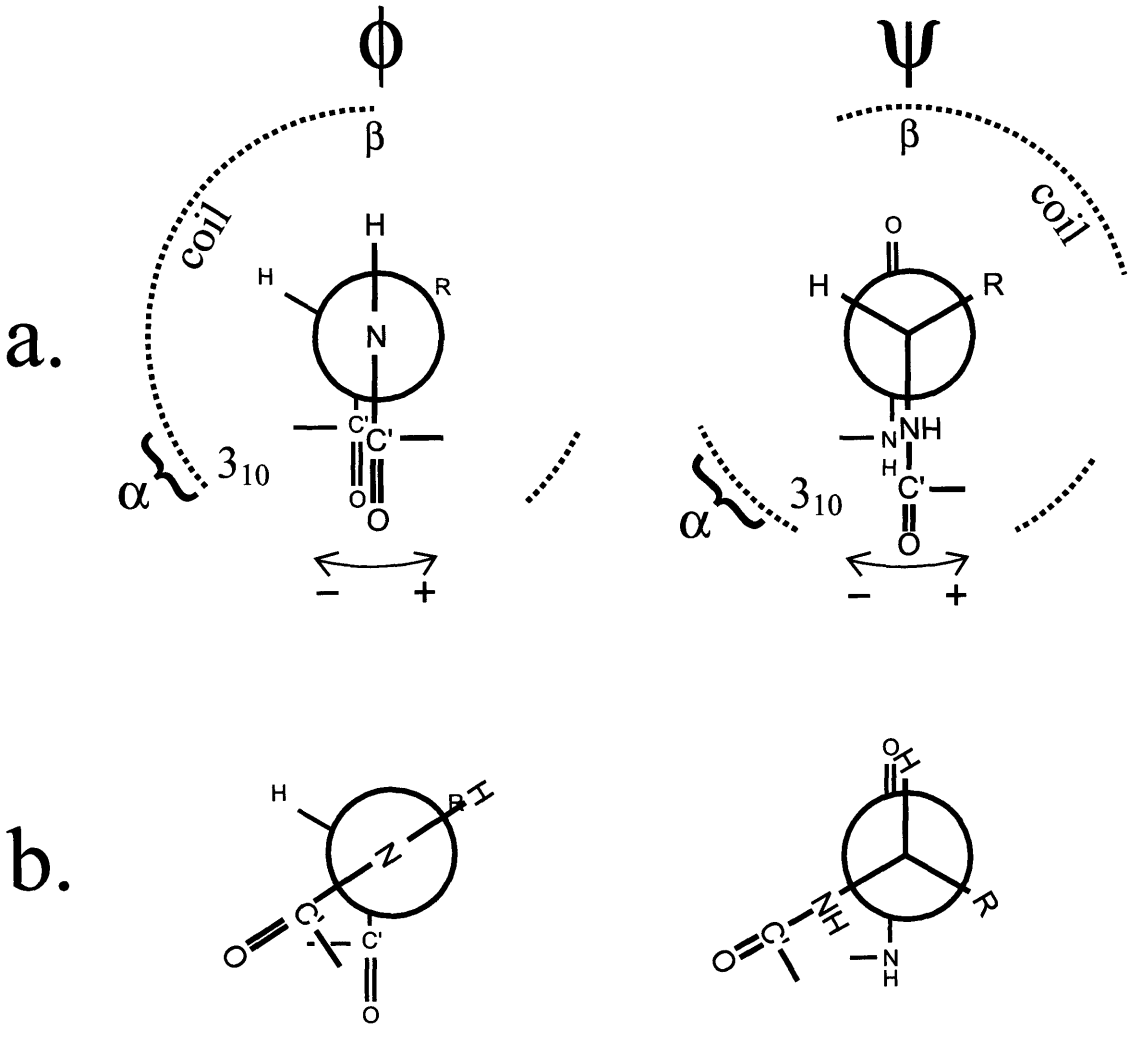

Figure 3: Newman projections for the ϕ and ψ angles of the peptide backbone. (a) Accessible regions with approximate indications for secondary structure. Both dihedral angles must fall in the indicated regions to attain helical and sheet structures. (b) Conformation of the α-helix; values for Pauling's helix are $\phi = -47°$ and $\psi = -57°$.

[13] Besley, N.A.; Hirst, J.D. "Theoretical Studies Toward Qunatitative Protein Circular Dichroism Calculations" *J. Am. Chem. Soc.* **1999**, *121*, 9636–9644.

It is worth a short digression to consider the helices that Pauling proposed and those he did not. In addition to the α-helix, Pauling debuted the left-handed γ-helix with an $i \rightarrow (i+5)$ hydrogen bonding pattern. The right-handed π-helix, with $i \rightarrow (i+5)$ hydrogen bonding, was absent from Pauling's papers, as was the right-handed 3_{10} helix, characterized by $i \rightarrow (i+3)$ hydrogen bonding. Pauling did evaluate the 3_{10} helix later, but rejected it on energetic grounds; the π-helix was not mentioned at all. In any event, the 3_{10} helix is much less abundant that the α-helix, as compared to the α-helix, it suffers from sub-optimal hydrogen bonding and increased intra-residue strain. The γ- and π-helices leave a void at the center of the helix, thereby reducing the energetically favorable van der Waals contacts; consequently, these structures are novelties.

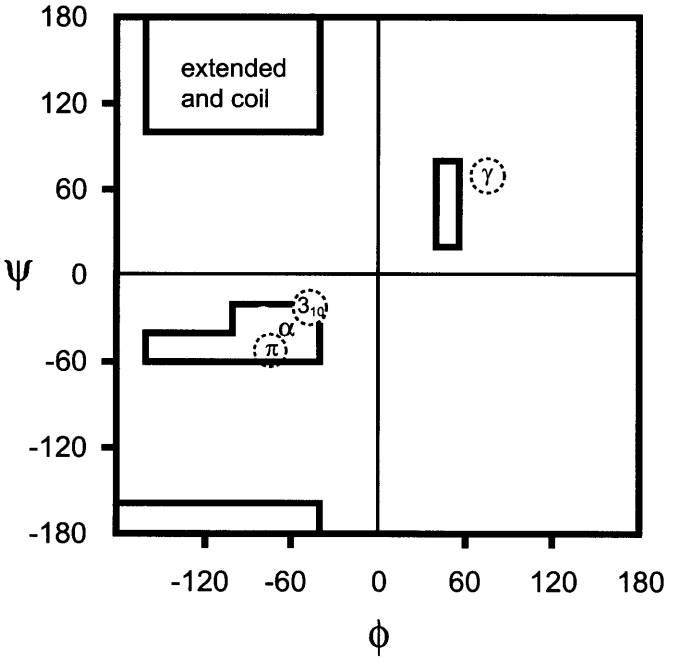

Figure 4: Ramachandran diagram with approximate contours indicating the accessible conformational space for the natural amino acids except proline and glycine. The shaded area for the α-helix demarcates the allowed helical regions for dihedral angle pairs, constrained by the relation $\phi + \psi = -103°$.

In their landmark series of communications, Pauling and Corey also noted that

elements of the diffraction patterns of synthetic polypeptides[14] and globular proteins[15] were consistent with α-helical structure. Moreover, others readily adopted the α-helix as the likely explanation for "rods" appearing in low resolution X-ray structures of globular proteins.[16] A definitive proof would appear almost a decade later in the 2 Å-resolved X-ray structure of myoglobin, itself a scientific triumph requiring years of painstaking effort.[17] Earlier low resolution data for myoglobin had indicated that approximately 85% of the residues were in rod-shaped structures with the dimensions of Pauling's helix; the high resolution data provided a precisely matching electron density map.

The various, disparate data on protein structure had coalesced by the mid nineteenth century. Sanger[18] proved the invariable amino acid sequence of insulin by his sequencing method, and as other proteins were sequenced it became clear that the primary structure of a given protein was constant. The availability of sequence data for proteins assisted the solution of protein crystal structures, the number of which grew steadily. Many more examples of the α-helix were discovered, as well as the pleated β-sheet and various turn motifs. These elements were found to represent the vast majority of internally hydrogen-bonded structures—collectively known as secondary structure—with the α-helix as the most abundant by far; approximately 1/3 of all residues in the protein X-ray crystallographic database (PDB) are found in α-helices. X-ray data also revealed the close packing of these secondary structures; this tertiary structure of a protein arises from dense interactions of side chains and secondary structure surfaces to maximize the van der Waals interactions.

X-ray diffraction provides static information on secondary and tertiary structure; however, it cannot be used to examine the structural dynamics of a protein under varying conditions. Moreover, crystallization of proteins is notoriously fickle and has created a

---

[14] Pauling, L.; Corey, R.B. "The Structure of Synthetic Polypeptides" *Proc. Natl. Acad. Sci USA.* **1951**, *37*, 241–250.

[15] Pauling, L.; Corey, R.B. "The Polypeptide-Chain Configuration in Hemoglobin and Other Globular Proteins" *Proc. Natl. Acad. Sci USA* **1951**, *37*, 282–285.

[16] Kendrew, J.C.; Pauling, P.J. "The Crystal Structure of Myoglobin II. Finback Whale Myoglobin" *Proc. R. Soc. London, Ser. A.* **1956**, *237*, 255–276.

[17] Kendrew, J.C.; Dickerson, R.E.; Strandberg, B.E.; Hart, R.G.; Davies, D.R.; Phillips, D.C.; Shore, V.C. "Structure of Myoglobin. A Three-Dimensional Fourier Synthesis at 2 Å Resolution" *Nature* **1960**, *185*, 422–427.

[18] Sanger, F. "Chemistry of Insulin" *Science* **1959**, *129*, 1340–1344.

bottleneck to protein structure determination. Clearly, complimentary solution-state techniques for structural data would be beneficial. In the coming years two spectroscopic techniques—circular dichroism (CD) spectroscopy and NMR—developed apace to meet this need. Of the two, NMR provides more data; information on both secondary and tertiary structure are obtained. CD is blind to tertiary structure and gives only cumulative information on secondary structure. Considering the one-dimensional nature of the CD technique, this apparent weakness actually simplifies data interpretation. In fact, CD remains the fastest way to assess protein secondary structure, despite continuing gains in NMR technology. Unfortunately, application of this useful technique has been hampered by uncertainties in fundamental CD spectroscopic properties of the α-helix. As will be developed, we have created highly helical, well-defined polyalanine helices that are soluble in water with no accompanying tertiary structure. These constructs provide fundamental CD data on the α-helix. Moreover, in this report, NMR is used extensively to verify the helicity of the constructs, thus providing an important correlation of the two techniques.

1.3. CD Spectroscopy Background

CD spectroscopy superseded the related method of optical rotary dispersion (ORD) spectroscopy; both operate on the principle that chiral entities interact nonequivalently with left- and right-handed circularly polarized light. Circularly polarized light (cpl) can be represented as two vectors rotating, one clockwise and the other counterclockwise, in a plane perpendicular to the direction of travel for a propagating, linearly polarized light wave; summation of the two vectors produces the characteristic sinusoidal oscillation in the direction of propagation. In ORD spectroscopy, the specific optical rotation of a sample—arising from the different refractive indices of cpl in a chiral medium—is recorded over a range of wavelengths whereas CD spectroscopy detects the differential absorption of cpl by a chiral medium.[19]

Synthetic homopolypeptides were the bridge between X-ray diffraction and solution-state CD spectroscopy. Films of the polydisperse synthetic homopeptides such

[19] Eliel, E.L.; Wilen, S.H. *Stereochemistry of Organic Compounds*; John Wiley & Sons, Inc.: New York, **1994**; Ch. 13.

as poly-γ-benzyl-L-glutamate (PBLG) gave diffraction patterns like the those of natural α-keratins. Moreover, measurements of viscosity and light scattering of PBLG in dimethylformamide gave clear evidence for rod-like structure, demonstrating that the helical conformation was retained in solution. Such measurements in dichloroacetic acid indicated a random coil conformation however, consistent with a disruption of the hydrogen-bonding pattern of the α-helix in a solvent with strong hydrogen bond donor ability.[20] Given the wealth of evidence for helical structure in the solid and solution states, PBLG was the natural choice for early investigations in visible-wavelength ORD.[21]

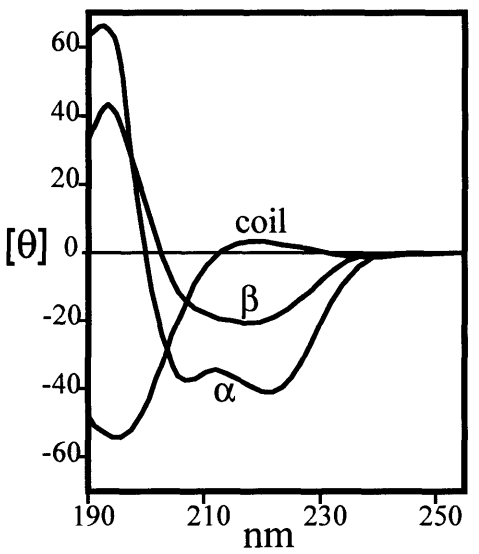

Figure 5: Representative CD spectra of the major secondary structures of proteins.

The transition from ORD to CD was accompanied by an effort to examine helical polypeptides under biological conditions. Water-soluble polyelectrolytes such as poly-L-

[20] (a) Tanford, C. *Physical Chemistry of Macromolecules*; Wiley & Sons: New York, **1967**, p.409. (b) Blout, E.R.; Karlson, R.H. "Polypeptides. III. The Synthesis of High Molecular Weight Poly-γ-benzyl-L-glutamates" *J. Am. Chem. Soc.* **1956**, *78*, 941–946.

[21] Yang, J.T.; Doty, P. "The Optical Rotary Dispersion of Polypeptides and Proteins in Relation to Configuration" *J. Am. Chem. Soc.* **1957**, *79*, 761–775.

glutamic acid[22] and poly-L-lysine were studied extensively. When fully charged, these polymers exist in random coil conformation, owing to electrostatic repulsion. Partial loss of charge, brought about by a change in pH, is accompanied by helix formation;[23] full loss of charge elicits precipitation of the peptide.

In addition to the early CD analyses of the synthetic polypeptides, spectra were taken of a significant number of globular proteins for which X-ray data were available. Two remarkable observations were made. First, to a reasonable approximation, each spectrum was a sum of the CD spectra of the constituent secondary structure (Figure 5), weighted by abundance. Second, because the helical chromophore signal is dominant at wavelengths greater than 215 nm, the CD signal at 222 nm—one of the minima for α-helical spectra—could be used to estimate the helical content of a protein.

1.4. CD Spectroscopy of the α-Helix

What is the relation between the number of helical residues in a helix and its signal intensity, typically measured at 222 nm? The CD signal at a given wavelength, θ_λ, obeys Beer's Law and is proportional to the concentration of the absorbing species and the path length of the cell (Equation 1); the CD proportionality constant at a given wavelength is called the molar ellipticity, $[\theta]_\lambda$. The UV-absorbing chromophore of the α-helix is the α-carbon of a helical amino acid residue flanked by two helically oriented amide groups—in other words, a single residue in a helix.[24] To account for this, molar ellipticity is often given as a per-residue value (Equation 2, n is the number of residues in the helix).

$$\theta_\lambda = [\theta]_\lambda cl \qquad \mathbf{1}$$

$$[\theta_n]_\lambda = [\theta]_\lambda / n \qquad \mathbf{2}$$

$$[\theta_n]_\lambda = [\theta_\infty]_\lambda (1 - X/n) \qquad \mathbf{3}$$

---

[22] Holzwarth, G.; Gratzer, W.B.; Doty, P. "The Optical Activity of Polypeptides in the Far Ultraviolet" *J. Am. Chem. Soc.* **1962**, *84*, 3194–3196.

[23] A reference spectrum for β-sheet structure can be obtained from helical poly-L-lysine solutions that are briefly warmed. Li, L.-K.; Spector, A. "The Cicular Dichroism of β-Poly-L-lysine" *J. Am. Chem. Soc.* **1969**, *91*, 220–222.

[24] Theoretical studies attribute the $[\theta]_{222}$ minimum to the $n \rightarrow \pi^*$ electronic transition of the amide group and the $[\theta]_{208}$ minimum to the $\pi \rightarrow \pi^*$ amide electronic transition.

$$FH = [\theta]_{\lambda,Exp} / n[\theta_n]_\lambda \qquad 4$$

$$n[\theta_n]_{222} = n[\theta_\infty]_\lambda - X[\theta_\infty]_\lambda \qquad 5$$

The absolute value of $[\theta]_{222}$ increases linearly with the number of helical residues in the protein, and empirical results fit Equation 3, in which the per-residue molar ellipticity of a helix, $[\theta_n]_\lambda$, is calculated as a fraction of the per-residue molar ellipticity of a theoretical helix of infinite length, $[\theta_\infty]_\lambda$. The amount by which the two differ is dependent on length n. As the length of a helix increases ($n \rightarrow \infty$), its per-residue molar ellipticity approaches the theoretical per-residue molar ellipticity of an infinite helix, known also as the limiting ellipticity for this reason. The difference between $[\theta_n]_\lambda$ and $[\theta_\infty]_\lambda$ is attributed to the fact that all residues of an infinite helix are identical whereas real helices have ends. The terminal residues are in an environment unlike that at the center of the helix where the environment is more similar to that of an infinite helix. This rationalization requires that the terminal residues of a helix give a reduced CD signal compared to the central residues. As the length of the helix increases, the ratio of central residues to end residues increases, and the diminished CD signal of the end residues is averaged over more residues. The value of X in Equation 3 is directly related to the number of terminal residues that reduce the overall helical signal.

Equation 3 has been used to quantify the helical content of proteins of unknown structure, and also to follow changes in secondary structure under varying conditions. The measure of a peptide's helical content is known as its fractional helicity FH (Equation 4), the ratio of measured molar ellipticity, $[\theta]_{\lambda,Exp}$, to the calculated potential molar ellipticity, $n[\theta_n]_\lambda$. Rearrangement of Equation 3 suggests a simple and direct method for determination of $[\theta_\infty]_\lambda$ and X (Equation 5). If a series of perfectly helical peptides could be obtained, the limiting ellipticity and X could readily be assigned by a graph like that in Figure 6. A plot of molar ellipticities ($n[\theta_n]_\lambda$) versus helix length (n) should give a straight line with a slope equal to the per-residue molar ellipticity for an infinite helix ($[\theta_\infty]_\lambda$) and an x-intercept equal to X.[25] Such a direct test has never been performed though, owing to the structural variability in short-to-medium peptides—

[25] Incidentally, if k were equal to zero and the line passes through the origin, then the per-residue molar ellipticity would not be length dependent.

hereafter called simply peptides. This is unfortunate because the lack of tertiary structure in peptides could allow a context-free investigation of the CD properties of the α-helix.

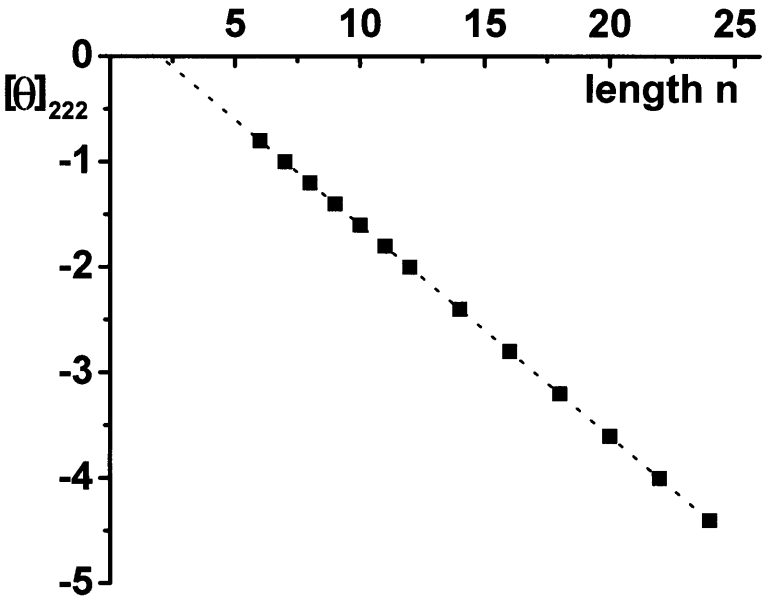

Figure 6: Theoretical plot of molar ellipticity at 222 nm versus helical length for a series of perfectly helical peptides. Slope = $[\theta_\infty]_{222}$, x-intercept = X.

1.5. Helix Formation

The problem with using peptides to explore helicity is that short peptides assume multiple conformations in solution. Peptide folding cannot be represented as a two state model, unlike protein folding which shows a sharp transition between folded and unfolded states. Proteins are not merely collections of secondary structure, but are stabilized by tertiary packing. The absence of such interactions in peptides lays bare the unfavorable thermodynamics of helix formation.

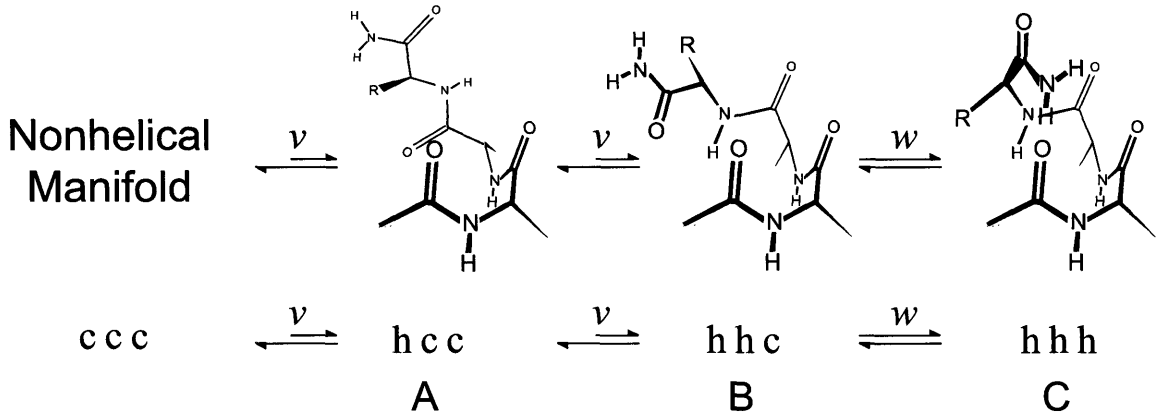

Figure 7: The equilibria leading to formation of an isolated helical loop. Constraint of the first two residues to helical conformation is very unfavorable (v^2). Hydrogen bond formation accompanies addition of the third residue to the helix; consequently, the equilibrium constant for the last step is more favorable than that of the two preceding steps ($w \gg v$).

The first difficulty in forming an α-helix is initiating the helix, as illustrated in Figure 7 with the simple Ac-Ala_3-NH_2 peptide; the equilibria constants v and w in the drawing pertain to the Lifson–Roig algorithm commonly used for modeling helix formation,[26] and the labels **h** and **c** refer to helical and random coil residues, respectively. In helix initiation, three sets of ϕ,ψ angles must be constrained—a large loss of entropy—before a hydrogen bond is made. This unfavorable situation is reflected in the small value for v, which consensus holds as approximately 0.05, owing to the low probability of any isolated amino acid residue being found in a helical conformation.[27] As the next residue in the chain assumes a helical conformation, the overall equilibrium constant becomes smaller still (v^2). Upon addition of the next helical residue a hydrogen bond is formed; even so, the equilibrium constant w for this step is only slightly greater than unity for helix-forming amino acids, such as alanine. This moderate equilibrium constant creates the second difficulty in forming a helix, as it leads to the presence of multiple

[26] Recent review on the L–R algorithm: Kemp, D.S. "Construction and Analysis of Lifson–Roig Models for the Helical Conformations of α-Peptides" *Helv. Chim. Acta* **2002**, *85*, 4392–4423.

[27] Compare the relatively small region of helical Ramachandran space with the total attainable conformational space.

helical conformations in solution, the number of which increase rapidly with increasing peptide length. For example, only one of the eight (2^n) conformations of the tripeptide in Figure 7 is helical whereas a decapeptide has 36 major helical conformers and a 25-mer has 276 major helical conformers.[28]

1.6. Summary

Although a length series of perfectly helical peptides would be ideal for calculation of $[\theta_\infty]_\lambda$ and X, a length series of highly helical peptides would suffice, so long as their fractional helicities could be accurately determined.[29] By 2002, research in the Kemp group had provided the tools necessary to attempt the synthesis of just such a length series. Development of helix-promoting N-terminal[30] and C-terminal[31] caps had raised the possibility of creating highly helical peptides with well-defined length, and validation of a scheme for separating a homopeptide region from solubilizing residues allowed the synthesis of long polyalanine peptides.[32]

Why polyalanine? Of the twenty natural α-amino acids, alanine is the most abundant in protein α-helices. It is the simplest of its kind and an obvious choice for modeling of helix formation; moreover, the transition from helical to sheet structure of alanine-rich regions in proteins are relevant to diseases such as Alzheimer's[33] and

---

[28] For example, a pentapeptide has six major helical conformations out of the 25 total conformations: hhhhh, hhhhc, chhhh, cchhh, chhhc, hhhcc. A conformation such as hhhch is not a major helical conformation since the isolated h does not extend the helix.

[29] Owing to practical constraints on the kinetic method used to calculate fractional helicity, highly helical peptides give data with smaller error. Furthermore, the use of highly helical peptides permits a simplification in compiling the kinetic data. Further explanation follows in the text and Experimental section.

[30] Maison W.; Arce, E.; Renold, P.; Kennedy, R.J.; Kemp, D.S. "Optimal N-Caps for N-Terminal Helical Templates: Effects of Changes in H-Bonding Efficiency and Charge" *J. Am. Chem. Soc.* **2001**, *123*, 10245–10254.

[31] Deechongkit, S.; Kennedy, R.J.; Tsang, K.Y.; Renold, P.; Kemp, D.S. "An Amino Acid that Controls Polypeptide Helicity: β-Amino Alanine, the First Strongly Stabilizing C-Terminal Helix Stop Signal" *Tetrahedron Lett.* **2000**, *41*, 9679–9683.

[32] (a) Miller, J.S.; Kennedy, R.J.; Kemp, D.S. "Short Solubilized Polyalanines Are Conformational Chameleons: Exceptionally Helical if N- and C-Capped with Helix Stabilizers, Weakly to Moderately Helical if Capped with Rigid Spacers" *Biochemistry* **2001**, *40*, 305–309. (b)Miller, J.S.; Kennedy, R.J.; Kemp, D.S. "Solubilized, Spaced Polyalanines: A Context-Free System for Determining Amino Acid a-Helix Propensities" *J. Am. Chem. Soc.* **2002**, *124*, 945–962.

[33] Perutz, M.F.; Pope, B.J.; Owen, D.; Wanker, E.E.; Schertzinger, E. "Aggregation of Proteins with Expanded Glutamine and Alanine Repeats of the Glutamine-rich and Asparagine-rich Domains of Sup35 and of the Amyloid β-Peptide of Amyloid Plaques" *Proc. Natl. Acad. Sci. USA* **2002**, *99*, 5596–5600.

spongiform encephaly.[34] Also, given that alanine has the highest helical propensity of the proteogenic amino acids, it was the best choice for our bid to create highly helical peptides.

The difficulty in using polyalanine for CD studies is its insolubility in water; peptides longer than Ala_8 precipitate. This is the reason poly-L-glutamate and poly-L-lysine have been used extensively for CD studies. Other groups have developed peptides with alanine regions interspersed with solubilizing Glu or Lys regions; [35] however, taking account of helix length and context dependencies makes imprecise the interpretation of the CD data for these peptides.

An important application for CD is the determination of amino acid helical propensities. The w value of alanine is especially important for understanding helix formation. Although it is agreed that the helical propensity of alanine is highest among the natural α-amino acids, the precise value has been strongly disputed. Two camps have formed—one favoring a w value near 1.1 and another favoring a value near 1.6. This apparently small difference has a great effect on helix formation.[36] Recent work in this group with solubilized polyalanines (without helix-promoting caps) is best interpreted as implying a previously unsuspected length dependence for w_{Ala}; because calculation of w_{Ala} is facilitated by assignment of $[\theta_\infty]_\lambda$, the work herein bolsters confidence in this important discovery. This issue is beyond the scope of this thesis, but has been thoroughly evaluated in the thesis of Dr. Robert Kennedy.[37]

---

[34] Ma, B.; Nussinov, R. "Molecular Dynamics Simulations of Alanine-Rich β-Sheet Regions: Insight into Amyloid Formation" *Protein Sci.* **2002**, *11*, 2335–2350.

[35] (a) Ingwall, R.T.; Scheraga, H.A.; Lotan, N.; Berger, A.; Katchalski, E. "Conformational Studies of Poly-L-Alanine in Water" *Biopolymers* **1968**, *6*, 331–368. (b) Gratzer, W.B.; Doty, P. "A Conformation Examination of Poly-L-Alanine and Poly-D,L-Alanine in Aqueous Solution" *J. Am. Chem. Soc.* **1963**, *85*, 1193–1197. (c) Marqsee, S.; Robbins, V.H.; Baldwin, R.J. "Unusually Stable Helix Formation in Short Alanine-Based Peptides" *Proc. Natl. Acad. Sci. USA* **1989**, *86*, 5286–8290.

[36] Consider, for example, the w^{n-2} weighting for the formation of a helical decapeptide: $1.1^8 = 2.1$ and $1.6^8 = 43$.

[37] Kennedy, R.J., III. "Experimental Characterization of Polyalanine Helices in Short and Long Contexts" Ph.D. Thesis, Massachusetts Institute of Technology, Cambridge, MA, 2004.

2. Highly Helical Peptide Design

2.1. Overview

A method for solubilizing a polyalanine region, developed by Dr. Justin Miller, is shown in Figure 8. The polyalanine region is separated from the solubilizing polylysine regions by a rigid tripeptide spacing element composed of a *tert*-Leu residue and two isonipecotic (Inp) residues. A Trp residue allows concentration determination by UV.

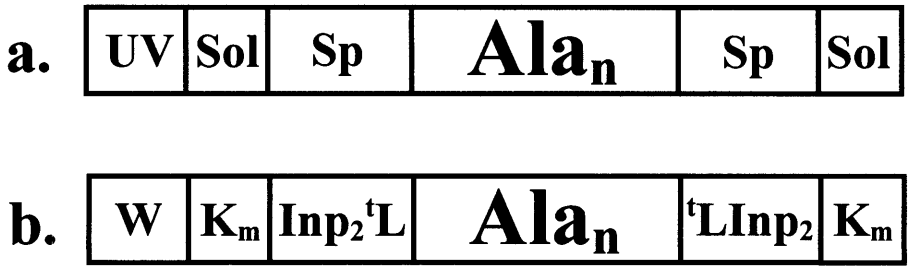

Figure 8: (a) Scheme for solubilization of polyalanine in water. UV = chromophore for concentration measurement by UV spectroscopy, Sol = solubilizing residues, Sp = spacing element to separate Sol from Ala_n. (b) Execution of the scheme for peptide series designed to study the helical propensity of alanine. Tryptophan (W) is the UV reporter, lysine (K) is the solubilizing amino acid (m = 4,5), and the spacer is a tripeptide segment with one *tert*-leucine (^{t}L) and two isonipecotic acid (Inp) residues.

In designing the N-terminal and C-terminal caps two characteristics of the α-helix were taken into account: (1) The terminal residues of an isolated α-helix have solvent-exposed hydrogen bonding sites, amide protons at the N-terminus and amide carbonyl oxygens at the C-terminus and (2) The alignment of the amide groups along the helical axis creates a helical dipole with a partial positive charge at the N-terminus and a partial negative charge at the C-terminus. Each helix-promoting cap provides hydrogen bonding sites for the terminal residues of the helix and a charge that is complimentary to the helix dipole.

2.2. Design of the N-terminal Helix-Initiating Cap

In 1991, the Kemp group introduced an N-terminal helix-initiating cap abbreviated Hel. The molecule is a constrained, tricyclic, prolyl proline dipeptide synthesized as its *N*-Ac derivative in 16 steps from proline and 4-hydroxyproline.[38] It was found to induce appreciable helicity in very short alanine-rich peptides.[39] Even though *N*-acylated Hel is quite rigid, there are still degrees of freedom: *cis* (c) and *trans* (t) rotamers of the *N*-acylamido group; rotation about the C8–C9 bond that gives rise to an eclipsed (e) or staggered (s) conformation; and the ψ angle of the carboxyamido group (Figure 9). Of the three major conformers, only the (te) state initiates helix formation. Fractional helicity of a Hel-capped peptide has been correlated with the ratio of ^{1}H NMR signal for the (cs) state versus the unresolved signals of the (ts) and (te) states, the so-called t/c ratio.

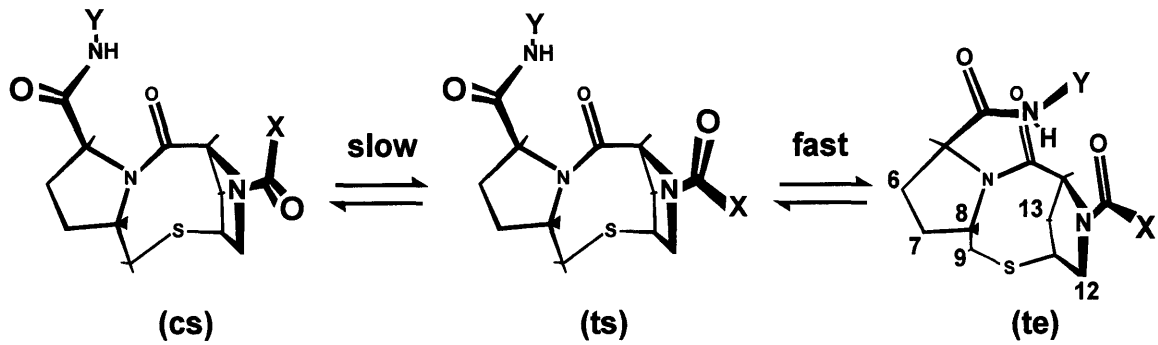

Figure 9: Three conformations of a peptide conjugate (Y = polypeptide chain) of the *N*-acyl-Hel N-cap, viewed from the concave side of the cap. On the NMR time scale in water, the (ts) and (te) states rapidly equilibrate and are indistinguishable. Because of slow interconversion between the amide rotamers, the (cs) and composite (ts + te) states can be resolved. The helix-stabilizing conformation is the (te) state. For our highly helical peptides, the (te) state is dominant, especially under helix-favoring conditions (2 °C, pH = 4.5 – 6.0). For AcHel, X = Me.

---

[38] Kemp, D.S.; Curran, T.P.; Davis, W.M.; Boyd, J.G.; Muendel, C. "Studies of N-Terminal Templates for α-Helix Formation. Synthesis and Conformational Analysis of (2*S*, 5*S*, 8*S*, 11*S*)-1-Acetyl-1,4-diaza-3-keto-5-carboxy-10-thiatricyclo[2.8.1.$0^{4,8}$]-tridecane (Ac-Hel$_1$-OH)" *J. Org. Chem.* **1991**, *56*, 6672–6682.

[39] Kemp, D.S.; Curran, T.P.; Boyd, J.G.; Allen, T.J. "Studies of N-Terminal Templates for α-Helix Formation. Synthesis and Conformational Analysis of Peptide Conjugates of (2*S*, 5*S*, 8*S*, 11*S*)-1-Acetyl-1,4-diaza-3-keto-5-carboxy-10-thiatricyclo[2.8.1.$0^{4,8}$]-tridecane (Ac-Hel$_1$-OH)" *J. Org. Chem.* **1991**, *56*, 6683–6697.

Not long after the introduction of Hel, efforts were made to improve it by replacement of the *N*-acetyl group.[30] The AcHel cap does not present a dedicated hydrogen bonding site to the first NH of the attached helix. Furthermore, it provides no negative charge to compliment the helix dipole. Of the many replacement groups for acetyl that were tested, the negatively charged malonyl and succinyl groups proved best for increasing the helix-inducing ability of Hel. So that the derivatized Hel cap could be incorporated anywhere in a peptide chain, Asp was chosen instead to replace Ac. The Asp residue is bound to Hel through its β-COOH ($^{\beta}$Asp) rather than its α-COOH so that the residues appended to the N-terminal side of the capped polyalanine region are directed along the helical axis. The choice of $^{\beta}$Asp mirrors the frequent appearance of Glu and Asp residues at the N-termini of protein α-helices.[40]

2.3. Design of the C-terminal Cap

The search for a C-cap identified the unnatural amino acid β-amino alanine (*beta*) as a strong helix helix-stabilizing terminator.[31] This residue carries a positive charge (pH < 11) that compliments the helix dipole. Also, the ammonium ion provides a hydrogen bonding site capable of interacting with the terminal amide carbonyls of the helix. In contrast to Hel, the *beta* does not have highly pre-organized hydrogen bonding sites, and is therefore a less effective cap. *Beta* also stops helix propagation, and in doing so defines the C-terminus of the helix. This is an important feature because uncertainties about helical length have complicated helical modeling with peptides.[41]

---

[40] (a) Presta, L.G; Rose, G.D. "Helix Signals in Proteins" *Science* **1988**, *240*, 1632–1641. (b) Aurora, R.; Rose, G.D. "Helix Capping" *Protein Sci.* **1998**, *7*, 21–38.

[41] NOESY analysis of the alanine-rich heteropeptide K_3-A_{12}-K_3-W-NH_2 has demonstrated that helical structure is not limited to the alanine region. Constructs of this type have been used by others to study the helical propensity of alanine by CD with the assumption that helical structure was confined to the alanine region. See PhD dissertation of Dr. Robert Kennedy, p.64.

3. Experimental Results

The above discussion lays the foundation for experimental results reported in this Chapter, presented in the following order:

(1) Synthesis of the N-terminal cap and capped peptides

(2) NMR structure determination of the capped alanine helix

(3) Quantitation of helical structure by amide NH→ND exchange

3.1. Synthesis of the N-Cap Hel

The peptides in this study were made by linear, N→C terminal, solid phase peptide synthesis using 9-fluorenylcarboxymethyl (Fmoc)-protected amino acids and [*O*-(7-azabenzotriazol-1-yl)-1,1,3,3-tetramethyluronium hexafluorophosphate] (HATU) to activate the free carboxylic group of the growing chain. All reagents were commercially available except FmocHel. At the start of the project, there was just enough FmocHel for the synthesis of a single test peptide, and therefore its synthesis was the first priority.

Dr. Kim McClure's synthetic route to AcHel[42] had been slightly modified by Dr. Wolfgang Maison[30] to provide FmocHel, permitting insertion of Hel anywhere along a peptide chain during solid-phase peptide synthesis. The more complicated branch of the convergent synthesis begins with the methyl ester of proline (Scheme 1). Electrochemical oxidation in methanol produces diastereomers **3** which are treated with $BF_3{\cdot}Et_2O$ to generate an *N*-acyl iminium ion *in situ*. At low temperature, this transient species is reacted with a vinyl cuprate reagent derived from a vinyl bromide via a vinyl lithium intermediate. Addition of the vinyl cuprate reagent to the *N*-acyl iminium ion occurs very diastereoselectively, yielding compound **4** which was then treated with ozone to cleave the olefin. A reductive work-up afforded the primary alcohol which was converted to a thiol by the Mitsunobu reaction.

---

[42] McClure, K.F.; Reynold, P.; Kemp, D.S. "An Improved Synthesis of a Template for α-Helix Formation" *J. Org. Chem.* **1995**, *60*, 454–457.

Scheme 1: Convergent 18-step synthesis of Fmoc-Hel.

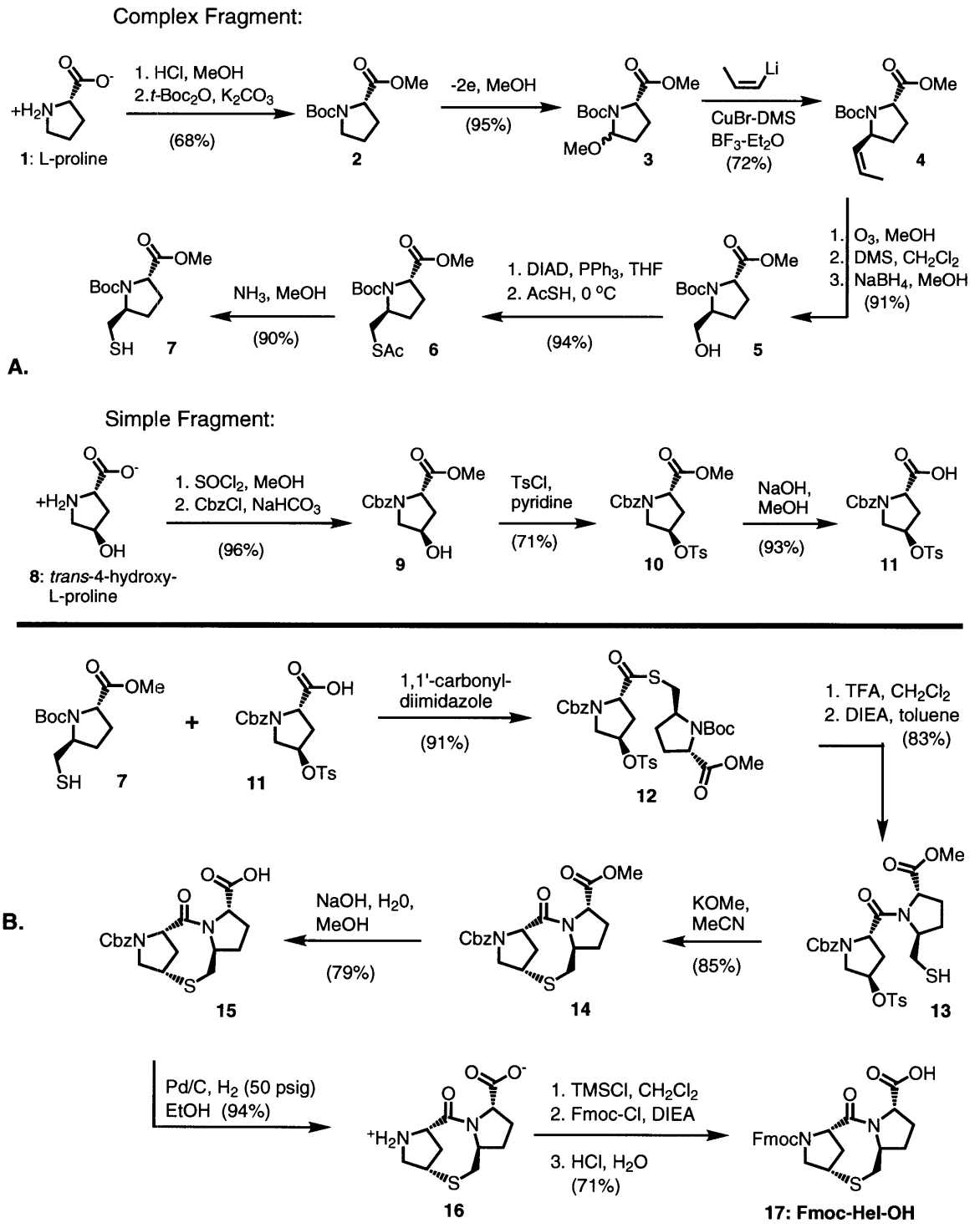

The simpler fragment, made from 4-hydroxy proline (Hyp), was combined with the thiol to form thioester **12**. Treatment with trifluoroacetic acid (TFA) removed the Boc group, giving the liberated amine as the TFA salt. The salt was exhaustively evaporated from methylene chloride and placed under high vacuum overnight to remove all traces of TFA. The free base was obtained by treatment with diisopropylethylamine (DIEA), and the compound was heated at 60 °C under argon in toluene to effect acyl transfer. The resulting tertiary amide **13** was then treated with KOMe under high dilution in boiling acetonitrile to trigger intramolecular S_N2 displacement of the tosylate group. The tricyclic compound thus formed was found to be free of the C5 epimer that had vexed earlier group members. I anticipated epimerization and took the precaution of reducing the amount of KOMe from 1.2 to 1.1 equivalents; also, the sample of **13** was thoroughly dried to ensure an accurate weight.

Despite successfully avoiding epimerization, I encountered another recurring problem with the published synthesis: failed hydrogenolysis of the Cbz protecting group. Previously, a procedure using a poisoned $Pd/BaSO_4$ catalyst[43] was used for the deprotection. The same batch of $Pd/BaSO_4$ catalyst that failed to deprotect compound **15** successfully deprotected Cbz-proline, and so I resorted to a stronger Pd catalyst—Pd/C. The Pd/C catalyst slowly but reliably cleaved the Cbz group from **15**. An Fmoc group was added to the free zwitterion using a procedure that nearly eliminates the dimer formed by carboxyl activation with FmocCl.[44] Previously, difficulties in using the zwitterion directly were overcome by protection of **15** as the *tert*-butyl ester before Cbz deprotection and Fmoc addition. After Fmoc addition, the *tert*-butyl group was removed by treatment with TFA. Happily, the extra two manipulations proved unnecessary, and the final product FmocHel was obtained in good yield. In all, approximately 15 grams of Cbz-protected intermediate **15** were synthesized, corresponding to approximately 12 grams of Fmoc-Hel-OH.

---

[43] Bodansky, M. and Bodansky A. *The Practice of Peptide Synthesis*; Springer–Verlag: Berlin, 1984; Vol. 21, p. 156.

[44] Bolin, D.R.; Sytwu, I.I.; Humiec, F.; Meienhofer, J. "Preparation of Oligomer-Free Nα-Fmoc and Nα-Urethane Amino Acids" *Intl. J. Pept. Protein Res.* **1989**, *33*, 353–359.

3.2. Design and Synthesis of the Helical Standards

a. **The three series:**

Ac-$^{\beta}$AspHel-Ala$_8$-*beta*-NH$_2$ **1 (sole member)**

Ac-$^{\beta}$AspHel-Ala$_n$-*beta*-Acc-Lys$_2$-Trp-NH$_2$ **2 (n = 4-16, even)**

Ac-Trp-Lys$_5$-Inp$_2$-^{t}Leu-$^{\beta}$AspHel-Ala$_n$-*beta*-^{t}Leu-Inp$_2$-Lys$_5$-NH$_2$

3 ($4 \le n \le 12$, n = 14-24 even)

b.

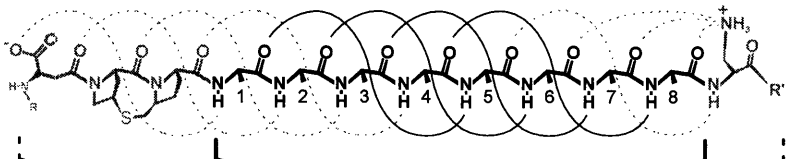

c.

d.

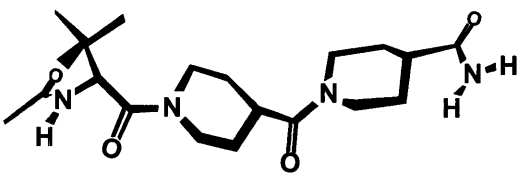

Ac-^{t}Leu-Inp$_2$-NH$_2$

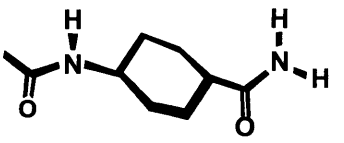

Ac-Acc-NH$_2$

Figure 10: (a) The three types of capped polyalanine peptides in this study. (b) The capped Ala$_n$ region (n = 8 in drawing) common to all peptides showing hydrogen bond connectivities; the series differ only in their R and R′ groups. (c) Schematic showing the design of the solubilized helical peptides for series 3. Sp = spacing element: ^{t}L/Inp tripeptide. Lysines were used to solubilize the polyalanines. The W residue was used for UV concentration determination. Series 2 peptides had a short Lys segment separated from the C-terminus of the capped core with a single Acc. (d) Structures of the spacing elements.

Three types of peptide incorporating a $^{\beta}$AspHelAla$_n$*beta* region were created for the helical standard project, each with a specific purpose (Figure 10a). Dr. Robert Kennedy synthesized our first N- and C-capped polyalanine, peptide **1**—Ac-$^{\beta}$AspHel-Ala$_8$-beta-NH_2—using the small amount of Fmoc present in the group at the beginning of the project. A line drawing of this peptide in Figure 10b (R = Ac and R′ = NH_2) demonstrates the helical hydrogen bonding pattern of the construct, distinguishing hydrogen bonds formed among alanines from those formed between alanine residues and the caps. The simple R groups of peptide **1** facilitated NMR studies verifying the proposed helical structure of the capped polyalanine region. Peptide **1** was suitable for structural studies, but the insolubility of polyalanine prevented us from using longer analogs for CD standards.

Application of the solubilizing scheme to our capped polyalanine peptides is shown in Figure 10c. Our first solubilized polyalanines were members of series **3**, which had ^{t}L/Inp$_2$ spacers and solubilizing Lys residues at both ends of the capped polyalanine region.[45] The large span of length in series **3** was suited for CD studies; however, the piperidine ring of Inp (Figure 10d) made the peptides impractical for many NMR studies. When placed in a peptide chain, Inp forms a tertiary amide with energetically comparable rotamers. Slow rotamer interconversion, on the time scale of NMR experiments, of the four Inp residues in the series **3** peptides gave rise to 16 diastereomers. A comparison of the Ala-1 amide resonances of peptide **1** and the series **3** Ala$_8$ peptide is shown in Figure 11a,b. The diastereomers produce a broad peak for the Inp-containing peptides instead of the sharp doublet observed for peptide **1**; although this is merely inconvenient for some NMR studies, it is incompatible with others. Two peptides were made to confirm Inp's role in the appearance of the proton NMR spectra. The first was a short peptide containing a single Inp residue—Ac-$^{\beta}$D-Hel-A$_8$-β-Inp-K$_2$-W-NH_2; its Ala$_1$ amide proton appears as two overlapping doublets, arising from the two Inp diastereomers (Figure 11c). The second was the series **2** Ala$_8$ peptide; its Ala$_1$ amide proton appears as a doublet, like the series **1** peptide (Figure 11d).

[45] Analytical ultracentrifugation proved the samples of peptide were unaggregated up to concentrations of approximately 1 mM.

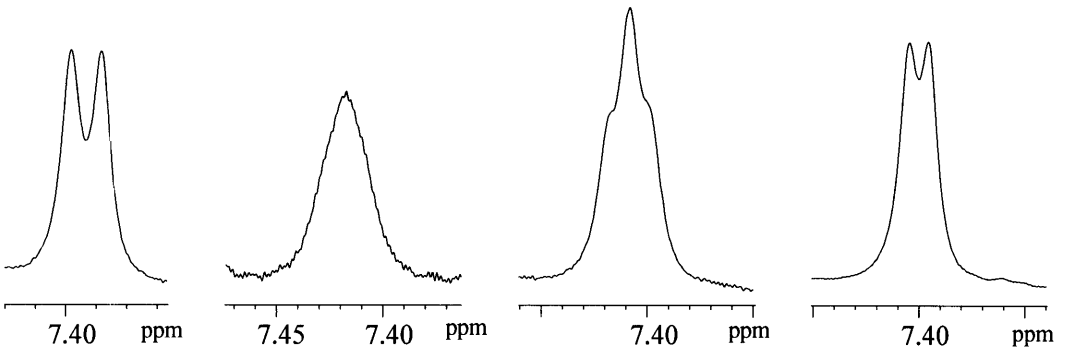

Figure 11: The Ala-1 amide proton NMR resonance from four different capped polyalanines. (a) Series 1 peptide (b) Series 3 Ala_8 peptide (c) Peptide = Ac-$^{\beta}$AspHel-Ala_8-Inp-Lys_2-W-NH_2 (d) Series 3 Ala_8 peptide.

Thus, replacement of Inp with *trans*-4-aminocyclohexane carboxylic acid (Acc) permitted detailed NMR analyses of soluble capped polyalanine peptides. The resulting series **2** peptides had fewer solubilizing lysines to further simplify NMR analysis. We were somewhat surprised to find that series **2** could be carried out to the Ala_{16} length without precipitation occurring. We surmised that the high helicity of the alanine regions prevented β-sheet aggregation.[45]

Inconveniently, *trans*-4-aminocyclohexane carboxylic acid is not widely available; a single commercial supplier of the HCl salt was found, but the cost was not negligible considering the minimum size available (100 g). Before committing to the purchase, I made the compound by a published Ru-catalyzed hydrogenation of *para*-aminobenzoic acid reported as giving the *trans* isomer in high yield after a single recrystallization.[46] Expectation did not match experience, and I obtained a mixture of both *cis* and *trans* isomers, with the *cis* predominating.[47] After failed attempts at thermal equilibration of the mixture, recrystallization was attempted. Several recrystallizations yielded a small sample of pure *trans*-Acc which was converted to Fmoc-*trans*-Acc. Following the successful demonstration described above, Acc·HCl was purchased from

[46] Ferber, E.; Brückner, H. "Über das Isochinuclidin" *Chem. Ber.* **1943**, *10*, 1019–1027.
[47] Determined by comparison of the spectrum with that of authentic *cis*-Acc, purchased from Aldrich.

Albany Molecular.[48]

Each peptide series was created for a specific purpose, and yet care was taken to ensure that the structure of the capped polyalanine region was constant, regardless of the identity of the R groups (Figure 10b). Although high quality data could not be obtained for all series in certain experiments, the collected data were nonetheless found to correlate qualitatively across all series.

3.3. Verification of N-cap and C-cap Structure

TOCSY and ROESY cross-peaks for the Hel moiety of peptide 1[49] closely corresponded to those of the helical, previously studied AcHel-A_6-OH peptide.[39] The data confirmed the (te) state of Hel required for helix-initiation, as well as the helical ψ dihedral angle of its carboxamido peptide linkage. Cross-peaks between the C-12 protons of Hel and a β-H of $^{\beta}$D verified the (t) conformation of the N-cap. Cross-peaks between the C-9 and C13 protons of the Hel template indicated the (e) conformation of the central ring. Cross-peaks between the amide NH of the first Ala residue and the C-6, C-7, and C-8 protons of Hel established the helical ψ dihedral angle of the carboxamido peptide linkage (Figure 12). TOCSY, NOESY, and ^{1}H NMR spectra taken for series 2 peptides (n = 8 – 16, n even)[49] were consistent with those taken for peptide **1**.

A second, minor peptide conformation observed by NMR for peptide **1** and series **2** peptides was consistent with the (c)-state. Under conditions creating maximal helicity, the t/c ratios were consistent with very high helicity. Conditions that reduced the helicity of our peptides—increased temperature and lower pH—increased the amount of (c)-state structure.

---

[48]Approximately a year afterwards, I interviewed with a chemist who had developed the synthesis of *trans*-Acc for Albany Molecular. He explained that the commercial route also relied on several recrystallizations to separate the isomers of Acc.

[49] Conditions: pH 4.5, 2 °C, 20 mM NaH_2PO_4.

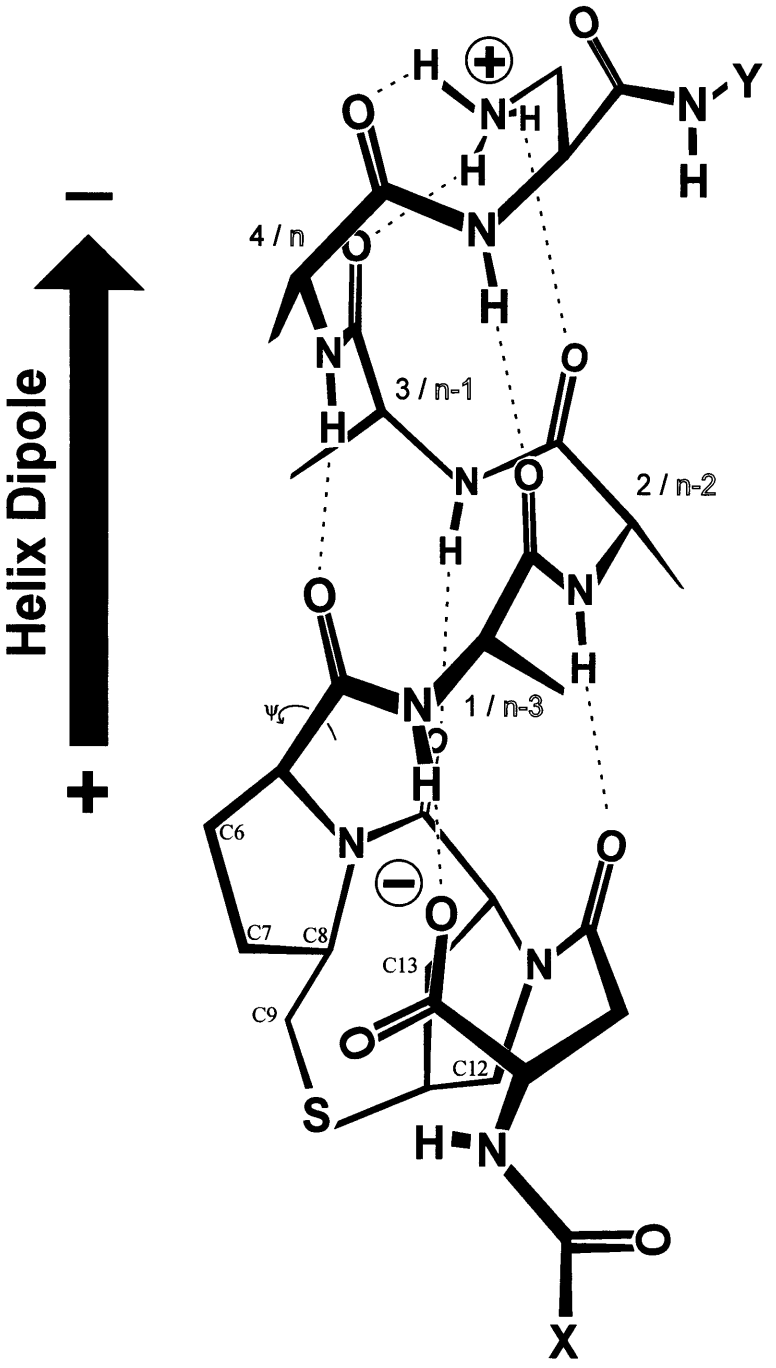

Figure 12: A perspective drawing of a Hel- and *beta*-capped Ala_4 peptide, with the concave side of Hel showing. In the proposed structure for our N- and C-capped polyalanines, four alanine residues are the minimum needed to demonstrate the interactions between the caps and the intervening amino acid residues. Hel interacts with the first four residues, and *beta* interacts with the last four (n through n-3). The configuration shown matches NOESY data for peptide 1, as explained in the text.

The position of the $^{\beta}$Asp COOH group was established indirectly. Because the charge of $^{\beta}$Asp was presumed to increase helical structure, selected series **2** and **3** peptides were titrated and the effects were monitored by CD (Figure 13). As pH decreased, the absolute value of the CD signal at 222 nm also decreased. The data fit well to a Henderson–Hasselbach plot, giving pKa values near 3.3, corresponding to ionization of the $^{\beta}$Asp carboxylate. A conspicuous feature of the CD titration curves is the decreasing effect of pH as the length of the capped alanine region increases. The stability of a helix is known to increase with the number of residues owing to the increasing weight of the *w* terms in the overall equilibrium constant; therefore, the diminished role of the caps with increasing alanine content is not surprising. Helix-promoting caps ought to have the greatest effect in short-to-medium length peptides.

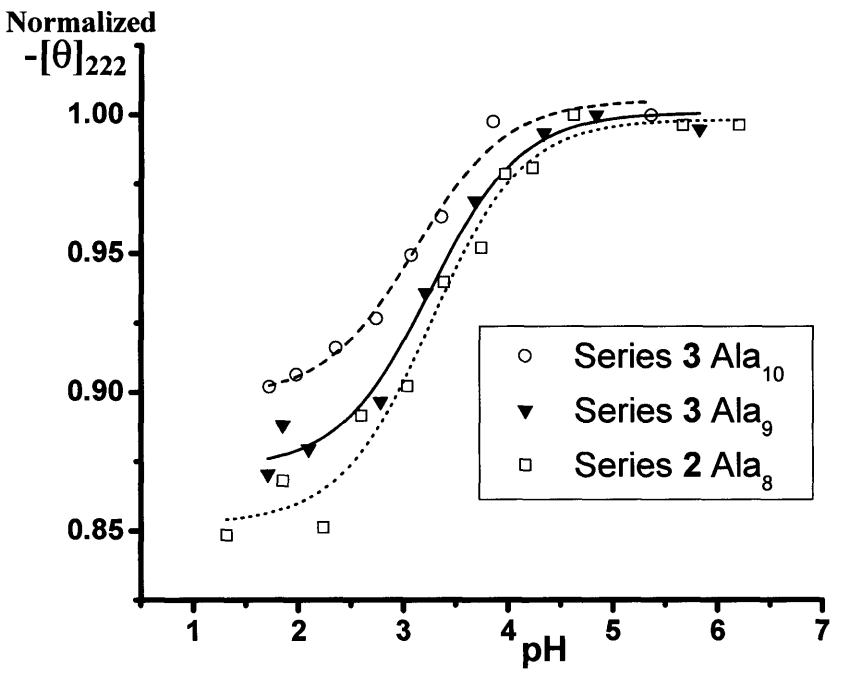

Figure 13: CD titration curves for series 2 Ala_8 and the Ala_9 and Ala_{10} members of series 3 (20 mM NaH_2PO_4, 2 °C, pH adjusted with conc. NaOH and H_3PO_4).

Another titration performed on peptide **1**[50] was monitored by NMR (Figure 14). Large chemical shift changes were observed for the amide protons of $^{\beta}$Asp (Δ 0.45 ppm), Ala-1 (Δ 0.19 ppm), and Ala-2 (Δ 0.13 ppm). The change in shift for $^{\beta}$Asp is rather uninformative; however, the changes in amide chemical shift for Ala-1 and Ala-2 imply that these protons are close to the aspartate carboxyl group as our model requires. Henderson–Hasselbach plots of the titration for the three amide resonances gave pKa values similar to those obtained from the CD measurements. The only other resonance to change significantly was the amide proton of Ala-4 which is hydrogen bonded to the carbonyl of the amide group formed from Hel and Ala-1, which is in turn hydrogen bonded to the α-COOH of $^{\beta}$Asp.

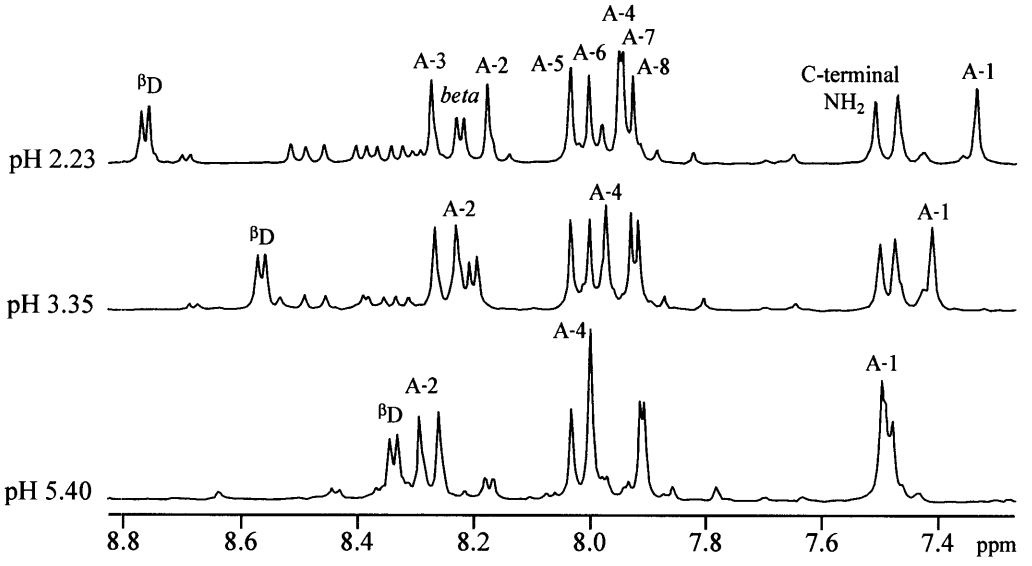

Figure 14: Titration of peptide 1 made with perdeuterated alanine, monitored by 1H NMR (2 °C, 40 mM NaH_2PO_4, pH adjusted with conc. NaOH and H_3PO_4). The large labeled peaks are the (t) state resonances. Small peaks correspond to the (c) state.

A pair of ROESY crosspeaks between the α-H and a β-H of β-amino alanine and the α-H resonance of Ala-6 ($Ala_{(n-2)}$) established the *left*-handed helical conformation of

[50] This peptide **1** was synthesized with perdeuterated alanine to simplify the ^{1}H NMR spectrum and facilitate interpretation of the titration experiment.

beta shown in Figure 12. This conformation is consistent with *beta*'s role as a terminating residue for the right-handed α-helix. Similar conformations of Asn and Gly residues at the C-termini of protein helices have been noted.[51]

3.4. ^{13}C Chemical Shift Evidence of Helical Structure

An extensive database of ^{13}Cα and ^{13}CO chemical shifts has been compiled for the residues of proteins in the PDB.[52] These backbone carbon shifts reliably indicate the secondary structure of residues. The average ^{13}CO chemical shifts for alanine residues in helix, coil, and β structure are 179.6, 177.6, and 175.0 ppm, respectively. The corresponding values for ^{13}Cα chemical shifts are 54.7, 52.4, and 50.3 ppm. It should be noted that although the dispersion of these values is great enough to make them useful, but the boundaries of the regions overlap somewhat.

Others have noticed a direct correlation between fractional helicity of peptides and the ^{13}CO/^{13}Cα chemical shifts,[53] and so we determined the chemical shift data for three of our series **2** peptides by synthesizing these peptides with uniformly-labeled ^{13}C,^{15}N alanine (^{U}*Ala*). Three such peptides were made—Ala$_6$^{U}*Ala*$_6$, ^{U}*Ala*$_6$Ala$_6$, and ^{U}*Ala*$_8$. These data are presented in Figure 15. The ^{13}Cα values all lie close to the reported PDB Ala average whereas the ^{13}CO values are substantially greater than the PDB average, excepting the two C-terminal Ala residues. We expected helix fraying to be greater at the C-terminus and so we were not surprised to find the C-terminal residues have the smallest chemical shift values; however, the very large values for the rest of the ^{13}CO shifts was noteworthy. Because random coil and β chemical shift values are less than those for the α-helix, we could confidently exclude the possibility that our peptides were forming non-helical secondary structure.

---

[51] Nagarajaram, H.A.; Sowdhamini, R.; Ramakrishnan, C.; Balaram, P. "Termination of Right Handed Helices in Proteins by Residues in Left Handed Helical Conformations" *FEBS Lett.* **1993**, *321*, 79–83.

[52] Wishart, D.S.; Sykes, B.D. "Chemical Shifts as a Tool for Structure Determination" *Methods Enzymol.* **1994**, *239*, 363–392.

[53] (a) Shalongo, W.; Dugad, L.; Stellwagen, E. "Analysis of the Thermal Transitions of a Model Helical Peptide Using ^{13}C NMR" *J. Am. Chem. Soc.* **1994**, *116*, 2500–2507. (b) Werner, J.H.; Dyer, R.B.; Fesinmeyer, R.M.; Andersen, N.H. "Dynamics of the Primary Processes of Protein Folding: Helix Nucleation" *J. Phys. Chem. B* **2002**, *106*, 487–494.

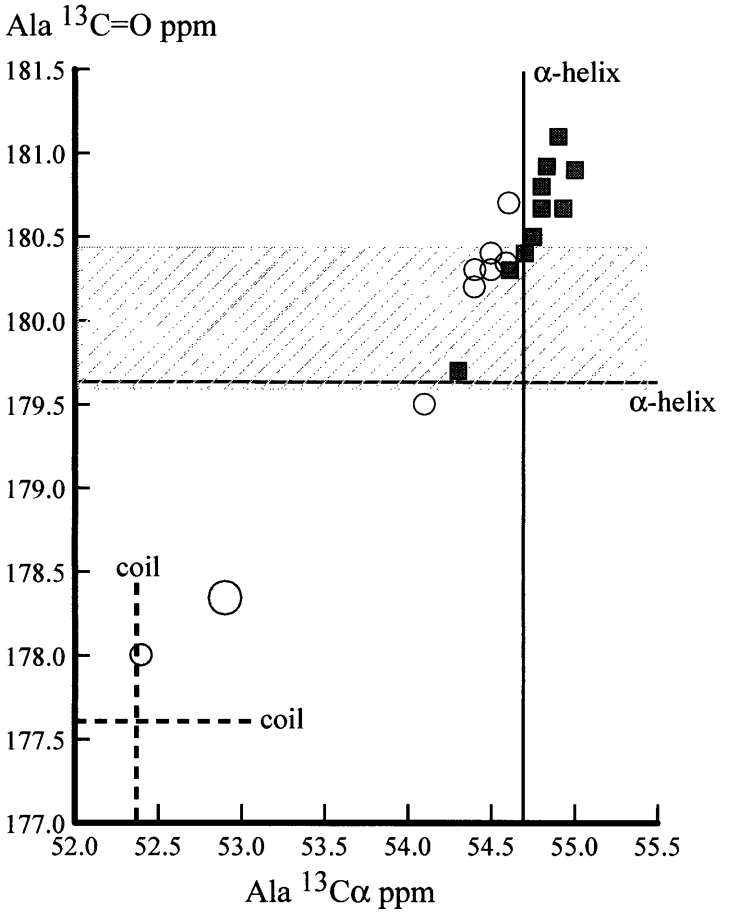

Figure 15: Alanine ^{13}CO and 13Cα chemical shifts for uniformly labeled ^{13}C,^{15}N alanine series 2 peptides (10 °C, 40 mM NaH_2PO_4, pH 4.5). Open circles correspond to the (te)-state Ala_8 peptide; solid squares correspond to the (te)-state Ala_{12} peptide. Two labeled Ala_{12} peptides were made because of overlap—one with six labeled Ala at sites 1–6 and one with six labeled Ala at sites 7–12. The solid lines mark the literature averages for α-helical Ala residues from the PDB; the averages for random coil Ala are marked with dashed lines. Average chemical shifts for β-sheet lie even further upfield. ^{13}CO chemical shifts within a single SD unit of the average for a highly helical peptide fall within the shaded rectangle. The large solid circle indicates the average for all (cs)-state resonances of both Ala_8 and Ala_{12}; the small solid circle indicates the Ala-1 pair for the (cs)-state of Ala_8.

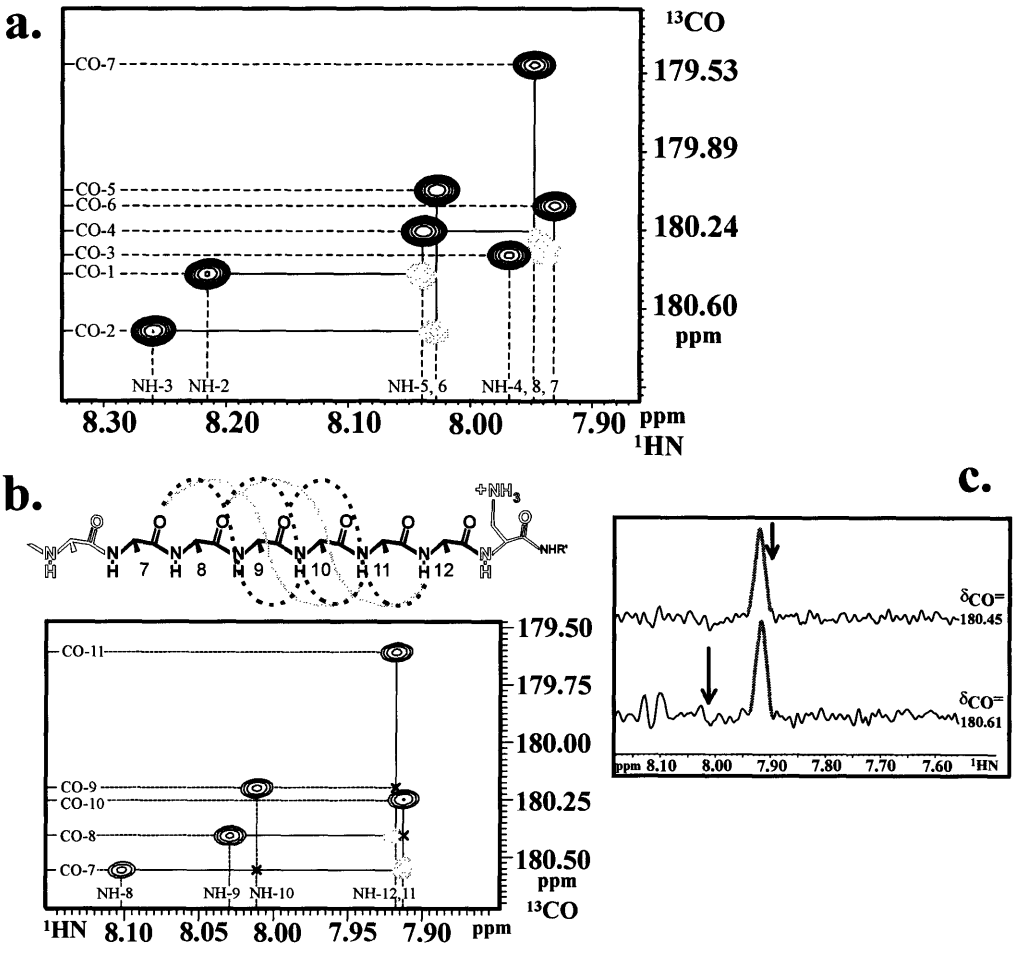

Figure 16: H-bonding NMR data (10 °C, 40 mM NaH_2PO_4, pH 4.5). (a) Overlay of two HNCO spectra for peptide 1 containing uniformly ^{13}C,^{15}N-labeled alanine. Solid contours are crosspeaks between ^{15}N and ^{13}C within an amide; dashed contours are crosspeaks between ^{15}N and ^{13}C in two hydrogen-bonded amides. In order to detect crosspeaks, the coupled nitrogen and carbon atoms must be labeled. Therefore, only seven solid crosspeaks and four dashed crosspeaks are evident. The four dashed hydrogen-bond crosspeaks are those that are indicated with a solid line in Figure 11b. (b) Overlay of two HNCO spectra for series 2 Ala_{12} with the last six alanines uniformly ^{13}C,^{15}N labeled. Contour conventions are the same as in part a. Two hydrogen-bond crosspeaks are evident; they are indicated with solid lines in the accompanying line drawing. The dashed hydrogen-bond lines indicate the pattern for the 3_{10} helix; these crosspeaks—black crosses—do not appear in the 2D NMR overlay. (c) Slices from an optimized Figure 15b spectrum at the residue 8 ^{13}CO resonance (top) and residue 7 ^{13}CO resonance (bottom) permit calculation of the signal-to-noise ratio.

In the NMR spectra of the labeled Ala_8 and Ala_{12} peptides, small resonances corresponding to the minor, sparingly helical (cs) state were evident.[54] These chemical shifts (shaded circles) are found closer to or in the random coil region, as expected.

3.5. Absence of 3_{10} Helical Structure

The 3_{10} helix has been found in protein structure, albeit less frequently than the α-helix.[55] Because the 3_{10} helix has a CD spectrum different from that of the α-helix, detection of its presence is important. The most reliable way to observe 3_{10} structure is X-ray crystallography; barring this, its presence has traditionally been deduced from relative intensities of NOESY crosspeaks.

A superior technique was recently introduced that permits direct observation of hydrogen bonding in a peptide by way of a modified HNCO experiment that detects the cross-hydrogen bond $^{15}N–^{13}C'$ scalar coupling ($^{3h}J_{NC'}$) for a pair of hydrogen bonded amides.[56] An overlay of two HNCO experiments for the series **2** $^{U}Ala_8$ peptide appears in Figure 16a. Dark contour lines are from an HNCO experiment optimized to detect the coupling between the NH and CO within a single amide group ($^{1}J_{C'N}$); the gray contours correspond to the H-bonding version of the HNCO. All four detectable $i\rightarrow(i+4)$ hydrogen bonding crosspeaks of the $^{U}Ala_8$ α-helix are evident;[57] however, none of the five detectable $i\rightarrow(i+3)$ 3_{10} helix crosspeaks are seen. The signal-to-noise ratio for the $^{U}Ala_8$ peptide experiments was low; results were better for the $Ala_6{}^{U}Ala_6$ series **2** peptide shown in Figure 16b. Two slices of the optimized spectrum (Figure 16c) indicate a signal-to-noise ratio of approximately 10, implying that the 3_{10} helix accounts for less than 10% of structure at the C-termini of our peptides, which are expected to be more

---

[54] The spectra were taken at pH 3, at which value the N-cap is not most effective. The Ala_{12} spectra were obtained at pH 4.5.

[55] Bolin, K.A.; Millhauser, G.L. "α and 3_{10}: The Split Personality of Polypeptide Helices" *Acc. Chem. Res.* **1999**, *32*, 1027–1033.

[56] Cordier, F.; Grzesiek, S.J. "Direct Observation of Hydrogen Bonds in Proteins by Interresidue $^{3h}J_{NC'}$ Scalar Couplings" *J. Am. Chem. Soc.* **1999**, *121*, 1601–1602.

[57] In principle, four more hydrogen bonds occurring between the caps and the labeled alanine region could be detected if appropriately ^{13}CO-labeled $^{\beta}$DHel and ^{15}N-labeled *beta* were available.

susceptible to 3_{10} structure than the N-termini owing to a lack of preorganization.[58]

3.6. Quantitation of Helicity by Hydrogen–Deuterium Exchange

In addition to verifying α-helicity, it was critical to determine the fractional helicity of our peptides by independent means. Previous attempts using peptides to calculate limiting ellipticity had lacked corroborating evidence for helical structure.[59]

The principle underlying the use of NH→ND exchange in D_2O to assign helicity is that a hydrogen-bonded amide proton exchanges slowly compared to one which is not hydrogen bonded. Because residues in the α-helix are hydrogen bonded, they are expected to exchange more slowly than unstructured, solvent-exposed residues such as the lysines in our peptides. The exchange rate of amide protons with water is the sum of contributions from separate acid-catalyzed, base-catalyzed, and water-catalyzed mechanisms, and the sum reaches its minimum at approximately pH 3.[60] So that data could be collected even for rapidly exchanging amide protons, the exchange experiments were conducted at low pH; however, the desire for slow exchange rates had to be balanced against the protonation of the $^{\beta}$Asp residue and the concomitant loss of helicity discussed earlier.

Exchange experiments were therefore conducted at pH values between 4.5 and 6.0, low enough for measurable rates of exchange and high enough for maximal helicity. The decrease in amide proton NMR signals was followed over several half-lives. Plots of the logarithm of the decreasing peak height versus time gave pseudo-first order rates for the exchange. The ratio of the calculated rate of exchange and the fundamental exchange rate for a residue is the protection factor (Equation 6); the fraction of non-helical residues at that position is correlated with the inverse of the protection factor (Equation 7).

---

[58] Assuming that the parameters for detection of the 3_{10} helix are similar to those for the α-helix. Dr. Heitmann spent significant time optimizing the parameters for the α-helix; during these trials, no peaks corresponding to 3_{10} helix were observed.

[59] (a) Luo, P.; Baldwin, R.L. "Mechanism of Helix Induction by Trifluoroethanol: A Framework for Extrapolating the Helix-Forming Properties of Peptides from Trifluoroethanol/Water Mixtures Back to Water" *Biochemistry* **1997**, *36*, 8413–8421. (b) Scholtz, J.M.; Barrick, D.; York, E.J.; Stewart, J.M.; Baldwin, R.L. "Urea Unfolding of Peptide Helices as a Model for Interpreting Protein Unfolding" *Proc. Natl. Acad. Sci. U.S.A.* **1995**, *92*, 185–189.

[60] Bai, Y.; Milne, J.S.; Mayne, L.; Englander, S.W. "Primary Stucture Effects on Peptide Group Hydrogen Exchange" *Proteins: Struct., Funct., Genet.* **1993**, *17*, 75-86.

$$PF_{NHi} = k_{StdNH} / k_{PeptideNH} \qquad \mathbf{6}$$

$$FH_{NHi} = 1 - (1 / PF_{NHi}) \qquad \mathbf{7}$$

The proton NMR spectra of series **2** peptides allowed a site-specific analysis of their fractional helicity. A stacked plot showing ^{1}H NMR spectra from the NH→ND exchange of series **2** peptides (n = 8, 10, 14, 16) appears in Figure 17. Some alanine amide resonances are distinguishable, and disappearance of the protons could be followed by peak area. Some alanine resonances overlap, in which case the signal decay was monitored by peak height and computer-fitted peak areas[61] with good agreement between the two methods. Selected members of the series **3** peptides were also investigated; although the spectra were not well resolved, collective rates for the loss of alanine amide signals were similar to the corresponding collective rates for the series **2** peptides.

Half-lives for the amide residues of our peptides ranged from 5 to 150 times longer than the reference half-life of an unprotected alanine amide.[60] The measurements permitted fine distinctions to be drawn between different regions of the polyalanine segments, since loss of amide protons occurs only from the minor unfolded conformations.[62] These fine distinctions appear in the compiled PF data for all measurements obtained from series **2** peptides (Figure 18). The helicity of the alanine region of our peptides is highest at the center and falls off at both termini. A decrease in helicity is most dramatic at the C-terminus, consistent with expectations. The central residues exhibit FH values above 0.994 and the FH of the ultimate alanine residue is approximately 0.5 as indicated by the PF of *beta*.[63] The following equations were used to compile the FH_i data, thus providing the overall FH for each peptide (Table 1).

---

[61] Origin graphing program, see Experimental section.

[62] For example, a $PF_i = 50$ corresponds to a $FH_i = 98$. A three-fold increase in PF_i (150) gives a mere 1% increase in FH_i. For highly helical peptides, PF is very sensitive to small structural changes whereas FH is not.

[63] The extremely rapid exchange of the *beta* amide proton was incompatible with the NH→ND exchange method. This protection factor was determined by the NH→NH′ indicated by relative changes in peak shape during pH titrations (*See experimental*).

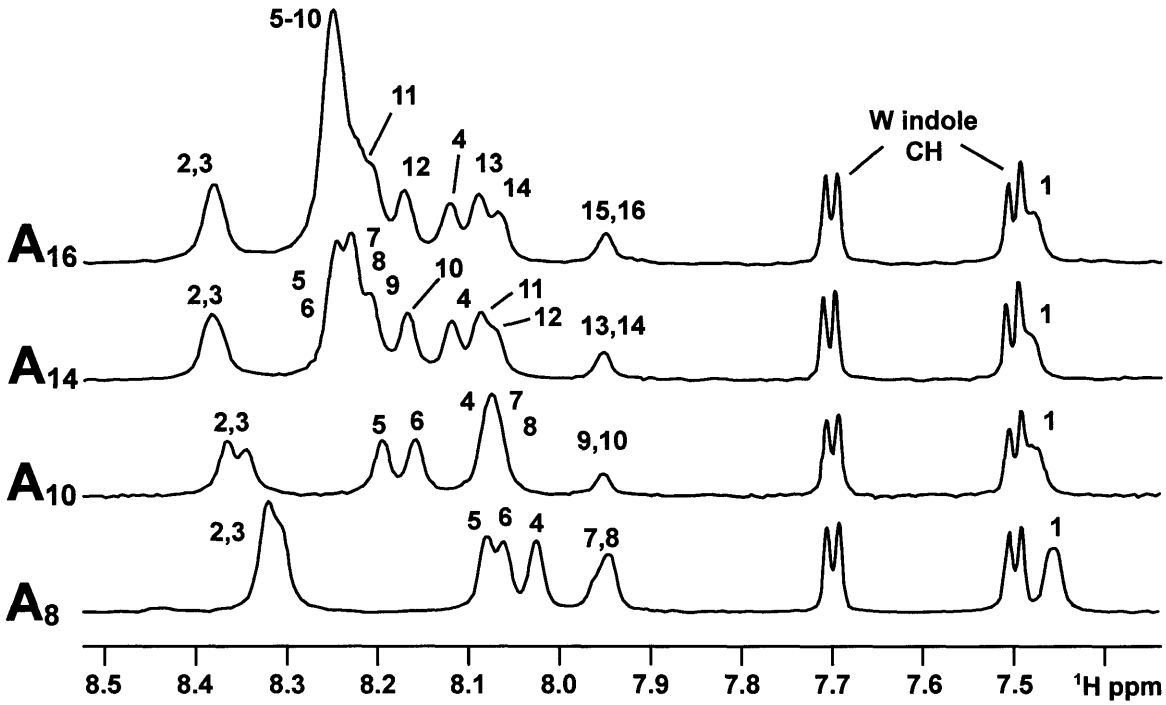

Figure 17: Stacked ^{1}H NMR spectra taken from NH→ND exchange experiments on series 2 peptides Ala_8, Ala_{10}, Ala_{14}, and Ala_{16} (2 °C, D_2O, pH = 4.5 – 6.0). All non-helical amide protons have fully exchanged; the alanine residues exchange much more slowly, consistent with protection by hydrogen bonding. The alanine residues of series 2 peptides could be assigned to specific residues, as indicated. Note the chemical shifts of the first four and last four alanine residues of each peptide are nearly identical throughout the length series.

$$FH_{NHi} \leq (FH_{i-3} + FH_{i-2} + FH_{i-1}) / 3 \qquad 8$$

$$\text{For } FH_{NHi} > 0.9 \text{ and } i < n/2\text{: } FH_{i-3} \cong FH_{NHi} \qquad 9$$

$$\text{For } FH_{NHi} > 0.9 \text{ and } i > n/2\text{: } FH_{i-1} \cong FH_{NHi} \qquad 10$$

$$(1/n)\Sigma FH_i \cong FH \qquad 11$$

It is important to note that the protection factor for a given amide proton FH_{NHi} is not identical to the corresponding site protection factor FH_i. An amide proton protection factor provides structural information on the three residues in the helical loop defined by

the hydrogen bond between that amide proton and the carbonyl group of the (*i*-4) residue.[64] The FH_{NHi} is the lower bound on the average helicity of the three preceding residues (Eq. 8); for highly helical peptides this relation approaches equality.[65] To illustrate the use of equations 9–12: the series **2** Ala_{12} peptide has FH_{NHi} values of 0.992 for $5 \leq i \leq 8$, indicating that $FH_i > 0.99$ at sites 2 through 7; Equation 9 gives $FH_1 = 0.987$, corresponding to the amide site value for Ala-4 (FH_{NH4}). All but one of the remaining assignments are obtained by use of Equation 10: $FH_{NH9} = FH_8 = 0.988$; $FH_{NH10} = FH_9 = 0.986$; $FH_{NH11} = FH_{10} = FH_{NH12} = FH_{11} = 0.955$. The last FH_i is defined by the limits for $FN_{beta}NH$ (0.1 to 0.7) supported by a NH→NH′ exchange titration experiment.

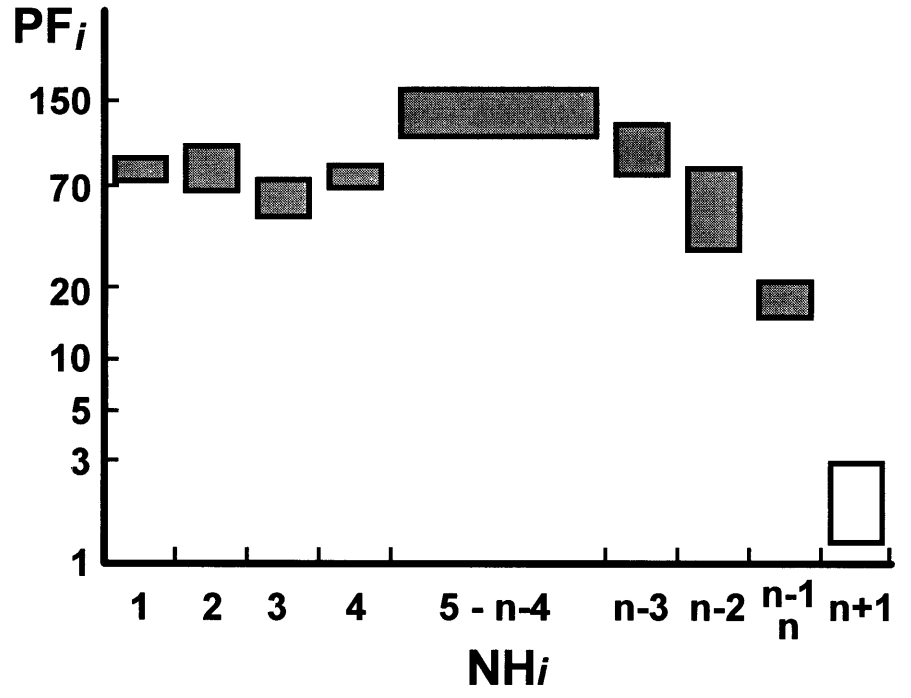

Figure 18: PF_{NHi} values for capped Alanine region. Gray rectangles: Values of site protection factors within one SD of the average for Ala_n region of series 2 peptides— D_2O, 2 °C, pH 4.5 – 6.0, n > 8. Open rectangle: Protection factor for *beta* (n+1); limits verified by titration experiments on peptide 1 in H_2O (see Experimental).

---

[64] Kemp, D.S. "Construction and Analysis of Lifson–Roig Models for the Helical Conformations of α-Peptides" *Helv. Chim. Acta* **2002**, *85*, 4392–4423.

[65] Thanks to Prof. Kemp for providing the derivations of these equations based on the Lifson–Roig algorithm (*See Experimental*).

Table 1: FH Values for Series 2 and 3 Peptides.

n	calculated FH[a]	extrapolated FH[b]	extrapolated $\langle n \rangle$[c]
8	0.862, 0.944	0.90 ± 0.04	7.2 ± 0.3
9		0.91 ± 0.04	8.2 ± 0.4
10	0.888, 0.954	0.92 ± 0.03	9.2 ± 0.3
11		0.92 ± 0.03	10.1 ± 0.3
12	0.905, 0.961	0.93 ± 0.03	11.2 ± 0.4
14	0.918, 0.966	0.94 ± 0.03	13.2 ± 0.4
16	0.927, 0.970	0.95 ± 0.02	15.2 ± 0.3
18		0.95 ± 0.02	17.1 ± 0.4
20		0.96 ± 0.02	19.2 ± 0.4
22		0.96 ± 0.02	21.1 ± 0.4
24		0.96 ± 0.02	23.0 ± 0.5

[a] Calculated FH derived from hydrogen-deuterium exchange on series **2** peptides; limits correspond to FH_n = 0.1 and 0.7, respectively. [b] FH extrapolated from mean values of series **2** data; these are applicable to both series **2** and **3** peptides. [c] average helical length $\langle n \rangle = n$FH.

4. Ellipticity Calculations

4.1. Calculation of Limiting Ellipticity

The positions of the first four and last four amide proton resonances for each peptide in the stacked spectra of Figure 17 are nearly constant and independent of the length of the alanine region. This is consonant with the fact that the first four alanine residues of our peptides are in contact with Hel, and the last four are in contact with *beta*. The series **2** Ala_8 peptide has all of its residues in contact with the caps; as the length of the alanine region increases, a "core" of alanine residues, separate from the caps, is formed. Helical amide ^1H chemical shifts are sensitive to hydrogen bond strength, solvent exposure, structural variations, and residue position. Constancy of these values thus provides an appropriate test for Ala_n structural convergence. The amide proton chemical shifts of the alanine core converge to a value of 8.21 ± 0.02, consistent with helical structure. A slight revision of the equation for molar ellipticity (Equation 12)

accommodates the two classes of residues in our capped peptides.

$$[\theta]_\lambda = [\theta_\infty]_\lambda (n - k) + [\theta_\infty]_\lambda (k - X) \quad \textbf{12}$$

$$[\theta]_{\lambda,core} = [\theta_\infty]_\lambda (n - k) \quad \textbf{13}$$

$$[\theta]_{\lambda,SS-Caps} = [\theta_\infty]_\lambda (k - X) \quad \textbf{14}$$

$$[\theta]_\lambda = [\theta]_{\lambda,core} + [\theta]_{\lambda,SS-Caps} \quad \textbf{15}$$

The new parameter k corresponds the number of capped alanines with properties that are perturbed by the capping groups—for our peptides, NMR data suggests k = 8. A stacked CD plot of series **3** peptides is given in Figure 19a; the dependence of signal on the number of alanines is obvious. However, is it reasonable to assume a constant CD contribution for the solubilizing residues, capping groups, and the eight alanine residues of the core's two extrema? A characteristic of the stacked spectra plot consistent with the concept underlying Equations 12 – 15 is the common value for all spectra at 201 nm. A change in the absorption of left and right cpl by a chiral entity is accompanied by a change in the sign of its CD spectrum. The point at which the absorption of left and right cpl is identical—the isoellipsoidal point—corresponds to zero CD signal; for the α-helix, this point is 201 nm. The constant value at 201 nm for all CD spectra is consistent with a zero contribution from the alanine core and a constant, non-zero contribution from the residues outside of the alanine core ($[\theta_\infty]_{\lambda,SS-Caps}$, Equation 15).[66]

A plot of molar ellipticity values at four wavelengths for the series **3** peptides (n = 9 – 12, 14 – 24 even) appears in Figure 19b. Comparison of extrapolated Ala_8 values from the figure with the actual values for the series **3** Ala_8 peptide showed very high agreement. One will also notice that the linear relations are, in fact, the CD calibration curve presented in the introduction (Figure 6). Having proven a constant, helical alanine core (FH > 99.5%) for the Ala_9 to Ala_{24} peptides, the slope of the line corresponds to the limiting ellipticity of alanine. A full spectrum of the limiting ellipticity from 195 to 255 nm can be compiled (Figure 19c), and the resulting spectrum represents the CD signal of a single alanine residue within an infinite polyalanine helix in water at 2 °C; the abscissa

[66] A plot of the molar ellipticity values at 201 nm for the series **3** peptides versus the number of alanine has a correlation coefficient of -0.002, signifying no length dependence at this wavelength.

at 222 nm—$[\theta_\infty]_{222}$— is –59,600 ± 1300 deg cm^2 dmol^{-1} residue^{-1}.

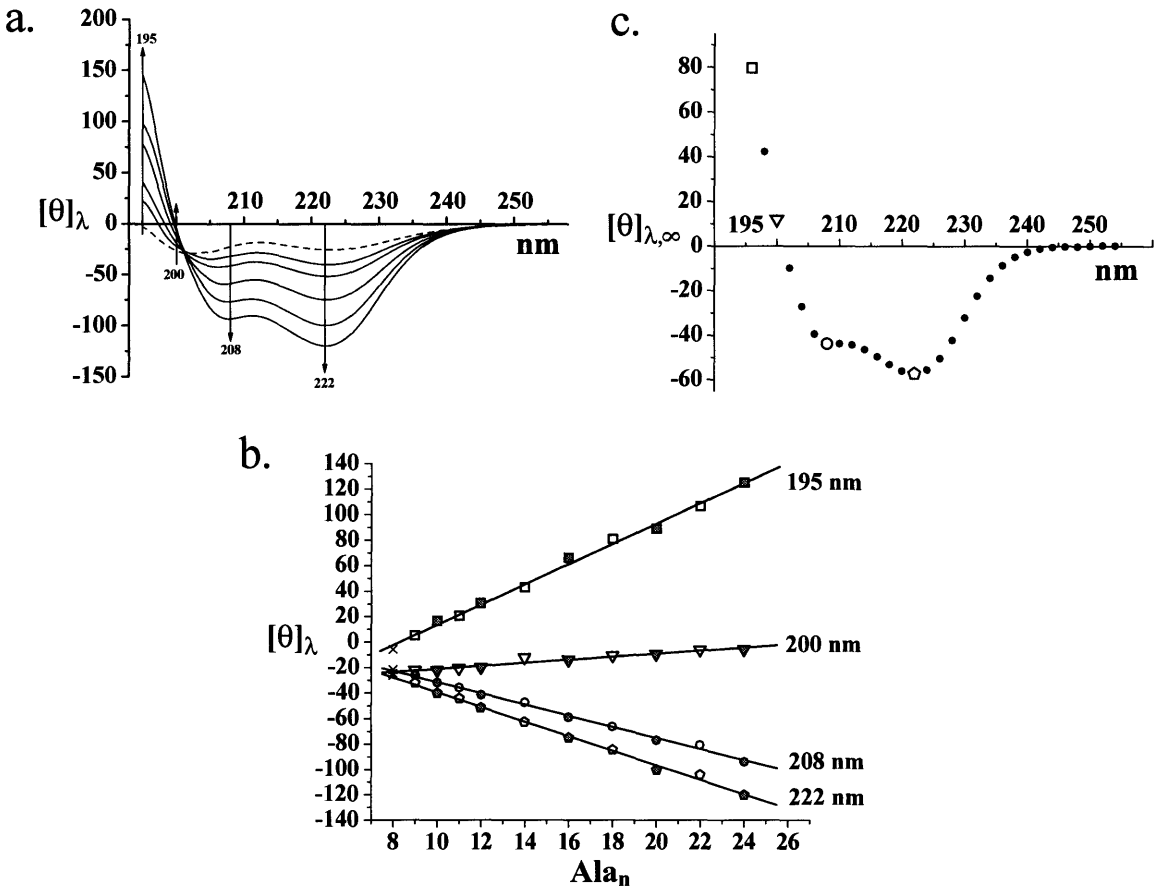

Figure 19: (a) Stacked CD spectra for series 3 (n = 10, 12, 16, 20, 24) peptides in water at 2 °C, pH = 4.5 – 6.0. Values are molar ellipticity (units = 10^{-4} deg cm^2 dmol^{-1}), uncorrected for contributions from solubilizing, capping, and spacing residues. (b) Linear regression plots at four wavelengths for series 3 peptides; data from the CD spectra appearing in part a. are shown as filled icons. Although data from series 3 Ala_8 were not used to calculate the regression line, the molar ellipticity values for the peptide are included (crosses) to demonstrate fit to extrapolated values. (c) The extrapolated CD spectrum of a completely helical alanine residue within an infinite α-helix—$[\theta_\infty]_\lambda$ units = 10^{-4} deg cm^2 dmol^{-1} residue^{-1}. The spectrum is a compilation of slopes from linear regressions in part b and others like those.

4.2. Calculation of X

Although the calculation of limiting ellipticity requires no correction for the contribution of non-alanine residues, determination of the value of X does. The CD data at 222 nm of series **3** peptides $[\theta_n]_{222}$ were corrected for capping and solubilizing contributions by subtracting $[\theta_0]_{222}$. The results were then divided by the corresponding average FH_{total} values (Table 1). The least-squares linear fit of the data gave X = 2.8 ± 0.3 and $[\theta_\infty]_{222}$ = –60,500 ± 1250 deg cm^2 dmol^{-1} residue^{-1}, very close to the value in the previous section. Moreover, analogous calculations using the low and high bounds for FH_{total} yielded X and $[\theta_\infty]_{222}$ values identical within the margin of error.

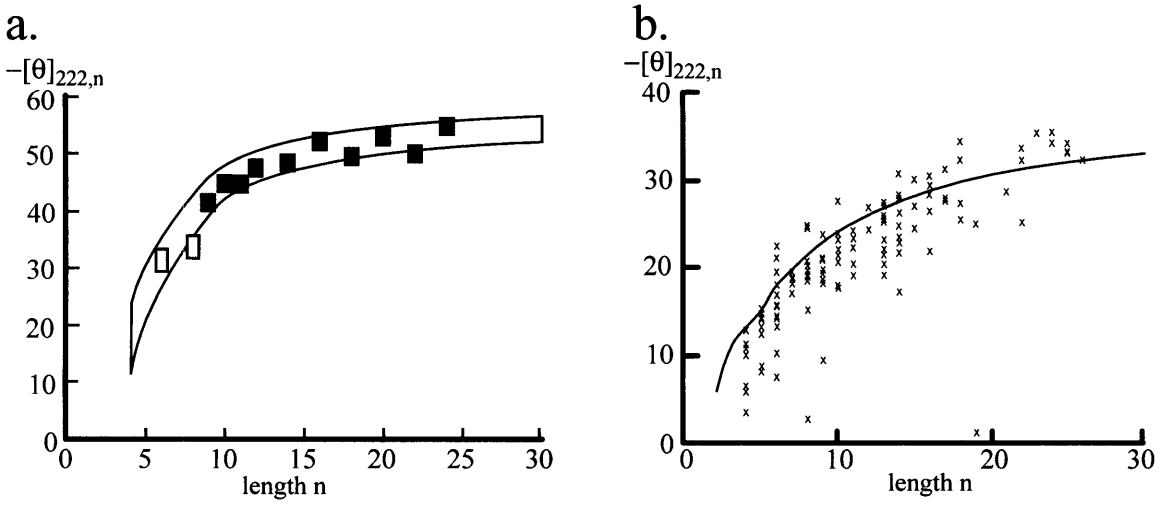

Figure 20: (a) Graph of the length dependence of per-residue molar ellipticity at 222 nm calculated from $[\theta_\infty]_{222}$ = –60,500 (± 1250) deg cm^2 dmol^{-1} residue^{-1} and X = 2.8 (± 0.3) residues. Ten experimental values for $[\theta_n]_{222}$ (units = deg cm^2 dmol^{-1} residue^{-1}) calculated from series 3 peptides, corrected for contributions from the non-helical regions, are shown as solid squares. Corresponding values calculated from series 3 Ala_6 and Ala_8 are shown as shaded squares. (b) Analogous graph of the length dependence of $[\theta_n]_{222}$ derived from analysis of the CD spectra for proteins from the PDB; $[\theta_\infty]_{222}$ = –37,000 deg cm^2 dmol^{-1} residue^{-1}, X = 2.6 – 3.0 residues. This graph was constructed from data appearing in reference 13.

5. Discussion

5.1. Comparison with PDB-Derived Results

The graph of $[\theta_n]_{222}$ versus alanine length (Figure 20a) was constructed using mean FH and X values for series **3** peptides. A similar per-residue graph, constructed from deconvolutions of CD spectra of proteins in the PBD, is presented in Figure 20b; the large amount of scatter contrasts with the graph derived from our peptide CD data. Furthermore, protein CD data give a value of –37,000 deg cm^2 dmol^{-1} residue^{-1} for $[\theta_\infty]_{222}$. What is the origin of this discrepancy? The α-helices found in proteins represent the full range of α-helical ϕ,ψ angles in the elliptical α-helical area of the Ramachandran diagram; this is not surprising given that close packing in proteins often requires some deviations from the Corey–Pauling values. In fact, three-quarters of the helices found in the PDB are curved or kinked.[70] On the other hand, our helical peptides have no such constraints, and one might expect a more uniform helical structure than that found in natural proteins. If a peptide is proven to be α-helical, the ϕ dihedral angle of a residue can be found from its $^3J_{HNH\alpha}$ coupling constant. E.COSY HNCA experiments on the uniformly labeled series **2** Ala_{12} peptides ($^{U}Ala_6A_6$ and $A_6{}^{U}Ala_6$) gave an average alanine value of 3.4 ± 0.5 Hz. The core residues gave a value of 3.0 Hz, which was fitted to the Karplus equation using parameters of Vuister,[67] Pardi,[68] and Ludvigsen.[69] The respective values for ϕ were –50.4°, –48.6°, and –52.7°, which are all close to the Pauling–Corey value but much lower than the average value from the PDB (–62 ± 7°).[70] Considering that the CD signal of a peptide helix arises from coupling between closely spaced, helically arrayed amides, it is plausible that the variation in the relative orientations of the amides associated with varying dihedral angles reduces the intensity of the CD signal. This is the likely explanation for the scatter of data points in Figure 20b and the

[67] Vuister, G.W.; Bax, A. "Quantitative *J* Correlation: A New Approach for Measuring Homonuclear Three-Bond $J(H^NH^\alpha)$ Coupling Constants in ^{15}N-Enriched Proteins" *J. Am. Chem. Soc.* **1993**, *115*, 7772–7777.

[68] Pardi, A.; Billeter, M.; Wüthrich, K. "Calibration of Angular Dependence of the Amide Proton–Cα Proton Coupling Constants, $^3J_{HN\alpha}$, in a Globular Protein" *J. Mol. Biol.* **1984**, *180*, 741–751.

[69] Ludvigsen, S.; Andersen, K.V.; Poulsen, F.M. "Accurate Measurements of Coupling Constants from Two-dimensional Nuclear Magnetic Resonance Spectra of Proteins and Determination of ϕ-Angles" *J. Mol. Biol.* **1991**, *217*, 731–736.

[70] Barlow, D.J.; Thornton, J.M. "Helix Geometry in Proteins" *J. Mol. Biol.* **1988**, *201*, 601–619.

accompanying value of $[\theta_\infty]_{222}$.

5.2. Other Peptide Models

We are not the first to calculate the limiting ellipticity for CD measurements using peptide models; however, the verification and quantitation of helical structure underlying our analysis is the most thorough so far. In addition to the problem of defining the length of the helical region, most peptide studies have relied on helix-promoting perfluorinated alcohol additives.

Much research on helicity has been conducted with alanine-rich peptides containing solubilizing lysine residues interspersed with the alanine residues; a typical motif is a repeating -A_4K- unit. Values of $[\theta_\infty]$ near –44,000 deg cm^2 dmol^{-1} residue^{-1} have been obtained as extrapolated limits of additive-dependent CD spectra; we are not the only group to find this value is too low to account for the helical CD spectra of alanine-rich peptides.[71] A significant difficulty with these methods is ensuring that the change in CD signal indicates only a change in peptide structure with no solvent-dependent contribution. A typical strategy is illustrated by the TFE-dependent study conducted by Baldwin.[59a] As TFE concentration increases, a peptide in a TFE/water solution exhibits a stronger helical CD signal. The increase in CD signal levels out at 40% TFE; the value at this point matches the limiting ellipticity the authors obtained by nonlinear least squares analysis of the data using a Lifson–Roig algorithm. No independent verification of the implied high helicity of the peptides in TFE solution was provided.

5.3. X Values

The value of X obtained from our peptides lies within the range of values found in the literature. However, because features of the helical termini may affect the X value, our value may not be relevant to other peptide series. Moreover, unlike the limiting ellipticity, the value of X will always have a relatively large error associated with it; relatively small changes in slope cause significant variation in the x-intercept. The large

[71] Farmer, R.S.; Kiick, K.L. "Conformational Behavior of Chemically Reactive Alanine-Rich Repetitive Protein Polymers" *Biomacromolecules* **2005**, *6*, 1531–1539.

error in X has a profound effect on calculation of the fractional helicity of small peptides. For a peptide with 24 residues, the error in $[\theta_{24}]_{222}$ calculated from our values for $[\theta_{\infty}]_{222}$ and X is 4%; for a peptide half as long, the error in $[\theta_{12}]_{222}$ increases to 7%. Thus, even if a value of X can be determined for a particular peptide series, calculation of the fractional helicity of short peptides by CD will be approximate.

5.4. Future Directions

The success of our helical standards project makes likely an extension to other helix-forming α-amino acids, both natural and unnatural. Provided our capping and solubilization strategies function for α-amino acids other than alanine, the assumption that side chains do not affect the CD signal of the α-helix could be tested.

Furthermore, although they are formal equivalents of UV extinction coefficients, $[\theta]_{\lambda}$ values differ in that they have been reported to vary with temperature. This phenomenon could be a consequence of conformational change in the α-helix with temperature; a gradual change in the tilt of the carbonyl group relative to the helical axis is one possibility. Variable temperature NMR and CD experiments with our helical standards offers a way to resolve this issue as well.

5.5. Summary

The Hel- and *beta*-capped polyalanine peptides in this study were found to lack tertiary structure. NMR and CD evidence demonstrated that the helical structure of the capped alanine region was not dependent on the solubilizing regions. The helix-initiating conformation of the N-terminal Hel cap was verified by NMR spectroscopy; the helix-promoting and terminating properties of the C-cap *beta* were likewise explained. To achieve maximal helicity, the carboxylate group of $^{\beta}$DHel must be fully ionized. Presence of significant 3_{10} helicity in the capped peptides was excluded by a recently introduced, modified HNCO NMR experiment that detects $^{3}J_{NC'}$ scalar couplings.

Fractional helicity of the peptides was calculated by NH→ND exchange experiments. The PF_i values, along with amide ^{1}H chemical shift data, indicated that Ala_n peptides with $n > 8$ possess a "core" of (n-8) alanine residues different from the first

and last four alanine residues, which are in contact with the caps. These core regions exhibit FH values greater than 99.5%; this constancy allows for calculation of $[\theta_\infty]_{222}$ without correction of $[\theta_n]_{222}$ values for contributions of the solubilizing regions and caps. Such a correction is necessary, though, to calculate the value of X; our value for X (2.8 ± 0.3) is similar to values previously reported. Linear regressions of the $[\theta_n]_\lambda$ values for series **2** and **3** peptides ($n > 8$) over the wavelength range of 195 – 255 nm gave slopes defining the spectrum of a single alanine residue in an infinite helix, $[\theta_\infty]_\lambda$. We calculated a value of (–60.5 ± 1.3) × 10^3 deg cm^2 $dmol^{-1}$, significantly greater than values derived from protein data but consistent with our previous approximate estimates.[32] This discrepancy is possibly caused by a variation in the structure of helices within proteins. Measurement of $^3J_{HNH\alpha}$ couplings for the core region of the series **2** Ala_{12} peptide indicated a dihedral angle of –50.5°, which is significantly closer to the ideal Corey–Pauling value than the average PDB value.

6. Experimental Procedures and Supplemental Data

6.1. Reagents

All reagents, organic solvents, and purchased chemicals were used as received from the supplier. The suppliers were as follows: all 9-fluorenyl-methoxycarbonyl (Fmoc)-amino acids from Novabiochem; [*O*-(7-azabenzotriazol-1-yl)-1,1,3,3-tetramethyluronium hexafluorophosphate] (HATU) and PAL-PEG-PS resin (polystyrene functionalized with poly(ethylene glycol) Peptide Amide Linker) from Applied Biosystems; biosynthesis-grade *N*,*N*-dimethylformamide (DMF), HPLC-grade acetonitrile, HPLC-grade methanol, and anhydrous diethyl ether from either EM Science or Mallinckrodt; diisopropylethylamine (DIEA) and 1,8-diazabicyclo[5.4.0]undec-7-ene (DBU) from Aldrich. *trans*-2-Aminocyclohexanecarboxylic acid (Acc) was purchased from Albany Molecular. All other materials were obtained from either Aldrich or Alfa Aesar. Water used for NMR and CD experiments and HPLC purification was deionized to 18 MΩ with a Millipore Gradient A10 system equipped with a total organic carbon (TOC) monitor reading under 5 ppb. Uniformly-labeled ^{13}C,^{15}N-alanine was purchased from Cambridge Isotope Laboratories, Inc. The Fmoc group was added using the same procedure used for synthesis of Fmoc-Acc.

6.2. Small Molecule Synthesis and Reagents

The synthesis of FmocHel differed slightly from the published procedure. The characterization data for the final compound were identical to an authentic sample produced by the original procedure. Only the zwitterion had not been previously reported. Unless otherwise noted, all precursors, reagents, and organic solvents were purchased from either Aldrich or Alfa-Aesar.

(1*S*, 4*S*, 7*S*, 10*S*)-2-Oxo-9-thia-3,12-diaza-tricyclo[8.2.1.03,7]tridecane-4-carboxylic acid (16)

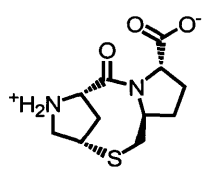

The acid **15** (1.0 g, 2.6 mmol) was dissolved in 60 mL ethanol and transferred to a Parr bottle containing 4 g Pd/C (10%, 50% H_2O by weight). The vessel was then placed

in the shaker, under a H_2 atmosphere (50 psig). After 24 h the reaction was stopped and the mixture was filtered; solvent was removed *in vacuo* to yield 0.47 g (72%) of the title compound as a light yellow foam. ^{1}H NMR ($CDCl_3$, 300 MHz) δ 8.19 (broad s, 2H), 5.35 (broad s, 1H), 4.53 (dd, 1H, J = 7.1, 3.0 Hz), 4.28 (d, 1H, J = 10.4 Hz), 3.54 (m, 2H), 3.37 (d, 1H, J = 10.2 Hz). ^{13}C NMR ($CDCl_3$, 125 MHz) δ 25.8, 34.2, 38.0, 38.8, 40.8, 55.1, 58.9, 61.9, 62.1, 172.3, 175.3. IR (cm^{-1}, film) 1408, 1588, 1710, 2954, 3364. $[\alpha]_D^{23}$ = +48.6 ($CHCl_3$, c 1.2). HRMS calcd for [$C_{11}H_{16}N_2O_3S$ + H] 257.0954, found 257.0963. A ^{1}H NMR spectrum of the TFA salt of **16** in d_6-DMSO appears below. The sample was purified by reverse-phase HPLC [1 to 35% MeCN in 0.05% TFA/H_2O, 30 min. gradient].

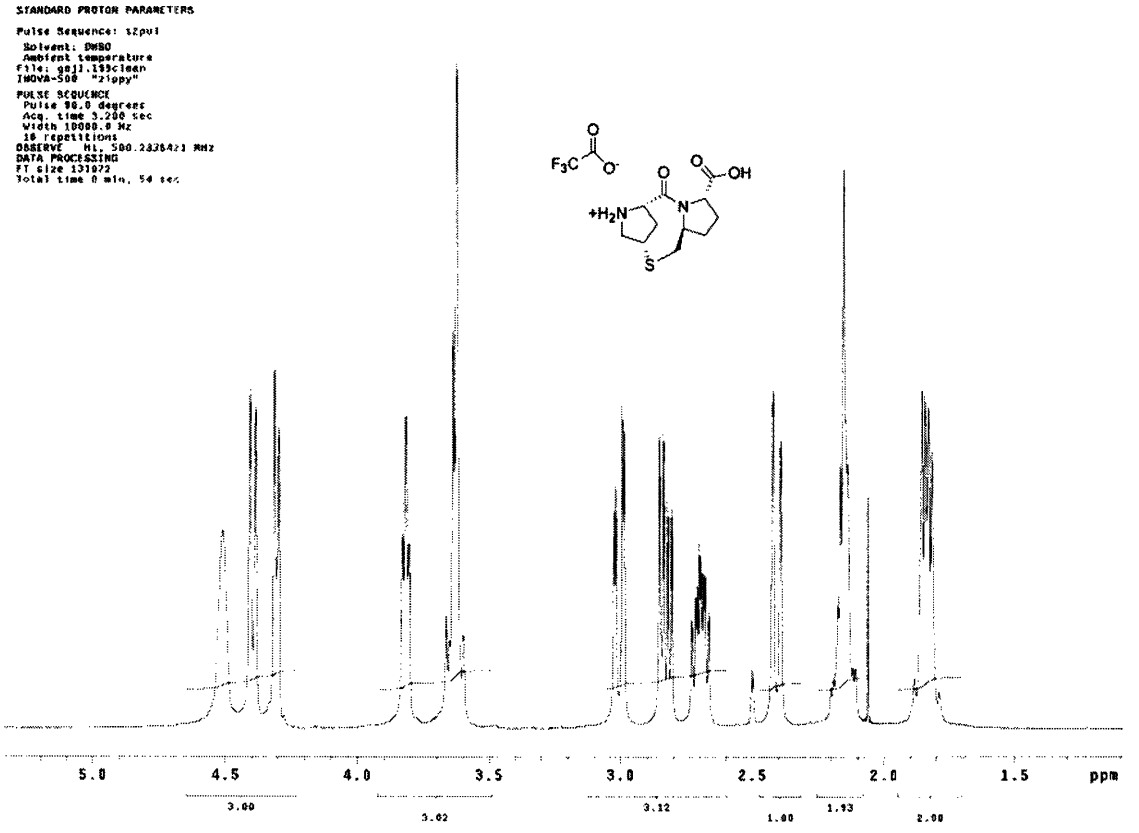

***trans*-4-(Fluorenylmethoxycarbonylamino)-cyclohexanecarboxylic acid (trans-Fmoc-Acc-OH)**

To a cold solution of 1 M K_2CO_3 (26 mL) and dioxane (10 mL) was added *trans*-Acc-OH (1.0 g, 5.6 mmol). FmocCl (1.45 g, 5.6 mmol) was added and the mixture was stirred at 0 °C for 5 h and then allowed to warm to room temperature overnight. Afterwards, the milky solution was poured into 300 mL water; with some shaking the mixture became homogeneous. The aqueous mixture was washed with diethyl ether (2 x 100 mL) and then cooled with an ice bath. The solution was adjusted to pH 2 using cold 6 M HCl; a solid formed and was collected by vacuum filtration. The filter cake was washed well with water, allowed to air dry overnight, and then placed under high vacuum to yield 1.65 g (81%) of an off-white powder. The crude product was sufficiently pure to use in the synthesis of peptides. A small sample was recrystallized from acetonitrile and characterized. ^{1}H NMR (d_6-DMSO, 500 MHz), major amide rotamer: δ12.02 (s, 1H), 7.89 (2H, d, J = 7.6 Hz), 7.68 (2H, d, J = 7.5 Hz), 7.41 (2H, t, J = 7.3 Hz), 7.33 (2H, t, J = 7.5 Hz), 7.24 (1H, d, J = 7.5 Hz), 4.27 (2H, d, J = 6.9 Hz), 4.20 (1H, t, J = 6.3 Hz), 3.22 (1H, m), 2.09 (1H, t, J = 11.8 Hz), 1.88 (2H, d, J = 12.1 Hz), 1.81 (2H, d, 10.4 Hz), 1.33 (2H, q, J = 11.9 Hz), 1.18 (2H, q, J = 11.1 Hz). Signals arising from the minor amide rotamer are visible; all of these signals are broad and poorly resolved: δ 7.63, 6.68, 4.44, 1.96, 1.75, 1.46, 1.10, 0.94. The minor peaks merge with those of the major rotamer at 60 °C. ^{13}C (d_6-DMSO, 125 MHz): δ 176.5, 155.4, 144.00, 141.0, 128.0, 127.1, 125.2, 120.2, 65.1, 49.1, 46.8, 41.6, 31.6, 27.6. IR (powder, cm^{-1}): 1045, 1451, 1540, 1686, 1697, 1712, 2945, 3338. Melting point: decomposition occurred at 230 °C. Elemental analysis calcd for $C_{22}H_{23}NO_4$ (found): C 72.31 (72.03), H 6.34 (6.34), N 3.83 (4.08). HRMS calcd for [M+H] 366.1700, found 366.1696.

6.3. Peptide Synthesis

Peptides were synthesized on a Pioneer Peptide Synthesizer using Fmoc solid phase synthesis (0.025 mmol scale). Nine equivalents of Fmoc-amino acids were activated by DIEA and nine equivalents of HATU before a 30 minute continuous-flow

coupling to the PAL-PEG-PS resin (0.2 meq/g). Resin washes were performed with biosynthesis grade DMF. Deblocking was done with a 48:1:1 (v:v:v) mixture of dimethyl formamide (DMF) : piperidine : DBU. After the final wash, the resin was washed with methanol and dried under a nitrogen flow.

Extended couplings of 1 h were needed to achieve adequate yields with 2-3 equivalents of FmocHel. A single recoupling was required to add the $^{\beta}$Asp residue to the Hel template in good yield.

Peptides were cleaved manually from the resin with 5 mL of a freshly made cocktail of trifluoroacetic acid (82.5% by vol.), water (5% by vol.), thioanisole (2.5% by vol.), phenol (5% by weight), and 1,2-dithioethane (2.5% by vol.) for two hours. Dropwise addition of the cleavage solution to cold diethyl ether precipitated the peptide as a white solid that was isolated by centrifugation and decanting the ether. The solid was washed and isolated three times with ether before drying under high vacuum.

6.4. Peptide Purification

A sample of crude peptide was taken up in 5 mL water and purified by semi-prep reverse phase HPLC using a gradient (1%/min) of 5 to 35% acetonitrile in 0.05% TFA/water—YMC ODS-AQ 200 Å, 4.5 x 150 mm stainless steel column (Waters), Waters 600 HPLC with a 996 PDA UV detector at 214 nm. Purity was assessed by analytical reverse-phase HPLC using a similar program method (Waters 2690 HPLC with auto injector and a 996 PDA UV detector at 214 and 280 nm). Typically, two prep runs were required to achieve purity >95%, as judged by analytical HPLC and mass spectroscopy. Samples were lyophilized and stored at –40 °C.

6.5. Peptide Mass Spectrometry

Mass spectra were obtained on a Waters Micromass ZMD 4000 mass spectrometer with electrospray ionization. The instrument was calibrated over the *m/z* range of 50 to 2000 Daltons with a NaI/RbI standard (2.0/0.05 μg/μL) in 1:1 water:isopropanol; a tolerance of ±1.0 mass units is observed. The multiple Lys residues in each peptide create a manifold of *m/z* peaks.

Series 3 Peptide	**Electrospray Mass Spectrometry (M+zH)/z Found (Expected)**
Ac-W-K_5-Inp_2-^{t}L-$^\beta$D-Hel-*beta*-^{t}L-Inp_2-K_5-NH_2	1318.84 (1320.30); 880.62 (879.56); 660.79 (659.92); 528.89 (528.14); 441.20 (440.28)
Ac-W-K_5-Inp_2-^{t}L-$^\beta$D-Hel-A_4-*beta*-^{t}L-Inp_2-K_5-NH_2	975.44 (974.28); 731.90 (730.96); 585.75 (584.97); 488.36 (487.64)
Ac-W-K_5-Inp_2-^{t}L-$^\beta$D-Hel-A_5-*beta*-^{t}L-Inp_2-K_5-NH_2	999.02 (997.95); 749.58 (748.72); 599.99 (599.18); 500.15 (499.48)
Ac-W-K_5-Inp_2-^{t}L-$^\beta$D-Hel-A_6-*beta*-^{t}L-Inp_2-K_5-NH_2	1022.72 (1021.63); 767.39 (766.48); 614.12 (613.38); 512.06 (511.32); 439.11 (438.42)
Ac-W-K_5-Inp_2-^{t}L-$^\beta$D-Hel-A_7-*beta*-^{t}L-Inp_2-K_5-NH_2	1046.42 (1045.31); 785.20 (784.24); 628.36 (627.59); 523.85 (523.16)
Ac-W-K_5-Inp_2-^{t}L-$^\beta$D-Hel-A_8-*beta*-^{t}L-Inp_2-K_5-NH_2	1070.00 (1068.99); 802.64 (802.00); 642.49 (641.80); 535.64 (535.00); 459.25 (458.72)
Ac-W-K_5-Inp_2-^{t}L-$^\beta$D-Hel-A_9-*beta*-^{t}L-Inp_2-K_5-NH_2	1093.83 (1092.67); 820.57 (819.75); 656.86 (656.01); 547.55 (546.84); 469.44 (468.86)
Ac-W-K_5-Inp_2-^{t}L-$^\beta$D-Hel-A_{10}-*beta*-^{t}L-Inp_2-K_5-NH_2	1117.53 (1116.35); 838.38 (837.51); 671.10 (670.21); 559.47 (558.68); 479.64 (479.01); 419.51 (419.26)
Ac-W-K_5-Inp_2-^{t}L-$^\beta$D-Hel-A_{11}-*beta*-^{t}L-Inp_2-K_5-NH_2	1141.24 (1140.03); 856.31 (855.27); 685.35 (684.42); 571.26 (570.52); 489.83 (489.16); 428.79 (428.14)
Ac-W-K_5-Inp_2-^{t}L-$^\beta$D-Hel-A_{12}-*beta*-^{t}L-Inp_2-K_5-NH_2	1164.94 (1163.71); 874.12 (873.03); 699.47 (698.63); 583.17 (583.36); 500.02 (499.31); 437.64 (437.02)
Ac-W-K_5-Inp_2-^{t}L-$^\beta$D-Hel-A_{14}-*beta*-^{t}L-Inp_2-K_5-NH_2	1212.47 (1211.07); 909.61 (908.55); 727.97 (727.04); 606.87 (606.04); 520.29 (519.60); 455.44 (454.78)
Ac-W-K_5-Inp_2-^{t}L-$^\beta$D-Hel-A_{16}-*beta*-^{t}L-Inp_2-K_5-NH_2	1259.87 (1258.42); 945.10 (944.07); 756.34 (755.46); 630.58 (629.72); 540.68 (539.90); 473.25 (472.54)
Ac-W-K_5-Inp_2-^{t}L-$^\beta$D-Hel-A_{18}-*beta*-^{t}L-Inp_2-K_5-NH_2	1307.40 (1305.78); 980.84 (979.59); 784.83 (783.87); 654.28 (653.39); 560.94 (560.20); 491.06 (490.30)
Ac-W-K_5-Inp_2-^{t}L-$^\beta$D-Hel-A_{20}-*beta*-^{t}L-Inp_2-K_5-NH_2	1354.56 (1353.14); 1016.21 (1015.11); 813.20 (812.29); 677.86 (677.07); 581.20 (580.49); 508.74 (508.06)
Ac-W-K_5-Inp_2-^{t}L-$^\beta$D-Hel-A_{22}-*beta*-^{t}L-Inp_2-K_5-NH_2	1401.97 (1400.50); 1051.83 (1050.63); 841.69 (840.70); 701.56 (700.75); 601.47 (600.79); 526.55 (525.82)
Ac-W-K_5-Inp_2-^{t}L-$^\beta$D-Hel-A_{24}-*beta*-^{t}L-Inp_2-K_5-NH_2	1449.50 (1447.86); 1087.44 (1086.14); 870.19 (869.12); 725.39 (724.43); 621.86 (621.09); 544.36 (543.58)

Series 2 Peptide	Electrospray Mass Spectrometry (M+zH)/z Found (Expected)
Ac-$^{\beta}$D-Hel-*beta*-Acc-K_2-W-NH_2	1066.98 (1066.55), 534.09 (533.78), 356.38 (356.19)
Ac Ac-$^{\beta}$D-Hel-A_4-*beta*-Acc-K_2-W-NH_2	675.95 (675.85); 451.01 (450.90)
Ac-$^{\beta}$D-Hel-A_6-*beta*-Acc-K_2-W-NH_2	747.06 (746.89); 497.87 (498.26)
Ac-$^{\beta}$D-Hel-A_8-*beta*-Acc-K_2-W-NH_2	818.28 (817.93); 545.76 (543.60)
Ac-$^{\beta}$D-Hel-A_{10}-*beta*-Acc-K_2-W-NH_2	889.02 (888.96); 593.41 (592.98)
Ac-$^{\beta}$D-Hel-A_{12}-*beta*-Acc-K_2-W-NH_2	960.87 (960.00); 640.57 (640.34)
Ac-$^{\beta}$D-Hel-A_{14}-*beta*-Acc-K_2-W-NH_2	1031.07 (1031.04); 687.91 (687.69)
Ac-$^{\beta}$D-Hel-A_{16}-*beta*-Acc-K_2-W-NH_2	1102.97 (1102.07); 735.75 (735.05); 552.15 (551.54)

Series 2 Peptide with Uniformly Labeled ^{13}C, ^{15}N Alanine	Electrospray Mass Spectrometry (M+zH)/z Found (Expected)
Ac(D_3)-$^{\beta}$D-Hel-A_8(2,3,3,3,-D_4)-*beta*-NH_2	1102.72 (1102.71), 552.02 (551.86)
Ac-$^{\beta}$D-Hel-A_8(U-$^{13}C_3$,^{15}N)-*beta*-Acc-K_2-W-NH_2	804.00 (833.95), 556.44 (556.31)
Ac-$^{\beta}$D-Hel-A_6-A_6(U-$^{13}C_3$,^{15}N)-*beta*-Acc-K_2-W-NH_2	971.88 (972.02); 647.96 (648.35)
Ac-$^{\beta}$D-Hel-A_6(U-$^{13}C_3$,^{15}N)-A_6-*beta*-Acc-K_2-W-NH_2	971.88 (972.02); 648.21 (648.35)

6.6. Analytical Ultracentrifugation Data

Data were acquired on a Beckman Optima X1-A centrifuge and a six-channel cell in a An-60 Ti analytical rotor.[72] Selected series **2** and **3** peptides were shown to be monomeric by sedimentation equilibrium analysis at 45,000 rpm. Samples were tested over the concentration range of NMR experiments (1 – 2 mM) because aggregation is more likely for concentrated samples. The linear distributions of $\ln(c_r)$ vs. $r^2/2$ for the samples in 20 mM NaH_2PO_4 at 2 °C are consistent with monomeric species (Figure 21).

[72] Facility maintained by the Imperiali group.

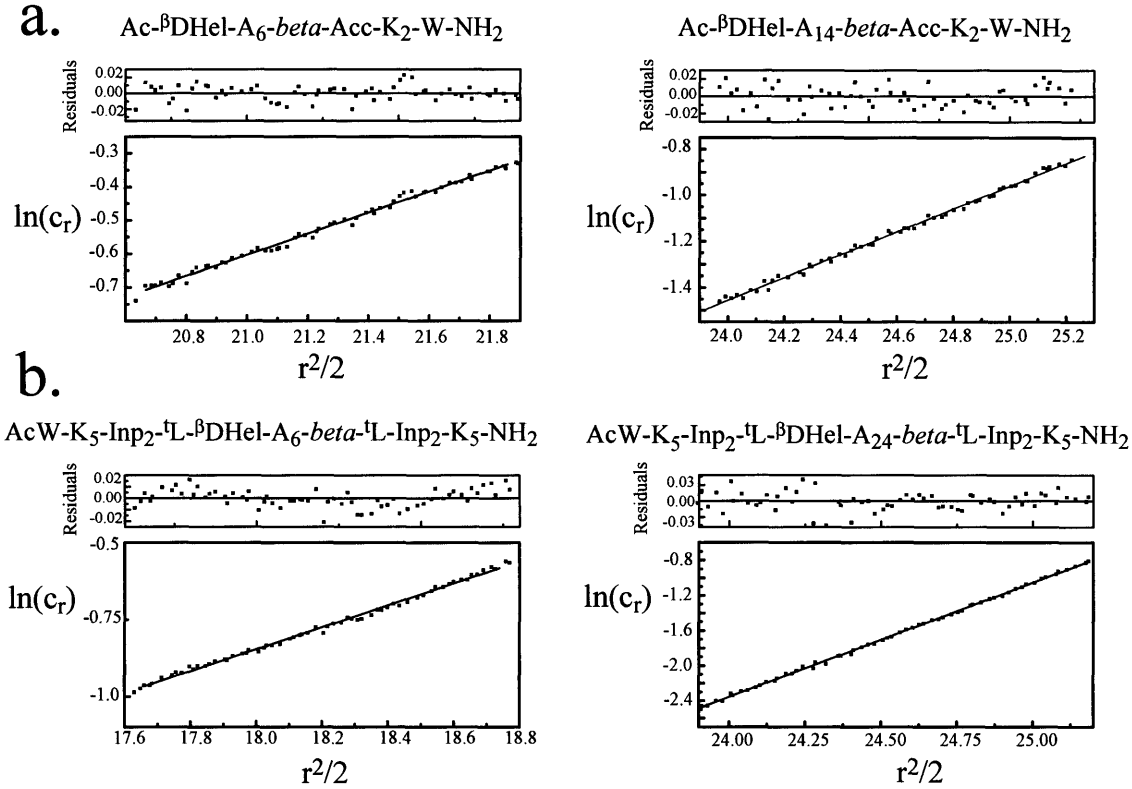

Figure 21: Sedimentation equilibrium analyses–45,000 rpm in 20 mM NaH_2PO_4 at 2 °C for (a) Ac-$^{\beta}$D-Hel-A_n-β-Acc-K_2-W-NH_2 in 20 mM NaH_2PO_4 at 2 °C (n = 6, 14) and (b) Ac-W-K_5-Inp_2-^{t}L-$^{\beta}$D-Hel-A_n-β-^{t}L-Inp_2-K_5-NH_2 (n = 6, 24).

6.7. Circular Dichroism

CD spectra were obtained on an Aviv 62DS spectrometer with a thermoelectric temperature controller and an Osram XBO 450W high-pressure Xenon lamp using a 10 mm QS cell (suprasil, Hellma). After a 12 min. temperature equilibration at 2 °C, measurements were made from 195 to 255 nm with a 1.0 nm bandwidth and a 0.5 nm step size; a total of five scans were averaged for each spectrum. The instrument was calibrated with titrated water solutions of sublimed 9-camphorsulfonic acid, as directed in the operating manual.

Peptides were dissolved in 20 mM NaH_2PO_4 solution. Concentration was determined by UV absorption of the Trp chromaphore (ε_{280} = 5560 cm^{-1} M^{-1})[32] on a Cary 300 UV–Vis instrument; CD measurements were made on peptides ranging from 10–20

μM. After blank correction, the data were divided by the concentration to obtain the molar ellipticity at each wavelength (Equations 16 and 17). The data were then smoothed using 5-point Fast Fourier Transform (FFT) smoothing in the Origin® 7.0 software package (OriginLab Corporation). Per-residue values were obtained by dividing the smoothed data by the number of alanine residues in the peptide.

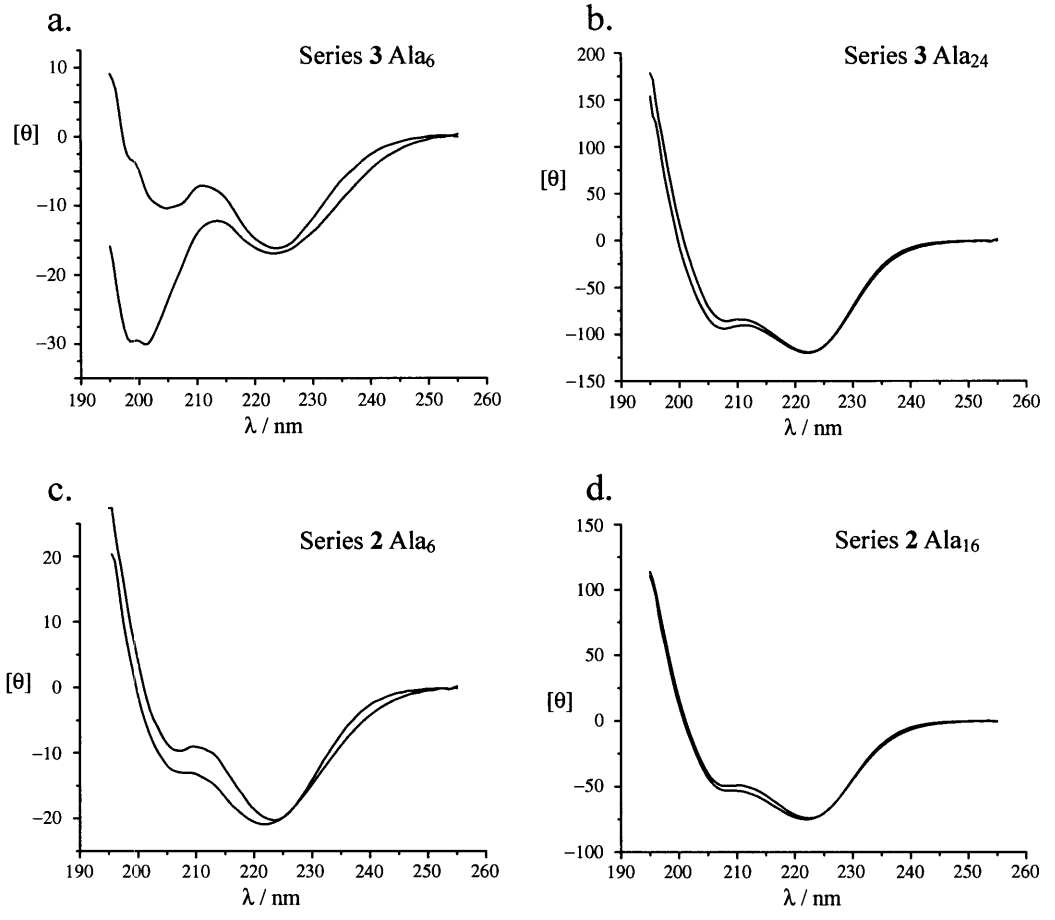

Figure 22: Comparison of CD spectra before and after correction for the contributions of residues other than alanine. [θ] units = deg cm^2 dmol^{-1}. For all spectra, $[\theta]_{corrected} \geq [\theta]_{uncorrected}$.

$$\theta_\lambda = [\theta]_\lambda cl \qquad \mathbf{1}$$

$$[\theta]_\lambda = \theta_\lambda / cl \qquad \mathbf{17}$$

$$10^{-1} \text{ mdeg / M cm} = \text{deg cm}^2 \text{ / dmol} \qquad \mathbf{18}$$

Data corrected for contributions from the non-helical caps, spacers, and solubilizing regions, were obtained by subtracting the smoothed molar ellipticity spectrum of Ac-W-K_5-Inp_2-^{t}L-$^{\beta}$DHel-*beta*-^{t}L-Inp_2-K_5-NH_2 for series **3** or Ac-$^{\beta}$DHel-*beta*-Acc-K_2-W-NH_2 for series **2**. The effects of the subtraction, and the associated measurement error, are most dramatic for short members of series **3** (Figure 22).

6.8. pH Measurement

Measurements were made at ambient temperature with a Radiometer Copenhagen PHM240 pH meter equipped with a Cole-Parmer EW-55529-08 glass electrode, standardized daily with pH 4.0 and pH 7.0 standard buffer solutions purchased from VWR Scientific. For measurements in D_2O, the meter reading was adjusted using the standard formula: pH = pD + 0.4.

6.9. NMR Experiments: General

I am indebted to my collaborator Dr. Bjorn Heitman for his NMR expertise; he collected all but a few of the spectra acquired during this research project. Spectra were collected on a Bruker Avance 600 instrument equipped with four channels and a pulsed field gradient triple probe with z gradients, unless otherwise noted. Processing and data analysis were done on an SGI O2 workstation running XWINNMR 3.5 software (Bruker). Unless otherwise stated, all spectra except those for the NH→ND exchange experiments were taken in H_2O/D_2O (95/5, v/v) 40 mM phosphate buffer using a relaxation delay of 1.8 s or greater. 2,2-Dimethyl-2-silapentane-5-sufonic acid (DSS) was used as the internal reference for ^{1}H chemical shifts; ^{13}C and ^{15}N chemical shifts were referenced in accordance with IUPAC recommendations.[73] For data processed in the indirect dimensions, zero filling was applied, and a square sine bell shifted by $\pi/2$ was used for apodization in all dimensions.

---

[73] Markley, J.L.; Bax, A.; Arata, Y.; Hilbers, C.W.; Kaptein, R.; Sykes, B.D.; Wright, P.E.; Wütrich, K. "IUPAC-IUBMB-IUPAB Inter-union Task Group on the Standardization of Data Bases of Protein and Nucleic Acid Structures Determined by NMR Spectroscopy." *Pure Appl. Chem.* **1998**, *70*, 117–142.

Table 2: Proton Chemical Shifts of Peptide 1

Residue	H_N	H_α	H_β	Miscellaneous
$^\beta$Asp	8.62	4.81	3.27, 2.74	*beta* NH_3: 8.00
Ala_1	7.39	4.29	1.44	
Ala_2	8.22	4.19	1.45	terminal NH_2: 7.51, 7.47
Ala_3	8.28	4.20	1.47	
Ala_4	7.97	4.21	1.48	Hel: H-2, 4.70; H-13a, 2.53; H-13b, 3.01; H-11, 3.89; H-12b, 4.20; H-12a, 4.12; H-5, 4.69; H-6a, 2.30; H-6b, 2.48; H-7a, 2.07; H-7b, 1.99; H-8, 4.65; H-9a, 3.20; H-9b, 2.86
Ala_5	8.04	4.22	1.47	
Ala_6	8.01	4.18	1.47	
Ala_7	7.93	4.21	1.47	
Ala_8	7.94	4.30	1.47	
beta	8.21	4.72	3.56, 3.36	

6.10. Peptide 1 Conformational Studies by NMR

Chemical shifts for peptide **1** (Table 2) were assigned from ^{1}H NMR, TOCSY (512c*4096c, τ_m = 70 ms),[74] and ROESY (512c*4096c, τ_m = 300 ms, Figure 23)[75] spectra using a sweep width of 6613.76 Hz and presaturation solvent suppression. The small amide peaks of the minor (cs) conformation lie downfield from the amide peaks of the major (t) conformation. A distinctive crosspeak between the C12-H and C9-H Hel protons indicated the (cs) state of Hel in the minor conformation, in accordance with previous characterization of Hel-Ala_6 conjugates (spectrum not shown).[76] The (cs) peaks increase relative to the (t) peaks as the temperature is raised or the pH is lowered; both of these actions are expected to decrease the helicity the peptide. At pH 3.8 and 280 K, a t/c value of approximately 12 was calculated for peptide **1**. Resonance areas were measured for baseline-corrected 1D ^{1}H spectra (16384c, sweep width 8992.9 Hz, presaturated for solvent suppression) using the integration menu of XWINNMR.

---

[74] Bax, A.; Davis, D.G. "MLEV-17-Based Two-Dimensional Homonuclear Magnetization Transfer Spectroscopy" *J. Magn. Res.* **1985**, *65*, 355–360.

[75] Bax, A.; Davis, D.G. "Practical Aspects of Two-Dimensional Transverse NOE Spectroscopy" *J. Magn. Res.* **1985**, *65*, 207–213.

[76] Kemp, D.S.; Allen, T.J.; Oslick, S.L. "The Energetics of Helix Formation by Short Templated Peptides in Aqueous Solution. 1. Characterization of the Reporting Helical Template Ac-Hel_1" *J. Am. Chem. Soc.* **1995**, *117*, 6641–6657.

The sample of peptide **1** that was used for the pH titration ^{1}H NMR studies was synthesized with perdeuterated alanine; the amide protons therefore appeared as singlets. The spectra were collected with a sweep width of 8992.0 Hz (16384c) over the pH range 1.3 – 8.

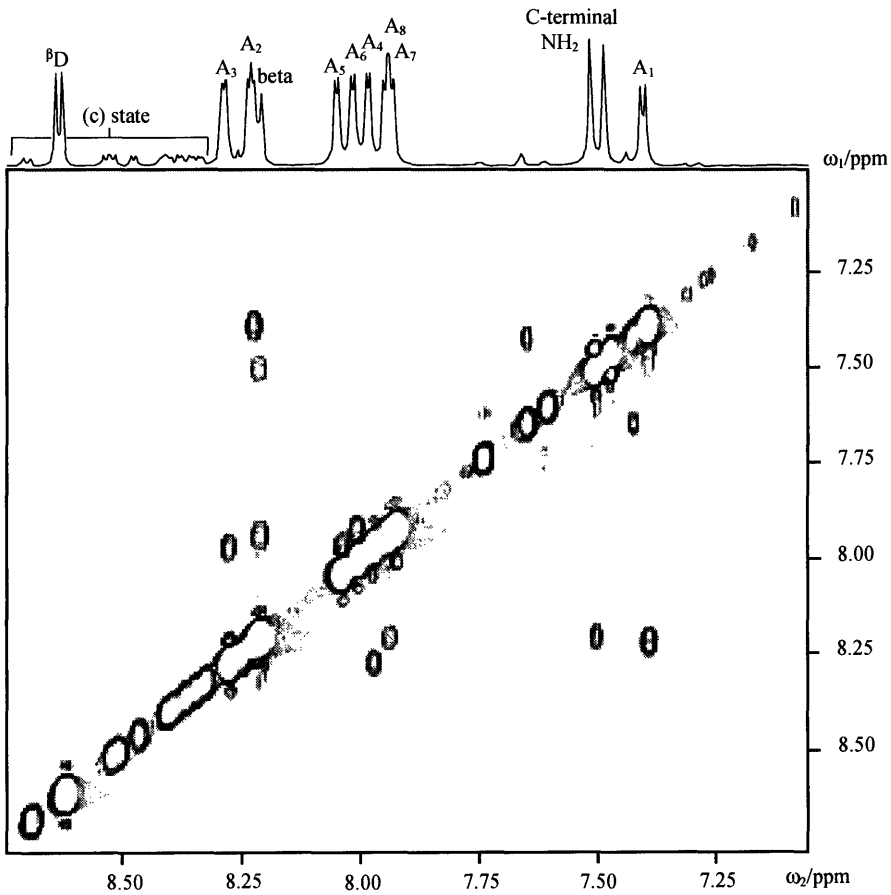

Figure 23: ROESY spectrum of peptide 1 in H_2O/D_2O (95/5, v/v), 40 mM NaH_2PO_4, 2 °C, pH 4.5, DSS internal standard.

6.11. Series 2 NMR Studies

The Ala amide proton resonances of each member of the series were assigned using TOCSY (512c*4096c, τ_m = 70 ms) and NOESY (512c*4096c, τ_m = 400 ms)[77] spectra obtained using a sweep width of 7183.9 Hz in both dimensions and watergate solvent suppression.

6.12. Amide Hydrogen–Deuterium Exchange

Peptide samples were prepared in 750 μL of 20 mM NaH_2PO_4 solution (1 – 2 mM) and the pH was adjusted to approximately 5.0 with additions of NaOH solution or H_3PO_4. Afterwards, the sample was lyophilized and the solid pellet was quickly taken up in ice-cold D_2O. The cold solution was transferred to an NMR tube and quickly placed in the NMR instrument, pre-equilibrated at 2 °C. A series of ^1H NMR spectra were collected over the course of 6 – 48 h, depending on the length of the peptide. After discarding initial spectra showing Lys, Trp, and spacer amide peaks, the remaining proton spectra were analyzed. Time-dependent peak heights and curve-fitted resonance areas for the alanine amide protons were conducted for series **2** peptides and selected members of the series **3** peptides. Satisfactory fits to pseudo-first order decay were observed for at least three half-lives. Curve fitting with Lorentzian peaks was performed using the Origin graphing software package. Each identifiable peak was fitted with a single peak; the central residues of the longer peptides were fitted with a single peak, as the resonances overlapped. R^2 values for the fits were typically greater than 0.99 with the lowest value being 0.96; all fitted peaks had appropriate line widths for amide protons, excepting large composite peaks comprising central, "core", alanine residues. Decay rates obtained from curve-fitted integrations agreed with rates for the same peak obtained from peak height (Table 3); FH calculations were performed using peak area values. Owing to the inverse relation between PF and FH, a fairly large difference in PF corresponds to a small difference in FH; as the FH of our peptides is dominated by PF_{NHi} values greater than 50, as much as a twenty percent variation in PF_{NHi} gives no significant

---

[77] Jeener, J.; Meier, B.H.; Bachmann, P.; Ernst, R.R. "Investigation of Exchange Processes by Two-Dimensional NMR Spectroscopy" *J. Chem. Phys.* **1979**, *71*, 4546–4553.

change in FH. Protection factor measurements for matching members of series **2** and **3** (Table 4) gave satisfactory agreement.

Table 3: Amide proton PF and total FH data for series 2 peptides

	PF_{NHi}																
Peptide	1	2	3	4	5	6	7	8	9	10	11	12	13	14	15	16	FH
Ala_{16} (H)	62.4	---63.4---		88.4	----------172.6----------							155.1	107.3	48.6	---15.0---		0.954
Ala_{16} (A)	68.3	---54.5---		69.7	----------177.6----------							154.3	106.9	31.1	---14.4---		0.953
Ala_{14} (H)	82.3	---74.0---		91.5	--154.0--		--188.6--		185.7	163.6	108.3	57.6	---17.5---				0.950
Ala_{14} (A)	83.5	---64.1---		59.8	--136.3--		--209.3--		194.3	154.7	113.5	32.3	---16.4---				0.948
Ala_{12} (A)	74.5	86.1	52.2	74.9	--131.3--		125.3	116.4	80.0	33.0	---22.5---						0.942
Ala_{10} (H)	84.9	74.6	55.8	69	91.5	94	---69---		---19.7---								0.935
Ala_{10} (A)	62.3	89.1	39.3	63.6	96.3	88.2	---63.6---		---17.9---								0.929
Ala_8 (H)	51.7	---32.4---		33	31.3	23.3	---17.9---										0.901
Ala_8 (A)	51.1	---32.4---		34.6	35.2	17.7	---11.1---										0.883
Ala_6 (A)	38.5	29.9	17.7	------10.4------													0.837
Ala_4 (A)	23.4	9.9	5.5	2.4													0.619

Protection factors for series **2** peptides calculated from amide hydrogen-deuterium exchange at 2 °C, 40 mM NaH_2PO_4, pH 4.5-6.0. (A) signifies values calculated from curve-fitted peak areas, (H) signifies values calculated from peak heights. PF values for overlapping amide peaks are indicated with dashed lines. FH values were calculated with equations 8 - 11, using $PF_{beta} = 0.5$.

Table 4: Amide proton PF and total FH for selected series 3 peptides

	PF_{NHi}																		
Peptide	1	2	3	4	5	6	7	8	9	10	11	12	13	14	15	16	17	18	FH
Ala_{18} (A)	62.5	44.7	97.1	97.5	----------190----------							---113.1---		97.5	97.1	32.5	26.9	17.3	0.961
Ala_{12} (A)	57.8	36.5	46.9	57.6	------70.0-------			----60.9----		21.4	21.2	6.4							*0.928*
Ala_8 (A)	46.4	36.8	62.5	105	33.7	28.1	16.1	8.8											0.894

Amide protection factors and total FH for series **3** peptides calculated from amide hydrogen-deuterium exchange at 2 °C, 40 mM NaH_2PO_4, pH 4.5 - 6.0 (except Ala_{12} for which pH = 4.4). (A) signifies values calculated from curve-fitted peak areas. PF values for overlapping amide peaks are indicated with dashed lines. Peak assignments are not supported by NOESY data; they were made by analogy with the series **2** peptides.

6.13. Proton-Proton Exchange—The PF of *beta*

Because the amide proton of *beta* exchanged too quickly, the NH→ND technique did not provide the $PF_{NH\mathit{beta}}$ needed to determine PF_{Alan}. Given that NOESY data for the C-terminal *beta* residue reveal organization consistent with the proposed hydrogen-bonded structure, it is reasonable to expect that $PF_{NH\mathit{beta}}$ will be greater than unity. Also, the monotonic decrease in PF_{NHi} from n/2 to n, implies that $PF_{NH\mathit{beta}}$ is less than the preceding PF_{NHi}. Inspection of Figure 24 provides a good first estimate for $PF_{NH\mathit{beta}}$ throughout the entire length series. The PF_{NHn} is remarkably similar for all series **2** peptides ($n \geq 8$); the range of values was 11 – 24. Because these values are an average of the last and penultimate alanine residues, the PF_{NHn} is undoubtedly smaller than this range suggests. The series **3** data provide a better estimate for PF_{NHn} owing to the fortuitous isolation of the ultimate alanine amide peak in those ^1H spectra. We established an upper estimate for PF_{beta} by dividing by two the lowest of the PF_n values in Table 4 to account for the monotonic decrease seen in Figure 24. Thus, a range of 1.1–3 for $PF_{NH\mathit{beta}}$ was assigned provisionally; line broadening in the ^1H NMR titration experiments on peptide **1** provided corroborating evidence for this provisional range.

Broadening of the amide resonances of the perdeuterated-Ala peptide **1** over the pH range of 3 – 7 is caused by increasing exchange rates of the amide protons with water. All peak heights were maximum at approximately pH 3, in agreement with the experimentally determined rate minimum for NH→ND amide exchange. As the pH is increased, the *beta* amide proton broadens significantly more than nearby alanine amide protons. Rather than compare these protons in the same peptide, a model peptide Ac-Ala_2-*beta*-Acc-K_2-W-NH_2 was titrated over the same pH range to provide a reference for the amide peaks in peptide **1**.

The rate of amide proton exchange, over the pH range 3.0 to 5.0, is pseudo first-order since the concentration of hydroxide is constant: Rate = $k[OH^-][amide] = k_{obs}[amide]$. Normalized[78] peak heights for the amide protons of a peptide, measured

[78] The amide proton peaks of the control peptide were normalized against a W indole proton peak which does not exchange with water and therefore has a constant height. The amide proton peaks of peptide **1** were normalized against a DSS peak because the peptide had no W.

over this pH range, give a line with slope equal to the intrinsic rate of the exchange: $k_{obs}/[OH^-] = k$. A comparison of these plots for the control peptide appears in Figure 25 which demonstrates that *beta* exchanges faster than either Ala residue, not surprisingly given its positively charged ammonium ion. Comparison of the control peptide[79] with peptide **1** gave rough estimates of the PF values for *beta* (11) and Ala-5 (50). The value determined by NH→ND exchange ($PF_{NH5} = 30$) was on par with that obtained by the NH→NH method; however, the error in measurement[80] was too great to use the PF_{beta} value for calculations, and the provisional range deduced from the PF_{NHi} data was used instead.

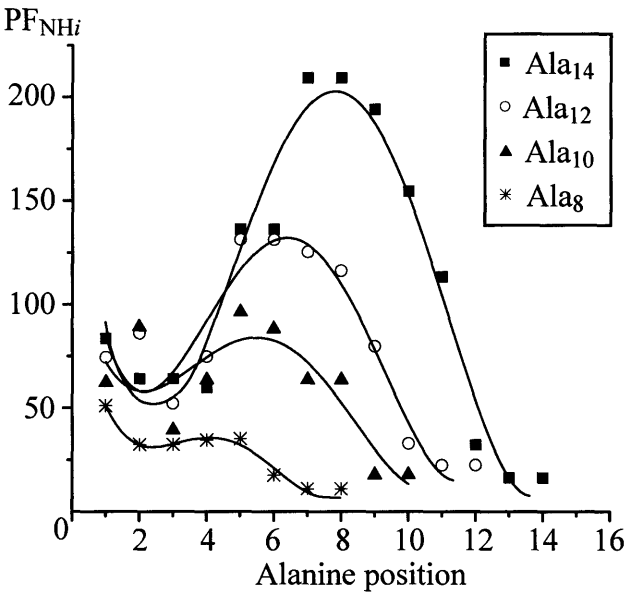

Figure 24: Graph of PF_{NHi} values determined from proton NMR peak heights for peptide series 2.

[79] The line broadening of the control peptide at 2 °C was extrapolated from five measurements taken at higher temperatures. This was necessary because a change to the cryoprobe on the Bruker 600 did not permit measurement at temperatures below 8 °C.

[80] The scatter in data gave error ranges equivalent to the values cited; also the temperature extrapolation added another degree of uncertainty. The variation in distance between the water peak and the amide proton peaks of interest was not great enough to warrant a correction.

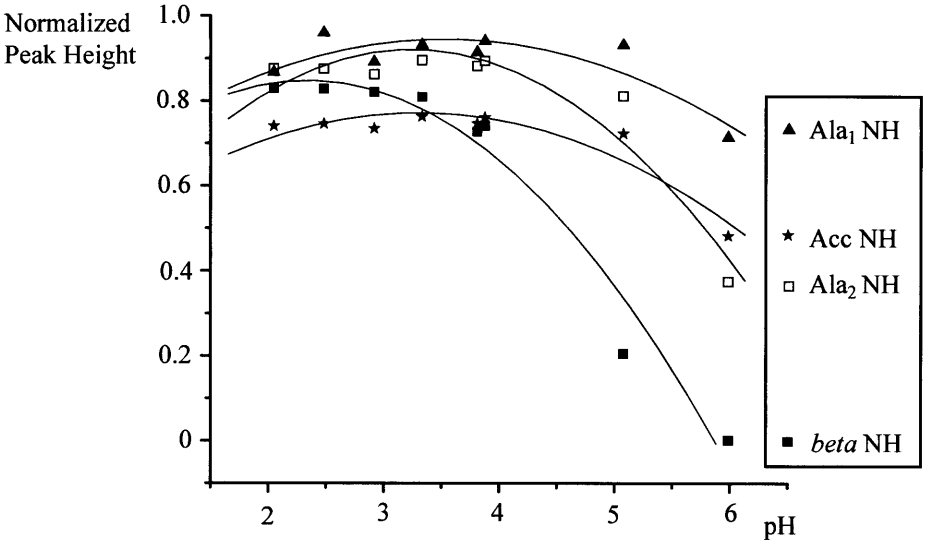

Figure 25: Variation in peak height over the pH range 2 – 6 for the peptide Ac-Ala$_2$-*beta*-Acc-K$_2$-W-NH$_2$. The steeper the slope, the faster the amide proton exchanges with water.

6.14. NMR Experiments on Peptides Synthesized with Uniformly ^{13}C,^{15}N-labeled Alanine

Three peptides were made with uniformly labeled ^{13}C,^{15}N alanine (^{U}Ala); they are as follows: Ac-$^{\beta}$DHel-$^{U}Ala_8$-*beta*-Acc-K$_2$-W-NH$_2$; Ac-$^{\beta}$DHel-$^{U}Ala_6$-Ala$_6$-*beta*-Acc-K$_2$-W-NH$_2$; Ac-$^{\beta}$DHel-Ala$_6$-$^{U}Ala_6$-*beta*-Acc-K$_2$-W-NH$_2$. The two labeled series **2** Ala$_{12}$ peptides were made to avoid overlap. The $^{13}C\alpha$ chemical shifts were assigned from a standard HNCA experiment, and the $^{3}J_{HNH\alpha}$ coupling constants were assigned from an E.COSY HNCA experiment (2048c*4c*64c); sweep widths for both were 5387.5, 426, and 1207 Hz for the ^{1}H, ^{13}C, and ^{15}N dimensions, respectively.

The ^{13}CO chemical shifts of the two labeled Ala$_{12}$ peptides were assigned from a 2D version of an HNCO experiment[81] (1024c*256c) with a sweep width of 5387 and 980 Hz for the ^{1}H and ^{13}C dimensions, respectively. For the peptide with the last six Ala residues labeled, the nitrogen to carbonyl dephasing time ($2T$) was set to 0.024 s, which is a value slightly shorter than $1/(2*{}^{1}J_{NCO})$, where $^{1}J_{NCO} = 15$.[82] Data for the H-bonding

[81] Grzesiek, S.; Bax, A. "title" *J. Magn. Reson. Ser. ?* **1992**, *96*, 432–440.
[82] This is a common value for correlations of chemical shifts $^{13}CO_i$ with $^{1}HN_{(i+1)}$.

experiments were collected on 2 – 4 mM samples (40 mM NaH_2PO_4, pH 4.5) in a Shigemi NMR tube on the Bruker spectrometer equipped with a ^1H, ^{13}C, ^{15}N triple resonance 5 mm CryoProbe. A data matrix of 2048c*32c was collected with a sweep width of 3894 and 203.7 Hz for the respective ^1H and ^{13}C dimensions. The H-bonding spectrum of the C-terminally labeled Ala_{12} peptide was acquired with $2T = 0.1316$ and 512 scans; similar measurements were carried out on the labeled Ala_8 peptide and the N-terminally labeled Ala_{12} peptide. The spectrum in Figure 16c was measured with $2T = 0.1303$ and 1024 scans; data from this experiment were used to determine the signal-to-noise ratio.

6.14. Calculational Justification

The following calculation justification for the revised limiting ellipticity equation and the Lifson–Roig justification of the simplified FH calculation from amide site protection factors were provided by Prof. Dan Kemp.

Equivalence of Eqs. 3 = 12 and 15.

Eq. **3** is justified by theory and by least squares deconvolution of CD spectra of proteins with known secondary structures. The residues in a helix may be divided into two classes: (1) central residues which exhibit constant conformation and experience identical environments; and (2) terminal residues which experience unique chemical environments, and whose p,psi dihedral angles may vary slightly. The introduction of a new parameter k makes explicit the contributions of these two classes of residues (Eq. **12** – **14**). Because the parameter k is both added and subtracted from the same side of Eq. **3**, there is no net change to the equation. If a peptide with $n > k$ were extended by several residues, each additional residue would contribute exactly the same amount ($[\theta_\infty]_\lambda$) to molar ellipticity. The length dependence of the per-residue ellipticity arises from the averaging of the constant cap contribution (Eq. **15**) over the total molar ellipticity value.

The peptide CD chromaphore is a peptide amide group flanked by two helical amino acid Cα; owing to the amide hydrogen bonding unique to the ends of the helix, it is reasonable to expect that the electronic transitions of these moieties will be perturbed from the state found in the center of a helix. Because the helical loops at each end

comprise three residues, a lower bound of k = 6 is indicated. Our data suggest that k = 8 is a better choice for our series.

$$[\theta_n]_\lambda = [\theta_\infty]_\lambda (1 - X/n) \quad \textbf{3}$$

$$[\theta]_\lambda = [\theta_\infty]_\lambda(n) + [\theta_\infty]_\lambda(X) = [\theta_\infty]_\lambda (n - k) + [\theta_\infty]_\lambda (k - X) \quad \textbf{12}$$

$$[\theta]_{\lambda,core} = [\theta_\infty]_\lambda (n - k) \quad \textbf{13}$$

$$[\theta]_{\lambda,SS-Caps} = [\theta_\infty]_\lambda (n - X) \quad \textbf{14}$$

$$[\theta]_\lambda = [\theta]_{\lambda,core} + [\theta]_{\lambda,SS-Caps} \quad \textbf{15}$$

Requirements for a calibration series.

Convergence of the core residues and constancy of the end residues must be demonstrated independently of CD in order to use a series of peptides for calculation of the parameters X and $[\theta_\infty]_\lambda$ used for calculation of fractional helicity. Moreover, the fractional helicity of the core residues must be nearly 100% (> 99.5%). NH→ND exchange experiments showed extremely high helicity for the core regions of our peptides. The convergent ^{1}HN chemical shifts implied minimal conformational variation within the helix core—^{1}H chemical shift is sensitive to changes in electronic environment that would likely accompany significant conformational changes in ϕ, ψ angles.

The ^{1}HN chemical shifts of the first four and last four alanine residues in our peptides are site-specific, but independent of length. Moreover, their FH values are, to a good approximation, constant throughout the series as well. These criteria permitted assignment of k = 8.

If FH is not constant for the core region of a series of peptides, the slope of the linear regression line, for a plot of $[\theta]_\lambda$ versus λ, will not equal $[\theta_\infty]_\lambda$—it is necessary to correct each peptide's $[\theta]_\lambda$ by its FH before calculating the regression line. This introduces additional error, especially since accurate quantitation of FH becomes more difficult with decreasing FH.

Once the conditions for a calibration series have been met, the series must be sufficiently large that a majority of the members have molar ellipticity values more than twice that of the k-length region; this ensures that the "core" term dominates the "cap" term for most of the series.

Problems associated with X assignments.

The parameter X reflects properties of the helix termini, and is therefore more influential in calculation of $[\theta]_\lambda$ for short peptides, in which central residues are few. Moreover, unlike $[\theta_\infty]_\lambda$, which for a homopeptide is affected only by measurement conditions and the nature of the residue, the value of X is probably sensitive to local structural features. X may therefore differ significantly among peptide sequences, entailing a specifically calculated value for a given context. In the present study, values of both $[\theta_\infty]_\lambda$ and X were assigned from a data base of $[\theta_n]_\lambda$ values measured for a large length range of N- and C-capped peptides by subtracting a $[\theta_0]_\lambda$ correction for the portion of each $[\theta_n]_\lambda$ that is contributed by the Trp UV reporter, solubilizers, spacers, and the helix-stabilizing caps βAsp-Hel and *beta*. A fundamental uncertainty that accompanies this use of cap-corrected $[\theta_n]_\lambda$ values arises from the likelihood that conformations and thus ellipticity contributions in the $^{\beta}$AspHel and *beta* region of the correction peptide are atypical of normal series members in which these functions flank an Ala_n core. A lower bound for this uncertainty is provided by comparing pairs of cap corrected $[\theta_n]_\lambda$ values for peptides of identical length taken from series **2** and series **3**. The error in measurement for each series is estimated as 3 to 5%, implying an error in the comparison that lies in the range of 6 to 10%. The actual average percentage differences calculated over the range of 208 to 228 nm is 5 % for n = 14 or 16; 11 % for n = 12, and 15 % for n = 10. These provide estimates for a lower bound to cap correction errors. As noted in the text, these uncertainties are likely to result in accuracy errors that are much larger for X than for $[\theta_\infty]_\lambda$ which is primarily sensitive to the ellipticities of the longer series members.

D. Calculation of FH_i and FH Values from PF_i-Derived FH_{NHi} Values.

The purpose of this section is to provide a verification of the inequalities **9** and **10** used in the text to calculate values of FH_i from PF_i-derived values of FH_{NHi}. Relationships between these different measures of site helicity have been reported, but this section focuses on semi-quantitative relationships that result for PF_i values of 20 to 200, corresponding to FH_{NHi} values that exceed 0.95. Within the body of an α-helix, a helical hydrogen bond between the carbonyl oxygen of the $(i - 4)$th residue and the NH

of the *i*th residue can form only if each of the ϕ,ψ dihedral angle pairs at residues $(i-1)$, $(i-2)$, and $(i-3)$ are helical. Since FH_i is defined as the site helicity at the ith α-carbon, $FH_{NHi} = 1.0$ implies that $FH_{(i-1)} = FH_{(i-2)} = FH_{(i-3)} = 1.0$. The analysis of the Table 5 generalizes this relationship by examining the possible conformational states that can influence values of FH_{NHi}, $FH_{(i-1)}$, $FH_{(i-2)}$, $FH_{(i-3)}$ within any four-residue helical sequence. In Lifson–Roig (h = helix, c = coil) notation, the 2^n conformations of an N- and C-capped peptide of n residues can be grouped within seven local sequences. Thus a partial sequence hhh symbolizes the collection of all helical conformations that include α-carbons at residues $(i-1)$, $(i-2)$, and $(i-3)$; ccc includes conformations that are nonhelical within these residues. Similarly, hcc and hhc respectively correspond to helical sequences that terminate at either residue $(i-3)$ or $(i-2)$, and cch and chh correspond to helical sequences that are initiated at either residue $(i-2)$ or $(i-1)$. Sequence hch corresponds to a pair of collective helical conformations, one terminated at residue $(i-3)$, the other initiated at residue $(i-1)$. Identifiers, mole fractions, and the contribution to FH_{NHi} by each of these appear in the first three columns of Table 5. The h symbols that appear in the three vertical columns identify mole fractions that comprise $FH_{(i-1)}$, $FH_{(i-2)}$, and $FH_{(i-3)}$. Reading down the first column of Table 5, $FH_{(i-3)}$ is found by adding all mole fractions corresponding to a helical α-carbon at this site: $FH_{(i-3)} = (\chi hhh + \chi hhc + \chi hcc + \chi hch)$. Similarly, $FH_{(i-2)} = (\chi hhh + \chi hhc + \chi cch)$, and $FH_{(i-1)} = (\chi hhh + \chi cch + \chi chh + \chi hch)$. Adding these and dividing by 3 yields $(FH_{(i-1)} + FH_{(i-2)} + FH_{(i-3)})/3 = \chi hhh + 2(\chi hhc + \chi chh + \chi hch)/3 + (\chi hcc + \chi cch)/3$. From the fifth column, one sees that $\chi hhh = FH_{NHi}$, which proves the inequality of eq. **9**: the mean of the three FH_i at sites that precede *i* must be greater than the value of FH_{NHi}. As noted previously, the presence of central peptide regions in which values of FH_{NHi} remain constant and exceed 0.99 implies that the helical manifold is dominated by the fully helical conformation, with a minor contribution from the nonhelical conformation. In these regions, FH_i and FH_{NHi} are in good agreement. For the last residues of peptides of series **2** or series **3**, the values of FH_{NHi} decrease monotonically with increasing *i*. This C-terminal fraying effect can be readily interpreted as due to a change in the relative magnitudes of the mole fractions of Table 5. Helical conformations corresponding to part structures hhh, hhc, or hcc contribute significantly, but conformations corresponding to

part structures cch, chh, or hch do not, since these initiate very short helical sequences. Inspection shows that for a Table comprised only of hhh, hhc, hcc, and ccc conformations, $FH_{NHi} = FH_{(i-1)}$, and $FH_{(i-3)} > FH_{(i-2)} > FH_{(i-1)}$, and the value of FH_{NHi} is to a good approximation given by Eq. **9**. From a similar argument, Eq. **10** models FH_{NHi} for $i \ll n$. For the two cases in which either $i = 4$, or $i = n + 1$, this argument implies that, as noted previously, the values of FH_i can be rigorously defined as $FH_{NH4} = FH_1$ for the former (for which χhhc , χhcc, and χhch are all zero) and $FH_{NH(i+1)} = FH_n$ for the latter (for which χcch, χchh, and χhch are all zero).

Table: Grouped Conformational States at Three Peptide α-Carbons that Precede a Site *i*

Peptide Site: (*i* - 3)	(*i* - 2)	(*i* - 1)	Mole Fraction	Contributes to FH_{NHi}?
h	h	h	χhhh	yes
h	h	c	χhhc	no
h	c	c	χhcc	no
c	c	h	χcch	no
c	h	h	χchh	no
h	c	h	χhch	no
c	c	c	χccc	no

In the Lifson–Roig formalism, helical ϕ,ψ angles at isolated single residues (chc) or pairs of residues (chhc) do not contribute to the helical state sum. As a result, in the context of Table 5, the symbolism ccc is an abbreviation for all global conformations that contain the following local sequences: |ccc|, |chc|, c|hcc|, c|hhc|, |cch|c, |chh|c.

Chapter 3. Simpler N-Terminal Helix-Initiating Caps

1. Introduction

1.1. Other Methods for Creating Helical Peptides

Efforts to create helical peptides by synthetic modification is not unique to our group.[1] In addition to small-molecule helix initiators like Hel, side-chain interactions and unnatural helix-promoting α-amino acids have been explored as a means for inducing helicity in peptides. The unnatural α-amino acid strategy is exemplified by use of α,α-disubstituted amino acids, such as amino-isobutyric acid (Aib),[2] in peptide synthesis. Insertion of these residues into peptides has been shown to appreciably increase helicity; however, these peptides are prone to adopt 3_{10} helical structure.[3] Additionally, the increased bulk of these amino acids can present a challenge to peptide synthesis.

Side-chain interactions—covalent, electrostatic, π-π stacking, hydrogen-bonding, and metal-binding—are also known to induce significant α-helical structure in peptides when suitable residues are spaced in an $i \rightarrow (i+4)$ arrangement. With these methods, the amino acid sequence is curtailed, and sometimes additives are required to mediate the stabilizing interaction. If the side chain interaction is covalent, post-synthetic modification is required; one example is a single helical turn imposed by a lactam bridge between the Lys and Asp residues in the Ac-KARAD-NH_2 pentapeptide.[4] Fractional helicity of this single turn peptide is similar to that of our N- and C-capped Ala_6 peptides, as judged by CD. No examples of longer peptides incorporating this constrained loop have been reported.

Examples **1**[5] and **2**[6] in Figure 1 present another method for constraining a single

---

[1] Reviews: (a) Schneider, J.P.; Kelly, J.W. "Templates that Induce α-Helical, β-Sheet, and Loop Conformations" *Chem. Rev.* **1995**, *95*, 2169–2187. (b) Andrews, M.J.I.; Tabor, A.B. "Forming Stable Helical Peptides Using Natural and Artificial Amino Acids" *Tetrahedron* **1999**, *55*, 11711–11743.

[2] Banerjee, R.; Basu, G.; Chene, P.; Roy, S. "Aib-Based Peptide Backbone as Scaffolds for Helical Peptide Mimics" *J. Peptide Res.* **2002**, *60*, 88–94.

[3] Karle, I.L. "Controls Exerted by the Aib Residue: Helix Formation and Helix Reversal" *Biopolymers* **2001**, *60*, 351–365.

[4] Shepherd, N.E.; Hoang, H.N.; Abbenante, G.; Fairlie, D.P. "Single Turn Peptide Alpha Helices with Exceptional Stability in Water" *J. Am. Chem. Soc.* **2005**, *127*, 2974–2983.

[5] Chapman, R.N.; Dimartino, G.; Aurora, P.S. "A Highly Stable Short α-Helix Constrained by a Main-Chain Hydrogen-Bond Surrogate" *J. Am. Chem. Soc.* **2004**, *126*, 12252–12253.

helix loop relying on post-synthetic modification. In each, the first hydrogen bond of a helix is replaced by a covalent analog. Of the two, the olefin is more stable; an octapeptide with this H-bond analog at its N-terminus has a $[\theta]_{222}$ value on par with those of our Ala_8 peptides.

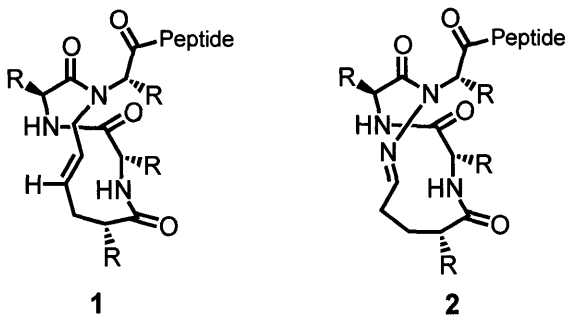

1 2

Figure 1: Two examples of a helix loop constrained by a covalent hydrogen bond analog.

A significant advantage to small-molecule helical templates is that they may be placed anywhere in a peptide chain by standard solid phase synthesis with no need for post-synthetic modification. The only constraint on peptide sequence for the small-molecule helical template approach is the exclusion of helix-breaking amino acids, which applies to the other strategies as well. Other templates have been reported in the literature (Figure 2), but none has been studied as thoroughly as Hel, and none has been shown to induce helicity as well as Hel.

The macrocyclic tetrapeptide **3**, reported by Gani, is very similar to a triproline template synthesized in this group.[7] The Kemp group efforts with the triproline template failed because the '*ttt*'form (all carbonyl groups aligned) that is required for helix initiation could not be made, presumably because of charge repulsion among the aligned carbonyl groups. Upon cyclization, the '*cct*' form, unsuitable for helix initiation, was formed. Gani also reported this problem with his attempt at a triproline template,[8] but

---

[6] Cabezas, E.; Satterthwait, A.C. "The Hydrogen Bond Mimic Approach: Solid-Phase Synthesis of a Peptide Stabilized as an α-Helix with a Hydrazone Link" *J. Am. Chem. Soc.* **1999**, *121*, 3862–3875.

[7] Kemp, D.S.; Rothman, J.H.; Curran, T.C.; Blanchard, D.E. "A Macrocyclic Triproline-Derived Template for Helix Nucleation" *Tetrahedron Lett.* **1995**, *36*, 3809–3812.

[8] (a) Lewis, A.; Ryan, M.D.; Gani, D. "Design, Construction and Properties of Peptide N-Terminal Cap Templates Devised to Initiate α-Helices. Part I. Caps Derived from *N*-(4-chlorobutyryl)-(2*S*)-Pro-(2*S*)-Pro-

overcame it by replacing the center Pro residue with D-Ala;[9] however, no applications of this putative helix-initiating template have appeared in the literature.

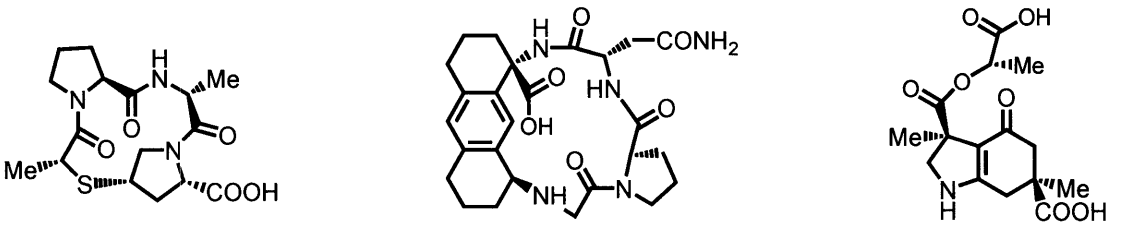

3 **4** **5**

Figure 2: Putative (3, 4) and proven (5) helical N-Caps.

The macrocycle **4**, containing an octahydroanthracene analog of lysine, is another example of a proposed helix-initiating template whose literature has not progressed past the initial synthetic report. This hydroanthracene moiety of the molecule was made in 18 steps and twice required diastereomer separations.[10]

Bartlett's hexahydroindalone **5** is one of the more promising helical templates to emerge from another group.[11] This relatively simple molecule is synthesized in seven steps from *tert*-butyl 3,5-dimethoxybenzoate with a diastereomeric separation before addition of L-lactate, and another after. At 0 °C, The $[\theta]_{222}$ signal of a hexapeptide (EALAKA) conjugate[12] was approximately 55% of the value for our series **3** Ala_6 peptide at 2 °C. Interestingly, replacement of L-lactate with L-alanine leads to a significant loss

(2*S*)-Ala-OMe and *N*-[(2*S*)-2-chloropropionyl]-(2*S*)-Pro-(2*S*)-Pro-(2*S*,4*S*)-4-hydroxyPro-OMe" *J. Chem. Soc., Perkin Trans. 1* **1998**, 3767–3775. (b) Lewis, A.; Wilkie, J.; Rutherford, T.J.; Gani, D. "Design, Construction and Properties of Peptide N-Terminal Cap Templates Devised to Initiate α-Helices. Part II. Caps Derived from *N*-[(2*S*)-2-chloropropionyl]-(2*S*)-Pro-(2*S*)-Pro-(2*S*,4*S*)-4-thioPro-OMe" *J. Chem. Soc., Perkin Trans. 1* **1998**, 3777–3793.

[9] Lewis, A.; Rutherford, T.J.; Wilkie, J.; Jenn, T.; Gani, D. "Design, Construction and Properties of Peptide N-Terminal Cap Templates Devised to Initiate α-Helices. Part III. Caps Derived from *N*-[(2*S*)-2-chloropropionyl]-(2*S*)-Pro-(2*R*)-Ala-(2*S*,4*S*)-4-thioPro-OMe" *J. Chem. Soc., Perkin Trans. 1* **1998**, 3795–3806.

[10] Stalker, R.A.; Munsch, T.E.; Tran, J.D.; Nie, X.; Warmuth, R.; Beatty, A.; Aakeroy, C.B. "Asymmetric Synthesis of Two New Conformationally Constrained Lysine Derivatives" *Tetrahedron* **2002**, *58*, 4837–4849.

[11] Austin, R.E.; Maplestone, R.A.; Sefler, A.M.; Liu, K.; Hruzewicz, H.N.; Liu, C.W.; Cho, H.S.; Wemmer, D.E.; Barlett, P.A. "A Template for Stabilization of a Peptide α-Helix: Synthesis and Evaluation of Conformational Effects by Circular Dichroism and NMR" *J. Am. Chem. Soc.* **1997**, *118*, 6461–6472.

[12] Also including a stabilizing, $i \rightarrow (i+4)$ Glu–Lys salt bridge.

of helix-inducing ability, presumably caused by a competitive intramolecular hydrogen bond formed between the resulting amide and the C-6 carboxylic group. The important role of the C-6 carboxylic group is also indicated by the dramatic loss in helicity for the **5**–EALAKA conjugate at low pH; during titration, the $[\theta]_{222}$ drops approximately 50% between pH 5 and pH 2. This result mirrors our experience with the modified $^{\beta}$DHel template.

1.2. Simplification of Hel

Although Hel is an effective helix initiator, the 18-step synthesis has prevented others from using it. If the α-helix is to be better understood, a simpler and commercially available helix initiator is needed.

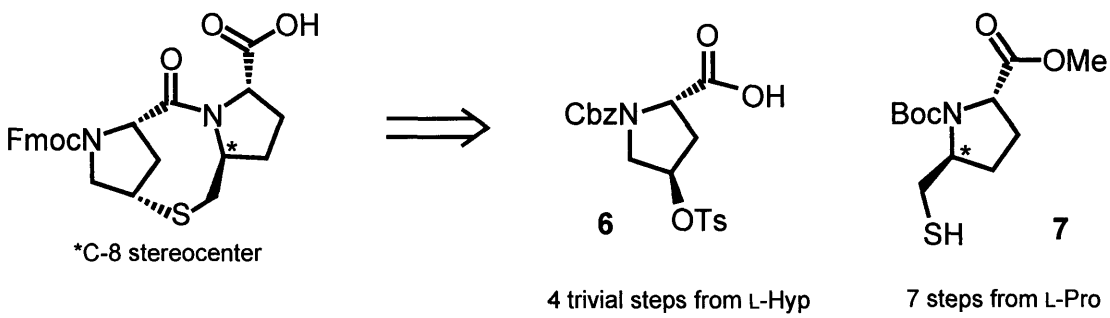

Figure 3: Key retrosynthetic step for FmocHel.

The convergent Hel synthesis[13] presents an opportunity for simplification in the C-terminal pyrrolidine fragment (Figure 3). This branch of the synthesis is seven steps long and contains the most demanding step of the synthesis—the *in situ* formation of a vinyl cuprate and its addition to an *N*-acyl iminium ion at low temperature. Furthermore, the equipment for the preceding electrochemical oxidation step is not common to an organic chemistry laboratory. The stereocenter at C-8 introduced by these manipulations is the only asymmetric carbon not already present in the naturally occurring precursors 4-hydroxyproline (Hyp) and Pro; if the stereocenter could be eliminated from the helical template as illustrated in Figure 4, the resulting analogues would be easier to make.

[13] Full route is given in Scheme 1 of Chapter 2.

Considering the large increase in Hel's helix-initiation ability brought about by adding $^{\beta}$D, we were curious whether the proposed simplification and the accompanying gain of a degree of freedom would greatly reduce the helix-initiating ability of the templates.

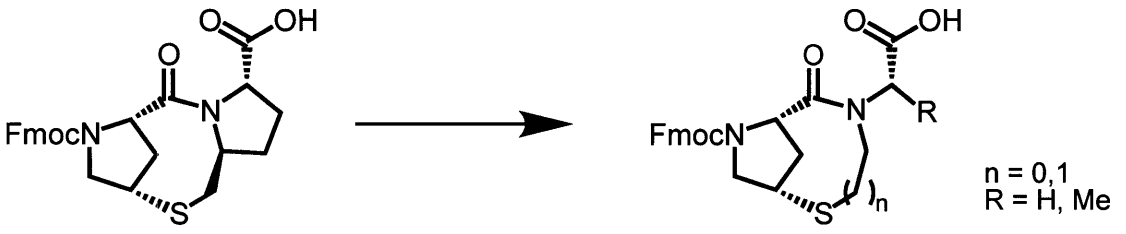

Figure 4: Proposed simplification of Hel by opening of the C-terminal pyrrolidine ring.

Two classes of Hel analogs lacking the C-8 stereocenter were proposed; the only difference being the size of the bridge that constrains the ψ angle of the pyrrolidine ring (Figure 4, n = 0 or 1). One can imagine three cyclization strategies for construction of the larger ring (Figure 5). In the first synthesis of AcHel, ring closure was by formation of the tertiary amide (1); this method gave poor and variable yields. The S_N2 method mentioned (2) in the preceding chapter was a great improvement in the synthesis of Hel and was therefore favored over the amide formation route for synthesis of the 8-member ring Hel analogs. The remaining route (3) in Figure 5 was employed for the synthesis of the 7-member ring Hel analogs, but failed for the 8-member ring Hel analogs. As a starting point, templates incorporating Gly or Ala fragments (R = H, Me) were the synthetic targets.

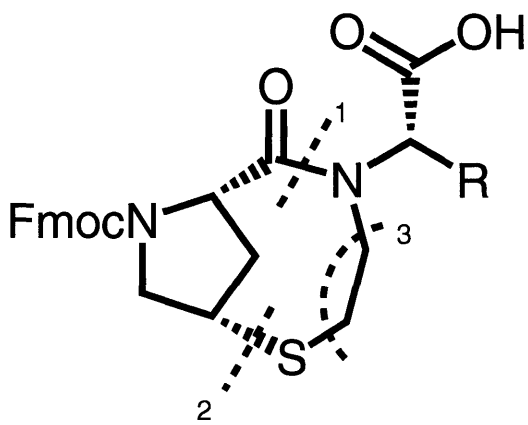

Figure 5: Three ring closing strategies for the proposed simpler N-terminal helix-initiating N-caps. Dashed lines indicate the bond(s) formed during ring closure.

2. Simpler Helix Initiators: Eight-member-ring N-Caps

2.1. NCap(8)Gly

We envisioned a synthesis combining Hel's Hyp fragment and a modified, natural α-amino acid with an ethylene sulfide group appended to the nitrogen (Figure 6). Of the retrosynthetic schemes for producing this modified 1,2-amino thiol residue **8**, the approach using ethylene sulfide failed under various conditions. A literature procedure for silver(II)-promoted addition of amines to ethylene sulfide failed;[14] compound **8**[15] could not be detected by electrospray mass spectroscopy (ES–MS) or ^{1}H NMR of the crude reaction. Although amino acids were listed as potential reaction partners in the claims of the patent, no examples were cited in the document.

The other two schemes, reductive amination and alkylation, were pursued simultaneously. Initial results from the *in situ* $NaBH(OAc)_3$ reductive amination[16] of *S*-Bz 2-thioacetaldehyde with H-Gly-OMe·HCl were promising; a major product was isolated by flash chromatography. The proton NMR spectrum of the product was

[14] Luhowy, R.R.; Meneghini, F.A. Mercaptoethylation of Amines. US Patent 3919277, 1975.
[15] R = Me, R′ = Me; R = H, R′ = *tert*-Bu; R = Me, R′ = H
[16] Abdel–Magid, A.F.; Maryanoff, C.S.; Carson, K.G. "Reductive Amination of Aldehydes and Ketones by Using Sodium Triacetoxyborohydride" *Tetrahedron Lett.* **1990**, *31*, 5595–5598.

consistent with the desired product, except for the integrations which were half their expected values for the glycine portion. ES–MS confirmed my suspicions that glycine had been doubly alkylated. Analysis of the crude reaction mixture by ES–MS indicated that the desired, singly alkylated glycine was formed, albeit in low yield.

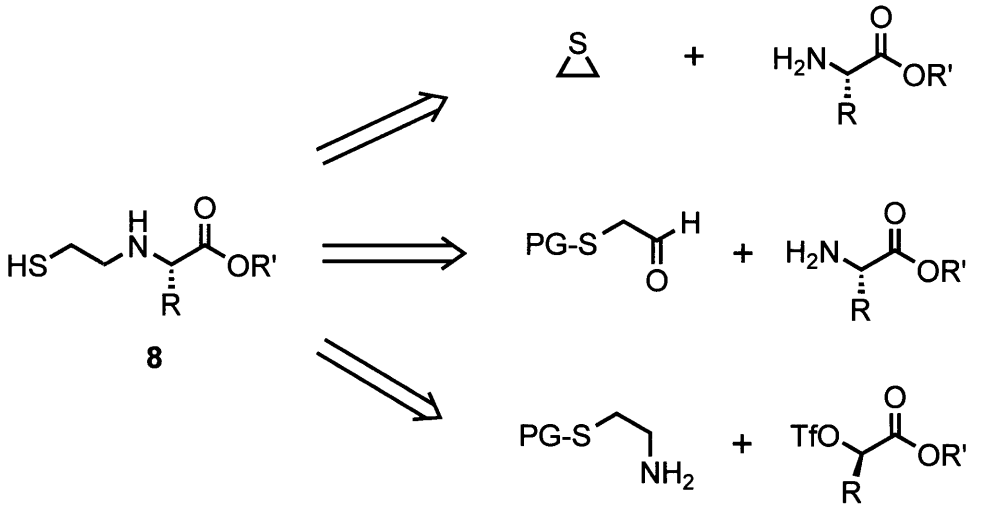

Figure 6: Synthetic routes to the 1,2-amino thiol fragment. PG = protecting group.

Synthesis of the mercaptoethylated amino acid was eventually accomplished by a straightforward alkylation route similar to a literature procedure[17] (Scheme 1). Thiol protection was achieved by use of the cheap symmetrical disulfide, cystamine. Reaction of cystamine with methyl bromoacetate in the presence of base, followed by treatment of the crude reaction mixture with Boc_2O gave compound **9** in acceptable yield. Careful flash chromatography is needed to remove the main by-product, doubly Boc-protected cystamine. Reductive cleavage of the disulfide was effected by treatment with tris(carboxyethyl)phosphine hydrochloride (TCEP·HCl).[18] A convenient aqueous extraction provided the modified amino acid **10** which was combined with the Hyp fragment from the original Hel synthesis to form thioester **11**. Treatment with

[17] Bitan, G.; Gilon, C. "Building Units for N-Backbone Cyclic Peptides. 2. Synthesis of Protected N-(ω-thioalkylene) Amino Acids and Their Incorporation into Dipeptide Units" *Tetrahedron* **1995**, *51*, 10513–10522.

[18] Burns, J.A.; Butler, J.C.; Moran, J.; Whitesides, G.M. "Selective Reduction of Disulfides by Tris(2-carboxyethyl)phosphine" *J. Org. Chem.* **1991**, *56*, 2648–2650.

trifluoroacetic acid (TFA) unmasked the secondary amine in preparation for the acyl transfer step. After the bulk TFA was removed by rotary evaporation, the residue was taken up in methylene chloride and carefully washed with saturated sodium bicarbonate ($NaHCO_3$); intramolecular acyl transfer occurred so readily with this compound that appreciable amounts of **12** were detected by ^1H NMR after rotary evaporation. These conditions are much milder than the 2 hours' heating in toluene required to effect the analogous transformation for Hel.

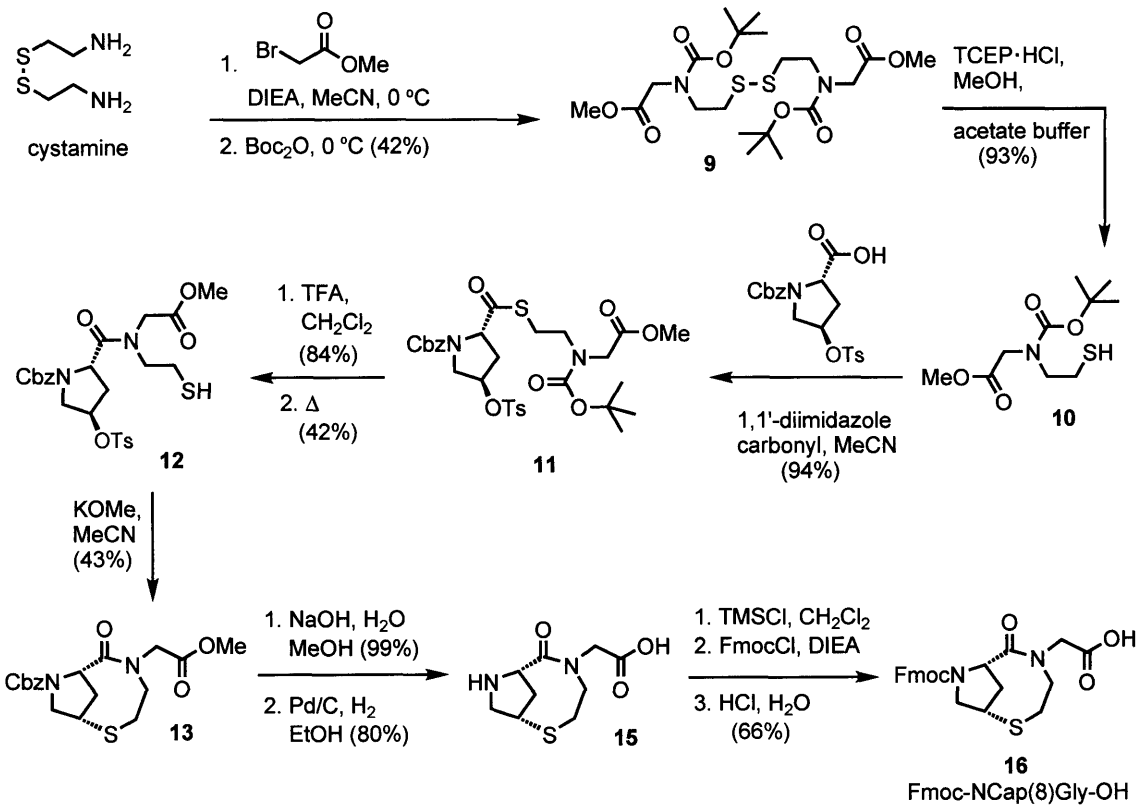

Scheme 1: Synthesis of the N-terminal helix-initiating cap NCap(8)Gly. Intermediate 14 is not shown.

A significant by-product was formed during cyclization; olefinic resonances in its ^1H NMR spectrum suggested competing elimination of the tosylate from **12**. Flash chromatography did not separate the by-product and **13**; fortunately, separation was accomplished by washing a toluene solution of the two with 0.1 M NaOH. Presumably, the by-product is rendered highly water soluble by deprotonation of its thiol group. Saponification of the methyl ester, deprotection of the benzyloxycarbonyl (Cbz) group,

and addition of the 9-fluorenylcarboxymethyl (Fmoc) group proceeded without incident. The new N-cap was christened NCap(8)Gly to denote its glycine moiety and eight-member ring.

2.2. NCap(8)Ala

With the addition of a single step—triflate formation from commercially available methyl-(*R*)-lactate[19]—the synthetic route to NCap(8)Gly was expected to furnished the analogous NCap(8)Ala (Scheme 2). The one-pot reaction yielded **17** in excellent yield; the amount of doubly Boc-protected cystamine was much reduced. Reductive cleavage of the disulfide, formation of the thioester **19**, and Boc deprotection all proceeded smoothly. However, the acyl transfer step was much more difficult than it had been for Hel and NCap(8)Gly; thioester **19** had to be boiled in toluene for five hours to drive the rearrangement to completion. During this time, the reaction became yellow and slightly cloudy, presumably owing to elimination of toluene sulfonic acid.

Cyclization proceeded in low yield; a significant amount of olefin by-product was observed by NMR. Additionally, at this step it became apparent that epimerization may have occurred. A portion of the ^{1}H NMR region for the isolated compound **21** is shown in Figure 7; the α-Me region has four sets of peaks rather than two as anticipated.[20] The suspected diastereomer mixture was subjected to the saponification and hydrogenolysis steps. The ^{1}H NMR spectrum of zwitterion **23** demonstrated unambiguously that epimerization had indeed occurred (Figure 8a), and the diastereomeric ratio of approximately 3:1 was confirmed by reverse-phase HPLC (Figure 8b).

Epimerization undoubtedly occurred at the α-H of the alanine moiety, as epimerization of the pyrrolidine ring α-H would prevent cyclization. Furthermore, the α-H region of the ^{1}H NMR spectrum in Figure 8a is analogous to that of epimerized Hel.[21] To determine if the problem had arisen during cyclization, this step was repeated with a sample of **20** from the same batch as before, but using DBU as the base. The yield from

---

[19] Effenberger, F.; Burkard, U.; Willfahrt, J. "Amino acids. 4. Enantioselective Synthesis of N-substituted α-Amino Carboxylic Acids from α-Hydroxy Carboxylic Acids" *Liebigs Ann. Chem.* **1986**, *2*, 314–333.
[20] The ^{13}C NMR spectrum also showed extra peaks, although not every peak was duplicated.
[21] This occurred during Dr. Wolfgang Maison's synthesis of FmocHel, as mentioned in Chapter 2 of this manuscript.

this reaction was very poor, but sufficient material was obtained for a ^{1}H NMR spectrum, which was identical to that in Figure 8a. Having eliminated the cyclization step from consideration, two others were suspected: the initial alkylation step and the acyl transfer step.

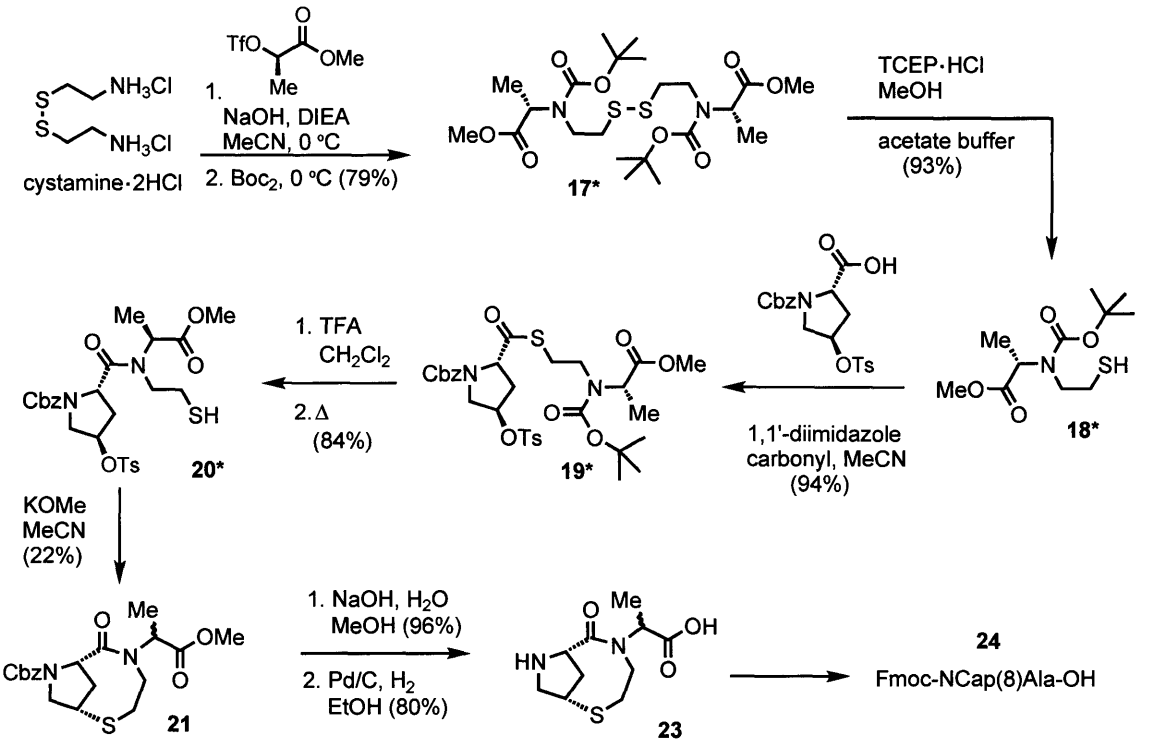

Scheme 2: The alkylation route to NCap(8)Ala produced a mixture of Ala Cα diastereomers. Although it was later learned that epimerization occurred at the alkylation step, it was not evident until cyclization. Asterisks denote that although the desired absolute configuration is shown, a significant amount of diastereomer was present. The last step to synthesize 24 was not performed in this reaction sequence, and intermediate 22 is not shown.

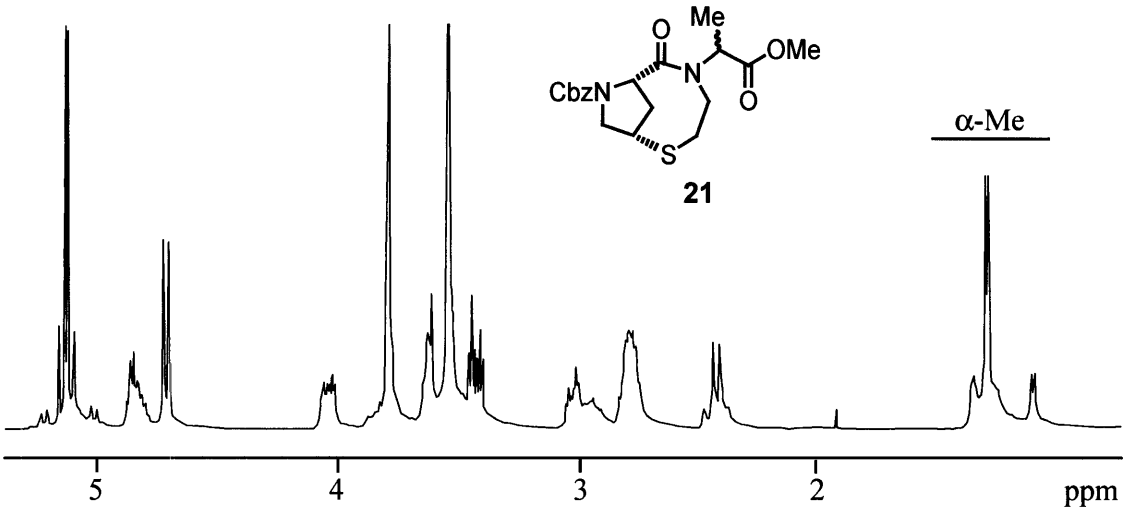

Figure 7: A portion of the ^{1}H NMR spectrum of 21 with the α-Me region indicated.

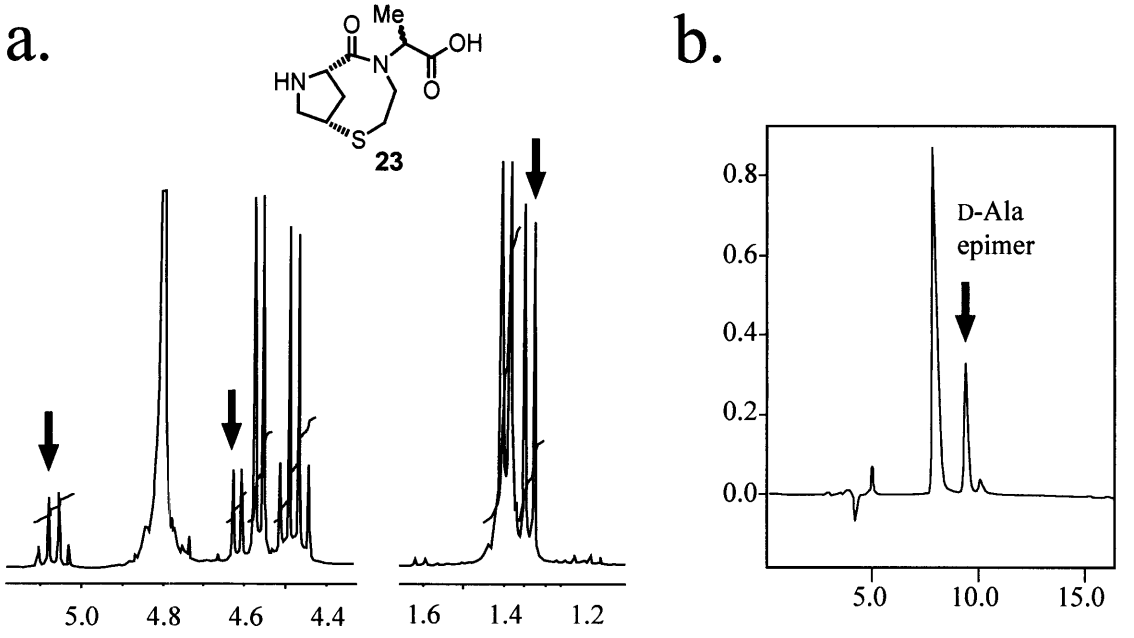

Figure 8: (a) The α-H and α-Me portions of the ^{1}H NMR spectrum of the epimers of 23 obtained by the alkylation route. Peaks of the minor epimer are indicated with arrows. (b) Reverse-phase HPLC of product 23 diastereomer mixture (1 to 35% MeCN in TFA (0.5%)/H_2O). Assignment of the D-Ala configuration to the minor diastereomer was supported by results from another synthetic scheme and comparison of the NMR spectrum with that of epimerized Hel.

The problematic step was revealed by synthesis of **18** using reductive amination (Scheme 3). The S_N2 reaction between *tert*-butyl thiol and the diethyl acetal of bromoacetaldehyde provided **25** in high yield, and hydrolysis of the acetal was readily accomplished in aqueous acetone with a catalytic amount of HCl. Simple extractions provided very clean material for each reaction in this beginning sequence. Reductive amination of aldehyde **26** was run using a slight excess of H-Ala-OMe·HCl. Column chromatography gave a pure sample of **27** in a rather disappointing yield, but because the reaction was run on a large scale, sufficient material was obtained to proceed with the synthesis. Deprotection with $Hg(O_2CCF_3)_2$/TFA was performed,[22] but mercury contamination of the isolated product made this method unappealing,[23] and a two-step route was used instead. The reaction of **27** with 2-nitrobenzylsulphenyl chloride[24] occurred quite cleanly, and the TFA salt **28** was obtained in high purity by precipitation.

Five equivalents of Boc_2O were necessary to obtain **29** in a reasonable time. Cleavage of the disulfide was accomplished by reaction with TCEP·HCl; an aqueous work-up provided **18** in high purity since the oxidized TCEP and the 2-nitrothiophenol both readily partitioned into saturated sodium bicarbonate.

The optical rotation of **18** made by the reductive amination route was approximately twice that of the sample obtained by the alkylation route,[25] consistent with the diastereomeric ratio of **23** from the alkylation route and indicative of epimerization during alkylation with the triflate ester of methyl-(*R*)-lactate. Because I had sufficient material to move forward with the synthesis, I did not return to the alkylation route to analyze the alkylation step although I suspected that the use of NaOH could have caused the epimerization.[26]

---

[22] Nishimura, O.; Kitada, C.; Fujino, M. " New Method for Removing the S-*p*-Methoxybenzyl and S-*t*-Butyl Groups of Cysteine Residues with Mercuric Trifluoroacetate" *Chem. Pharm. Bull.* **1978**, *26*, 1576–1585.

[23] Determined by electrospray mass spectroscopy.

[24] Moore, C.G.; Porter, M. "The Reaction of 2,4-Dinitrobenzenesulphenyl Chloride with Organic Monosulphides" *Tetrahedron* **1960**, *9*, 58–64.

[25] Reductive amination route: $[\alpha]_D^{23} = -30.1$ ($CHCl_3$, c 5.84). Alkylation route: $[\alpha]_D^{23} = -15.0$ ($CHCl_3$, c 5.85).

[26] I had attempted to treat the solution of cystamine·2HCl with 1.95 equivalents of NaOH; for such a close margin, a small variation in measurements or NaOH concentration could introduce a catalytic amount of NaOH which could epimerize the triflate ester in the subsequent alklyation step.

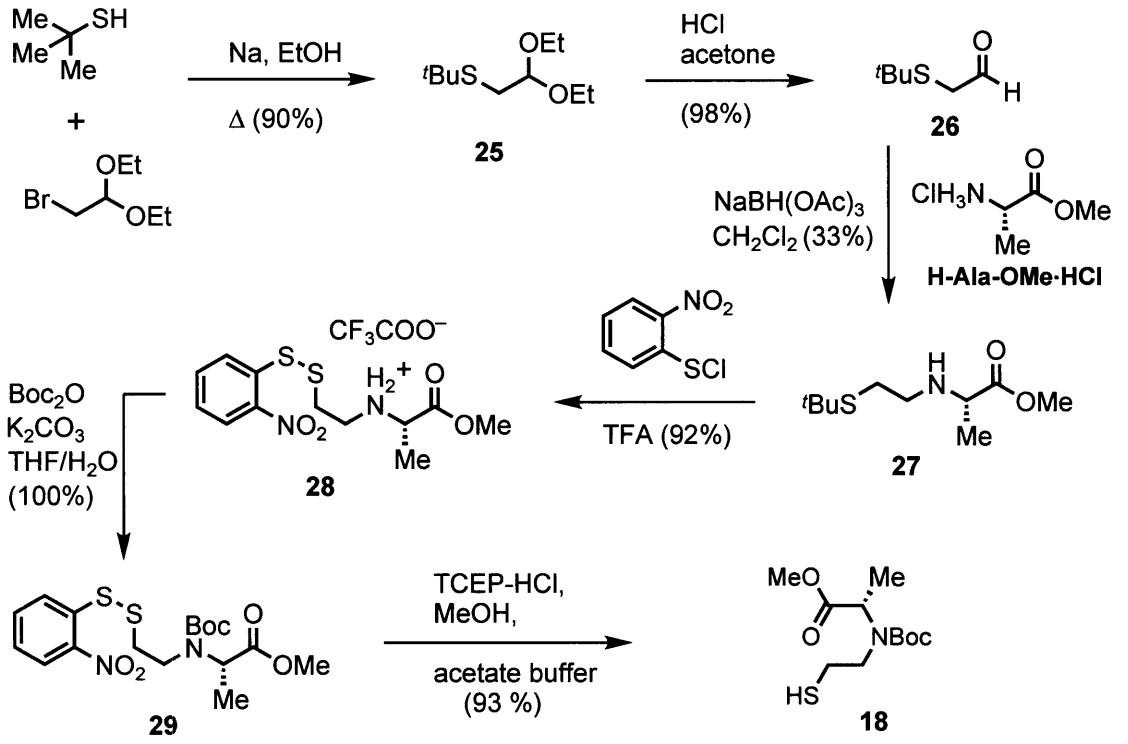

Scheme 3: Synthesis of enantiopure 18 by the reductive amination route.

Enantiopure **18** was combined with the Hyp fragment; the spectrum of the resulting thioester **19** is compared in Figure 9 with the spectrum of the mixture of thioester diastereomers from the alkylation route. The spectra illustrate the difficulty in using ^{1}H NMR to detect epimerization early in the synthesis (^{13}C NMR was no better). Not only do the amide and urethane rotamers complicate the spectrum, the conformational flexibility of the pyrrolidine ring broadens the resonances.

The diastereopure thioester was submitted the acyl transfer and cyclization reactions. Inspection of the ^{1}H NMR spectrum of the cyclized compound revealed a small amount of epimerization had occurred over the two steps, and comparison of the ^{1}H NMR spectra of **20** for the two routes suggested that the slight epimerization had occurred at the acyl transfer step. After hydrogenolysis of the Cbz group and hydrolysis of the methyl ester, analysis of the zwitterion by reverse-phase HPLC (Figure 10) confirmed the presence of approximately 4% of the epimer which was removed from the

product by HPLC. With addition of the Fmoc group (Scheme 4), NCap(8)Ala was ready to be tested in a peptide. Peptide conjugates of all templates are presented in the final section of this chapter.

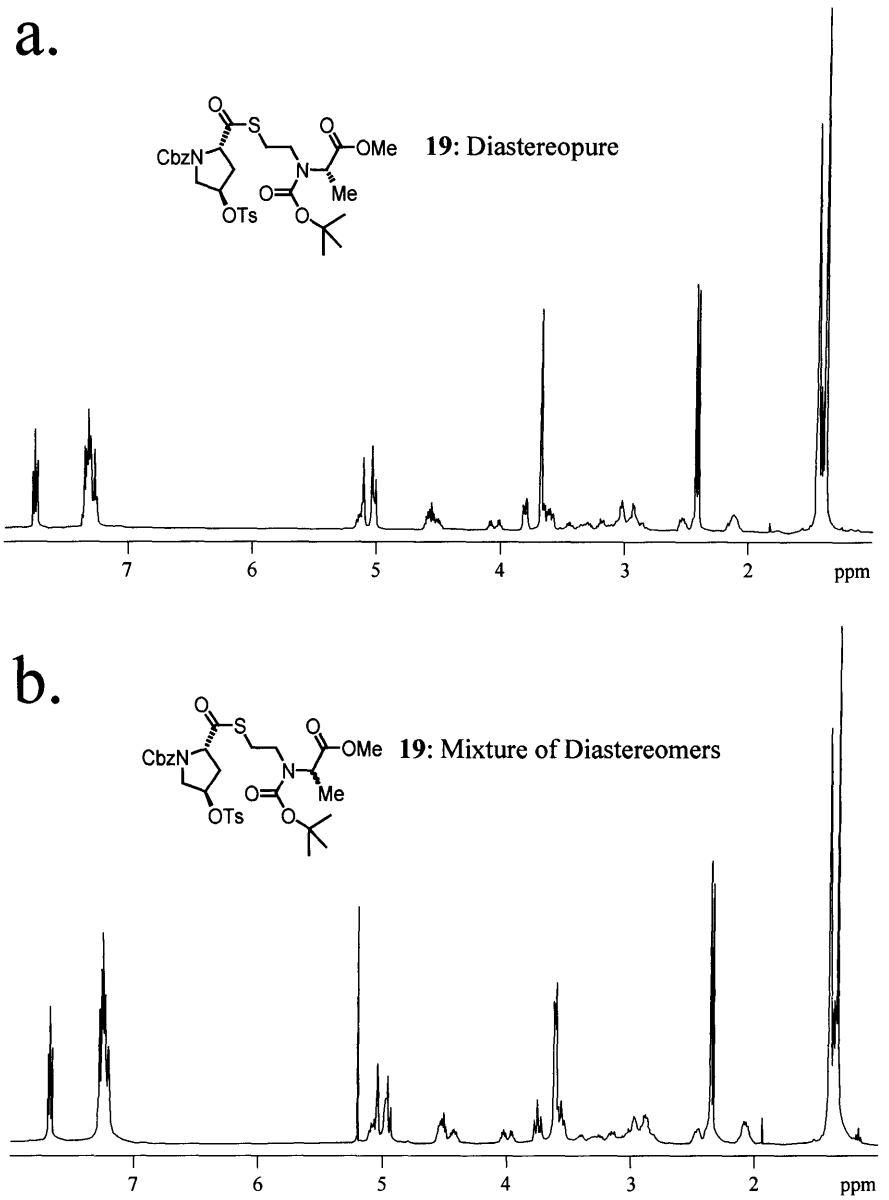

Figure 9: Comparison of ^{1}H NMR spectra for compound 19. (a) Diastereopure thioester obtained from the reductive amination route, and (b) Mixture of Diastereomers obtained from the alkylation route.

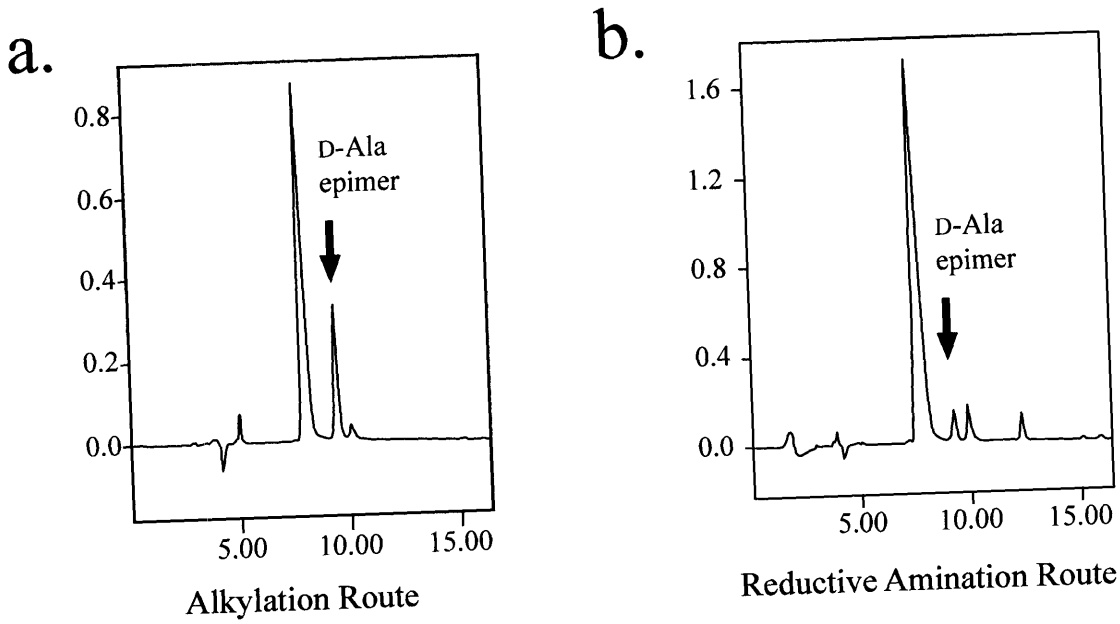

Figure 10: Reverse-phase HPLC chromatograms of 23 obtained from (a) the alkylation route and (b) the reductive amination route. (1 to 35% MeCN in (0.05%) H_2O /TFA).

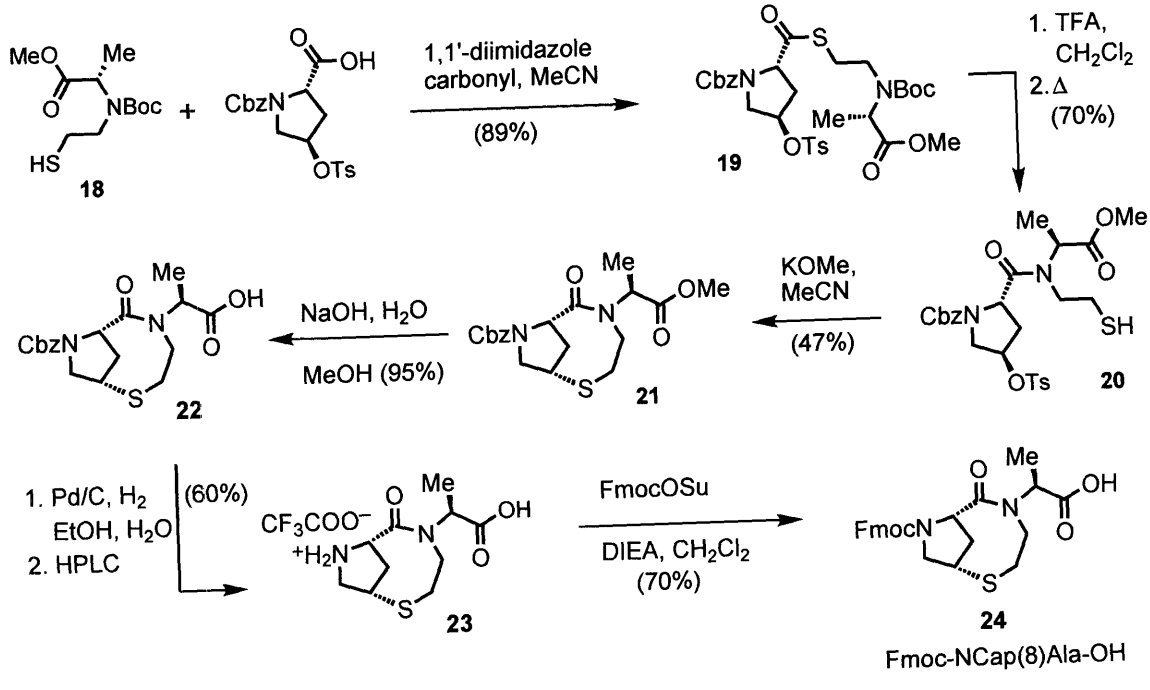

Scheme 4: Continuation of the reductive amination synthetic route to NCap(8)Ala

3. Simpler N-Terminal Helix Initiators: Seven-Member-Ring N-Caps

3.1. NCap (7)Ala

The key reaction in the syntheses of the 7-member ring N-Caps was an acid-catalyzed condensation of formaldehyde with a γ-thio amide (Figure 11) reported in the literature.[27] The moderate yield of **30** was not encouraging since the compound has a primary thiol and an unhindered secondary amide whereas our proposed dipeptide precursor contains a secondary thiol and a hindered secondary amide.

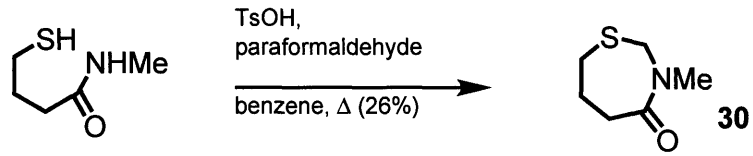

Figure 11: Literature precedent for key reaction in formation of 7-member-ring N-Caps.

The hydroxyl group of dipeptide Cbz-Hyp-Ala-OMe was converted to thiol **31** with inversion of configuration by Mitsunobu reaction with thiolacetic acid followed by treatment with ammonia (Scheme 5). Compound **33** was then heated at reflux overnight in benzene with paraformaldehyde and *p*-toluene sulfonic acid (TsOH); water was azeotropically removed using a Dean–Stark trap filled with molecular sieves. A good yield of the cyclized compound was obtained, but small peaks in the ^{1}H NMR spectrum of the purified material suggested the presence of an α-H epimer (approximately 13%). The most significant by-product in the reaction was the formaldehyde thioacetal formed from two molecules of thiol **33**.

[27] Kigasawa, K.; Hiiragi, M.; Wagatsuma, N.; Kohagizawa, T.; Inoue, H. "A Simple Synthesis of 4-Thiazolidinones, Tetrahydro-1,3-thiazin-4-one and Hexahydro-1,3-thiazepin-4-ones from Amide-Thiols (Studies on the Syntheses of Heterocyclic Compounds 749)" *Heterocycles* **1978**, *9*, 831–840.

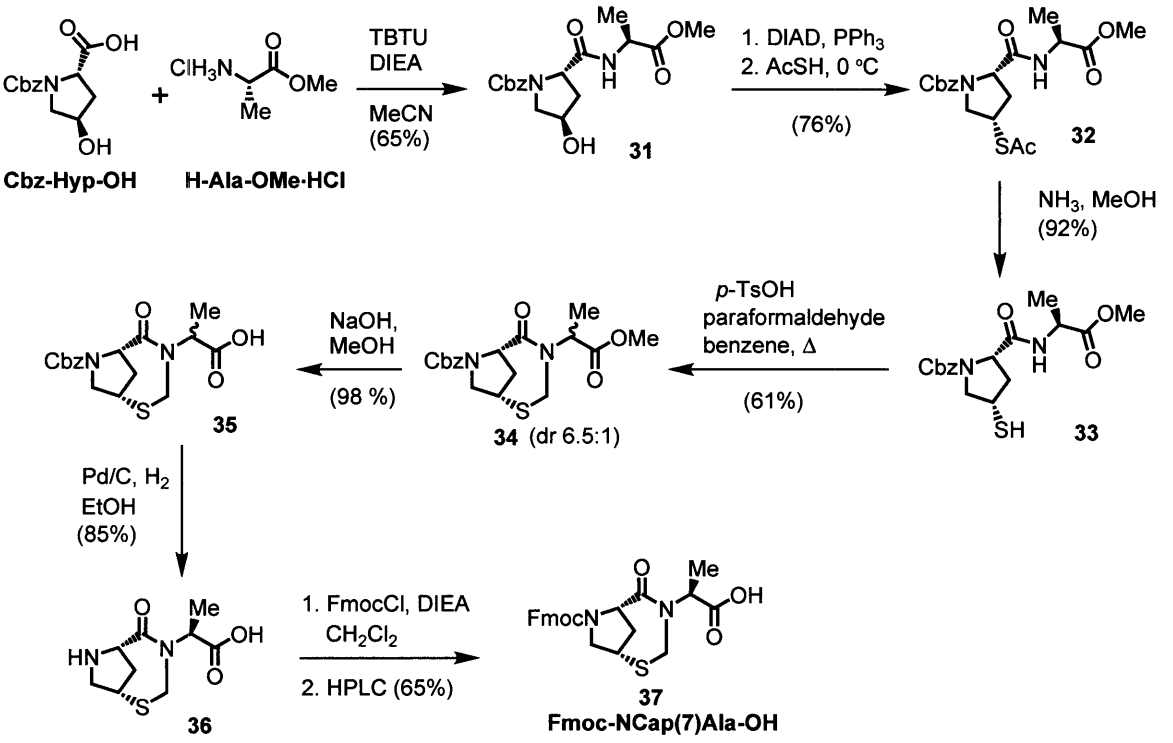

Scheme 5: Synthesis of NCap(7)Ala. The major diastereomer for 34, 35, and 36 is the desired L-Ala epimer, as demonstrated by subjecting H-D-Ala-OMe·HCl to this synthetic scheme.

Epimerization of the α-C of the alanine moiety was confirmed by comparison of the reverse-phase HPLC chromatogram and ^{1}H NMR spectrum of **34** with those for a sample derived from D,L-alanine (Figure 12). Although purification could be performed at this point, it was deferred until the zwitterion stage because the separation of the diastereomers was better at that point.

With no other evidence corroborating the absolute configuration of **34**, the synthesis was repeated using methyl-D-alanate in place of methyl-L-alanate. No significant difference in reactivity was observed, and Scheme 6 shows only the cyclization step. Paraformaldehyde is insoluble in most solvents, benzene included, and the reaction mixture was cloudy at the beginning of the condensation. After approximately one hour, the solution in the reaction vessel was clear, and the reaction was stopped rather than heating it at reflux overnight. Gratifyingly, the yield of the reaction was unchanged, and the reverse-phase HPLC chromatogram (Scheme 6) showed

only a trace of the α-H epimer in addition to proving the absolute configuration of the cyclized compound. Clearly, heating the cyclized product for hours in the presence of acid is detrimental and unnecessary. Compound **40** was submitted to the rest of the reaction sequence to generate NCap(7)DAla **44**;[28] the small amount of epimer was removed by reverse-phase HPLC at the zwitterion stage.

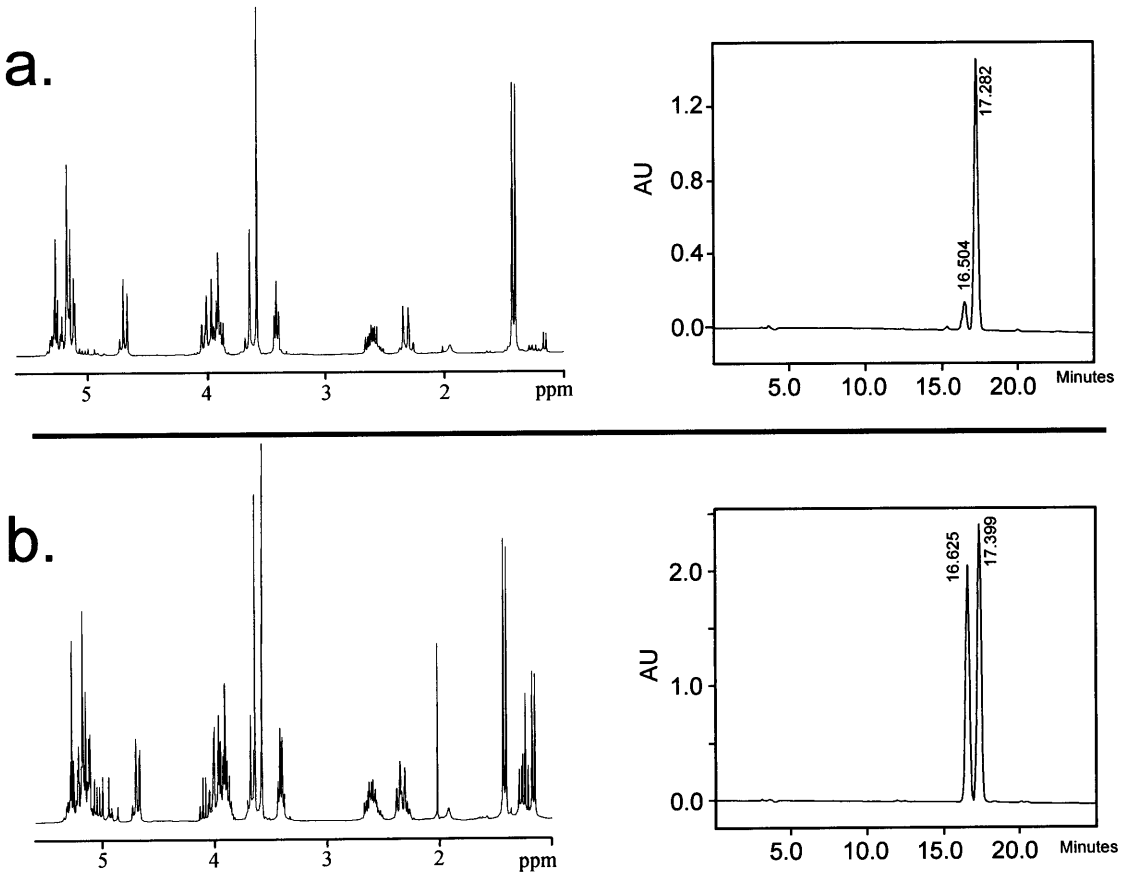

Figure 12: Comparison of ^{1}H NMR and reverse-phase HPLC (5 to 35% MeCN in TFA (0.05%)/H_2O) for (a) epimerized compound 34 derived from L-Ala and (b) compound 34 derived from racemic Ala.

Modeling of the putative helical conformation of the NCap(7)Ala identified a possible steric interaction—similar to 1,3-allylic strain—between the alanine α-Me and the methylene group derived from formaldehyde. Replacement of the L-Ala moiety with

[28] Because of the similarity between the reaction sequence for NCap(7)Ala and NCap(7)DAla, steps other than the cyclization reaction are only shown in the Experimental section. Although compounds **32**, **33**, and **36**–**38** do not appear here, the numbering scheme is still used.

D-Ala alleviated this strain, and therefore both templates **36** and **43** were investigated.

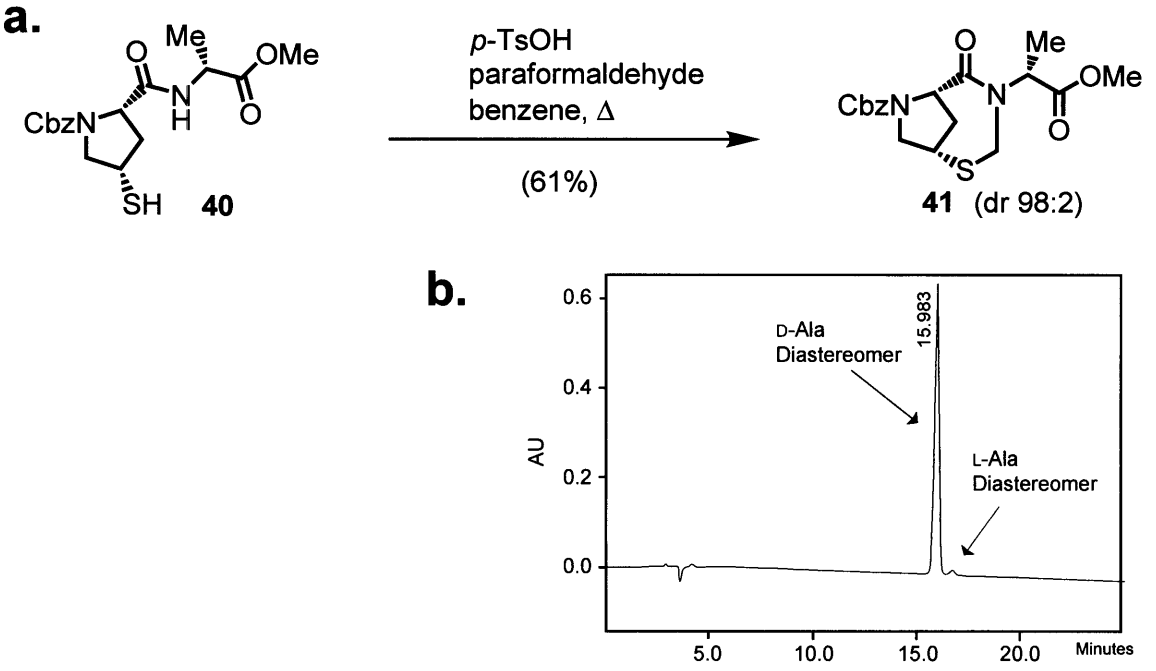

Scheme 6: (a) Key cyclization step in the synthesis of NCap(7)DAla; compounds 38, 39, and 42–44 are not shown—See experimental. (b) Reverse-phase HPLC chromatogram of 35 showing a trace of the Ala α-C epimer.

3.2. NCap(7)Gly

Epimerization problem during the ring-forming condensation spurred the development of a glycine analog. The dipeptide Boc-Hyp-Gly-OMe was synthesized in good yield and the secondary hydroxy group was converted to a thiol as before, in preparation for the cyclization step (Scheme 7). The most notable difference arising from the substitution of Gly for Ala was the markedly lower yield for the formaldehyde condensation reaction. No significant impurity was evident by TLC; however, a large amount of insoluble material was noted. Compound **48** was subjected to base hydrolysis followed by acid hydrolysis to obtain zwitterion **49** which was reacted with FmocOSu to generate Fmoc-NCap(7)Gly-OH. The low yield for the final step is possibly caused by the high water solubility of the compound.

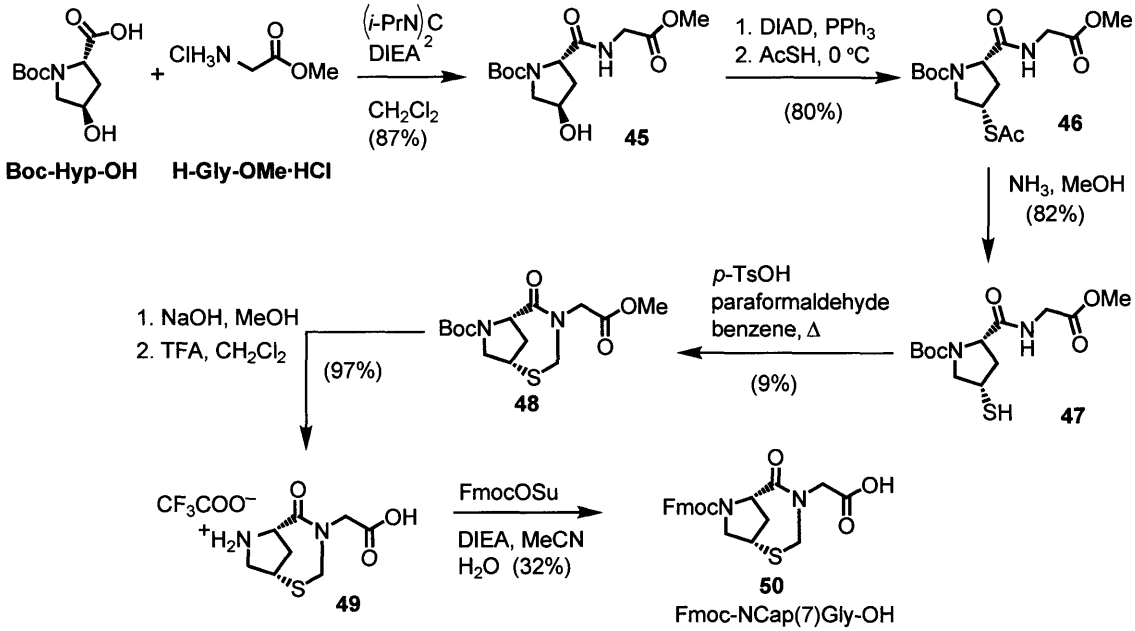

Scheme 7: Synthesis of NCap(7)Gly

3.3. NCap(7)Aib

The use of Aib in place of Ala was also investigated as another way to avoid the issue of epimerization. The helix-promoting property of Aib was alluring, but the possibility for the 1,3-allylic-like interaction still existed. After an earlier attempt using dipeptide Cbz-Hyp-Aib-OMe failed at the ester hydrolysis step,[29] a *tert*-butyl ester protecting group strategy for the synthesis of Fmoc-NCap(7)Aib-OH was pursued.

A commercial source for H-Aib-O^{t}Bu·HCl was found and the dipeptide Boc-Hyp-Aib-O^{t}Bu was made in good yield. A common problem with the Mitsunobu reaction was encountered though—the reduced DIAD reagent could not be separated from thioacetate **56** by flash chromatography.[30] Although reverse-phase HPLC separated the compounds, this was not feasible for a large scale purification. The mixture was treated with ammonia in methanol in hopes that thiol **57** would be separable from the impurity by

[29] Aranda, G.; Fétizon, M. "A New Method for the Hydrolysis of Hindered Esters" *Synthesis* **1975**, *5*, 330–332.

[30] (a) Dembinski, R. "Recent Advances in the Mitsunobu Reaction: Modified Reagents and the Quest for Chromatography-Free Separation" *Eur. J. Org. Chem.* **2004**, *13*, 2763–2772. (b) Barrett, A.G.M.; Roberts, R.S.; Schröder, J. "Impurity Annihilation: Chromatography-Free Parallel Mitsunobu Reactions" *Org. Lett.* **2000**, *2*, 2999–3001.

flash chromatography, but this was not the case. Again, an analytical sample was prepared by reverse-phase HPLC; after standing overnight, the thiol in the aqueous HPLC sample was converted to the disulfide which is readily separated from the reduced DIAD impurity by flash chromatography.

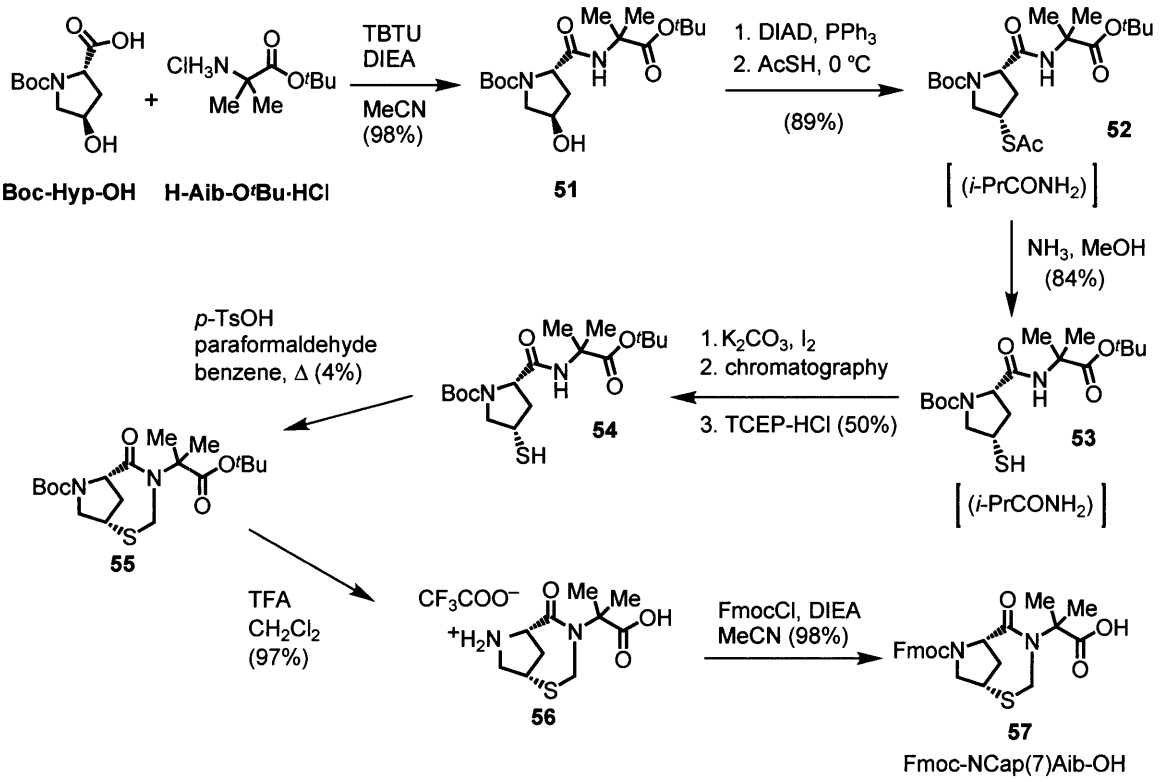

Scheme 8: Synthesis of Fmoc-NCap(7)Aib-OH

Attempts at forming the disulfide by stirring overnight in aqueous acetonitrile under ambient atmosphere failed; so too did an attempt under an atmosphere of oxygen. I therefore treated the mixture of reduced DIAD and **56** with iodine in basic aqueous methanol. Pure disulfide was obtained by flash chromatography, and thiol **57** was recovered by treatment of the disulfide with TCEP·HCl. I later learned that the key to disulfide formation was base; ammonolysis of thioacetate **56** under ambient atmosphere rather than argon gave the disulfide in good yield. Cyclization yielded compound **59** in poor yield; however, sufficient material was obtained to allow synthesis of Fmoc-NCap(7)Aib-OH (Scheme 8). In this case, the chief impurity in the cyclization reaction

was easily identified as the thioacetal dimer.

4. Evaluation of Peptides Incorporating the New N-Caps

4.1. CD Analysis

For initial tests of our new N-Caps, six analogs of the series **2** Ala_{10} peptide Ac-$^{\beta}$DHel-A_{10}-*beta*-Acc-K_2-W-NH_2 were made by substituting our new caps for Hel (Table 1). We chose Ala_{10} because the peptides would have two "core" alanine residues not directly affected by the caps, and because short peptides permit fine distinctions among the caps to be discerned.

Table 1: Analogs of the Series 2 Ala_{10} Peptide

Ac-**N-Cap**-Ala_{10}-*beta*-Acc-K_2-W-NH_2

Peptide	N-Cap
Series **2** Ala_{10} peptide	$^{\beta}$D-Hel
NC(8)Gly	$^{\beta}$D-NCap(8)Gly
NC(8)Ala	$^{\beta}$D-NCap(8)Ala
NC(7)Gly	$^{\beta}$D-NCap(7)Gly
NC(7)Ala	$^{\beta}$D-NCap(7)Ala
NC(7)DAla	$^{\beta}$D-NCap(7)DAla
NC(7)Aib	$^{\beta}$D-NCap(7)Aib

An overlay of the CD spectra (2 °C, pH > 4.5) of the series **2** Ala_{10} peptide and the seven-member-ring analogs appears in Figure 13a. Spectra of peptides NC(7)Gly and NC(7)DAla are absent from the plot because they are nearly superimposable with the spectrum for peptide NC(7)Ala. NCap(7)Aib is clearly the least effective helix-stabilizer, and NCap(7)Ala emerges as the most cost-effective helix initiator of its class; even so, judging by CD, its helicity is much less than that of the series **2** peptide. A notable characteristic of the NC(7)Xxx peptides is the slightly different shape of their CD spectrum: the distance between the two minima is greater than that in the CD spectrum of the Hel peptides.

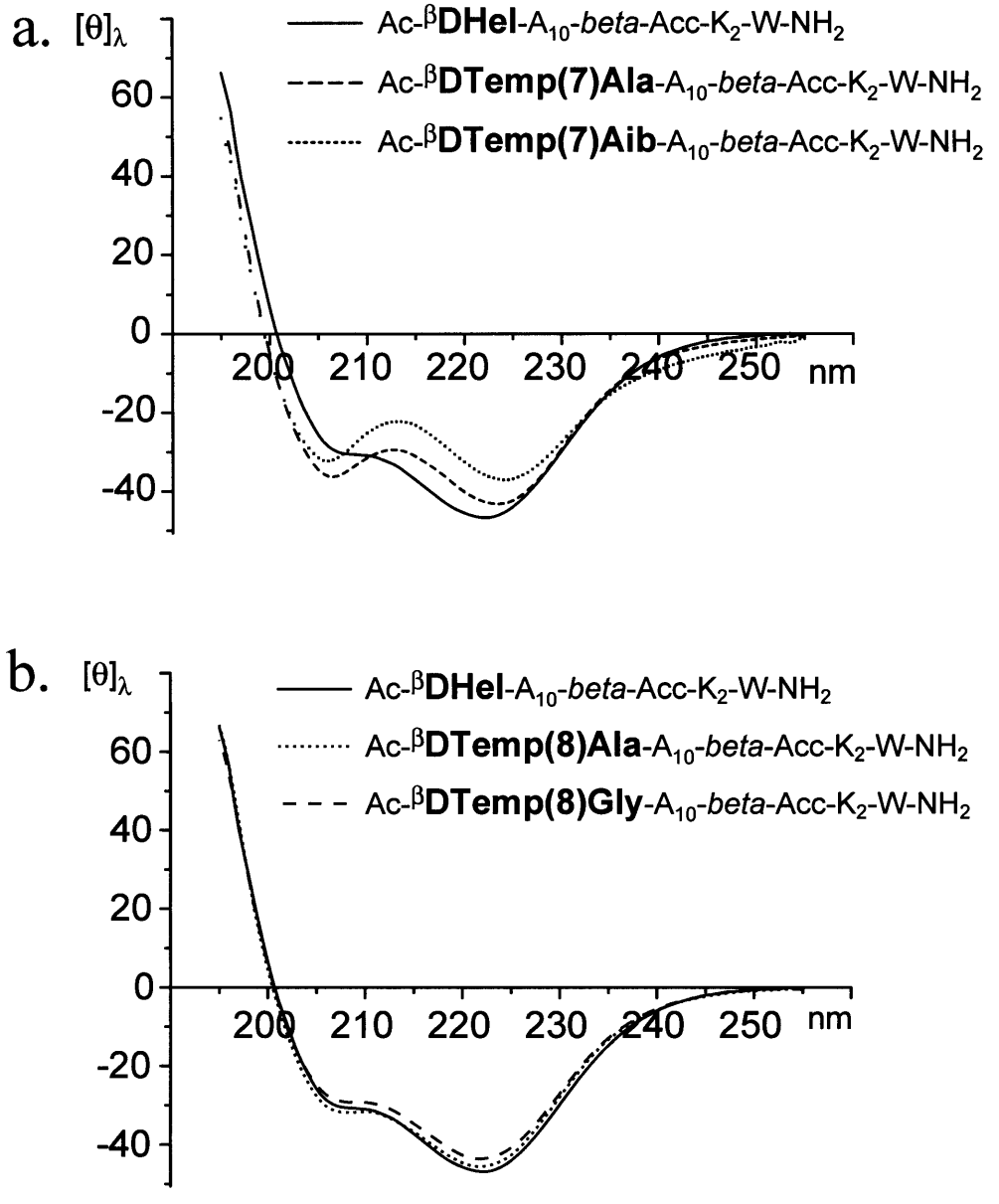

Figure 13: (a) Overlay of CD spectra (2 °C, pH > 4.5) for the NCap(7)Xxx Ala_{10} peptides and the series 2 Ala_{10} peptide. (b) Overlay of CD spectra (2 °C, pH > 4.5) for the NCap(8)Xxx Ala_{10} peptides and the series 2 Ala_{10} peptide.

Peptides constructed with the new eight-member-ring N-Caps have CD spectra that very closely approach that of the series **2** Ala_{10} reference (Figure 13b). The CD curve of NC(8)Gly closely matches that of the series **2** peptide and the CD curve of NC(8)Ala is closer still. Differences among the three peptides become more pronounced

with higher temperatures; even so, all three peptides are quite helical at 30 °C (pH > 4.5).

The CD spectrum of the series **2** Ala_{10} peptide places an upper bound on the $[\theta]_{222}$ for a decapeptide, and the CD spectrum of the peptide W-K_4-Inp_2-^{t}L-Ala_{10}-^{t}L-Inp_2-K_4-NH_2, which contains no helix-stabilizing caps, defines the lower bound of $[\theta]_{222}$ for a decapeptide as approximately zero (Figure 14). However, we felt that the appropriate references for gauging the effects of ϕ,ψ constraint in our synthetic N-caps were peptides incorporating a simple $^{\beta}$D-Pro-Xxx N-cap (Figure 15). We were astonished to find that, at 2 °C, the $[\theta]_{222}$ value of the series **2** Ala_{10} peptide was flanked by the values for the control peptides Ac-$^{\beta}$DProXxx-A_{10}-*beta*-Acc-K_2-W-NH_2 (Figure 16, Xxx = Gly or Ala). Direct comparison of these data is not warranted because the Xxx residues of the control peptides ought to be counted with the ten alanine residues; in other words, the two should be considered undecapeptides with a $^{\beta}$DPro N-cap.

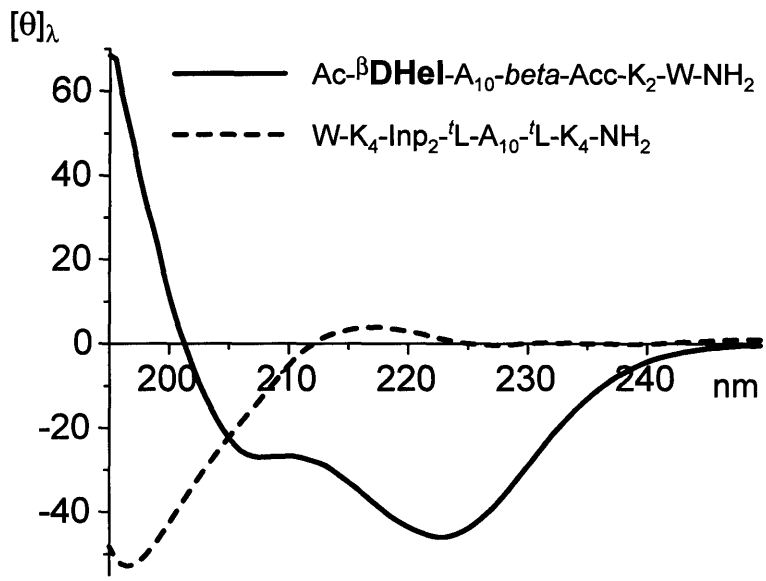

Figure 14: Comparison of the series 2 Ala_{10} peptide with an Ala_{10} peptide capped only by spaced solubilizers.

Our values of $[\theta_{\infty}]_{222}$ and X can be applied to compare the helicity of these $^{\beta}$DPro-capped peptides with our Hel-capped peptides, but only approximately owing to the

likely series specificity of X. Even so, the $-[\theta]_{222}$ value[31] at 2 °C for the peptide Ac-$^{\beta}$DProAla-A_{10}-*beta*-Acc-K_2-W-NH_2 (479,000 deg cm^2 dmol^{-1}) is within the calculated range of $-[\theta]_{222}$ for fully helical Ala_{11}: 468,000 – 525,000 deg cm^2 dmol^{-1}.

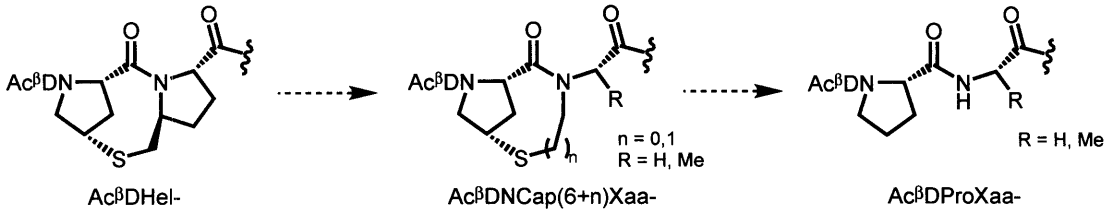

Figure 15: N-caps of increasing simplicity and decreasing ϕ,ψ constraint from left to right.

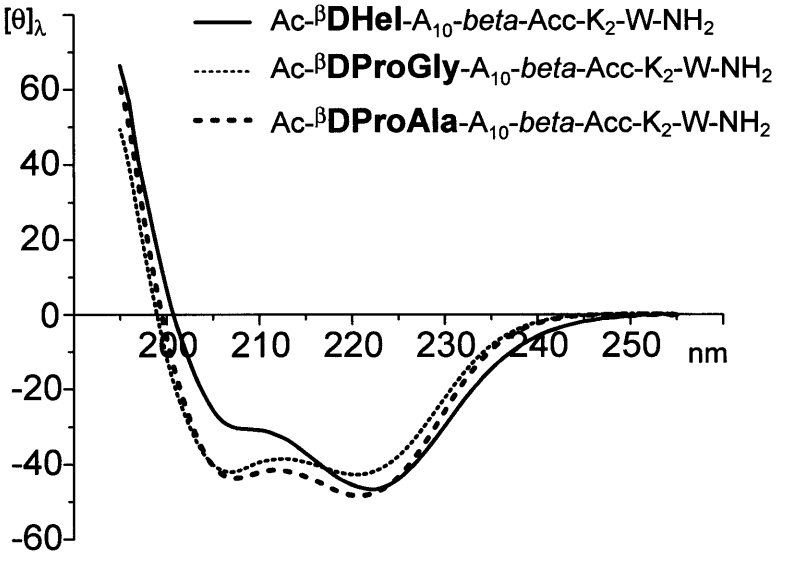

Figure 16: Comparison of the series 2 Ala_{10} peptide with Ala_{10} peptides containing the N-cap $^{\beta}$DProXaa (2 °C, pH > 4.5, 20 mM NaH_2PO_4).

4.2. NMR Analysis

As noted in the previous Chapter, ^{13}C chemical shifts have proven useful for structure determination, and we expected that a comparison of highly analogous peptides would be informative. A preliminary study of ^{13}CO NMR chemical shifts was conducted on Ac-$^{\beta}$DProGly-A_{10}-*beta*-Acc-K_2-W-NH_2 peptides synthesized with ^{13}CO-labeled Ala

[31] Uncorrected for contributions of non-alanine residues.

(*^{l}Ala*). Dr. Robert Kennedy had recently developed a method whereby each alanine site is encoded by its signal intensity, thus reducing the number of peptides needed to observe all alanine resonances. This is accomplished as follows: for peptide Ac-$^{\beta}$DPro-Gly-*^{l}Ala*-AAA-*^{l}Ala*-AAA-*^{l}Ala*-A-*beta*-Acc-K_2-W-NH_2 the alanine at site 1 is 100% labeled, the alanine at site 5 is 66% labeled, and the alanine at site 9 is 33% labeled.[32] Thus, the identities can be assigned by ^{13}CO peak integrations. Data from three labeled $^{\beta}$DPro peptides appear in Figure 17 along with Dr. Kennedy's data for Ala_5, Ala_9, and Ala_{11} peptides capped only by spaced solubilizers. The Ala_5 peptide sets a lower bound for ^{13}CO chemical shift values, and the upper bound is defined by the ^{13}CO chemical shift of the central residues of the labeled series **2** Ala_{12} peptide from the previous chapter.

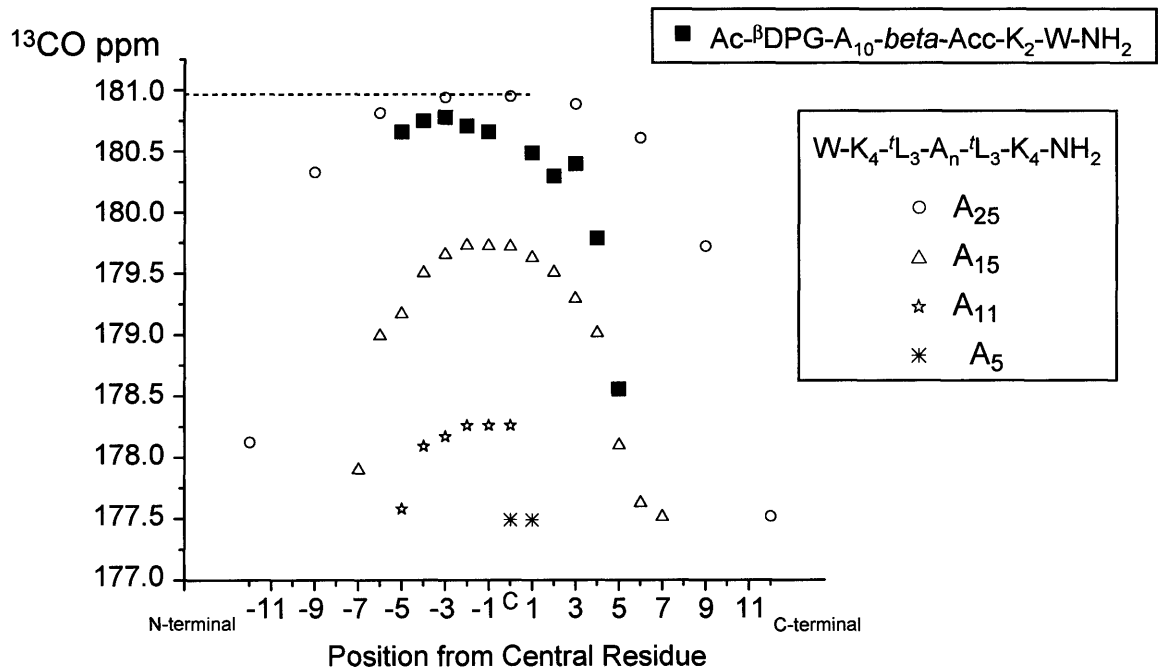

Figure 17: Plot of ^{13}CO chemical shifts for the peptide Ac-$^{\beta}$DProGly-A_{10}-*beta*-Acc-K_2-W-NH_2 (2 °C, pH > 4.5) and for a series of peptides without helix-stabilizing caps: W-K_4-$^{t}L_3$-A_n-$^{t}L_3$-K_4-NH_2 where n = 25, 15, 9, and 5 (2 °C, pH ~7). The dashed line marks the ^{13}CO chemical shifts for the central residues of the (> 95% helical) series 2 Ala_{12} peptide from the preceding chapter.

[32] Some may recognize this as an application of the traditional puzzle of identifying, with a single measurement, which of ten sacks contains coins weighing only 9/10^{ths} as much as the coins in the other sacks. See Gamow, G. and Stern, M. *Puzzle Math;* New York, Viking Press, **1958**.

4.3. Discussion

The proliferation of X-ray crystal structures of proteins in the last two decades has prompted analysis of the frequency with which amino acids appear at specific sites in α-helices.[33] Others have built on this work, and the motif XaaP (where Xaa = Ser, Thr, Asp, Asn) has been identified as a frequent dipeptide sequence at the N_{cap}-N_1 positions of α-helices in proteins.[34] These investigators have considered Pro a part of the helix, which is seemingly at odds with our convention of referring to it as part of the N-cap. Our rationale stems from our work with CD spectroscopy of Hel-capped peptides in which the contribution of a tertiary amide to a helical CD spectrum is different from the contribution of a secondary amide. The uncertainty illustrates the difficulty in defining helical length.

In any event, CD and ^{13}CO evidence demonstrate that the $^{\beta}$DPro motif creates highly helical polyalanines. It is striking that, despite the well-known helix-promoting properties of the XaaPro dipeptide,[35] no examples of highly helical peptides with such N-caps have been widely reported, especially considering the broad interest in the α-helix. A natural question is whether our $^{\beta}$DPro-capped polyalanines are atypical. How does the $^{\beta}$DPro cap function at high temperatures, at low pH, and with amino acids other than alanine? Furthermore, is $^{\beta}$DPro significantly different from the natural peptide N-caps XaaPro? Although our preliminary results cannot address the final question, they can address the first.

---

[33] (a) Presta, L.G.; Rose, G.D. "Helix Signals in Proteins" *Science* **1988**, *240*, 1632–1640. (b) Aurora, R.; Rose, G.D. "Helix Capping" *Prot. Sci.* **1998**, *7*, 21–38.

[34] (a) Wako, H.; An, J.; Sarai, A. "Environment-dependent and Position-specific Frequencies of Amino Acid Occurrences in α-Helices" *Chem-Bio Informatics Journal* **2003**, *3*, 58–77. (b) Pal, L.; Chakrabarti, P.; Basu, G. "Sequence and Structure Patterns in Proteins from an Analysis of the Shortest Helices: Implications for Helix Nucleation" *J. Mol. Biol.* **2003**, *326*, 273–291. (c) Hollenbeck, J.J.; McClain, D.L.; Oakley, M.G. "The Role of Helix-stabilizing Residues in GCN4 Basic Region Folding and DNA Binding" *Protein Science* **2002**, *11*, 2740–2747.

[35] Xaa = Asp, Asn, Ser, Thr.

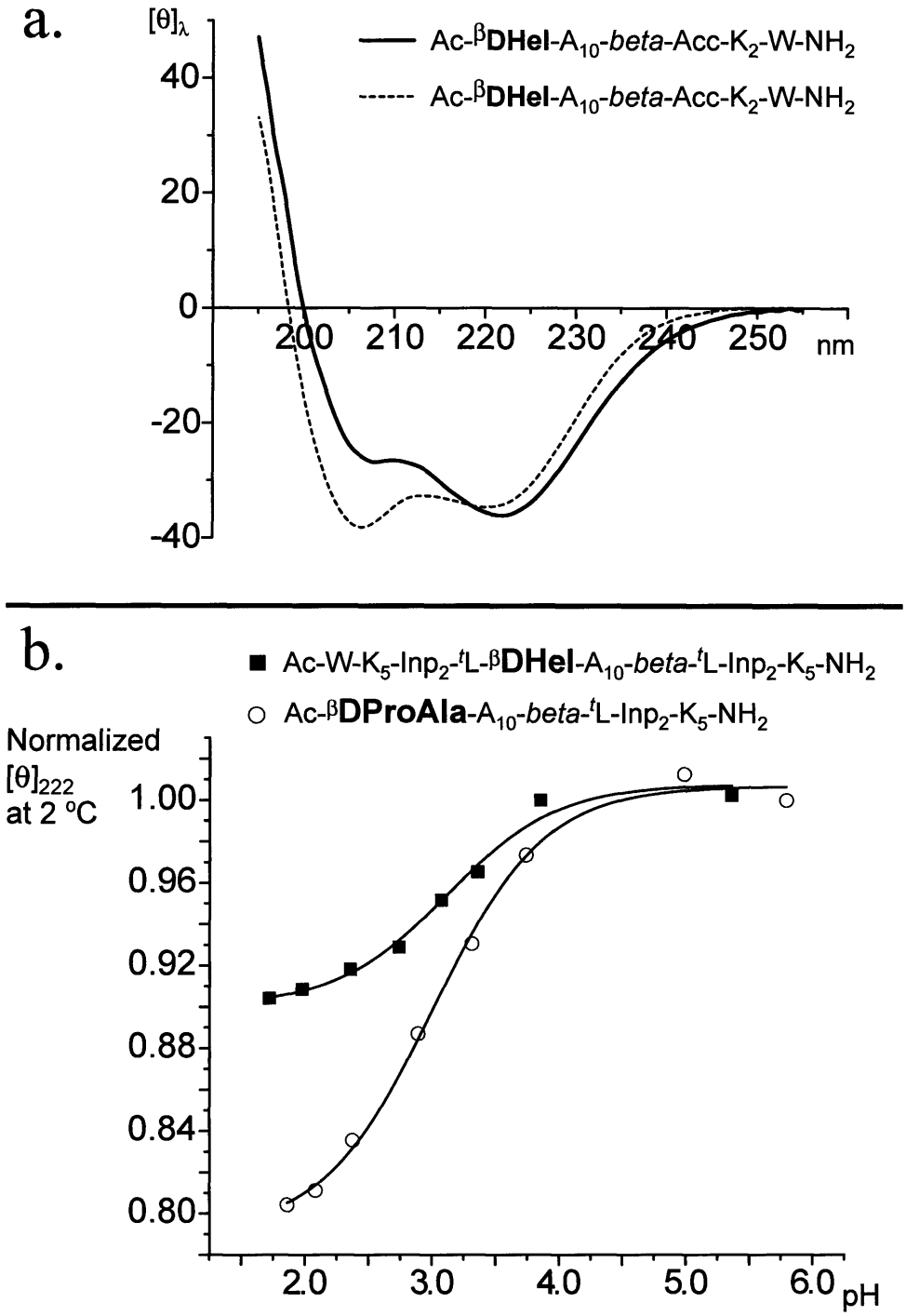

Figure 18: (a) CD spectra of the series 2 Ala_{10} peptide and the $^{\beta}$DProAla-capped Ala_{10} peptide (30 °C, pH > 4.5, 20 mM NaH_2PO_4). (b) Normalized titration curves for the series 2 Ala_{10} peptide and the $^{\beta}$DProAla-capped Ala_{10} peptide (2 °C, pH adjusted with conc. NaOH and H_3PO_4, 20 mM NaH_2PO_4 initially).

Subtle differences among helix-stabilizing caps are apt to be more apparent under non-ideal conditions. At 30 °C, the $^{\beta}$DPro-Ala$_{11}$ peptide loses helicity more than does the series **2** Ala$_{10}$ peptide (Figure 18a); yet the $^{\beta}$DPro-Ala$_{11}$ peptide still compares favorably with the $^{\beta}$DNCap(8)Xaa-Ala$_{10}$ peptides. Moreover, the difference between the $^{\beta}$DPro cap and Hel is greater at pH < 4.5. The $^{\beta}$DPro-Ala$_{11}$ peptide $[\theta]_{222}$ value drops by 20% from pH 4.5 to pH 1.5, whereas the corresponding value for the Hel-capped series **3** Ala$_{10}$ peptide drops by only 10% (Figure 18b). This result signifies that, although charge plays a role in helix-stabilization, an uncharged hydrogen-bonding site can also effectively stabilize helical structure. Although this pH dependence is not physiologically relevant, it does reveal that constraint of ϕ,ψ angles in the N-cap contributes appreciably to helical structure under non-optimal conditions. Another non-optimal condition that is physiologically relevant is the replacement of alanine residues with amino acids having lower helical propensities. The relative helix-stabilizing properties of Hel, our new N-Caps, and $^{\beta}$DPro in non-alanine models is unknown, and must be determined before application of our helical constructs to broader issues can proceed.

4.4. Summary

In the search for easily synthesized N-terminal helix-initiating caps, a series of Hel analogs were made which have one less rotational constraint. Ala$_{10}$ peptides made with the eight-member-ring N-Caps exhibited CD spectra very similar in shape and intensity to their Hel analogs. Results for the seven-member-ring N-Caps were less encouraging. A surprising and promising discovery was the high helicity of $^{\beta}$DPro-capped polyalanine peptides initially synthesized as control sequences to judge the helix-initiating ability of our new synthetic N-Caps.

The availability of a cheap, effective, and commercially available N-Cap will likely engender new interest in this fundamental protein structure. Although the results reported herein are promising, they are also preliminary and their ability to induce helicity in peptides other than polyalanine is unproven.

5. Experimental Procedures

5.1. General Considerations

Reactions were stirred magnetically and run open to the atmosphere with no effort made to exclude water, unless otherwise stated. Organic solvents were evaporated / removed / stripped by rotary evaporation at ~50 mmHg. All solvents and reagents were obtained from commercial sources—Aldrich and Alfa Aesar—and used as received. L-Alanine-N-Fmoc (1-13C, 99%) was purchased from Cambridge Isotope Laboratories, Inc.

5.2. Chromatography

Flash chromatography was performed using Merck 230-400 mesh silica gel using high pressure liquid chromatography (HPLC)-grade solvents and monitored by thin layer chromatography (TLC). TLC was performed using precoated, glass silica gel 60 plates from EMD Chemicals Inc. All R_f values refer to the chromatography solvent unless otherwise stated. Visualization was by short-wave UV or a Mo–Ce stain, as appropriate. The Mo–Ce stain was prepared by mixing 50 g of ammonium molybdate(VI) tetrahydrate $(NH_4)_6Mo_7O_{24}{\cdot}4H_2O$, 1 g cerium(IV) sulfate $Ce(SO_4)_2$, 100 mL concentrated H_2SO_4, and 900 mL H_2O; heating is required for visualization.

Semi-prep HPLC was performed using a 25 minute gradient (#6, 1%/min.) with a YMC ODS-AQ 200 Å, 10 × 150 mm stainless steel column (Waters) on a Waters 600 HPLC system, monitoring at 214 nm, with a 996 PDA UV detector. Analytical HPLC was performed using a 40 minute gradient (#6, 1%/min.) with a smaller version (4.5 × 150 mm) of the same column on a Waters 2690 HPLC, monitoring at 214 and 280 nm, with a 996 PDA UV detector. No isocratic hold was used at the beginning of either the semi-prep or analytical HPLC methods. For all methods, the solvents were HPLC-grade acetonitrile (MeCN) and a mixture of 0.05% trifluoroacetic acid (TFA) in deionized, 18 MΩ water (Millipore gradient A10 system).

5.3. Synthesis of Fmoc-NCap(8)Gly-OH

(*tert*-Butoxycarbonyl-{2-[2-(tert-butoxycarbonyl-methoxycarbonylmethyl-amino)-ethyldisulfanyl]-ethyl}-amino)-acetic acid methyl ester (9)

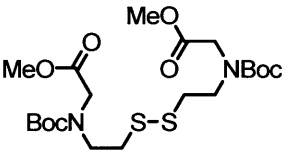

DIEA (2.4 mL, 13.9 mmol) and methyl bromoacetate (2.4 mL, 13.8 mmol) were added to a round bottom flask containing cystamine (1.0 g, 6.6 mmol) in methylene chloride (80 mL), and the solution was allowed to warm to room temperature overnight. Boc_2O (3.0 mL, 13.8 mmol) was added, and stirring was continued for 8 h. Methylene chloride was evaporated, and the white solid which remained was triturated with hexanes–ethyl acetate (2:1). After filtration, the solution was concentrated to a clear, highly viscous oil. Purification by silica gel chromatography (hexanes–ethyl acetate, 3:2), provided 1.48 g (42%) of the analytically pure title compound. TLC: Mo–Ce, blue, R_f = 0.41. Careful chromatography is required to separate the title compound from the di-Boc-cystamine for which R_f = 0.46. ^{1}H NMR ($CDCl_3$, 300 MHz, 2 rotamers): δ 1.42 (s, 9H), 1.48 (s, 9H), 2.84 (m, 4H), 3.53 (t, 2H, J = 7.4 Hz), 3.57 (t, 2H, J = 6.9 Hz), 3.737 (s, 3H), 3.741 (s, 3H), 3.94 (s, 2H), 4.01 (s, 2H). ^{13}C NMR ($CDCl_3$, 125 MHz, 4 diastereomers evident by NMR): δ 28.3, 28.4, 36.4, 36.6, 36.6, 36.6, 48.4, 48.5, 49.6, 49.7, 50.6, 52.1, 52.2, 52.2, 80.6, 80.7, 80.8, 80.9, 155.02, 155.03, 155.4, 155.5, 170.57, 170.61, 170.6, 170.7. IR (film, cm^{-1}): 1693, 1751, 2933, 2976. Elemental analysis found C 48.46, H 7.38, N 5.62; calcd. C 48.37, H 7.31, N 5.64.

[*tert*-Butoxycarbonyl-(2-mercapto-ethyl)-amino]-acetic acid methyl ester (10)

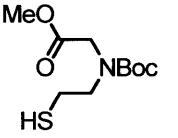

NaOAc–AcOH buffer (0.1 M, pH = 4.7) was added to a solution of disulfide **9** (1.0 g, 2.0 mmol) in 20 mL MeOH (~5mL, stopped just before solution became cloudy). TCEP·HCl (1.04 g, 3.6 mmol) was then added in one portion, and the contents of the flask were stirred for 6 h. Afterwards, most of the MeOH was stripped, and 30 mL of brine were added to the flask. The cloudy mixture was extracted with ether (3 x 20 mL), and the combined organic layers were washed with saturated $NaHCO_3$ (2 x 20 mL), dried

over $MgSO_4$, and filtered. The solvent was removed *in vacuo* yielding 0.93 g (93%) of the analytically pure title compound as a clear oil. Thiol **10** is much less viscous than its disulfide precursor **9**; furthermore, **10** quickly stains blue with Mo–Ce, unlike the disulfide which requires prolonged heating. TLC: R_f = 0.61, hexanes–ethyl acetate (3:2). ^{1}H NMR ($CDCl_3$, 500 MHz, 2 rotamers): δ 1.42 (s, 4.8H), 1.48 (s, 4.2H), 2.69 (app quint, 2H, J = 7.2 Hz), 3.42 (t, 0.9H, J = 7.2 Hz), 3.46 (t, 1.1H, J = 7.2 Hz), 3.735 (s, 1.4H), 3.742 (s, 1.6H), 3.95 (s, 1.05H), 4.03 (s, 0.95H). ^{13}C NMR ($CDCl_3$, 125 MHz, 2 rotamers): δ 23.2, 23.5, 28.4, 28.5, 49.9, 50.6, 52.25, 52.31, 52.46, 52.52, 80.8, 81.0, 155.3, 155.6, 170.68, 170.73. IR (film, cm^{-1}): 1689, 1751, 2565, 2953, 2976. Elemental analysis found C 48.22, H 7.76, N 5.64; calcd. C 48.17, H 7.68, N 5.62.

(*2S,4R*)-2-[2-(*tert*-Butoxycarbonyl-methoxycarbonylmethyl-amino)-ethylsulfanylcarbonyl]-4-(toluene-4-sulfonyloxy)-pyrrolidine-1-carboxylic acid benzyl ester (11)

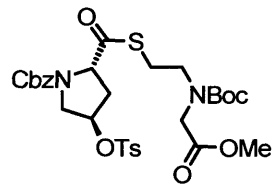

A round bottom flask was charged with N-Cbz-4-(*R*)-tosyl-L-proline (4.36 g, 10.4 mmol), 1,1′-diimidazole carbonyl (1.69 g, 10.4 mmol), and MeCN (150 mL). Thiol **10** (2.16 g, 8.7 mmol) was added ½ h later, and stirring was continued overnight. Evaporation of the solvent provided a light yellow oil; purification by flash chromatography [hexanes-ethyl acetate (11:9)] yielded 1.61 g (88%) of the title compound as a white foam under high vacuum. TLC: R_f = 0.56, Mo–Ce, blue. ^{1}H NMR ($CDCl_3$, 500 MHz, 2 rotamers): δ 1.41 (s, 4.8H), 1.47 (4.2H), 2.14 (m, 1H), 2.44 (s, 1.6H), 2.46 (s, 1.4H), 2.50 (m, 1H), 2.92 (m, 1H), 3.04 (m, 1H), 3.20 (m, 1H), 3.36 (m, 1H), 3.61 (dd, J = 4.0, 12.8Hz, 0.45H), 3.66 (dd, J = 4.4, 12.7Hz, 0.55H), 3.72 (s, 1.4H), 3.73 (s, 1.6H), 3.82 (m, 1H), 3.92 (s, 1H), 3.99 (s, 0.6H), 4.59 (m, 1H), 5.10 (m, 3H), 7.35 (m, 7H), 7.75 (t, J = 8.2Hz, 2H). ^{13}C NMR ($CDCl_3$, 125 MHz, 2 rotamers): δ 21.8, 26.7, 26.8, 27.2, 27.4, 28.3, 28.5, 36.8, 38.1, 38.2, 48.2, 48.4, 49.6, 49.7, 50.2, 50.4, 52.2, 52.27, 52.31, 52.8, 53.1, 64.3, 64.6, 67.8, 68.0, 78.1, 78.3, 78.7, 78.8, 80.8, 80.9, 81.0, 81.1, 127.90, 127.94, 128.1, 128.2, 128.36, 128.42, 128.6, 128.7, 130.28, 130.32, 133.3, 133.4, 133.4, 133.5, 135.9, 136.0, 136.1, 145.6, 145.7, 154.1, 154.7, 155.0, 155.2, 155.3, 155.5, 170.5, 170.6, 170.67, 170.72, 199.7, 200.1, 200.19, 200.6. IR (film, cm^{-1}): 1598, 1695, 1751, 2976, 3066.

HRMS $[M+Na]^+$ found (calcd): 673.1947 (673.1866). Opt. Rot. $[\alpha]_D^{22}$ = –36.0 (c 2.56, $CHCl_3$).

(*2S,4R*)-2-[(2-Mercapto-ethyl)-methoxycarbonylmethyl-carbamoyl]-4-(toluene-4-sulfonyloxy)-pyrrolidine-1-carboxylic acid benzyl ester (12)

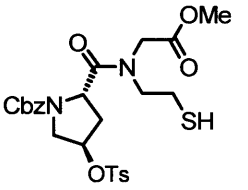

Thioester **11** (1.61 g, 2.5 mmol) was cooled to 0 °C in methylene chloride (20 mL); TFA (25 mL, 333 mmol) was added and the mixture was allowed to warm to room temperature for 2 h. The solvent was evaporate, and the resulting yellow oil was evaporated twice again from methylene chloride (50 mL each), dissolved in 50 mL methylene chloride, and washed carefully with ice-cold saturated $NaHCO_3$ (3 x 50 mL). The organic layer was dried over $MgSO_4$, filtered, transferred to a round bottom flask with condenser, and heated at reflux under argon for 3 h. The thiol ester has an R_f = 0.76 in ethyl acetate and the tertiary amide has an R_f = 0.50; both stain blue by Mo–Ce. The crude oil, obtained by stripping the methylene chloride, was purified by flash chromatography [hexanes–ethyl acetate (1:3), R_f = 0.54, Mo–Ce, blue], and 1.16 g (84%) of the title compound were obtained as a white foam under high vacuum. ^{1}H NMR ($CDCl_3$, 500 MHz, 4 rotamers): δ 1.27 (t, J = 8.5 Hz, 0.2H), 1.36 (t, J = 8.7 Hz, 0.3H), 1.56 (t, J = 8.6 Hz, 0.2H), 1.73 (t, J = 8.7 Hz, 0.3H), 2.34 (m, 2H), 2.43 (s, 1.6H), 2.46 (s, 1.4H), 2.58 (m, 0.6H), 2.73 (m, 0.6H), 2.80 (m, 0.3H), 3.18 (m, 0.3H), 3.34 (m, 1H), 3.46 (d, J = 17.3 Hz, 0.3H), 3.59 (m, 0.3H), 3.70 (m, 5.6H), 4.01 (d, J = 18.8Hz, 0.3H), 4.18 (d, J = 18.8Hz, 0.2H), 4.26 (d, J = 17.2Hz, 0.3H), 4.45 (t, J = 7.5Hz, 0.3H), 4.52 (m, 0.6H), 4.77 (t, J = 7.6Hz, 0.3H), 4.93 (t, J = 7.6Hz, 0.6H), 4.99 (m, 0.6H), 5.09 (m, 2.4H), 7.35 (m, 7H), 7.79 (m, 2H). ^{13}C NMR ($CDCl_3$, 125 MHz, 4 rotamers): δ 21.84, 21.86, 22.3, 23.0, 23.5, 36.8, 37.0, 37.9, 38.5, 48.7, 49.1, 50.5, 51.5, 52.0, 52.4, 52.6, 52.7, 52.8, 53.0, 54.3, 54.6, 54.9, 55.0, 67.5, 67.6, 67.9, 68.1, 79.1, 79.4, 79.9, 80.2, 127.91, 127.95, 127.97, 128.26, 128.31, 128.64, 128.66, 128.68, 128.70, 128.80, 128.98, 129.03, 130.23, 130.26, 130.32, 133.26, 133.32, 133.37, 133.44, 135.9, 136.09, 136.17, 136.23, 145.41, 145.45, 145.51, 145.53, 153.6, 153.8, 154.7, 154.8, 169.4, 169.6, 169.8, 170.4, 172.67,

172.74, 172.9, 173.0. IR (film, cm^{-1}): 1597, 1658, 1704, 1748, 2566, 2954, 3065. HRMS $[M+H]^+$ found (calcd): 551.1501 (551.1516). Opt. Rot. $[\alpha]_D^{23}$ = +18.9 (c 2.16, $CHCl_3$).

(2*S*,7*S*)-5-Methoxycarbonylmethyl-6-oxo-2-thia-5,8-diaza-bicyclo[5.2.1]decane-8-carboxylic acid benzyl ester (13)

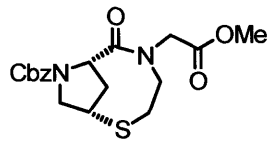

In a round bottom flask, 800 mL of acetonitrile were heated at reflux under argon for 1 h before the sequential addition, by syringe, of compound **12** (0.659 g, 1.2 mmol) in 10 mL of acetonitrile and KOMe (0.092 g, 1.3 mmol) in 10 mL dry MeOH. The mixture was stirred at reflux for 2 h, and the solvent was evaporated *in vacuo* to provide an oily yellow solid which was triturated in hexanes–ethyl acetate (1:1). This suspension was filtered, dried over $MgSO_4$, and concentrated to a crude oil which was taken up in 50 mL toluene. The toluene solution was washed with ice-cold 0.5 M NaOH (3 x 20 mL) to remove the presumed elimination (olefin/thiol) by-product. The toluene was stripped, and flash chromatography [hexanes–ethyl acetate (1:2)] of the crude oil provided 0.199 g (44%) of the title compound as a white foam under high vacuum. TLC: R_f = 0.34, Mo–Ce, blue. ^1H NMR ($CDCl_3$, 500 MHz, 2 rotamers): δ 2.46 (dd, J = 4.8, 16.7Hz, 0.1H), 2.53 (d, J = 14.5Hz, 0.9H), 2.85 (m, 1H), 3.02 (m, 1.8H), 3.21 (broad m, 0.2H), 3.36 (dt, J = 5.8, 11.0Hz, 0.8H), 3.49 (broad m, 0.2H), 3.61 (t, J = 6.9Hz, 1H), 3.72 (s, 3H), 3.85 (m, 2H), 3.92 (d, J = 17.4Hz, 1H), 4.02 (d, J = 16.9Hz, 1H), 4.13 (m, 0.8H), 4.24 (broad m, 0.2H), 4.45 (d, J = 16.8Hz, 0.1H), 4.76 (dd, J = 1.6, 10.8Hz, 0.9H), 5.10 (d, J = 12.5Hz, 0.8H), 5.13 (d, J = 11.3Hz, 0.2H), 5.21 (d, J = 11.3Hz, 0.2H), 5.26 (d, 12.7Hz, 0.8H), 7.32 (m, 5H). ^{13}C NMR ($CDCl_3$, 125 MHz, 2 rotamers): δ 30.1, 30.4, 36.1, 37.8, 39.2, 40.2, 40.4, 49.2, 50.3, 52.1, 52.3, 52.8, 55.2, 56.2, 62.0, 62.8, 67.6, 128.0, 128.3, 128.7, 136.5, 154.5, 169.8, 172.1. IR (film, cm^{-1}): 1637, 1703, 1748, 2952, 3062. HRMS $[M+H]^+$ found (calcd): 379.1308 (379.1322). Opt. Rot. $[\alpha]_D^{23}$ = +96.1 ($CHCl_3$, c 0.67).

(*2S,7S*)-5-Carboxymethyl-6-oxo-2-thia-5,8-diaza-bicyclo[5.2.1]decane-8-carboxylic acid benzyl ester (14)

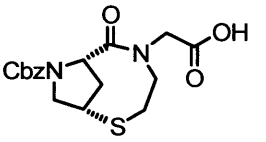

A solution of compound **13** (0.165 g, 0.44 mmol) in 15 mL MeOH was cooled with an ice bath, and 3 M NaOH (0.22 mL, 0.65 mmol) was added. The mixture was allowed to warm to room temperature overnight. Afterwards, 10 mL H_2O were added, and the MeOH was removed *in vacuo*. Ice was added, and the mixture was acidified to pH 1 with cold 3 M HCl. A white solid formed and the mixture was extracted with methylene chloride (2 x 30 mL). The combined organic extracts were dried over $MgSO_4$, filtered, and concentrated. Evaporation of solvent gave 0.14 g (96%) of analytically pure title compound as a white foam under high vacuum. ^{1}H NMR ($CDCl_3$, 500 MHz, 2 rotamers): δ 2.51 (d, J = 14.6 Hz, 1H), 2.84 (m, 1H), 3.01 (m, 1H), 3.06 (broad m, 1H), 3.60 (dt, J = 16.8, 5.5 Hz, 0.6H), 3.50 (broad d, J = 15.0 Hz, 0.4H), 3.59 (t, J = 5.2 Hz, 1H), 3.83 (m, 2H), 3.97 (m, 1.6H), 4.10 (dt, J = 16.5, 7.3 Hz, 1H), 4.19 (broad d, J = 14.0 Hz, 0.4H), 4.31 (d, J = 17.5 Hz, 0.4H), 4.77 (d, J = 10.1 Hz, 1H), 5.08 (d, J = 12.3 Hz, 0.6H), 5.14 (broad d, J = 12.6 Hz, 0.4H), 5.20 (broad d, J = 12.5 Hz, 0.4H), 5.25 (d, J = 12.6 Hz, 0.6H), 7.30 (m, 5H), 9.00 (s, 1H). ^{13}C NMR ($CDCl_3$, 125 MHz, 2 rotamers): δ 29.8, 30.0, 37.8, 39.1, 40.0, 40.1, 49.1, 50.1, 52.1, 52.7, 55.2, 56.0, 61.8, 62.5, 67.6, 67.8, 127.9, 128.2, 128.4, 128.5, 128.6, 136.0, 136.3, 154.4, 154.7, 172.1, 172.2, 172.6, 172.8. IR (film, cm^{-1}): 1610, 1633, 1703, 1735, 2604, 2730, 2948, 3033, 3466. HRMS $[M+Na]^+$ found (calcd): 387.0993 (387.0985). Opt. Rot. $[\alpha]_D^{23}$ = +76.2 (MeOH, c 0.52).

(*1S,7S*)-(6-Oxo-2-thia-5,8-diaza-bicyclo[5.2.1]dec-5-yl)-acetic acid (15)

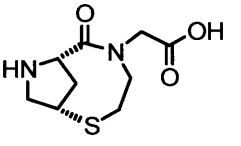

A solution of compound **14** (0.140 g, 0.4 mmol) in 15 mL ethanol was transferred to a Parr bottle containing 1.22 g of Pd–C (10% Pd by weight, 0.57 mmol Pd). The bottle was placed in a Parr shaker, filled with H_2 (50 psig), and shaken for 66 h. Afterwards, the contents were filtered and concentrated to a dark yellow, viscous oil. Evaporation from ethanol–methylene chloride *in vacuo* gave the title compound as a yellow foam in

80% yield. An pure sample was obtained by reverse-phase HPLC (5 to 35% acetonitrile in H_2O/TFA, t_R = 6.0 min); all characterization data were obtained with the resulting TFA salt. ^{1}H NMR (d_6-DMSO, 500 MHz): δ 2.08 (ddd, J = 15.7, 6.0, 4.3 Hz, 1H), 2.80 (dt, J = 15.7, 9.3 Hz, 1H), 3.06 (m, 3H), 3.33 (dd, 12.2, 4.9 Hz, 1H), 3.61 (dd, J = 15.7, 8.9 Hz, 1H), 3.86 (d, J = 17.1 Hz, 1H), 3.89 (t, J = 4.3 Hz, 1H), 4.15 (ddd, J = 16.3, 10.4, 6.3 Hz, 1H), 4.25 (d, J = 17.1 Hz, 1H), 4.51 (d, J = 6.3 Hz, 1H), 9.00 (broad s, 1H), 10.6 (broad s, 1H), 12.9 (broad s, 1H). ^{13}C NMR (d_6-DMSO, 125 MHz): δ 30.2, 35.4, 41.0, 48.0, 51.1, 51.9, 60.7, 117.0 (q, J_{CF} = 300.3 Hz), 158.8 (q, J_{CF} = 32.3 Hz), 170.1, 170.3. IR (film, cm^{-1}): 1632, 1670, 1733, 2737, 2971, 3107, 3366. HRMS $[M+H]^+$ found (calcd): 231.0802 (231.0798). Opt. Rot. $[\alpha]_D^{23}$ = +18.3 (c 1.51, H_2O).

(*S,S*)-5-Carboxymethyl-6-oxo-2-thia-5,8-diaza-bicyclo[5.2.1]decane-8-carboxylic acid 9H-fluoren-9-ylmethyl ester (16)

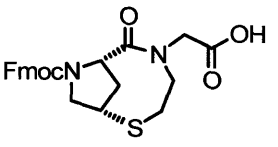

Trimethylsilyl chloride (0.10 mL, 0.8 mmol) was added to a solution of **15** (0.09 g, 0.4 mmol) in 25 mL methylene chloride. The mixture was heated at reflux for ½ h; after this time a fine white solid was evident. The heat source was removed and the reaction vessel was cooled with an ice bath before the addition of DIEA (0.14 mL, 0.8 mmol) and FmocCl (0.154 g, 0.4 mmol). The mixture was allowed to warm to room temperature over 3 h, after which time the solvent was removed to yield an orange oil. A solution of $NaHCO_3$ (2.5%, 25 mL) and diethyl ether (25 mL) were added to the vessel and stirred vigorously until no solids remained. The layers were then separated and the aqueous layer was washed again with diethyl ether (1 x 25 mL). The aqueous layer was then cooled by adding ice and acidified to pH 1 with cold 3 M HCl. A solid formed and the solution was extracted with diethyl ether (3 x 25 mL). The organic extracts were dried over $MgSO_4$, filtered, and concentrated. The title compound was obtained as a light yellow foam under high vacuum in 66% yield. Note: A simplified procedure using Schotten–Bauman conditions was investigated. The final product was found to be contaminated with an appreciable amount of the dimer Fmoc-Template(8)Gly-Template(8)Gly-OH, which is easily removed by HPLC. ^{1}H NMR ($CDCl_3$, 500 MHz, 2

rotamers): δ 2.39 (d, J = 12.1 Hz, 0.4H), 2.47 (d, J = 14.4 Hz, 0.6H), 2.71 (m, 0.4H), 2.81 (m, 1H), 2.99 (m, 1.6H), 3.43 (m, 3H), 3.80 (m, 3H), 4.12 (m, 3H), 4.43 (m, 0.6H), 4.59 (m, 1H), 4.79 (d, J = 9.8 Hz, 0.4 H), 7.32 (m, 4H), 7.53 (m, 1.4H), 7.64 (m, 0.6H), 7.74 (m, 2H), 9.00 (broad s, 1H). ^{13}C NMR ($CDCl_3$, 125 MHz, 2 rotamers): δ 29.8, 30.0, 38.3, 39.0, 40.0, 41.2, 47.1, 47.5, 48.7, 49.8, 52.1, 52.8, 54.8, 55.3, 62.0, 62.4, 67.5, 68.5, 120.0, 120.1, 124.9, 125.2, 125.7, 127.3, 127.4, 127.8, 127.9, 141.2, 141.3, 141.4, 143.5, 143.7, 144.1, 154.5, 154.7, 172.1, 172.7. IR (film, cm^{-1}): 1605, 1638, 1707, 1737, 2599, 2718, 2951, 3039, 3456. HRMS $[M+H]^+$ found (calcd): 453.1473 (453.1479). Opt. Rot. $[\alpha]_D^{23}$ = +47.1 (c 2.15, $CHCl_3$).

5.4. Synthesis of NCap(8)Ala-OH: Alkylation Route

The only significant changes in the alkylation protocol described for the synthesis of Fmoc-Template(8)Gly-OH are (1) the use of the triflate ester of methyl-(*R*)-lactate as the alkylation reagent in place of methyl bromoacetate and (2) the use of cystamine·2HCl rather than cystamine, and the deprotonation of the salt with sodium hydroxide. Because the products obtained were diastereomeric mixtures, characterization data is not given.

5.5. Synthesis of NCap(8)Ala-OH: Reductive Amination Route

2-(2,2-diethoxy-ethylsulfanyl)-2-methyl-propane (24)

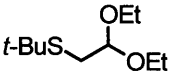

In a round bottom flask, sodium (1.68 g, 73 mmol) was dissolved in 100 mL of ethanol, and *tert*-butyl thiol (8.22 mL, 73mmol) was added to the warm solution, followed by bromoacetaldehyde diethyl acetal (10 mL, 73 mmol). The mixture was heated to 70 °C and stirred for 4 h; as the reaction progressed, a fine white precipitate formed. Afterwards, the mixture was allowed to cool to room temperature and concentrated. The residue was partitioned between water (50 mL) and Et_2O (50 mL), and the aqueous layer was washed with Et_2O (50 mL). The combined organic layers were washed with 1 M NaOH (2 x 75 mL), dried over $MgSO_4$, filtered, and concentrated to yield 12.3 g (90%) of a light yellow oil with low viscosity. ^1H NMR ($CDCl_3$, 500 MHz,): δ 1.18 (t, J = 5.0 Hz, 6H), 1.28 (s, 9H), 2.71 (d, J = 5.8 Hz, 2H), 3.51 (m, 2H), 3.63 (m, 2H), 4.57 (t, J =

5.8 Hz, 1H). ^{13}C NMR ($CDCl_3$, 125 MHz,): δ 15.4, 31.0, 32.1, 42.0, 61.7, 102.5. IR (film, cm^{-1}): 1055, 1123, 1364, 1459, 2899, 2930, 2973.

tert-butylsulfanyl-acetaldehyde (25)

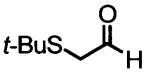

Compound **24** (12 g, 58 mmol) was dissolved in 100 mL acetone, and 20 mL of 3 M HCl (60 mmol) were added. The reaction mixture was stirred at room temperature for 7 h, after which time another 50 mL H_2O were added, and the acetone was stripped. The aqueous mixture was extracted with Et_2O (3 x 30 mL). The extracts were washed with saturated $NaHCO_3$ (1 x 25 mL) and brine (1 x 25 mL), dried over $MgSO_4$, and filtered. The solvent was evaporated to yield 6.18 g (98%) of the title compound as an orange, freely flowing oil. ^1H NMR ($CDCl_3$, 500 MHz,): δ 1.28 (s, 9H), 3.23 (d, J = 3.3 Hz, 2H), 9.51 (t, J = 3.3 Hz, 1H). ^{13}C NMR ($CDCl_3$, 125 MHz,): δ 31.1, 39.9, 43.5, 197.6. IR (film, cm^{-1}): 1461, 1721, 2819, 2901, 2964.

2-(2-_tert_-butylsulfanyl-ethylamino)-propionic acid methyl ester (26)

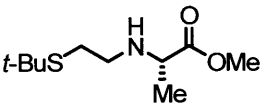

H-Ala-OMe·HCl (3.3 g, 23.6 mmol) and **25** (2.6 g, 19.7 mmol) were combined in 75 mL CH_2Cl_2. To this suspension was added sodium triacetoxy borohydride (6.26 g, 30 mmol) in portions. After 6 h the clear solution was washed with saturated $NaHCO_3$ (2 x 25 mL), dried over $MgSO_4$, filtered, and concentrated. Flash chromatography [ethyl acetate–hexanes (4:1), R_f= 0.41, Mo–Ce, blue] provided 1.42 g (33%) of the title compound as a clear oil. ^1H NMR ($CDCl_3$, 500 MHz,): δ 1.28 (d, J = 7.0 Hz, 3H), 1.29 (s, 9H), 1.82 (s, 1H), 2.65 (m, 3H), 2.76 (m, 1H), 3.35 (q, J = 7.0 Hz, 1H), 3.63 (s, 3H). ^{13}C NMR ($CDCl_3$, 125 MHz,): δ 19.2, 28.9, 31.2, 42.3, 47.8, 52.0, 56.6, 176.0. IR (film, cm^{-1}): 1459, 1737, 2864, 2959, 3320. High resolution mass spectroscopy found (calculated) $[M+Na]^+$ 242.1187 (242.1185). Opt. Rot. $[\alpha]_D^{23}$ = –26.3 ($CHCl_3$, c 3.95).

(1-methoxycarbonyl-ethyl)-[2-(2-nitro-phenyldisulfanyl)-ethyl]-ammonium; trifluoro-acetate (27)

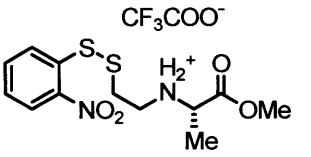

Compound **26** (2.91 g, 13.3 mmol) was dissolved in 40 mL CH_2Cl_2, and TFA was added slowly at room temperature, with stirring. Next, 2-nitrosulphenyl chloride (2.52 g, 13.3 mmol) was added in portions, and the solution was stirred overnight (16 h). Afterwards, the solvent was removed *in vacuo*, and the resulting orange oil was placed under high vacuum until a solid formed. Diethyl ether (75 mL) was added and the mixture was stirred until a solution with fine precipitate was obtained. The precipitate was collected by vacuum filtration, and the filter cake was washed well with cold diethyl ether. After drying thoroughly under high vacuum, 5.24 g (92%) of the title compound were obtained as a light yellow solid. ^{1}H NMR ($CDCl_3$, 500 MHz,): δ 1.57 (d, J = 7.2 Hz, 3H), 3.08 (t, J = 7.3 Hz, 2H), 3.37 (m, 2H), 3.79 (s, 3H), 3.95 (q, J = 7.2Hz, 1H), 7.39 (t, J = 7.0 Hz, 1H), 7.70 (t, J = 6.9 Hz, 1H), 8.21 (d, J = 8.1 Hz, 1H), 8.27 (d, J = 8.2 Hz, 1H), 9.40 (s, 2H). ^{13}C NMR ($CDCl_3$, 125 MHz,): δ 14.6, 32.6, 44.7, 53.5, 55.4, 116.4 (q, J_{CF} = 292.5 Hz), 126.5, 126.9, 127.2, 134.6, 136.0, 145.8, 162.4 (q, J_{CF} = 35.7 Hz), 169.6. IR (film, cm^{-1}): 1668, 1748, 2463, 2756, 2961, 3008. High resolution mass spectroscopy found (calculated) $[M+H]^+$ 317.0622 (317.0624). Opt. Rot. $[\alpha]_D^{23}$ = –24.3 ($CHCl_3$, c 1.73).

2-{*tert*-butoxycarbonyl-[2-(2-nitro-phenyldisulfanyl)-ethyl]-amino}-propionic acid methyl ester (28)

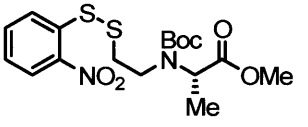

The TFA salt **27** (2.23 g, 5.18 mmol) was dissolved in 90 mL THF in a round bottom flask, yielding a clear yellow solution. A solution of K_2CO_3 (0.716 g, 5.18 mmol) in 10 mL H_2O was added with vigorous stirring; within 15 min. a clear yellow solution with white precipitate was obtained. Boc_2O (4.53 g, 20.7 mmol) was added to the vessel, and the mixture was stirred overnight at room temperature. Afterwards, the reaction mixture was concentrated, and equal volumes of water and methylene chloride (50 mL) were added to the residue. The layers were separated, and the aqueous layer was washed again with methylene chloride (25 mL). The combined organic layers were dried over $MgSO_4$,

filtered, and concentrated. Flash chromatography [ethyl acetate–hexanes (4:1), R_f= 0.17, UV) yielded 2.64 g (100%) of the title compound as a clear oil. ^{1}H NMR ($CDCl_3$, 500 MHz,): δ 1.32 (s, 4.5H), 1.38 (m, 7.5H), 2.81 (m, 0.5H), 2.93 (m, 1.5H), 3.39 (m, 1H), 3.58 (m, 1H), 3.65 (s, 3H), 4.05 (q, J = 7.2 Hz, 0.5H), 4.50 (q, J = 7.3 Hz, 0.5H), 7.34 (dd, J = 15.1, 7.9 Hz, 1H), 7.68 (dd, J = 15.7, 7.8 Hz, 1H), 8.24 (m, 1H), 8.27 (d, J = 8.2 Hz, 1H). ^{13}C NMR ($CDCl_3$, 125 MHz,): δ 15.7, 16.3, 28.27, 28.32, 36.4, 45.4, 47.1, 52.3, 54.7, 56.6, 80.9, 81.0, 126.26, 126.31, 126.35, 126.39, 127.2, 127.4, 134.3, 137.4, 137.5, 145.7, 154.7, 155.1, 172.5, 172.8. IR (film, cm^{-1}): 1695, 1745, 2950, 2978, 3093. High resolution mass spectroscopy found (calculated) $[M+Na]^+$ 439.0956 (439.0968). Opt. Rot. $[\alpha]_D^{23}$ = –7.1 ($CHCl_3$, c 0.79).

2-[*tert*-butoxycarbonyl-(2-mercapto-ethyl)-amino]-propionic acid methyl ester (17)

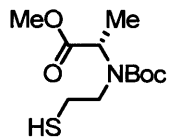

Disulfide **28** (4.82 g, 11.6 mmol) was dissolved in 200 mL of methanol and 20 mL of acetate buffer (0.1 M, pH 4.7). TCEP·HCl (3.66 g, 12.8 mmol) was added in portions, and after 2.5 h, the MeOH was removed and the residue was partitioned between brine (50 mL) and Et_2O (75 mL). The layers were separated and the ether layer was washed exhaustively with a saturated solution of $NaHCO_3$ to remove the thiophenol by-product. Upon addition of the bicarbonate solution to the ether layer, both layers would become dark yellow, presumably owing to the deprotonation of the thiophenol. After each wash, the color change became less pronounced until only faint yellow aqueous washed were obtained. In all, 30 washes of 50 mL bicarbonate solution were performed. The ether layer was dried over $MgSO_4$, filtered, and concentrated *in vacuo* to yield 2.84 g (93%) of the title compound as a light yellow oil. ^{1}H NMR ($CDCl_3$, 500 MHz,): δ 1.35 (m, 13H), 2.62 (m, 2H), 3.16 (m, 1H), 3.41 (m, 1H), 3.62 (s, 3H), 3.99 (q, J = 6.4 Hz, 0.5H), 4.43 (q, J = 7.2 Hz, 0.5H). ^{13}C NMR ($CDCl_3$, 125 MHz,): δ 15.6, 16.1, 23.1, 23.8, 28.3, 49.6, 51.0, 52.1, 54.7, 56.3, 80.5, 80.6, 154.6, 155.1, 172.5, 172.7. IR (film, cm^{-1}): 1690, 1744, 2563, 2951, 2977. High resolution mass spectroscopy found (calculated) $[M+Na]^+$ 286.1081 (286.1083). Opt. Rot. $[\alpha]_D^{23}$ = –30.1 ($CHCl_3$, c 5.84).

2-{2-[*tert*-butoxycarbonyl-(1-methoxycarbonyl-ethyl)-amino]-ethylsulfanylcarbonyl}-4-(toluene-4-sulfonyloxy)-pyrrolidine-1-carboxylic acid benzyl ester (18)

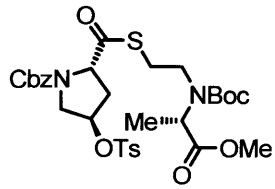

The carboxylic acid (4.34 g, 10.3 mmol) and 1,1′-carbonyl diimidazole (1.67 g, 10.3 mmol) were dissolved in 60 mL acetonitrile and stirred for ½ h. Afterwards, **17** (2.72 g, 10.3 mmol) was added, and stirring continued overnight.. The reaction mixture was concentrated *in vacuo*, and flash chromatography [ethyl acetate–hexanes (1:1), R_f= 0.46, Mo–Ce, blue) provided 6.08 g (89%) of the title compound as a clear oil. ^{1}H NMR ($CDCl_3$, 500 MHz,): δ 1.43 (m, 12H), 2.12 (m, 1H), 2.41 (s, 1.5H), 2.43 (s, 1.5H), 2.43 (m, 0.5H), 2.54 (m, 0.5H), 2.8-3.5 (m, 4H), 3.64 (m, 1H), 3.68 (s, 3H), 3.81 (m, 1H), 4.02 (q, J = 7.3 Hz, 0.25H), 4.09 (q, J = 7.0 Hz, 0.25H), 4.55 (m, 1.5H), 5.06 (m, 3H), 7.30 (m, 7H), 7.76 (m, 2H). ^{13}C NMR ($CDCl_3$, 125 MHz,): δ 15.7, 16.14, 16.19, 21.79, 21.81, 26.9, 27.17, 27.24, 27.6, 28.3, 28.4, 36.8, 38.05, 38.14, 45.3, 45.4, 46.5, 46.6, 52.2, 52.3, 52.7, 53.0, 54.7, 54.8, 56.2, 56.4, 64.2, 64.5, 67.7, 78.1, 78.2, 78.6, 78.8, 80.8, 80.9, 127.81, 127.85, 128.0, 128.1, 128.25, 128.33, 128.5, 128.6, 130.2, 130.3, 133.28, 133.34, 135.9, 136.1, 145.5, 154.0, 154.65, 154.72, 155.18, 155.24, 172.57, 172.64, 172.8, 172.9, 199.7, 200.15, 200.19, 200.6. IR (film, cm^{-1}): 1692, 1743, 2881, 2946, 2976, 3034, 3067. High resolution mass spectroscopy found (calculated) $[M+Na]^+$ 687.2039 (687.2017). Opt. Rot. $[\alpha]_D^{23}$ = –40.4 ($CHCl_3$, c 6.96).

2-[(2-mercapto-ethyl)-(1-methoxycarbonyl-ethyl)-carbamoyl]-4-(toluene-4-sulfonyloxy)-pyrrolidine-1-carboxylic acid benzyl ester (19)

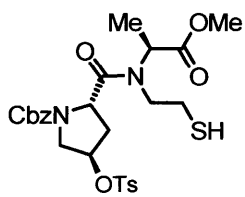

Compound **19** (6.0 g, 9.0 mmol) was dissolved in 90 mL CH_2Cl_2 and cooled with an ice bath; TFA (85 mL, 1.1 mol) was added, and the solution was stirred at 0 °C for 2 h. The mixture was concentrated *in vacuo* and evaporated from CH_2Cl_2 twice. The resulting residue was dissolved in 100 mL CH_2Cl_2 and sequentially washed with a cold, saturated solution of $NaHCO_3$ (2 × 75 mL) and brine (1 × 25 mL). The organic solution was then dried over $MgSO_4$, filtered, and concentrated *in vac*uo to yield an oil which was taken up

in 200 mL toluene and placed under an argon atmosphere. The solution was heated at reflux for 5 h. Afterwards, the mixture was concentrated to a yellow oil, and 3.58 g (70%) of the title compound were obtained as a clear oil after flash chromatography [ethyl acetate-hexanes (9:1), R_f = 0.63, Mo–Ce, blue) to yield. ^{1}H NMR ($CDCl_3$, 500 MHz,): δ 1.18 (d, J = 7.3 Hz, 1.5H), 1.37 (t, J = 8.7 Hz, 0.5H), 1.40 (d, J = 7.3 Hz, 1.5H), 1.59 (t, J = 8.7 Hz, 0.5H), 2.17 (m, 2H), 2.39 (s, 1.5H), 2.41 (m, 0.5H), 2.42 (s, 1.5H), 2.51 (m, 0.5H), 2.65 (m, 0.5H), 2.93 (m, 0.5H), 3.18 (t, J = 7.9 Hz, 1H), 3.52 (m, 1H), 3.60 (s, 1.5H), 3.61 (1.5H), 3.69 (m, 2H), 4.56 (q, J = 7.2 Hz, 0.5H), 4.65 (t, J = 7.4 Hz, 0.5H), 4.66 (q, J = 7.3 Hz, 0.5H), 4.78 (t, J = 7.0 Hz, 0.5H), 5.03 (m, 3H), 7.29 (m, 7H), 7.74 (m, 2H). ^{13}C NMR ($CDCl_3$, 125 MHz,): δ 14.5, 14.7, 21.7, 21.72, 23.7, 24.0, 36.4, 37.6, 48.9, 49.4, 52.3, 52.4, 52.5, 52.8, 53.8, 54.1, 55.1, 55.4, 67.2, 67.8, 78.8, 79.6, 127.7, 127.78, 127.81, 128.1, 128.5, 128.6, 128.8, 130.1, 130.2, 133.1, 133.2, 135.8, 136.2, 145.3, 145.4, 153.6, 154.4, 171.8, 172.0, 172.3, 172.4. IR (film, cm^{-1}): 1658, 1708, 1741, 2564, 2886, 2951, 3033. High resolution mass spectroscopy found (calculated) $[M+Na]^+$ 587.1501 (587.1492). Opt. Rot. $[\alpha]_D^{23}$ = –10.5 ($CHCl_3$, c 1.39).

5-(1-methoxycarbonyl-ethyl)-6-oxo-2-thia-5,8-diaza-bicyclo[5.2.1]decane-8-carboxylic acid benzyl ester (20)

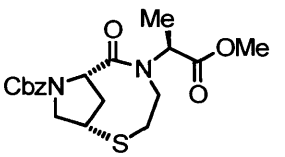

In a round bottom flask, 3.2 L of acetonitrile were heated at reflux under argon for 1 h before the sequential addition, by syringe, of **19** (2.73 g, 4.84 mmol) in 10 mL acetonitrile and a solution of KOMe (0.35 g, 5.0 mmol) in dry MeOH (20 mL). The mixture was heated at reflux for 2 h, and the solvent was evaporated *in vacuo* providing an oily residue which was triturated in that ethyl acetate–hexanes (1:1). This suspension was filtered, and the mother liquor was concentrated to an oil which was purified by flash chromatography [ethyl acetate–hexanes (2:1), R_f = 0.21, Mo–Ce, blue). The product was contaminated with a by-product, presumably the olefin resulting from elimination of the tosylate group. The contaminated product was taken up in 50 mL toluene and washed with cold 0.1 M NaOH (2 × 25 mL) to remove the olefin-thiol. After the toluene layer was dried over $MgSO_4$ and filtered, the solvent was removed *in vacuo* to yield 0.9 g (47%) of the title compound as a clear oil. ^{1}H NMR ($CDCl_3$, 500 MHz,): δ 1.31 (d, J =

7.3 Hz, 1.8H), 1.36 (s, 1.2H), 2.42 (d, J = 14.3 Hz, 1H), 2.79 (m, 2H), 3.02 (m, 1H), 3.41 (t, J = 5.5 Hz, 0.4H), 3.45 (t, J = 5.5 Hz, 0.6H), 3.55 (s, 3H), 3.63 (m, 1H), 3.79 (m, 2H), 4.02 (dd, J = 7.6, 5.2 Hz, 0.6H), 4.06 (dd, J = 7.3, 4.9 Hz, 0.4H), 4.71 (d, J = 9.8 Hz, 1H), 4.85 (m, 1H), 5.13 (m, 3H), 7.29 (m, 5H). ^{13}C NMR ($CDCl_3$, 125 MHz,): δ 14.7, 30.9, 38.1, 38.6, 39.6, 39.8, 45.0, 45.4, 51.9, 54.8, 54.9, 55.7, 56.0, 62.0, 62.6, 67.1, 127.2, 127.6, 127.8, 128.18, 128.23, 136.0, 136.2, 153.9, 154.1, 170.5, 170.7, 171.6. IR (film, cm^{-1}): 1639, 1706, 1740, 2886, 2949, 2983, 3030. High resolution mass spectroscopy found (calculated) $[M+Na]^+$ 415.1281 (415.1298). Opt. Rot. $[\alpha]_D^{23}$ = +47.5 ($CHCl_3$, c 1.42).

5-(1-carboxy-ethyl)-6-oxo-2-thia-5,8-diaza-bicyclo[5.2.1]decane-8-carboxylic acid benzyl ester (21)

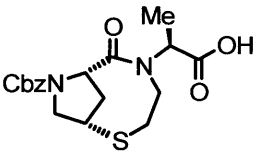

A solution of **20** (0.69 g, 1.76 mmol) in 30 mL MeOH was cooled with an ice bath, and 0.19 M NaOH (10 mL, 1.9 mmol) was added. The mixture was allowed to warm to room temperature overnight. Afterwards, 10 mL H_2O were added, and the MeOH was removed *in vacuo*. Ice was added, and the mixture was acidified to pH 1 with cold 3 M HCl. A white precipitate formed and was isolated by extraction with CH_2Cl_2 (2 x 25 mL). The organic extracts were dried over $MgSO_4$, filtered, and concentrated to yield 0.635 g (95%) of the title compound as a white foam under high vacuum. ^{1}H NMR ($CDCl_3$, 500 MHz,): δ 1.35 (d, J = 7.2 Hz, 1.8H), 1.42 (d, J = 5.8 Hz, 1.2H), 2.45 (d, J = 14.3 Hz, 1H), 2.81 (m, 2H), 3.01 (m, 1H), 3.46 (m, 1H), 3.56 (s, 1H), 3.82 (s, 2H), 4.06 (m, 1H), 4.77 (m, 2H), 4.85 (m, 1H), 5.14 (m, 2H), 7.29 (m, 5H). ^{13}C NMR ($CDCl_3$, 125 MHz,): δ 14.8, 31.1, 31.3, 38.0, 39.0, 40.0, 45.8, 46.3, 55.2, 55.6, 56.6, 62.2, 62.8, 67.8, 127.9, 128.2, 128.3, 128.6, 128.7, 136.2, 154.7, 171.7, 174.9, 175.7. IR (film, cm^{-1}): 1605, 1634, 1705, 1732, 2593, 2943, 2983, 3030, 3477. High resolution mass spectroscopy found (calculated) $[M+Na]^+$ 401.1129 (401.1142). Opt. Rot. $[\alpha]_D^{23}$ = +58.5 ($CHCl_3$, c 1.09).

2-(6-Oxo-2-thia-5,8-diaza-bicyclo[5.2.1]dec-5-yl)-propionic acid (22)

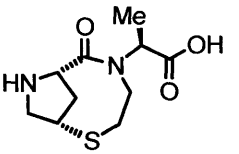

Compound **21** (0.61 g, 1.61 mmol) was taken up in EtOH (20 mL) and transferred to a Parr flask containing 3 g Pd/C (10% Pd, 50% water by weight). The contents of the flask were placed under 50 psig H_2 and shaken for 68 h, after which time the reaction mixture was filtered and concentrated *in vacuo* to yield a dark yellow foam (0.29 g, 75%) which was taken up in water and purified by reverse-phase HPLC (1 to 35% acetonitrile in 0.05% TFA/water). After lyophilization, the title compound was obtained as its TFA salt. ^{1}H NMR (D_2O, 500 MHz,): δ 1.24 (d, J = 7.2 Hz, 3H), 2.08 (ddd, J = 16.3, 6.4, 3.8 Hz, 1H), 2.69 (ddd, J = 15.6, 9.9, 5.7 Hz, 1H), 2.95 (d, J = 16.2 Hz, 1H), 3.01 (dd, J = 15.5, 6.4 Hz, 1H), 3.16 (d, J = 12.5 Hz, 1H), 3.30 (dd, J = 12.5, 4.7 Hz, 1H), 3.57 (dd, J = 15.6, 9.2 Hz, 1H), 3.90 (t, J = 4.0 Hz, 1H), 4.04 (ddd, J = 17.1, 10.8, 6.7 Hz, 1H), 4.33 (q, J = 7.2 Hz, 1H), 4.41 (d, J = 6.4 Hz, 1H). ^{13}C NMR (CD_3OD/D_2O (1:9, v:v), 125 MHz,): δ 14.6, 32.2, 36.2, 42.6, 48.2, 52.3, 61.0, 63.0, 117.5 (q, J_{CF} = 292 Hz), 163.9 (q, J_{CF} = 35.1 Hz), 171.4, 175.5. IR (film, cm^{-1}): 1626, 1670, 1723, 2766, 2945, 2980, 3094, 3420. High resolution mass spectroscopy found (calculated) $[M+H]^+$ 245.0949 (245.0954). Opt. Rot. $[\alpha]_D^{23}$ = –29.7 (H_2O, c 0.66).

5-(1-carboxy-ethyl)-6-oxo-2-thia-5,8-diaza-bicyclo[5.2.1]decane-8-carboxylic acid 9H-fluoren-9-ylmethyl ester (23)

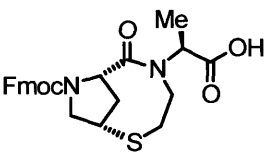

Upon addition of DIEA (0.115 mL, 0.66 mmol) to a suspension of the TFA salt of zwitterion **22** (0.079 g, 0.22 mmol) in 15 mL methylene chloride, the solution became homogeneous. The clear solution was cooled with an ice bath and FmocOSu (0.0816 g, 0.24 mmol) was added. The ice bath was removed and the mixture was allowed to warm to room temperature for 4 h. The reaction mixture was concentrated in vacuo, and the resulting oil was partitioned between diethyl ether (20 mL) and a solution of sodium bicarbonate (2.5%, 20 mL). The layers were separated and the aqueous layer was washed

again with diethyl ether (20 mL). The aqueous layer was cooled on ice and cold 3 M HCl was added to adjust to pH 1. A white precipitate formed and was extracted with CH_2Cl_2 (2 × 25 mL). The combined organic extracts were dried over $MgSO_4$, filtered, and concentrated to yield 0.072 g (70%) of the title compound as a white foam under high vacuum. The product could be further purified by reverse-phase HPLC (35 to 60% acetonitrile in 0.05% TFA/water, elutes at 12 min.). ^{1}H NMR ($CDCl_3$, 500 MHz,): δ 1.31 (d, J = 6.7 Hz, 1.2H), 1.36 (d, J = 7.1 Hz, 1.8H), 2.31 (d, J = 14.6 Hz, 0.4H), 2.47 (d, J = 14.3 Hz, 0.6H), 2.72 (m, 2H), 3.05 (dt, J = 15.5, 5.3 Hz, 0.6H), 3.19 (m, 0.4H), 3.50 (m, 3H), 3.80 (m, 1H), 4.10 (m, 2.6H), 4.43 (dd, J = 11.7, 6.5 Hz, 0.4H), 4.52 (dd, J = 10.1, 6.1 Hz, 0.6H), 4.63 (d, J = 10.4 Hz, 0.4H), 4.68 (dd, J = 10.1, 5.3 Hz, 0.4H), 4.80 (q, J = 7.0 Hz, 0.4H), 4.86 (d, J = 10.4 Hz, 0.6H), 5.03 (q, J = 7.2 Hz, 0.6H), 7.30 (m, 4H), 7.54 (m, 2H), 7.70 (m, 2H), 10.9 (s, 1H). ^{13}C NMR ($CDCl_3$, 125 MHz,): δ 14.7, 15.0, 31.2, 31.4, 38.4, 38.9, 39.8, 40.7, 45.0, 45.7, 47.0, 47.5, 54.8, 55.7, 56.5, 62.3, 62.4, 67.4, 68.9, 119.9, 120.1, 124.9, 125.1, 125.3, 126.1, 127.3, 127.4, 127.5, 127.8, 127.9, 141.0, 141.4, 141.5, 141.6, 143.2, 143.7, 143.8, 144.5, 154.6, 154.7, 171.8, 172.1, 174.5, 175.5. IR (film, cm^{-1}): 1599, 1639, 1705, 1735, 2589, 2949, 3040, 3065. High resolution mass spectroscopy found (calculated) $[M+Na]^+$ 489.1440 (489.1455). Opt. Rot. $[\alpha]_D^{23}$ = +21.1 ($CHCl_3$, c 1.66).

5.6. Synthesis of Fmoc-NCap(7)Ala-OH

(*2S,4R*)-4-Hydroxy-2-(1-(*S*)-methoxycarbonyl-ethylcarbamoyl)-pyrrolidine-1-carboxylic acid benzyl ester (30)

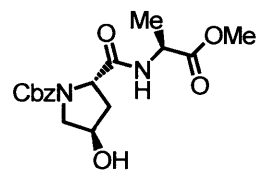

Cbz-Hyp-OH (4.24 g, 16.0 mmol), H-Ala-OMe·HCl (3.35 g, 24.0 mmol), and DIEA (8.36 mL, 48 mmol) were combined in 110 mL acetonitrile. TBTU (5.65 g, 17.6 mmol) was added to the stirred solution in portions, and a slight warming was noted. After 5 h the reaction mixture was concentrated to an oil which was taken up in 250 mL ethyl acetate. This solution was washed with 1 M HCl (2 x 50 mL), sat. $NaHCO_3$ (2 x 50 mL), and brine (1 x 25 mL), dried over $MgSO_4$, and filtered. The solvent was stripped *in*

vacuo, and 3.65 g (65%) of the title compound was obtained as a clear oil that slowly solidified under high vacuum. ^{1}H NMR ($CDCl_3$, 500 MHz, 2 rotamers): δ 1.17 (d, J = 5.5 Hz, 1.2H), 1.39 (d, J = 6.7 Hz, 1.8H), 2.11 (s, 1H), 2.30 (m, 1 H), 2.84 (broad s, 1H), 3.58 (m, 2H), 3.71 (m, 3H), 4.44 (m, 3H), 5.10 (m, 2H), 6.57 (s, 0.4H), 7.20 (s, 0.6H), 7.30 (m, 5H). ^{13}C NMR ($CDCl_3$, 125 MHz, 2 rotamers): δ 18.1, 37.6, 39.7, 48.1, 48.4, 52.6, 54.9, 55.9, 59.2, 59.5, 67.6, 69.6, 70.2, 128.0, 128.3, 128.7, 136.3, 136.4, 155.4, 156.2, 171.4, 172.0, 173.5. IR (film, cm^{-1}): 1546, 1665, 1744, 2952, 3068, 3306. Elemental analysis found C 58.19, H 6.63, N 7.93; calcd. C 58.28, H 6.33, N 8.00. Opt. Rot. $[\alpha]_D^{23} = -63.1$ ($CHCl_3$, c 2.29). Melting point: 109 – 110 °C.

(*2S,4R*)-4-Acetylsulfanyl-2-(1-(*S*)-methoxycarbonyl-ethylcarbamoyl)-pyrrolidine-1-carboxylic acid benzyl ester (31)

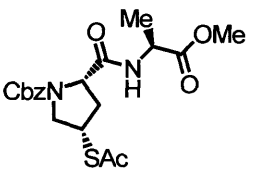

Triphenylphosphine (2.99 g, 11.4 mmol) was dissolved in 50 mL THF in a flame-dried round bottom flask under an argon atmosphere. The solution was cooled to 0 °C and DIAD (2.24 mL, 11.4 mmol) was added. The mixture quickly became viscous as white particles formed, and stirring was continued at 0 °C for 15 min. Meanwhile, compound **30** (3.65 g, 10.4 mmol) and thiolacetic acid (0.78 mL, 11.0 mmol) were combined in 200 mL of dry THF in another flame-dried round bottom flask. The mixture of thiolacetic acid and **30** were transferred quickly by funnel to the flask containing the triphenylphosphine–DIAD adduct at 0 °C, and an argon atmosphere was reestablished (compound **30** is only moderately soluble in THF; the compound was not fully dissolved when added to the reaction). Upon addition of the mixture, the reaction became dark green, and as the reaction progressed, the color became light green and the particulates disappeared. After 5 h, the reaction mixture was concentrated to an oil, and flash chromatography [ethyl acetate-hexanes (1:1), Mo–Ce blue, R_f = 0.23) provided 3.22 g (76%) of the title compound as a clear oil that slowly solidified under high vacuum. ^{1}H NMR ($CDCl_3$, 500 MHz, 2 rotamers): δ 1.29 (s, 1.2H), 1.41 (s, 1.8H), 2.20 (broad s, 0.4H), 2.29 (s, 3H), 2.37 (broad s, 0.6H), 2.52 (broad s, 0.6H), 2.70 (broad s, 0.4H), 3.36 (m, 1H), 3.70 (s, 3H), 3.98 (quint, J = 6.7 Hz, 1H), 4.06 (s, 1H), 4.39 (s, 1H), 4.54 (s, 1H), 5.15 (m, 2H), 6.56 (s, 0.4H), 7.19 (s, 0.6H), 7.31 (m, 5H). ^{13}C NMR ($CDCl_3$, 125

MHz, 2 rotamers): δ 18.18, 30.70, 33.62, 36.77, 39.36, 39.97, 48.20. 48.45, 52.61, 53.54, 60.23, 67.87, 128.20, 128.38, 128.69, 136.12, 154.91, 155.92, 170.48, 173.26, 194.75, 195.59. IR (film, cm^{-1}): 1537, 1688, 1743, 2880, 2953, 2986, 3034, 3066, 3310. Elemental analysis found C 55.62, H 5.89, N 6.70; calcd. C 55.87, H 5.92, N 6.86. Melting point = 105 – 107 °C. Opt. Rot. $[\alpha]_D^{23} = -73.2$ ($CHCl_3$, c 3.67).

(*2S,4R*)-4-Mercapto-2-(1-(*S*)-methoxycarbonyl-ethylcarbamoyl)-pyrrolidine-1-carboxylic acid benzyl ester (32)

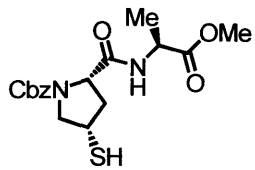

To a solution of **31** (3.22 g, 7.88 mmol) in 100 mL methanol was added 7 N NH_3/MeOH (100 mL), and stirring was continued for 2 h. Afterwards, the solution was concentrated to an oil; flash chromatography (EtOAc, R_f = 0.68, Mo–Ce blue; the product appears as a light yellow band on the column) provided 2.89 g (92%) of the title compound as a light yellow oil that solidified slowly under high vacuum. ^1H NMR ($CDCl_3$, 500 MHz, 2 rotamers): δ 1.22 (s, 1.2H), 1.34 (s, 1.8H), 1.85 (d, J = 6.9 Hz, 1H), 2.10 (m, 1H), 2.58 (m, 1H), 3.25 (s, 2H), 3.63 (s, 3H), 3.99 (s, 1H), 4.28 (s, 1H), 4.47 (s, 1H), 5.10 (m, 2H), 6.70 (s, 0.4H), 7.20 (s, 0.6H), 7.27 (s, 5H). ^{13}C NMR ($CDCl_3$, 125 MHz, 2 rotamers): δ 17.90, 34.71, 35.28, 38.99, 41.08, 48.24, 52.41, 56.38, 60.37, 67.52, 127.92, 128.15, 128.49, 136.08, 154.54, 155.29, 170.81, 173.13. IR (film, cm^{-1}): 1541, 1668, 1697, 1742, 2552, 2879, 2952, 2985, 3034, 3066, 3309. Elemental analysis found C 55.81, H 6.07, N 7.61; calcd. C 55.72, H 6.05, N 7.64. Opt. Rot. $[\alpha]_D^{22} = -50.4$ ($CHCl_3$, c 1.47). Melting point = 94 – 96 °C.

(*1S,6S*)-4-(1-(*S*)-Methoxycarbonyl-ethyl)-5-oxo-2-thia-4,7-diaza-bicyclo[4.2.1]nonane-7-carboxylic acid benzyl ester (33)

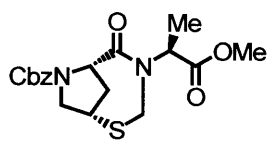

Compound **32** (2.67 g, 7.29 mmol), *p*-toluene sulfonic acid (0.46 g, 2.41 mmol), and paraformaldehyde (2.0 g) were combined in a flame-dried round bottom flask fitted with a Dean–Stark trap and a condenser. The apparatus was evacuated and backfilled with argon twice before filling the Dean–Stark trap with benzene/molecular sieves and adding 250 mL benzene to the round bottom flask. The stirred solution was heated at reflux for

12 h. Afterwards, the reaction mixture was concentrated to an orange oil that was purified by flash chromatography [ethyl acetate–hexanes (3:2), Mo–Ce blue, R_f = 0.58] yielding 1.76 g (64%) of a clear oil that was a mixture of the alanine α-H epimers in an approximately 13:1 ratio favoring the desired product. The diastereomers may be separated by reverse-phase HPLC (30 to 60 % acetonitrile in 0.5 % TFA/water; analytical column retention times: L-Ala epimer t_R = 17.4 min, D-Ala epimer t_R = 16.6 min); however, it is best to wait until the cyclized zwitterion is formed. A small sample of this product was purified and carried on to the methyl ester hydrolysis so that an analytical sample of the carboxylic acid could be obtained. ^{1}H NMR ($CDCl_3$, 500 MHz, 2 rotamers): δ 1.39 (d, J = 7.3 Hz, 3H), 2.27 (d, J = 13.6 Hz, 0.3H), 2.31 (d, J = 13.6 Hz, 0.7H), 2.55 (ddd, J = 13.5, 9.5, 5.7 Hz, 0.3H), 2.60 (ddd, J = 13.6, 9.6, 5.8 Hz, 0.7H), 3.40 (t, J = 5.5 Hz, 1H), 3.56 (s, 2.10H), 3.62 (s, 0.9H), 3.87 (m, 1H), 3.93 (m, 1H), 4.00 (m, 1H), 4.67 (d, J = 9.6 Hz, 0.7H), 4.69 (d, J = 10 Hz, 0.3H), 5.14 (m, 3H), 5.24 (m, 1H), 7.29 (m, 5H). ^{13}C NMR ($CDCl_3$, 125 MHz, 2 rotamers): δ 14.49, 14.64, 38.11, 38.90, 40.03, 40.94, 42.83, 52.37, 53.71, 53.83, 54.24, 54.51, 62.38, 62.93, 67.47, 67.56, 127.43, 127.91, 128.10, 128.27, 128.42, 128.59, 136.11, 136.30, 153.81, 171.68, 171.91, 172.64, 172.74. IR (film, cm^{-1}): 1647, 1700, 17.39, 2883, 2951, 2983, 3032, 3064. HRMS $[M+Na]^+$ found (calcd): 401.1148 (401.1142). Opt. Rot. $[\alpha]_D^{23}$ = +86.1 ($CHCl_3$, c 5.48).

(*1S,6S*)-4-(1-(*S*)-Carboxy-ethyl)-5-oxo-2-thia-4,7-diaza-bicyclo[4.2.1]nonane-7-carboxylic acid benzyl ester (34)

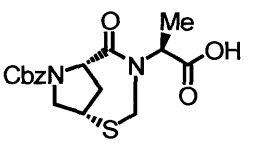

A solution of compound **33** (0.200 g, 0.53 mmol) in 20 mL methanol was cooled with an ice bath before the addition of 0.19 mL 3 M NaOH (0.57 mmol), and then allowed to warm to room temperature overnight. Afterwards, 10 mL of water were added and the solution was concentrated to remove most of the methanol. Ice was added to the residue, followed by 3 M HCl to adjust to pH 1. A white precipitate formed and was collected by extraction with CH_2Cl_2 (3 × 20 mL). The combined organic extracts were dried over $MgSO_4$ and filtered. The extraction solvent was stripped to yield 0.18 g (98%) of a clear oil that formed a white foam under high vacuum. ^{1}H NMR ($CDCl_3$, 500 MHz, 2

rotamers): δ 1.40 (d, J = 7.3 Hz, 0.7H), 1.41 (d, J = 7.2 Hz, 0.3H), 2.25 (d, J = 13.9 Hz, 0.3H), 2.29 (d, J = 13.6 Hz, 0.7H), 2.51 (ddd, J = 15.0, 9.3, 5.7 Hz, 0.3H), 2.54 (ddd, J = 13.7, 9.6, 5.6 Hz, 0.7H), 3.36 (t, J = 5.5 Hz, 0.7H), 3.37 (t, J = 5.5 Hz, 0.3H), 3.84 (dd, J = 11.8, 5.5 Hz, 1H), 3.92 (m, 1H), 3.98 (m, 1H), 4.68 (d, J = 9.4 Hz, 0.7H), 4.71 (d, J = 9.6 Hz, 0.3H), 5.11 (m, 3H), 5.30 (q, J = 7.3 Hz, 1H), 7.28 (m, 5H), 10.6 (broad s, 1H). ^{13}C NMR ($CDCl_3$, 125 MHz, 2 rotamers): δ 14.35, 14.55, 38.01, 38.76, 40.01, 40.93, 43.00, 43.05, 53.95, 54.26, 54.44, 62.27, 62.83, 67.65, 67.77, 127.42, 127.91, 128.14, 128.29, 128.42, 128.59, 135.98, 136.13, 154.01, 173.07, 173.14, 174.65, 174.84. IR (film, cm^{-1}): 1607, 1650, 1703, 1735, 2592, 2944, 3030, 3470. HRMS $[M+H]^+$ found (calcd): 365.1166 (365.1166). Opt. Rot. $[\alpha]_D^{23}$ = +86.2 ($CHCl_3$, c 1.69).

4-(1-Carboxy-ethyl)-5-oxo-2-thia-4-aza-7-azonia-bicyclo[4.2.1]nonane trifluoro-acetate (35)

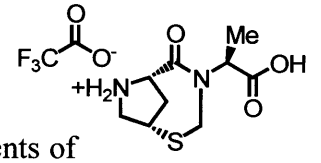

Compound **34** (0.18 g, 0.49 mmol) was taken up in 20 mL ethanol. The solution was added to a Parr bottle containing 1.5 g of Pd/C (10% by dry weight, 50% water by weight). The contents of the Parr bottle were placed under 50 psig of H_2 and shaken for 68 h, after which time the reaction mixture was filtered and concentrated. A light yellow oil was obtained (0.099 g, 87%) and formed a foam under high vacuum. This crude product was taken up in a minimum of acetonitrile and water (approximately 1:10 by volume), and purified by reverse-phase HPLC chromatography (5 to 35 % acetonitrile in 0.05% TFA/water). The D-Ala epimer from the cyclization step is readily removed at this point. The retention times on the analytical column are L-Ala epimer t_R = 10.2 min., D-ala epimer t_R = 7.4 min. The TFA salt of the title compound was obtained as a white powder after lyophilization in 32% yield (0.37 g). The crude product is greater than 90% pure as judged by ^1H NMR and reverse-phase HPLC. Because a semi-prep size HPLC column was used for the purification of the compound, substantial loss of product occurred. ^1H NMR ($CDCl_3$, 500 MHz): δ 1.31 (d, J = Hz, 3H), 2.31 (m, 1H), 2.49 (m, 1H), 3.71 (s, 2H), 3.85 (s, 1H), 4.33(d, J = Hz, 1H), 4.52 (d, J = Hz, 1H), 4.62 (q, J = Hz, 1H), 5.00 (d, J = Hz, 1H). ^{13}C NMR ($CDCl_3$, 125 MHz): δ 14.42, 37.99, 41.31, 43.97, 52.75, 56.38,

63.23, 116.87 (q, J_{CF} = 269.5 Hz), 159.40 (q, J_{CF} = 51.6 Hz), 168.77, 171.99. IR (film, cm^{-1}): 1412, 1648, 1730, 2596, 2949, 3372. HRMS $[M+H]^+$ found (calcd): 231.0797 (231.0798). Opt. Rot. $[\alpha]_D^{23}$ = +12.2 (c 6.58, H_2O).

(*1S,6S*)-4-(1-(*S*)-carboxy-ethyl)-5-oxo-2-thia-4,7-diaza-bicyclo[4.2.1]nonane-7-carboxylic acid 9H-fluoren-9-yl methyl ester (36)

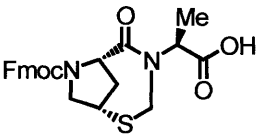

Upon addition of DIEA (0.36 mL, 2.1 mmol) to a suspension of **35** (0.235 g, 0.68 mmol) in 30 mL acetonitrile, the solution became homogeneous. The reaction mixture was cooled with an ice bath, and FmocCl (0.21 g, 0.82 mmol) was added in one portion. The ice bath was then removed, and the reaction was stirred overnight. The contents of the flask were concentrated to an oil which was partitioned between a solution of $NaHCO_3$ (2.5% in water) and diethyl ether. The layers were separated and the aqueous layer was washed again with diethyl ether. Ice was added to the aqueous layer, and it was acidified to pH 1 with 3 M HCl. A white precipitate formed and was collected by extraction with CH_2Cl_2 (2 × 25 mL). The organic extracts were combined, dried over $MgSO_4$, filtered, and concentrated to yield 0.258 g (84%) of the title compound as a light yellow oil. The product could be used without further purification for solid-phase peptide synthesis, but an analytical sample was obtained by reverse-phase HPLC (30 to 60% acetonitrile in 0.05% TFA/water; t_R = 22.7 min. on analytical column). After lyophilization, a white powder was obtained. Appreciable loss of product occurred on the semi-prep column. ^1H NMR ($CDCl_3$, 300 MHz, three conformations evident): δ 1.36 (d, J = 7.2Hz, 0.6H), 1.37 (d, J = 7.2Hz, 0.6H), 1.43 (d, J = 7.5 Hz, 1.8H), 2.25 (d, J = 13.4 Hz, 0.4H), 2.38 (d, J = 13.7 Hz, 0.6H), 2.50 (m, 0.4H), 2.62 (ddd, J = 14.0, 9.9, 5.8 Hz, 0.6H), 3.50 (m, 1H), 3.92 (m, 1H), 4.16 (m, 2H), 4.50 (m, 2H), 4.70 (m, 2.6H), 5.14 (d, J = 16.2Hz, 0.4H), 5.18 (q, J = 7.3 Hz, 0.4H), 5.31 (q, J = 7.4Hz, 0.6H), 7.32 (m, 4H), 7.65 (m, 4H), 8.65 (s, 1H). ^{13}C NMR ($CDCl_3$, 125 MHz, 4 conformations): δ 14.4, 14.5, 14.69, 14.75, 37.7, 38.1, 38.8, 39.1, 40.0, 40.1, 40.8, 40.9, 42.8, 43.4, 44.3, 47.1, 47.2, 47.4, 47.6, 53.7, 54.0, 54.1, 54.6, 54.7, 55.2, 56.2, 62.4, 62.5, 62.7, 63.0, 67.3, 67.8, 68.8, 68.9, 119.96, 120.01, 120.1, 120.2, 124.9, 125.0, 125.1, 125.3, 125.4, 125.8, 125.9, 127.2, 127.2, 127.3, 127.4,

127.8, 127.85, 127.88, 127.9, 130.0, 141.1, 141.3, 141.36, 141.38, 141.50, 141.52, 143.4, 143.5, 143.8, 144.0, 144.2, 144.5, 153.8, 154.1, 154.28, 154.32, 172.9, 173.1, 173.3, 173.4, 174.8, 175.1, 175.5. IR (film, cm^{-1}): 1413, 1617, 1651, 1704, 1735, 2589, 2948, 3066, 3457. HRMS $[M+H]^+$ found (calcd): 453.1485 (453.1479). Opt. Rot. $[\alpha]_D^{23}$ = +72.9 ($CHCl_3$ c 3.00).

5.7. Synthesis of Fmoc-NCap(7)DAla-OH

(*2S,4R*)-4-Hydroxy-2-(1-(*R*)-methoxycarbonyl-ethylcarbamoyl)-pyrrolidine-1-carboxylic acid benzyl ester (37)

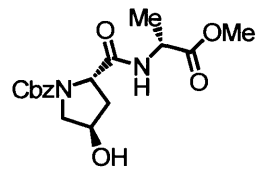

Cbz-Hyp-OH (3.71 g, 14 mmol), H-D-Ala-OMe·HCl (1.95 g, 14 mmol), and DIEA (2.73 mL, 16.8 mmol) were combined in 80 mL CH_2Cl_2. Diisopropyl carbodiimide (2.19 mL, 14 mmol) was added in portions, and a slight warming was noted. After 22 h, the reaction mixture was concentrated to an oil which was taken up in 50 mL ethyl acetate and placed in the refrigerator for ½ h. A white precipitate formed and was removed by vacuum filtration. The mother liquor was concentrated to an oil; purification by flash chromatography [EtOAc, R_f = 0.32, Mo–Ce blue] provided 3.66 g (75%) of the title compound as a clear oil. ^1H NMR ($CDCl_3$, 500 MHz, 2 rotamers): δ 1.19 (d, J = 5.9 Hz, 1.5H), 1.38 (d, J = 5.4 Hz, 1.5H), 2.11 (m, 1H), 2.34 (m, 1H), 3.56 (m, 2H), 3.69 (s, 3H), 4.46 (m, 3H), 5.10 (m, 2H), 6.54 (s, 0.5H), 7.30 (m, 5.5H). ^{13}C NMR ($CDCl_3$, 125 MHz, 2 rotamers): δ 18.2, 37.5, 39.7, 47.9, 48.3, 52.6, 54.8, 55.8, 59.4, 59.8, 67.6, 69.4, 70.0, 128.0, 128.3, 128.7, 136.4, 155.7, 156.4, 171.4, 172.0, 173.3. IR (film, cm^{-1}): 1540, 1674, 1743, 2952, 3035, 3315. Opt. Rot. $[\alpha]_D^{23}$ = –56.3 ($CHCl_3$, c 1.12).

(*2S,4R*)-4-Acetylsulfanyl-2-(1-(*R*)-methoxycarbonyl-ethylcarbamoyl)-pyrrolidine-1-carboxylic acid benzyl ester (38)

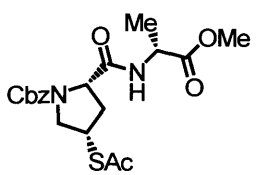

Triphenylphosphine (3.02 g, 11.6 mmol) was dissolved in 40 mL THF in a flame-dried round bottom flask under an argon atmosphere. The solution was cooled to 0 °C and

DIAD (2.27 mL, 11.6 mmol) was added. The mixture quickly became viscous as white particles formed, and stirring was continued at 0 °C for 15 min. Meanwhile, compound **37** (3.66 g, 10.5 mmol) and thiolacetic acid (0.78 mL, 11 mmol) were combined in 150 mL of dry THF in another flame-dried round bottom flask. The mixture was transferred quickly by funnel to the flask containing the triphenylphosphine–DIAD adduct at 0 °C, and an argon atmosphere was reestablished. Upon addition of the mixture, the reaction became dark green; as the reaction progressed, the color became light yellow and the particulates disappeared. After 5 h, the reaction mixture was concentrated to an oil, and flash chromatography [ethyl acetate–hexanes (1:1), R_f = 0.23, Mo–Ce blue], provided 3.4 g (79%) of the title compound as a clear oil that solidified slowly under high vacuum. A faint yellow band precedes the desired compound on the column. Compound **37** is only moderately soluble in THF; the compound was not fully dissolved when added to the reaction. ^{1}H NMR ($CDCl_3$, 500 MHz, 2 rotamers): δ 1.20 (s, 1.2H), 1.40 (s, 1.8H), 2.12 (broad s, 0.4H), 2.30 (s, 3H), 2.37 (broad s, 0.6H), 2.54 (broad s, 0.6H), 2.70 (broad s, 0.4H), 3.35 (m, 1H), 3.71 (s, 3H), 3.94 (quint, J = 6.9 Hz, 1H), 4.10 (s, 1H), 4.39 (s, 1H), 4.54 (s, 1H), 5.17 (m, 2H), 6.53 (s, 0.4H), 7.21 (s, 0.6H), 7.31 (m, 5H). ^{13}C NMR ($CDCl_3$, 125 MHz, 2 rotamers): δ 18.3, 30.7, 33.5, 36.7, 39.1, 39.8, 48.4, 52.5, 53.4, 60.2, 60.5, 67.8, 128.2, 128.4, 128.7, 136.1, 155.0, 156.0, 170.4, 173.1, 194.8, 195.6. IR (film, cm^{-1}): 1532, 1688, 1743, 2878, 2953, 2982, 3034, 3066, 3310. Melting point = 84 – 87 °C. HRMS $[M+H]^+$ found (calcd): 409.1430 (409.1428). Opt. Rot. $[\alpha]_D^{23}$ = –73.0 ($CHCl_3$, c 2.73).

(*2S,4R*)-4-Mercapto-2-(1-(*R*)-methoxycarbonyl-ethylcarbamoyl)-pyrrolidine-1-carboxylic acid benzyl ester (39)

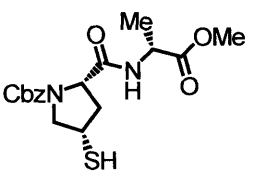

A 7 N solution of NH_3 in methanol was added to a solution of compound **38** (3.4 g, 8.3 mmol) in 30 mL methanol under an argon atmosphere; the mixture was stirred at room temperature for 2 h. Afterwards, the solution was concentrated to an oil and flash chromatography [EtOAc, R_f = 0.68, Mo–Ce blue) provided 2.8 g (92%) of the title compound as a light yellow oil that solidified slowly under high vacuum. ^{1}H NMR ($CDCl_3$, 500 MHz, 2 rotamers): δ 1.19 (s, 1.4H), 1.38 (s, 1.6H), 1.90 (d, J = 6.3 Hz, 1H),

2.13 (m, 1H), 2.65 (m, 1H), 3.30 (s, 2H), 3.68 (s, 3H), 4.04 (m, 1H), 4.31 (s, 1H), 4.50 (m, 1H), 5.10 (m, 2H), 6.62 (s, 0.45H), 7.13 (s, 0.55H), 7.31 (s, 5H). ^{13}C NMR ($CDCl_3$, 125 MHz, 2 rotamers): δ 18.1, 34.7, 35.4, 38.9, 41.2, 47.9, 48.2, 56.6, 60.6, 60.8, 67.6, 128.1, 128.3, 128.6, 136.1, 154.9, 155.7, 170.6, 171.0, 173.1. IR (film, cm^{-1}): 1533, 1668, 1697, 1741, 2551, 2877, 2952, 2985, 3033, 3065, 3308. HRMS $[M+H]^+$ found (calcd): 367.1320 (367.1322). Opt. Rot. $[\alpha]_D^{22} = -43.5$ ($CHCl_3$, c 1.53).

(*1S,6S*)-4-(1-(*R*)-Methoxycarbonyl-ethyl)-5-oxo-2-thia-4,7-diaza-bicyclo[4.2.1]nonane-7-carboxylic acid benzyl ester (40)

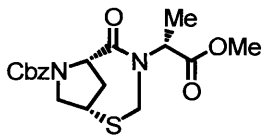

Compound **39** (1.79 g, 4.9 mmol), *p*-toluene sulfonic acid (0.466 g, 2.45 mmol), and paraformaldehyde (2.0 g) were combined in a flame-dried round bottom flask fitted with a Dean–Stark trap and a condenser. The apparatus was evacuated and backfilled with argon twice before filling the Dean–Stark trap with benzene/molecular sieves and adding 150 mL benzene to the round bottom flask. The stirred solution was heated at reflux for 1 h. Afterwards, the reaction mixture was concentrated to an oil and flash chromatography [ethyl acetate–hexanes (1:1), $R_f = 0.19$, Mo–Ce blue) provided 1.13 g (61%) of the title compound as a clear oil that was contaminated with less than 2% of the α-H alanine epimer, as determined by ^1H NMR. The characterization data for this compound were obtained with this slightly contaminated compound. ^1H NMR ($CDCl_3$, 500 MHz, 2 rotamers): δ 1.16 (d, J = 7.4 Hz, 2H), 1.26 (m, 1H), 2.35 (m, 1H), 2.55 (ddd, J = 16.2, 9.6, 6.5 Hz, 0.3H), 2.62 (ddd, J = 14.0, 8.9, 5.8 Hz, 0.7H), 3.41 (t, J = 5.2 Hz, 1H), 3.65 (s, 2H), 3.68 (s, 1H), 3.94 (m, 3H), 4.70 (d, J = 9.4 Hz, 1H), 4.90 (d, J = 16.0 Hz, 0.3H), 4.99 (d, J = 16.2 Hz, 0.7H), 5.14 (m, 3H), 7.31 (m, 5H). ^{13}C NMR ($CDCl_3$, 125 MHz, 2 rotamers): δ 14.8, 15.0, 38.0, 38.8, 39.9, 40.8, 42.4, 42.7, 52.3, 53.3, 53.7, 54.2, 54.5, 62.5, 63.0, 67.4, 67.7, 127.8, 128.2, 128.4, 128.5, 128.6, 128.7, 136.4, 136.5, 153.81, 171.7, 171.9, 172.7, 172.8. IR (film, cm^{-1}): 1652, 1704, 1738, 2879, 2950, 2982, 3032, 3064. HRMS $[M+Na]^+$ found (calcd): 401.1144 (401.1142). Opt. Rot. $[\alpha]_D^{23} = +123.7$ ($CHCl_3$, c 1.09).

(*1S,6S*)-4-(1-(*R*)-Carboxy-ethyl)-5-oxo-2-thia-4,7-diaza-bicyclo[4.2.1]nonane-7-carboxylic acid benzyl ester (41)

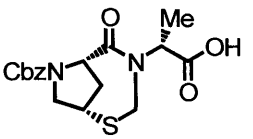

A solution of **40** (1.1 g, 2.9 mmol) in 25 mL methanol was cooled with an ice bath before the addition of 1.07 mL 3 M NaOH (3.19 mmol). The solution was allowed to warm to room temperature overnight; afterwards, 15 mL of water were added, and the methanol was stripped. Ice was added to the residue, followed by 3 M HCl to adjust to pH 1. A white precipitate formed and was isolated by extraction with CH_2Cl_2 (3 × 25 mL). The combined organic extracts were dried over $MgSO_4$ and filtered. The extraction solvent was stripped to yield 0.95 g (90%) of the title compound as a clear oil that formed a white foam under high vacuum. ^1H NMR ($CDCl_3$, 500 MHz, 2 rotamers): δ 1.20 (d, J = 7.2 Hz, 2H), 1.31 (d, J = 7.2 Hz, 1H), 2.36 (m, 1H), 2.53 (ddd, J = 14.5, 9.5, 5.7 Hz, 0.3H), 2.58 (ddd, J = 13.9, 9.6, 5.8 Hz, 0.7H), 3.38 (t, J = 5.5 Hz, 0.7H), 3.41 (t, J = 5.5 Hz, 0.3H), 3.86 (dd, J = 11.8, 5.5 Hz, 1H), 3.97 (m, 2H), 4.69 (d, J = 9.5 Hz, 1H), 4.89 (m, 1H), 5.02 (m, 1H), 5.15 (m, 2H), 7.29 (m, 5H), 10.1 (broad s, 1H). ^{13}C NMR ($CDCl_3$, 125 MHz, 2 rotamers): δ 14.7, 14.8, 37.9, 38.7, 39.9, 40.8, 43.1, 43.4, 54.2, 54.4, 54.5, 54.9, 62.4, 62.9, 67.6, 67.8, 128.0, 128.3, 128. 4, 128.5, 128.6, 128.7, 136.29, 136.34, 154.0, 173.36, 173.43, 175.0, 175.1. IR (film, cm^{-1}): 1616, 1653, 1705, 1734, 2592, 2944, 2979, 3034, 3470. HRMS $[M+Na]^+$ found (calcd): 387.0985 (387.0985). Opt. Rot. $[\alpha]_D^{23}$ = +150 ($CHCl_3$, c 0.9).

4-(1-Carboxy-ethyl)-5-oxo-2-thia-4-aza-7-azonia-bicyclo[4.2.1]nonane trifluoro-acetate (42)

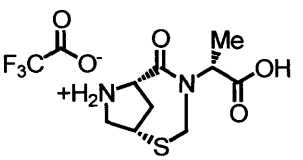

Compound **41** (0.86 g, 2.36 mmol) was dissolved in 30 mL ethanol. The solution was added to a Parr bottle containing 4.0 g of Pd/C (10% by dry weight, 50% water by weight). The contents of the Parr bottle were placed under 50 psig of H_2 and shaken for 78 h, after which time the reaction mixture was filtered and concentrated. A light yellow oil which formed a foam under high vacuum was obtained (0.535 g, 99%). This crude product was taken up in a minimum of acetonitrile and water (approximately 1:10 by volume). Reverse-phase HPLC chromatography (5 to 35% acetonitrile in 0.05%

TFA/water) was used to purify the title compound. The retention times on the analytical column are given in the preceding section. The TFA salt of the title compound was obtained as a white powder after lyophilization in 44% yield (0.36 g). The crude product is greater than 90% pure as judged by ^{1}H NMR and reverse-phase HPLC; because a semi-prep size HPLC column was used for the purification of the compound, substantial loss of product occurred. ^{1}H NMR (d_6-DMSO, 500 MHz): δ 1.32 (d, J = Hz, 3H), 2.43 (m, 2H), 3.60 (s, 2H), 3.84 (s, 1H), 4.38 (d, J = Hz, 1H), 4.59 (s, 1H), 4.68 (s, 1H), 4.90 (s, 1H), 10.0 (broad s, 2H), 12.5 (broad s, 1H). ^{13}C NMR ($CDCl_3$, 125 MHz): δ 13.8, 39.0, 41.3, 43.9, 54.4, 56.8, 64.6, 117.0 (q, J_{CF} = 269.5 Hz), 162.2 (q, J_{CF} = 51.6 Hz), 169.1, 173.4. IR (film, cm^{-1}): 1647, 1665, 1730, 2594, 2988, 3405. HRMS $[M+H]^+$ found (calcd): 231.0805 (231.0798). Opt. Rot. $[\alpha]_D^{23}$ = +67.8 (c 0.56, H_2O).

(*1S,6S*)-4-(1-(*S*)-carboxy-ethyl)-5-oxo-2-thia-4,7-diaza-bicyclo[4.2.1]nonane-7-carboxylic acid 9H-fluoren-9-yl methyl ester (43)

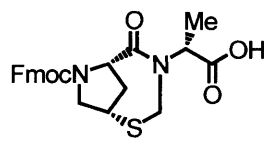

Upon addition of DIEA (0.35 mL, 2.0 mmol) to a suspension of **42** (0.228 g, 0.66 mmol) in 15 mL of acetonitrile, the solution became homogeneous. The reaction mixture was cooled with an ice bath, and FmocCl (0.19 g, 0.73 mmol) was added in one portion. The ice bath was then removed, and the reaction was stirred for 7 h. The contents of the flask were concentrated to an oil which was partitioned between a solution of $NaHCO_3$ (2.5% in water) and diethyl ether. The layers were separated and the aqueous layer was washed again with diethyl ether. Ice was added to the aqueous layer before it was acidified to pH 1 with 3 M HCl. A white precipitate formed and was collected by extraction with CH_2Cl_2 (2 × 25 mL). The organic extracts were combined, dried over $MgSO_4$, filtered, and concentrated to yield 0.268 g (89%) of the title compound as a light yellow oil. An analytical sample was purified by reverse-phase HPLC (30 to 60% acetonitrile in 0.05% TFA/water, t_R = 21.5 min. on the analytical column). ^{1}H NMR ($CDCl_3$, 300 MHz, three conformations evident): δ 1.34 (d, J = 7.7 Hz, 0.6H), 1.35 (d, J = 7.7 Hz, 0.6H), 1.41 (d, J = 7.3 Hz, 1.8H), 2.20 (m, 0.4H), 2.32 (d, J = 13.6 Hz, 0.6H), 2.40 (m, 0.2H), 2.50 (m, 0.2H), 2.58 (ddd, J = 13.9, 9.5, 5.6 Hz, 0.6H), 3.30 (m, 1H), 3.61 (m, 1H), 3.89 (m, 2H),

4.10 (m, 2H), 4.40–4.80 (m, 2H), 5.11 (d, J = 16.5 Hz, 0.8H), 5.17 (q, J = 7.6 Hz, 0.4H), 5.31 (q, J = 7.6 Hz, 0.6H), 7.30 (m, 4H), 7.54 (m, 1H), 7.68 (m, 3H), 11.1 (broad s, 1H). ^{13}C NMR ($CDCl_3$, 125 MHz, 4 conformations): δ 14.36, 14.45, 14.65, 14.72, 37.7, 38.0, 38.7, 39.0, 39.9, 40.0, 40.7, 40.9, 42.8, 42.9, 43.3, 44.3, 47.0, 47.1, 47.4, 47.5, 53.7, 53.97, 54.05, 54.5, 54.7, 55.1, 56.2, 62.3, 62.4, 62.6, 62.8, 67.3, 67.7, 68.8, 68.9, 119.9, 120.0, 120.09, 120.14, 124.8, 124.9, 125.0, 125.2, 125.3, 125.7, 125.8, 127.15, 127.20, 127.26, 127.32, 127.7, 127.81, 127.84, 127.87, 127.90, 141.0, 141.2, 141.29, 141.31, 141.43, 141.44, 141.6, 143.35, 143.37, 143.7, 143.9, 144.0, 144.1, 144.4, 153.8, 154.0, 154.26, 154.29, 173.0, 173.2, 173.3, 173.4, 174.7, 174.9, 175.3. IR (film, cm^{-1}): 1626, 1646, 1704, 1730, 2603, 2945, 3043, 3395. HRMS $[M+Na]^+$ found (calcd): 489.1440 (489.1455). Opt. Rot. $[\alpha]_D^{23}$ = +50.4 ($CHCl_3$ c 1.47).

5.8. Synthesis of Fmoc-NCap(7)Gly-OH

(*2S,4R*)-4-Hydroxy-2-(methoxycarbonylmethyl-carbamoyl)-pyrrolidine-1-carboxylic acid *tert*-butyl ester (44)

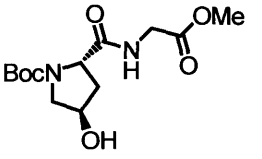

Boc-Hyp-OH (0.92 g, 4.0 mmol), H-Gly-OMe·HCl (0.63 g, 5.0 mmol), and DIEA (0.87 mL, 5.0 mmol) were combined in 20 mL methylene chloride. 1,1′-Diisopropyl carbodiimide (0.63 mL, 4.0 mmol) was added, and the reaction mixture was stirred at room temperature overnight (17 h). Afterwards, the reaction mixture was concentrated to an oil that was suspended in 50 mL ethyl acetate; the white precipitate that formed was removed by vacuum filtration, and the supernatant was concentrated to an oil. Purification by flash chromatography [MeOH:EtOAc (5:95), R_f = 0.17, Mo-Ce blue] provided 1.05 g (87%) of the title compound as a clear oil that foamed under high vacuum. ^{1}H NMR ($CDCl_3$, 500 MHz, 2 rotamers): δ 1.40 (s, 4.5H), 1.43 (s, 4.5H), 2.09 (s, 1H), 2.30 (s, 1H), 3.42 (m, 1H), 3.50 (dd, J = 11.4, 4.6 Hz, 1H), 3.58 (m, 1H), 4.00 (m, 2H), 4.40 (m, 2H), 6.83 (s, 0.5H), 7.37 (s, 0.5H). ^{13}C NMR ($CDCl_3$, 125 MHz, 2 rotamers): δ 28.1, 28.3, 37.6, 39.5, 40.9, 41.1, 52.2, 54.8, 54.9, 58.6, 59.6, 69.0, 69.5, 80.5, 80.7, 154.7, 155.6, 170.0, 170.2, 172.8, 173.5. IR (film, cm^{-1}): 1668, 1755, 2954,

2978, 3085, 3313. HRMS $[M+Na]^+$ found (calcd): 325.1378 (325.1370). Opt. Rot. $[\alpha]_D^{23} = -77.2$ ($CHCl_3$, c 1.02).

(*2S,4S*)-4-Acetylsulfanyl-2-(methoxycarbonylmethyl-carbamoyl)-pyrrolidine-1-carboxylic acid *tert*-butyl ester (45)

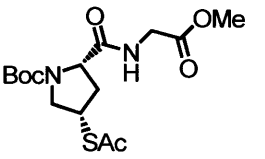

Triphenylphosphine (4.29 g, 16.4 mmol) was dissolved in 40 mL THF in a flame-dried round bottom flask under an argon atmosphere. The solution was cooled to 0 °C and DIAD (3.23 mL, 16.4 mmol) was added. The mixture quickly became white and viscous, and stirring was continued at 0 °C for 15 min. During this time, compound **44** (4.37 g, 14.9 mmol) and thiolacetic acid (1.12 mL, 15.6 mmol) were combined in 125 mL of dry THF in another round bottom flask. The mixture was transferred quickly by funnel to the round bottom flask containing the triphenylphosphine–DIAD adduct at 0 °C, and the reaction mixture was then returned to an argon atmosphere. Upon addition of the adduct, the reaction became dark yellow, and particulates were evident. As the reaction progressed the color became a light yellow, and the particulates disappeared within 3 h. The reaction mixture was then concentrated to an oil; flash chromatography [ethyl acetate–hexanes (1:1), R_f = 0.15, Mo–Ce blue] provided 4.45 g (80%) of the title compound as a light yellow oil. Careful chromatography is required to purify the compound as a yellow impurity precedes the product, and triphenylphosphine oxide elutes closely after the product. ^{1}H NMR ($CDCl_3$, 500 MHz, 2 rotamers): δ 1.39 (s, 9H), 2.08 (s, 0.4H), 2.25 (s, 3H), 2.29 (s, 0.6H), 2.47 (s, 0.6H), 2.64 (s, 0.4H), 3.21 (m, 1H), 3.68 (s, 3H), 3.92 (m, 4H), 4.28 (m, 1H), 6.70 (s, 0.4H), 7.34 (s, 0.6H). ^{13}C NMR ($CDCl_3$, 125 MHz, 2 rotamers): δ 28.3, 30.6, 33.3, 36.7, 39.1, 39.8, 41.3, 52.3, 52.6, 53.9, 59.5, 60.5, 81.2, 154.1, 155.4, 170.0, 171.5, 171.9, 194.7, 195.6. IR (film, cm^{-1}): 1536, 1694, 1755, 2872, 2933, 2977, 3085, 3313. HRMS $[M+Na]^+$ found (calcd): 383.1251 (383.1247). Opt. Rot. $[\alpha]_D^{23} = -90.9$ ($CHCl_3$, c 4.1).

(*2S,4S*)-4-Mercapto-2-(methoxycarbonylmethyl-carbamoyl)-pyrrolidine-1-carboxylic acid *tert*-butyl ester (46)

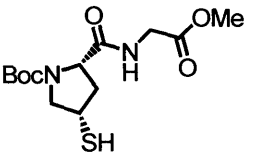

A saturated solution of NH_3 in methanol (20 mL) was added to a solution of compound **45** (4.66 g, 12.9 mmol) in 25 mL methanol under argon, and the contents of the reaction vessel were stirred at room temperature for 2 h. Afterwards, the solution was concentrated to an oil which was purified by flash chromatography [ethyl acetate-hexanes (4:1), R_f= 0.35, Mo–Ce blue]. After stripping the chromatography solvent, 3.37 g (82%) of the title compound were obtained as a light yellow oil. ^{1}H NMR ($CDCl_3$, 500 MHz, 2 rotamers): δ 1.40 (s, 9H), 1.84 (s, 1H), 2.01 (s, 0.4H), 2.22 (s, 0.6H), 2.61 (m, 1H), 3.19 (m, 1H), 3.28 (m, 1H), 3.99 (m, 3H), 4.24 (m, 1H), 6.75 (s, 0.4H), 7.24 (s, 0.6H). ^{13}C NMR ($CDCl_3$, 125 MHz, 2 rotamers): δ 28.3, 34.8, 35.3, 38.8, 41.2, 52.4, 56.2, 56.7, 60.0, 61.0, 81.2, 154.1, 155.2, 170.1, 171.8, 172.3. IR (film, cm^{-1}): 1538, 1670, 1752, 2544, 2873, 2934, 2977, 3085, 3304. HRMS $[M+Na]^+$ found (calcd): 341.1151 (341.1142). Opt. Rot. $[\alpha]_D^{22}$ = –63.1 ($CHCl_3$, c 2.22).

(*2S,4S*)-4-Methoxycarbonylmethyl-5-oxo-2-thia-4,7-diaza-bicyclo[4.2.1]nonane-7-carboxylic acid *tert*-butyl ester (47)

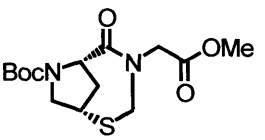

The thiol **46** (1.68g, 5.28 mmol), *p*-toluene sulfonic acid·H_2O (0.66 g, 3.48 mmol), and paraformaldehyde (4.0 g) were combined in a round bottom flask fitted with a Dean–Stark trap and a condenser. The apparatus was evacuated and backfilled with argon twice before adding 250 mL benzene to the reaction vessel, and filling the Dean–Stark trap with benzene and molecular sieves. The stirred solution was heated at reflux under argon for 1.5 h, after which time the reaction was clear. After stripping the solvent, the orange oil was purified by flash chromatography [ethyl acetate–hexanes (1:1), R_f= 0.72, Mo–Ce blue] yielding 0.18 g (10%) of the title compound as a clear oil. ^{1}H NMR ($CDCl_3$, 500 MHz, 2 rotamers): δ 1.41 (s, 6.75H), 1.46 (s, 2.25H), 2.33 (d, J = 13.5 Hz, 0.75H), 2.34 (d, J = 13.2 Hz, 0.25H), 2.57 (m, 1H), 3.38 (t, J = 5.5 Hz, 1H), 3.67 (s, 0.75H), 3.69 (s, 2.25H), 3.84 (m, 2.75H), 3.96 (d, J = 11.8 Hz, 1H), 4.11 (d, J = 17.4 Hz, 0.25H), 4.25 (d,

J = 17.1 Hz, 0.25H), 4.51 (m, 1.75H), 4.58 (d, J = 9.3 Hz, 0.25H), 5.29 (d, J = 15.9 Hz, 1H). ^{13}C NMR ($CDCl_3$, 125 MHz, 2 rotamers): δ 28.2, 28.4, 37.8, 38.8, 40.1, 41.0, 47.6, 50.8, 51.1, 52.3, 53.8, 54.4, 62.3, 81.1, 81.5, 169.1, 169.3, 173.6, . IR (film, cm^{-1}): 1654, 1696, 1752, 2875, 2954, 2978. HRMS $[M+Na]^+$ found (calcd): 353.1150 (353.1142). Opt. Rot. $[\alpha]_D^{23}$ = +148.7 ($CHCl_3$, c 0.38).

(*2S,4S*)-4-Carboxymethyl-5-oxo-2-thia-4-aza-7-azonia-bicyclo[4.2.1]nonane; trifluoro-acetate (48)

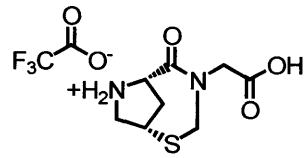

A solution of compound **47** (0.126 g, 0.39 mmol) in 10 mL MeOH was cooled with an ice bath, and a solution of 3 M NaOH (0.14 mL, 0.42 mmol) was added. The ice bath was removed to allow the solution to warm to room temperature over 8 h. Afterwards, 10 mL water were added to the reaction vessel and the MeOH was removed *in vacuo*. Ice was added to the residue, followed by cold 3 M HCl to adjust to pH 1. The solution became cloudy, but no precipitate formed. The mixture was frozen immediately and lyophilized to yield a white solid. The solid was suspended in CH_2Cl_2, and TFA was added whereupon most of the precipitate went into solution. The reaction vessel was placed in the refrigerator overnight, and afterwards the solution was filtered, and the supernatant was concentrated. The residue was taken up in water, frozen immediately, and lyophilized. A light yellow solid was obtained. Although the crude ^{1}H NMR was quite clean, the sample was purified by reverse-phase HPLC (1 to 35% MeCN in 0.05% TFA/H_2O, t_R = 3.8 min. on the analytical column). After lyophilization of the fractions, 0.122 g (97%) of a white powder was obtained. ^{1}H NMR (CD_3CN, 500 MHz): δ 2.58 (m, 2H), 3.81 (s, 3H), 4.06 (d, J = 17.4 Hz, 1H), 4.20 (d, J = 17.4 Hz, 1H), 4.45 (d, J = 15.0 Hz, 1H), 4.60 (d, J = 8.7 Hz, 1H), 5.02 (d, J = 8.5 Hz, 1H), 10.9 (s, 3H). ^{13}C NMR (CD_3CN, 125 MHz): δ 37.8, 42.3, 48.1, 53.0, 54.1, 64.3, 118.2 (q, J_{CF} = 296.5 Hz), 162.8 (q, J_{CF} = 51.6 Hz), 171.0, 172.6. IR (film, cm^{-1}): 1669, 2746, 2996, 3427. Opt. Rot. $[\alpha]_D^{23}$ = +40.4 (CH_3CN, c 0.87).

(*2S,4S*)-4-Carboxymethyl-5-oxo-2-thia-4,7-diaza-bicyclo[4.2.1]nonane-7-carboxylic acid 9H-fluoren-9-ylmethyl ester (49)

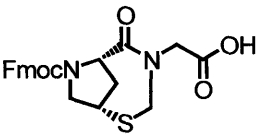

A clear solution was obtained after addition of DIEA (0.05 mL, 0.3 mmol) to a suspension of the zwitterion salt **48** (0.033g, 0.1 mmol) in acetonitrile:water (10:1, v:v). The reaction vessel was cooled with an ice bath, and FmocOSu (0.04 g, 0.12 mmol) was added; afterwards, the ice bath was removed, and the reaction was stirred for 7 h. Water (10 mL) was added to the mixture, and the solution was frozen and lyophilized. The white solid thus obtained was taken up in 0.05% TFA/water and chromatographed by reverse-phase HPLC (35 to 60% MeCN in 0.05% TFA/water, 30 min., t_R = 10 min. on the analytical column). After lyophilization of the fractions, 0.0142 g (32%) of the title compound was obtained as a white powder. ^{1}H NMR ($CDCl_3$, 500 MHz): δ 2.33 (d, J = 13.8 Hz, 0.35H), 2.42 (d, J = 13.7 Hz, 0.65H), 2.45 (ddd, J = 14.0, 9.8, 5.8 Hz, 0.35H), 2.63 (ddd, J = 13.8, 9.9, 5.8 Hz, 0.65H), 3.32 (t, J = 5.5Hz, 0.35H), 3.42 (t, J = 5.5 Hz, 0.65H), 3.54 (d, J = 5.3 Hz, 0.65H), 3.66 (dd, J = 11.6, 5.3Hz, 0.35), 3.86 (m, 2.35H), 4.03 (d, J = 11.9 Hz, 0.65H), 4.19 (m, 2H), 4.52 (m, 2H), 4.74 (m, 1.35H), 5.30 (d, J = 17.2 Hz, 0.65H), 7.38 (m, 4H), 7.60 (m, 5H). ^{13}C NMR ($CDCl_3$, 125 MHz): δ 37.9, 39.0, 40.2, 40.9, 47.2, 47.6, 48.0, 51.3, 51.5, 54.0, 54.7, 62.3, 62.6, 67.5, 68.8, 120.0, 120.1, 120.2, 120.23, 125.0, 125.2, 125.4, 125.9, 127.3, 127.4, 127.88, 127.94, 128.0, 141.3, 141.4, 141.5, 141.7, 143.6, 143.8, 144.4, 154.2, 154.3, 172.3, 172.6, 173.4, 173.6. IR (film, cm^{-1}): . HRMS $[M+Na]^+$ found (calcd): 461.1130 (461.1142). Opt. Rot. $[\alpha]_D^{23}$ = +50.3 ($CHCl_3$, c 1.56).

5.9. Synthesis of Fmoc-NCap(7)Aib-OH:

(*2S,4R*)-2-(1-*tert*-Butoxycarbonyl-1-methyl-ethylcarbamoyl)-4-hydroxy-pyrrolidine-1-carboxylic acid *tert*-butyl ester (54)

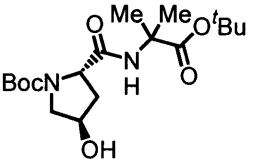

Boc-Hyp-OH (7.09 g, 30.7 mmol), *tert*-butyl α-aminoisobutyrate·HCl (5.0 g, 25.5 mmol), and DIEA (13.4 mL, 76.5 mmol) were combined in 250 mL acetonitrile. TBTU (9.84 g, 30.7 mmol) was added to this stirred solution in portions, and the solution warmed slightly. Stirring was continued overnight (18 h); afterwards, the reaction mixture was concentrated to an oil which was dissolved in 250 mL ethyl acetate, and the solution was washed with sat. NH_4Cl (2 × 50 mL), sat. $NaHCO_3$ (2 x 50 mL), and brine (1 × 50 mL). The organic solution was dried over $MgSO_4$, filtered, and the solvent was stripped *in vacuo* yielding 9.3 g (98%) of title compound as a clear oil that slowly solidified under high vacuum. ^1H NMR ($CDCl_3$, 500 MHz, 2 rotamers): δ 1.40 (m, 24H), 2.01 (s, 1H), 2.25 (s, 1H), 3.49 (m, 2H), 3.75 (broad s, 1H), 4.24 (m, 1H), 4.36 (s, 1H), 6.83 (s, 0.5H), 7.41 (s, 0.5H). ^{13}C NMR ($CDCl_3$, 125 MHz, 2 rotamers): δ 24.5, 24.7, 27.9, 28.4, 37.0, 39.7, 54.6, 55.2, 56.7, 58.8, 60.0, 69.1, 69.7, 80.6, 81.1, 81.7, 154.9, 155.8, 171.1, 172.0, 173.5. IR (film, cm^{-1}): 1666, 1734, 2934, 2980, 3077, 3327. HRMS $[M+H]^+$ found (calcd): 373.2333 (373.2333). Opt. Rot. $[\alpha]_D^{23} = -71.5$ ($CHCl_3$, c 1.81). Melting point: 155 – 158 °C.

(*2S,4S*)-4-Acetylsulfanyl-2-(1-*tert*-butoxycarbonyl-1-methyl-ethylcarbamoyl)-pyrrolidine-1-carboxylic acid *tert*-butyl ester (55)

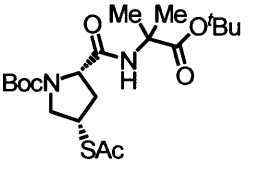

Triphenylphosphine (6.61 g, 25.3 mmol) was dissolved in 40 mL THF in a flame-dried round bottom flask under an argon atmosphere. The solution was cooled to 0 °C and DIAD (4.98 mL, 25.3 mmol) was added. The mixture quickly became white and viscous, and stirring was continued at 0 °C for 15 min. During this time, compound **54** (8.55 g, 23.0 mmol) and thiolacetic acid (1.8 mL, 25.3 mmol) were combined in 200 mL of dry

THF in another round bottom flask. The mixture of thiolacetic acid and compound **54** was transferred quickly by funnel to the round bottom flask containing the triphenylphosphine–DIAD adduct at 0 °C, and an argon atmosphere was reestablished. Upon addition of the mixture, the reaction became dark green, and particulates were evident. Within 5 h, the color became a light green and the particulates disappeared. Afterwards, the reaction mixture was concentrated to an oil, and the crude mixture was purified by flash chromatography [ethyl acetate–hexanes (1:4); TLC plates were developed in ethyl acetate–hexanes (1:1), for which R_f = 0.43; Mo–Ce blue] yielding 6.89 g of the title compound as a clear oil. This sample was contaminated with the reduced DIAD by-product, diisopropylhydrazodicarboxylate. After ^{1}H NMR analysis, a corrected yield of 4.48 g (83%) was determined for the reaction. An analytical sample was prepared by reverse-phase HPLC [35 to 60% acetonitrile in TFA/water (0.5%), t_R = 12 min. on the semi-prep column]. All characterization data were collected with the pure compound. ^{1}H NMR ($CDCl_3$, 500 MHz, 2 rotamers): δ 1.41 (m, 24H), 2.09 (s, 0.5H), 2.23 (s, 3H), 2.28 (s, 0.5H), 2.42 (s, 0.5H), 2.62 (s, 0.5H), 3.22 (s, 1H), 3.86 (app quint, J = 6.9 Hz), 3.92 (s, 1H), 4.15 (m, 1H), 6.81 (s, 0.5H), 7.35 (s, 0.5H). ^{13}C NMR ($CDCl_3$, 125 MHz, 2 rotamers): δ 24.1, 24.4, 27.8, 28.3, 30.6, 33.0, 36.6, 39.3, 39.8, 52.9, 53.6, 56.8, 59.8, 60.9, 81.0, 81.2, 81.8, 154.2, 155.2, 170.1, 170.6, 173.5, 194.7, 195.6. IR (film, cm^{-1}): 1538, 1671, 1734, 2874, 2933, 2979, 3323. HRMS $[M+H]^+$ found (calcd): 431.2214 (431.2214). Melting point = 139 – 140 °C. Opt. Rot. $[\alpha]_D^{23}$ = -79.0 ($CHCl_3$, c 1.76).

(*2S,4S*)-2-(1-*tert*-Butoxycarbonyl-1-methyl-ethylcarbamoyl)-4-mercapto-pyrrolidine-1-carboxylic acid *tert*-butyl ester (56)

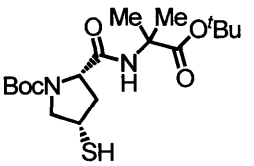

A saturated solution of NH_3 in methanol (15 mL) was added to a solution of compound **55** (0.255 g, 0.566 mmol) in 15 mL methanol, under argon. The contents of the reaction vessel were stirred at room temperature for 3 h; afterwards, the solution was concentrated to an oil. Flash chromatography [EtOAc, R_f = 0.78, Mo–Ce blue, mod. UV] provided 0.169 g (77%) of the title compound as a light yellow oil. The sample **55** described above was the analytical sample from the preceding step; however, if contaminated **55** is

used for the reaction, contaminated **56** is obtained. In this case, disulfide formation provides a means for separating the thiol from the contaminant. ^{1}H NMR ($CDCl_3$, 500 MHz, 2 rotamers): δ 1.38 (s, 18H), 1.45 (s, 6H), 2.00 (m, 2H), 2.55 (m, 1H), 3.23 (m, 2H), 3.91 (s, 1H), 4.10 (m, 1H), 6.81 (s, 0.5H), 7.28 (s, 0.5H). ^{13}C NMR ($CDCl_3$, 125 MHz, 2 rotamers): δ 24.2, 24.5, 27.9, 28.3, 34.7, 35.3, 38.4, 41.0, 56.3, 56.7, 60.2, 61.3, 80.9, 81.8, 154.2, 155.0, 170.3, 170.7, 178.5. IR (film, cm^{-1}): 1539, 1668, 1688, 1732, 2549, 2871, 2933, 2979, 3310. HRMS $[M+H]^+$ found (calcd): 389.2103 (389.2105). Opt. Rot. $[\alpha]_D^{22} = -58.7$ ($CHCl_3$, c 1.45). Melting point = 115 – 116 °C.

Disulfide Synthesis and Recovery of Pure (*2S,4S*)-2-(1-*tert*-Butoxycarbonyl-1-methyl-ethylcarbamoyl)-4-mercapto-pyrrolidine-1-carboxylic acid *tert*-butyl ester (56)

A solution of K_2CO_3 (0.55 g, 4.0 mmol) in 10 mL water was added to a solution of contaminated thiol **56** (2.8 g, 7.2 mmol, corrected) in 90 mL of acetonitrile. Iodine (1.87 g, 7.2 mmol) was added, and stirring was continued for 7 h, after which time $Na_2S_2O_3$ was added until the solution was light yellow. The reaction mixture was concentrated in vacuo, and the resulting yellow sludge was partitioned between 50 mL water and 100 mL diethyl ether. The layers were separated, and the water layer was washed again with diethyl ether (1 × 50 mL). The combined organic extracts were dried over $MgSO_4$, filtered, and concentrated. Flash chromatography [ethyl acetate–hexanes (3:1), R_f = 0.27, Mo–Ce blue, UV] provided 1.9 g (68%) of the title compound as a light yellow oil. ^{1}H NMR revealed that the disulfide was contaminated with a small amount of an unknown impurity.

The disulfide (1.9 g, 2.7 mmol) was dissolved in 40 mL of methanol and approximately 5 mL of an acetate buffer (0.1 M, pH = 4.7). TCEP·HCl (1.0 g, 3.5 mmol) was added to the reaction vessel, and the reaction was stirred overnight. Afterwards, 20 mL of brine were added to the vessel and the MeOH was removed *in vacuo*. The aqueous solution was extracted with diethyl ether (40 mL); the organic extract was dried over $MgSO_4$, filtered, and concentrated to yield 1.1 g (55%) of the thiol as a clear oil.

The characterization data for the product exactly matched the analytical sample prepared from the contaminated thiol.

(*2S,4S*)-4-(1-*tert*-Butoxycarbonyl-1-methyl-ethyl)-5-oxo-2-thia-4,7-diaza-bicyclo[4.2.1]nonane-7-carboxylic acid *tert*-butyl ester (58)

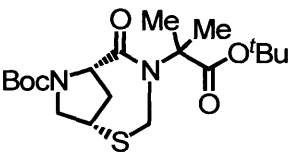

Thiol **57** (3.18 g, 8.18 mmol), *p*-toluene sulfonic acid·H_2O (0.78 g, 4.09 mmol), and paraformaldehyde (4.0 g) were combined in a round bottom flask fitted with a Dean–Stark trap and a condenser. The apparatus was evacuated and backfilled with argon twice before adding 200 mL benzene to the reaction vessel, and the Dean–Stark trap was filled with benzene and molecular sieves. The stirred solution was heated at reflux under argon for 4 h, after which time another 2 g of paraformaldehyde were added. An aliquot was removed 1 h after the second addition of paraformaldehyde; mass spectroscopy demonstrated that starting material was still present. Another 5 g of paraformaldehyde were added and the reaction was heated at reflux for another 3 h. Afterwards, the reaction mixture was concentrated to an orange oil; flash chromatography [ethyl acetate–hexanes (1:1), R*f* = 0.72, Mo–Ce blue] provided 0.19 g of product. The material was further purified by reverse-phase HPLC [35 to 60% acetonitrile in TFA/water (0.05%)], and after lyophilization, the title compound was obtained in 4% yield (0.129 g). ^{1}H NMR ($CDCl_3$, 500 MHz, 2 rotamers): δ 1.42 (m, 24H), 2.34 (d, J = 13.5 Hz, 0.25H), 2.42 (d, J = 13.5 Hz, 0.75H), 2.54 (m, 0.25H), 2.59 (ddd, J = 13.5, 9.4, 5.8 Hz, 0.75H), 3.41 (t, J = 5.5 Hz, 1H), 3.88 (dd, J = 11.5, 5.5 Hz, 1H), 4.00 (dd, J = 11.8, 1.4 Hz, 1H), 4.26 (d, J = 16.5 Hz, 1H), 4.50 (d, J = 9.3 Hz, 0.75H), 4.59 (d, J = 9.1 Hz, 0.25H), 5.12 (d, J = 16.5 Hz, 0.75H), 5.13 (d, J = 16.5 Hz, 0.25H). ^{13}C NMR ($CDCl_3$, 125 MHz, 2 rotamers): δ 23.3, 24.0, 24.5, 24.8, 27.9, 28.0, 28.3, 28.4, 37.7, 38.1, 40.4, 40.5, 41.2, 54.6, 55.0, 62.9, 63.1, 63.2, 80.5, 81.2, 153.2, 171.9, 172.2, 172.4, 172.5. IR (film, cm^{-1}): 1652, 1696, 1731, 2880, 2933, 2978. HRMS $[M+Na]^+$ found (calcd): 423.1941 (423.1924). Opt. Rot. $[\alpha]_D^{23}$ = +97.1 ($CHCl_3$, c 3.5). Melting point: 121 – 124 °C.

(*2S,4S*)-4-(1-Carboxy-1-methyl-ethyl)-5-oxo-2-thia-4-aza-7-azonia-bicyclo[4.2.1]nonane; trifluoro-acetate (59)

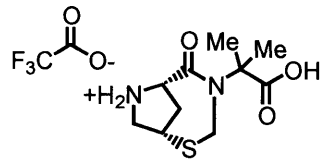

Compound **58** (0.128 g, 0.32 mmol) was dissolved in 5 mL CH_2Cl_2 and cooled with an ice bath. TFA (10 mL, 13 mmol) was added, and stirring was continued at 0 °C for approximately 15 min. After this time the ice bath was removed and the solution was allowed to warm to room temperature over 10 h. The reaction mixture was concentrated and evaporated from methylene chloride, and the title compound was obtained in 100% yield (0.115 g) after being kept under high vacuum overnight. ^{1}H NMR ($CDCl_3$, 500 MHz): δ 1.31 (s, 3H), 1.40 (s, 3H), 2.36 (s, 1H), 2.49 (s, 1H), 3.71 (m, 2H), 3.88 (t, J = 6.0 Hz, 1H), 4.28 (d, J = 9.0 Hz, 1H), 4.65 (d, J = 15.7 Hz, 1H), 4.89 (d, J = 13.4 Hz, 1H), 10.2 (s, 2H), 12.2 (s, 1H). ^{13}C NMR (d_6-DMSO, 125 MHz, 2 rotamers): δ 22.9, 23.4, 37.8, 40.2, 41.6, 53.2, 62.4, 63.7, 117.3 (q, J =), 158.8 (q, J =), 169.2, 174.3. IR (film, cm^{-1}): 1626, 1672, 2757, 2985, 3402. HRMS $[M]^+$ found (calcd): 245.0952 (245.0954). Opt. Rot. $[\alpha]_D^{23}$ = +30.7 (H_2O, c 0.5).

(*2S,4S*)-4-(1-Carboxy-1-methyl-ethyl)-5-oxo-2-thia-4,7-diaza-bicyclo[4.2.1]nonane-7-carboxylic acid 9H-fluoren-9-ylmethyl ester (60)

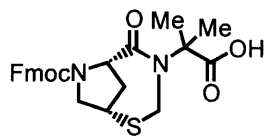

The TFA salt **59** (0.154 g, 0.43 mmol) was dissolved in 10 mL acetonitrile, and DIEA (0.22 mL, 1.3 mmol) was added, followed by FmocCl (0.112 g, 0.43 mmol). Stirring was continued at room temperature for 5 h, after which time the reaction mixture was concentrated, and the resulting oil was partitioned between diethyl ether (15 mL) and a 2.5% solution of $NaHCO_3$ in water (7 mL). The layers were separated and the aqueous layer was cooled by the addition of ice. The aqueous layer was acidified to pH 1 by the addition of 3 M HCl. A white precipitate formed and was collected by extraction with methylene chloride (2 × 15 mL). The organic extracts were dried over $MgSO_4$, filtered, and concentrated to yield 0.196 g (98%) of the title compound as a clear oil that foamed under high vacuum. ^{1}H NMR ($CDCl_3$, 500 MHz, 2 rotamers): δ 1.24 (s, 2.1H), 1.28 (s, 0.9H), 1.35 (s, 0.9H), 1.41 (s, 2.1H), 2.30 (d, J = 13.4 Hz, 0.3H), 2.40 (d, J = 13.3 Hz,

0.7H), 2.56 (ddd, J = 15.1, 9.8, 5.8 Hz, 1H), 3.29 (t, 5.3 Hz, 0.3H), 3.37 (t, J = 5.5 Hz, 0.7H), 3.58 (d, J = 11.5 Hz, 0.3H), 3.68 (dd, J = 11.5, 5.4 Hz, 0.3H), 3.87 (m, 1.4H), 4.00 (m, 1H), 4.17 (m, 2H), 4.50 (m, 1.3H), 4.66 (d, J = 16.6 Hz, 0.3H), 4.73 (d, J = 9.3 Hz, 0.7H), 5.08 (d, J = 16.6 Hz, 0.7H), 7.31 (m, 4H), 7.5 – 7.8 (m, 4H), 11.09 (s, 1H). ^{13}C NMR ($CDCl_3$, 125 MHz, 2 rotamers): δ 23.0, 23.5, 24.2, 24.5, 37.2, 38.4, 40.4, 41.2, 46.7, 47.6, 54.8, 55.0, 62.4, 62.5, 63.0, 63.3, 67.1, 68.9, 119.8, 119.9, 120.0, 120.1, 124.8, 125.1, 125.3, 126.3, 127.2, 127.3, 127.7, 127.79, 127.83, 141.0, 141.3, 141.4, 141.5, 143.2, 143.7, 143.9, 144.9, 153.6, 154.1, 172.1, 172.6, 177.7, 178.6. IR (film, cm^{-1}): 1653, 1706, 1737, 2873, 2976, 3040, 3150. HRMS $[M+Na]^+$ found (calcd): 489.1456 (489.1455). Opt. Rot. $[\alpha]_D^{23}$ = +42.7 ($CHCl_3$, c 1.5).

5.10. Peptide Characterization Tables

Peptide synthesis was performed as described in the previous Chapter. Whereas 9 equivalents of commercially available Fmoc-amino acids were used for each coupling, only 3 – 5 equivalents of the new, synthetic Fmoc-N-Caps were used.

Peptide	Electrospray Mass Spectrometry (M+zH)/z Found (Expected)
Ac-$^{\beta}$D-NCap(8)Gly-A_{10}-*beta*-Acc-K_2-W-NH_2	876.3 (876.0), 584.6 (584.3)
Ac-$^{\beta}$D-NCap(8)Ala-A_{10}-*beta*-Acc-K_2-W-NH_2	883.0 (882.8), 589.0 (588.9)
Ac-$^{\beta}$D-NCap(7)Gly-A_{10}-*beta*-Acc-K_2-W-NH_2	868.5 (869.0), 579.5 (579.6)
Ac-$^{\beta}$D-NCap(7)Ala-A_{10}-*beta*-Acc-K_2-W-NH_2	876.2 (876.0), 584.5 (584.3)
Ac-$^{\beta}$D-NCap(7)DAla-A_{10}-*beta*-Acc-K_2-W-NH_2	875.5 (876.0), 584.1 (584.3)
Ac-$^{\beta}$D-NCap(7)Aib-A_{10}-*beta*-Acc-K_2-W-NH_2	882.6 (883.0), 588.8 (589.0)
Ac-$^{\beta}$D-ProGly-A_{10}-*beta*-Acc-K_2-W-NH_2	847.2 (847.0), 565.2 (565.0)
Ac-$^{\beta}$D-ProAla-A_{10}-*beta*-Acc-K_2-W-NH_2	854.4 (854.0), 570.0(569.7)
Ac-$^{\beta}$D-ProGly-AA-^{U}*Ala*-^{U}*Ala*-AA-^{U}*Ala*-^{U}*Ala*-AA-*beta*-Acc-K_2-W-NH_2	848.1 (849.0), 565.8 (566.3)
Ac-$^{\beta}$D-ProGly-^{U}*Ala*-AAA-^{U}*Ala*-AAA-^{U}*Ala*-A-*beta*-Acc-K_2-W-NH_2	847.6 (849.0), 565.1 (566.3)
Ac-$^{\beta}$D-ProGly-A-^{U}*Ala*-AAA-^{U}*Ala*-AAA-^{U}*Ala*-*beta*-Acc-K_2-W-NH_2	847.6 (849.0), 565.1 (566.3)

5.11. ^{1}H NMR Spectra

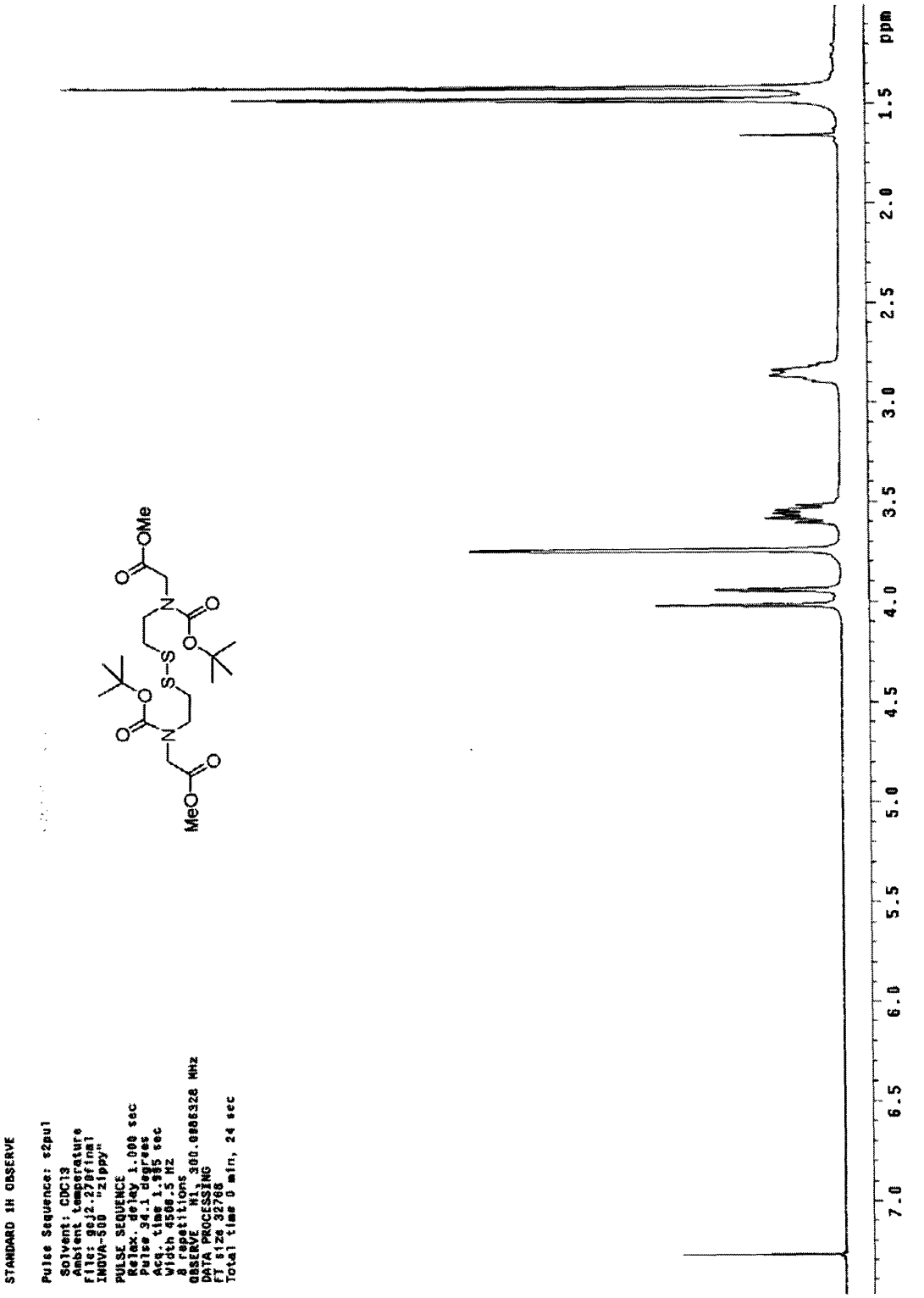


STANDARD PROTON PARAMETERS
Pulse Sequence: s2pul
Solvent: CDCl3
Ambient temperature
File: gej2.29ifinal
INOVA-500 "zippy"
PULSE SEQUENCE
Pulse 90.0 degrees
Acq. time 3.200 sec
Width 10000.0 Hz
8 repetitions
OBSERVE H1, 500.2312669 MHz
DATA PROCESSING
FT size 131072
Total time 0 min, 28 sec
Me
Me
Me
O
O
SH
N
O
O
MeO
ppm
7
6
5
4
3
2

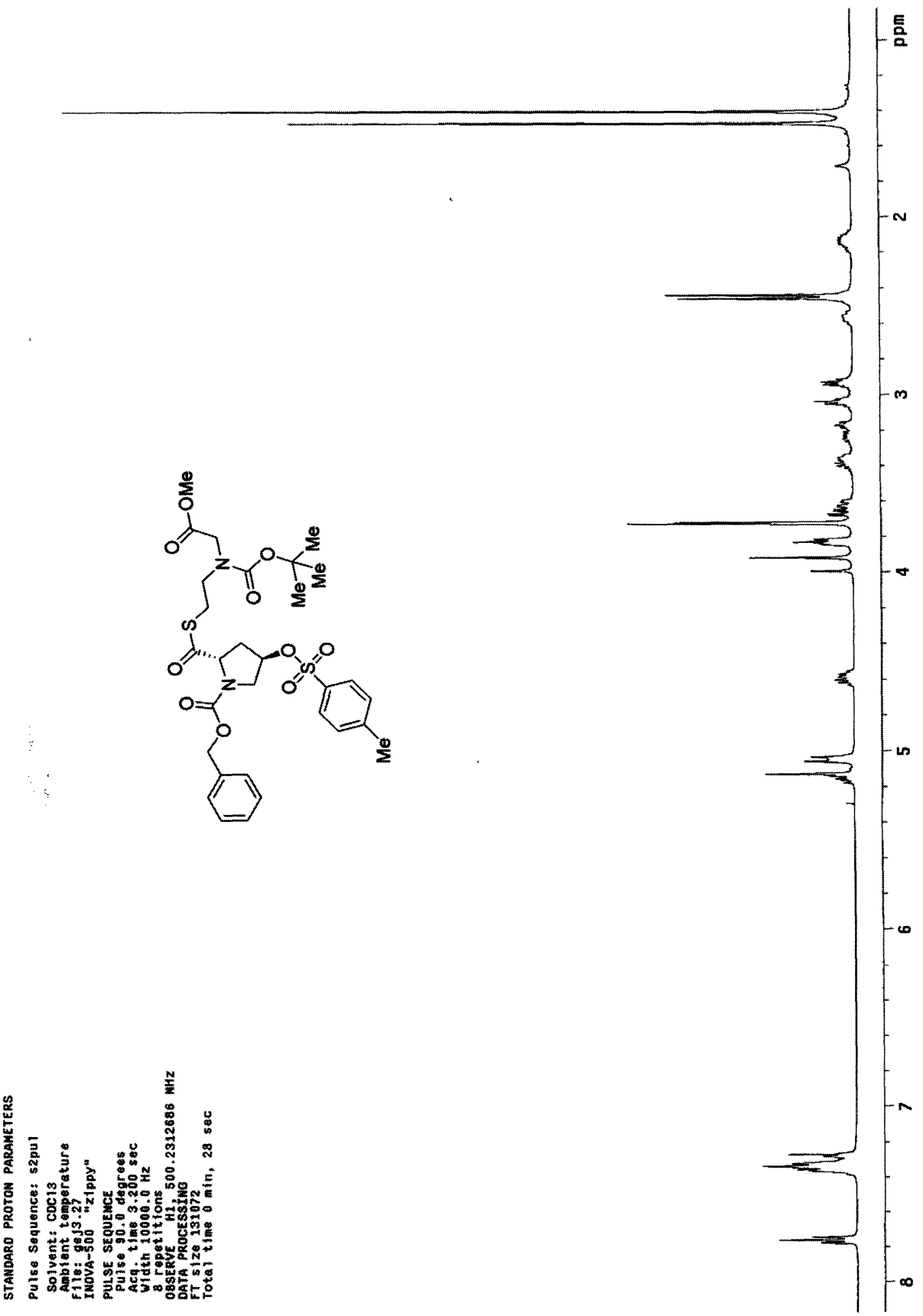
STANDARD PROTON PARAMETERS
Pulse Sequence: s2pul
Solvent: CDCl3
Ambient temperature
File: gaj3.27
INOVA-500 "zippy"
PULSE SEQUENCE
Pulse 90.0 degrees
Acq. time 3.200 sec
Width 10000.0 Hz
8 repetitions
OBSERVE H1, 500.2312686 MHz
DATA PROCESSING
FT size 131072
Total time 0 min, 28 sec
OMe
Me
Me
Me
Me
ppm
8
7
6
5
4
3
2

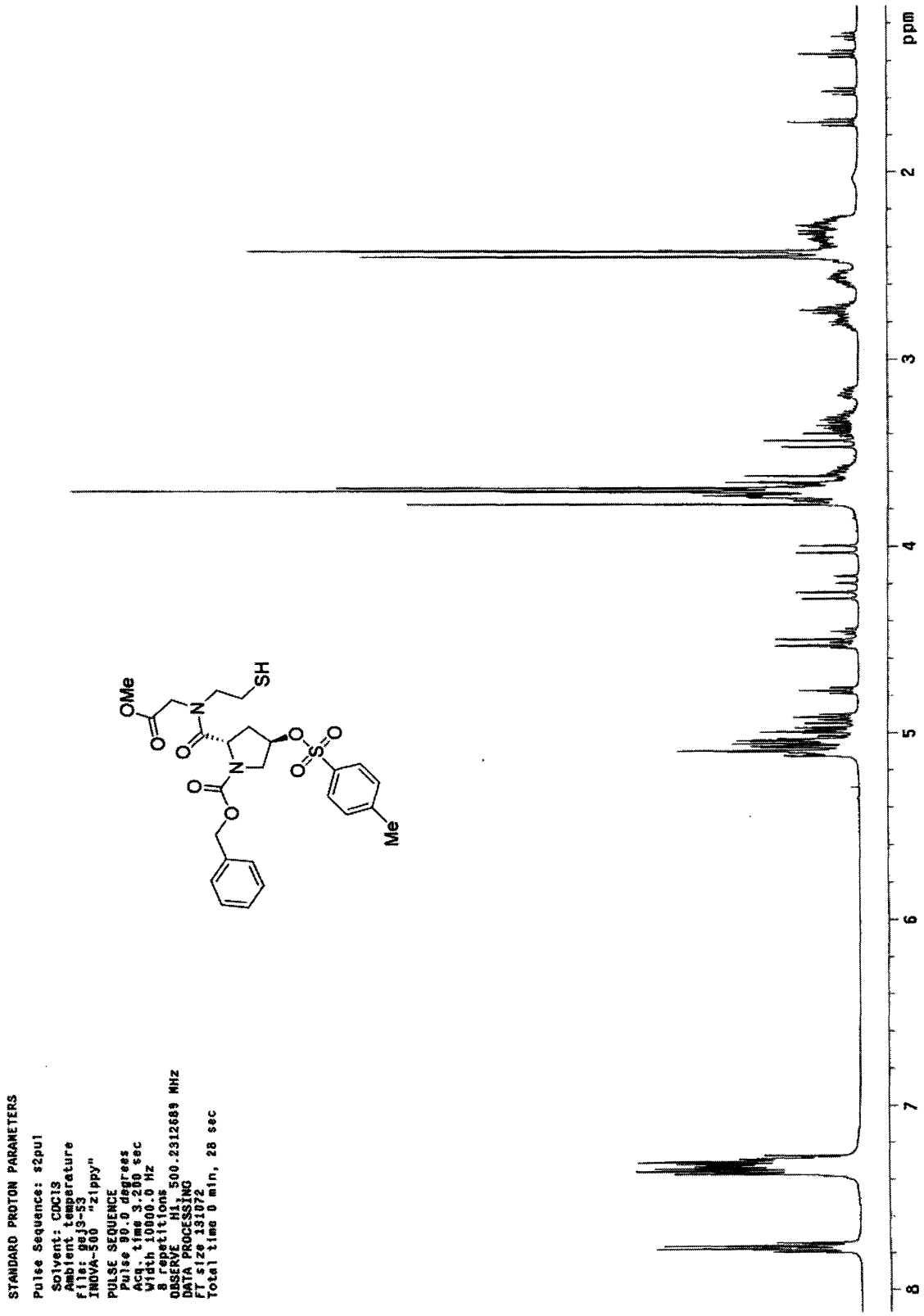
STANDARD PROTON PARAMETERS
Pulse Sequence: s2pul
Solvent: CDCl3
Ambient temperature
File: gaj3-53
INOVA-500 "zippy"
PULSE SEQUENCE
Pulse 90.0 degrees
Acq. time 3.200 sec
Width 10000.0 Hz
8 repetitions
OBSERVE H1, 500.2312689 MHz
DATA PROCESSING
FT size 131072
Total time 0 min, 28 sec
OMe
SH
Me
ppm
8
7
6
5
4
3
2

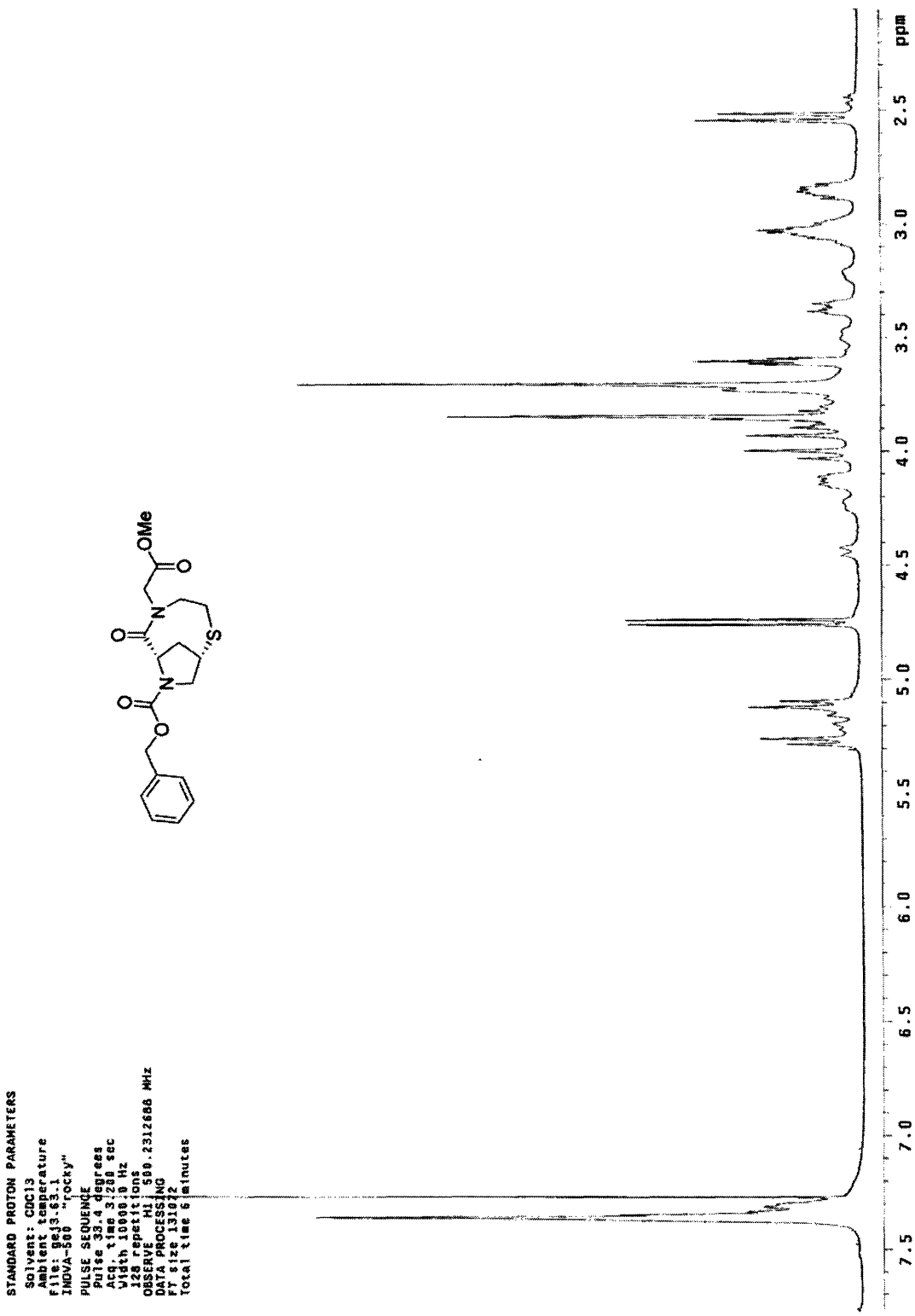
STANDARD PROTON PARAMETERS
Solvent: CDCl3
Ambient temperature
File: gej3-63-1
INOVA-500 "rocky"
PULSE SEQUENCE
Pulse 33.4 degrees
Acq. time 3.728 sec
Width 10000.0 Hz
128 repetitions
OBSERVE H1, 499.2312688 MHz
DATA PROCESSING
FT size 131072
Total time 6 minutes
OMe
O
N
S
7.5
7.0
6.5
6.0
5.5
5.0
4.5
4.0
3.5
3.0
2.5
ppm

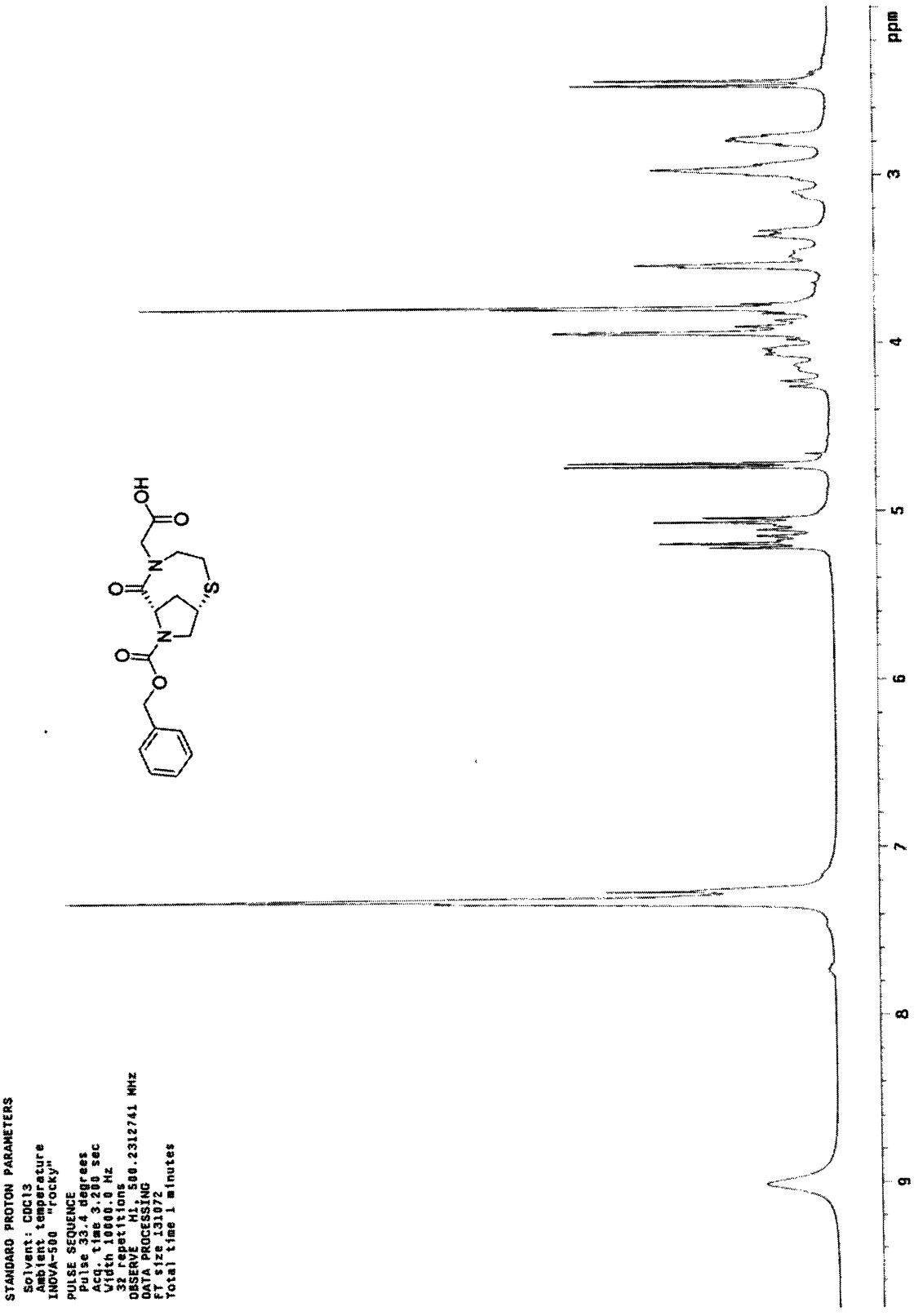
STANDARD PROTON PARAMETERS
Solvent: CDCl3
Ambient temperature
INOVA-500 "rocky"
PULSE SEQUENCE
Pulse 33.4 degrees
Acq. time 3.288 sec
Width 10000.0 Hz
32 repetitions
OBSERVE H1, 500.2312741 MHz
DATA PROCESSING
FT size 131072
Total time 1 minutes
OH
O
N
O
S
N
O
O
ppm
9
8
7
6
5
4
3

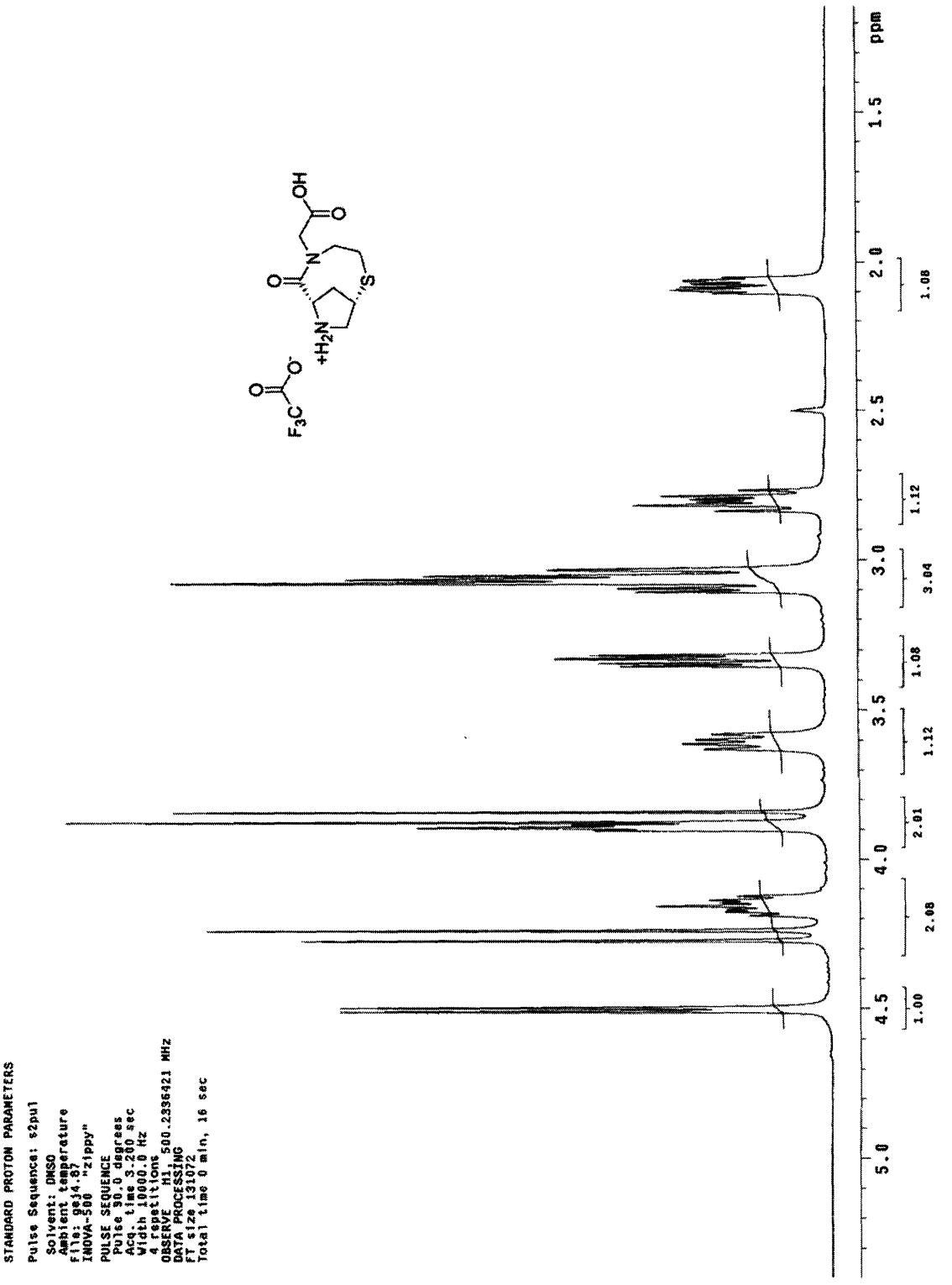
STANDARD PROTON PARAMETERS
Pulse Sequence: s2pul
Solvent: DMSO
Ambient temperature
File: ge34.87
INOVA-500 "zippy"
PULSE SEQUENCE
Pulse 30.0 degrees
Acq. time 3.200 sec
Width 10000.0 Hz
4 repetitions
OBSERVE H1, 500.2336421 MHz
DATA PROCESSING
FT size 131072
Total time 0 min, 16 sec
5.0
4.5
4.0
3.5
3.0
2.5
2.0
1.5
ppm
1.00
2.08
2.01
1.12
1.08
3.04
1.12
1.08

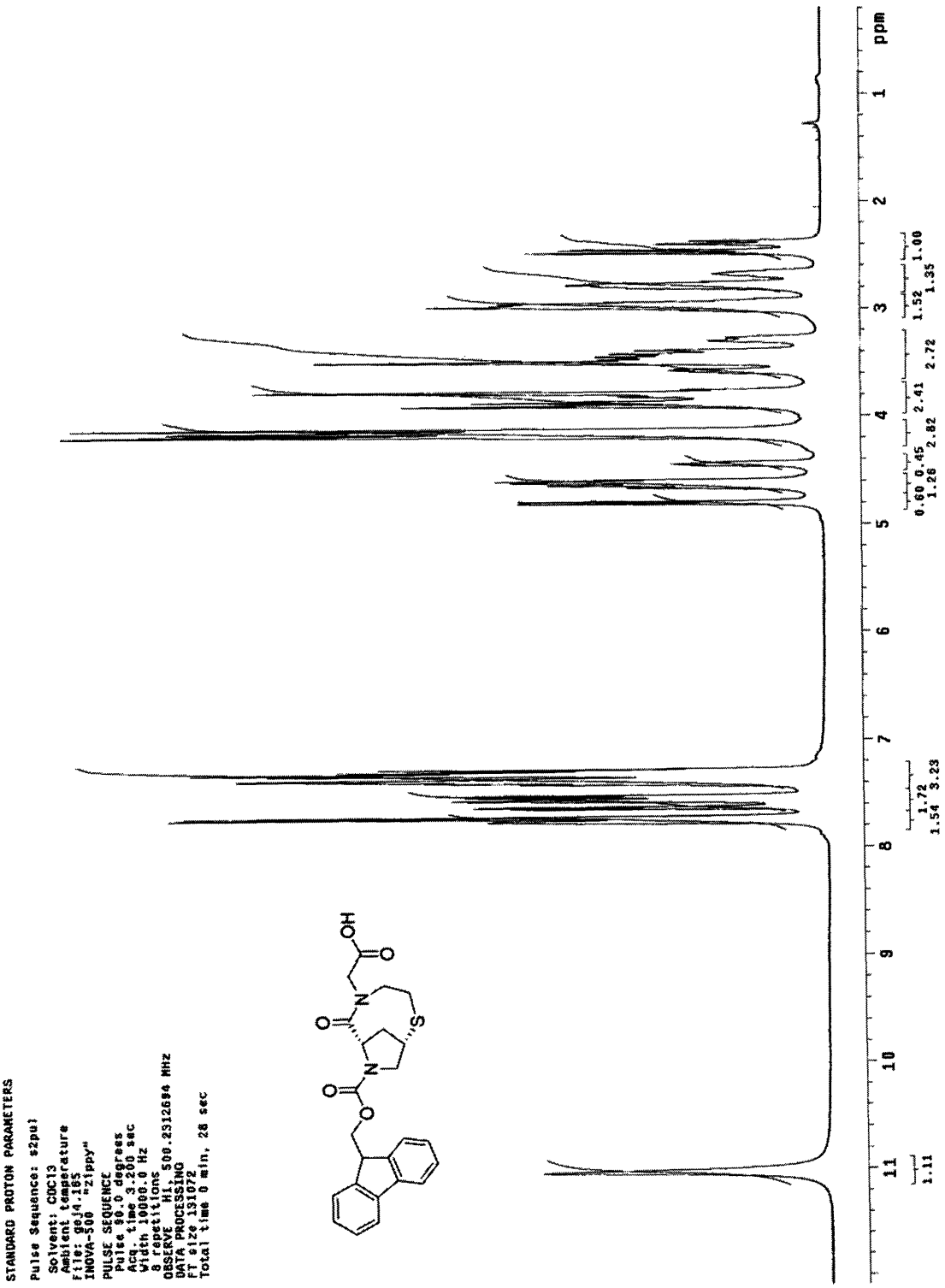
STANDARD PROTON PARAMETERS
Pulse Sequence: s2pul
Solvent: CDCl3
Ambient temperature
File: gej4.185
INOVA-500 "zippy"
PULSE SEQUENCE
Pulse 90.0 degrees
Acq. time 3.200 sec
Width 10000.0 Hz
8 repetitions
OBSERVE H1, 500.2312694 MHz
DATA PROCESSING
FT size 131072
Total time 0 min, 28 sec
OH
O
N
O
N
O
O
S
ppm
1
2
3
4
5
6
7
8
9
10
11
1.11
1.72
1.54
3.23
0.60
0.45
1.28
2.82
2.41
2.72
1.52
1.35
1.00

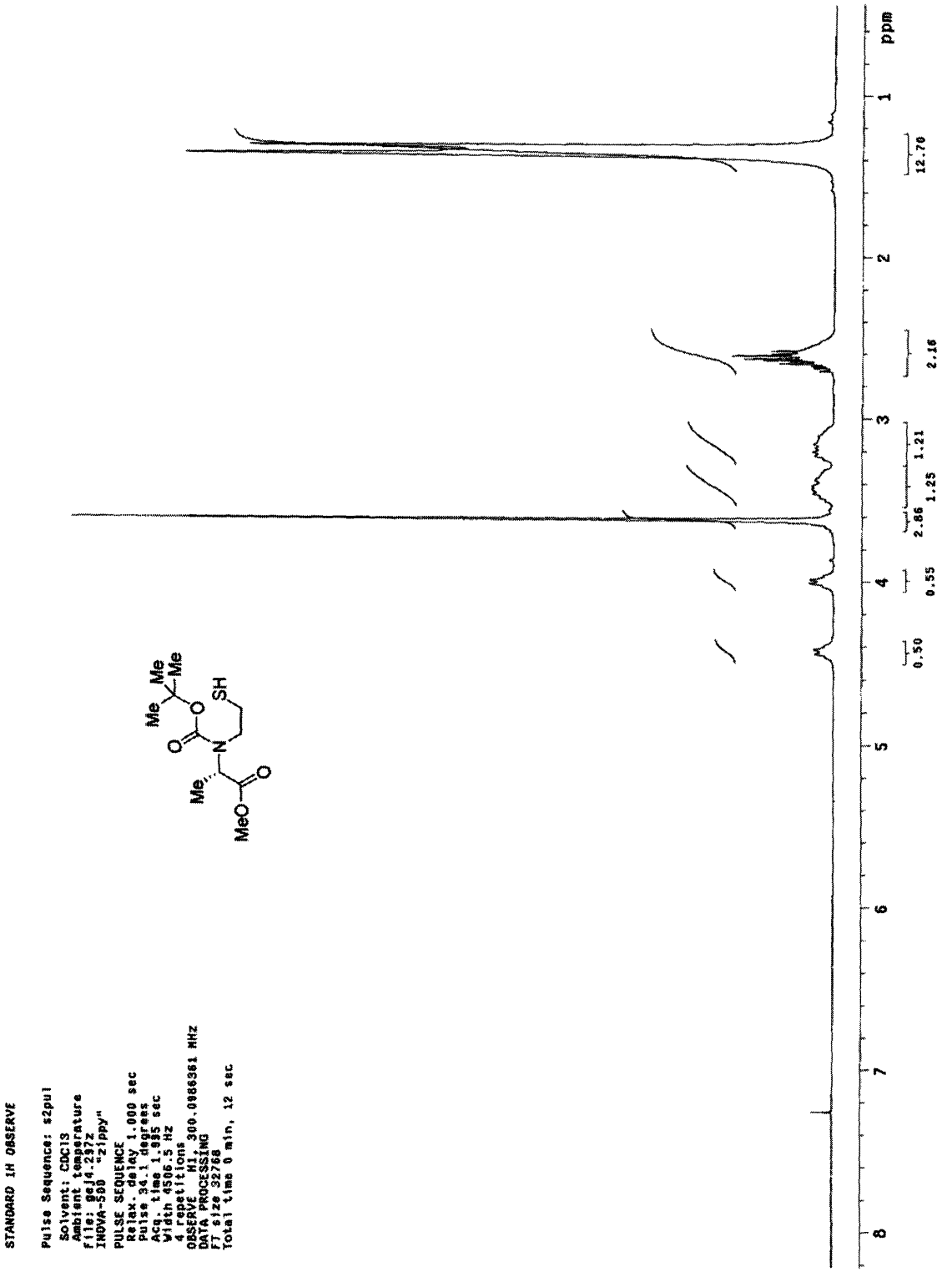
STANDARD 1H OBSERVE
Pulse Sequence: s2pul
Solvent: CDCl3
Ambient temperature
File: gej4.237z
INOVA-500 "zippy"
PULSE SEQUENCE
Relax. delay 1.000 sec
Pulse 34.1 degrees
Acq. time 1.995 sec
Width 4506.5 Hz
4 repetitions
OBSERVE H1, 300.0866361 MHz
DATA PROCESSING
FT size 32768
Total time 0 min, 12 sec
Me
Me
Me
O
O
SH
N
Me
O
MeO
O
ppm
1
2
3
4
5
6
7
8
0.50
0.55
2.86
1.25
1.21
2.16
12.70

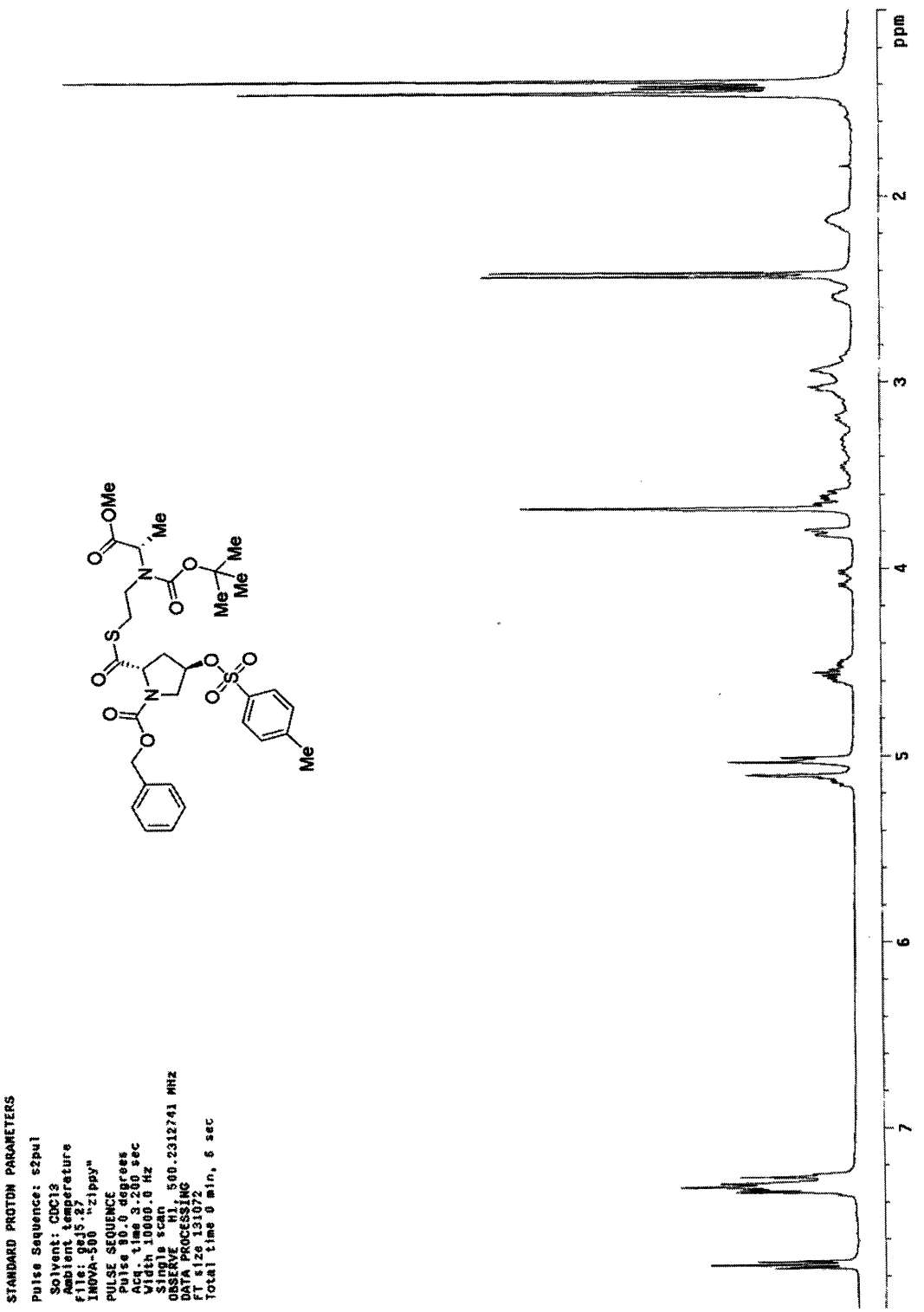
STANDARD PROTON PARAMETERS
Pulse Sequence: s2pul
Solvent: CDCl3
Ambient temperature
File: gmi5-27
INOVA-500 "zippy"
PULSE SEQUENCE
Pulse 90.0 degrees
Acq. time 3.280 sec
Width 10000.0 Hz
Single scan
OBSERVE H1, 500.2312741 MHz
DATA PROCESSING
FT size 131072
Total time 0 min, 6 sec
OMe
Me
Me
Me
Me
Me
ppm
7
6
5
4
3
2

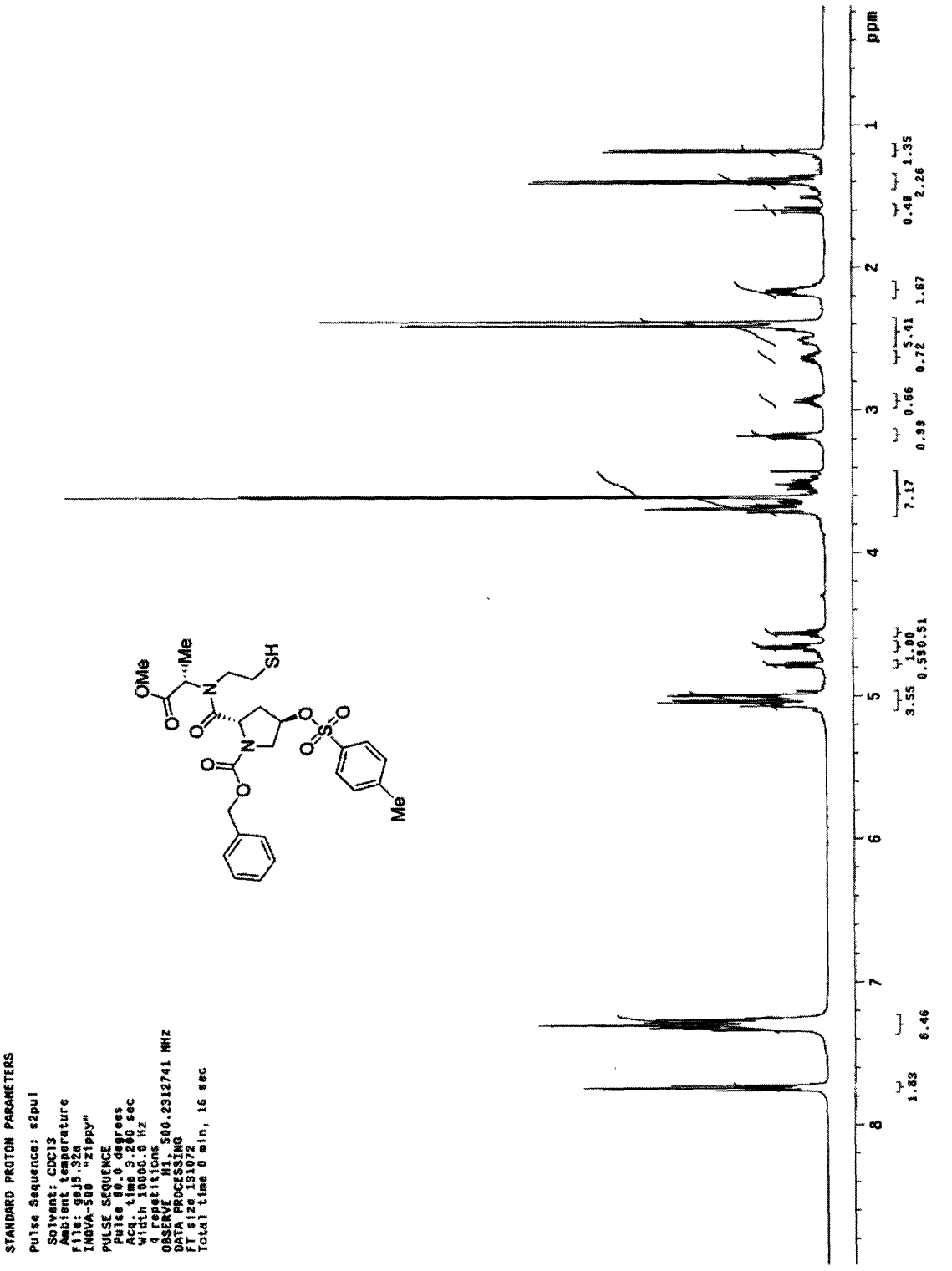
STANDARD PROTON PARAMETERS
Pulse Sequence: s2pul
Solvent: CDCl3
Ambient temperature
File: gmj5-32a
INOVA-500 "zippy"
PULSE SEQUENCE
Pulse 90.0 degrees
Acq. time 3.200 sec
Width 10000.0 Hz
4 repetitions
OBSERVE H1, 500.2312741 MHz
DATA PROCESSING
FT size 131072
Total time 0 min, 16 sec
OMe
Me
N
SH
O
S
Me
ppm
1.83
6.46
3.55
1.00
0.590.51
7.17
0.39
0.66
0.72
5.41
1.67
0.49
2.26
1.35

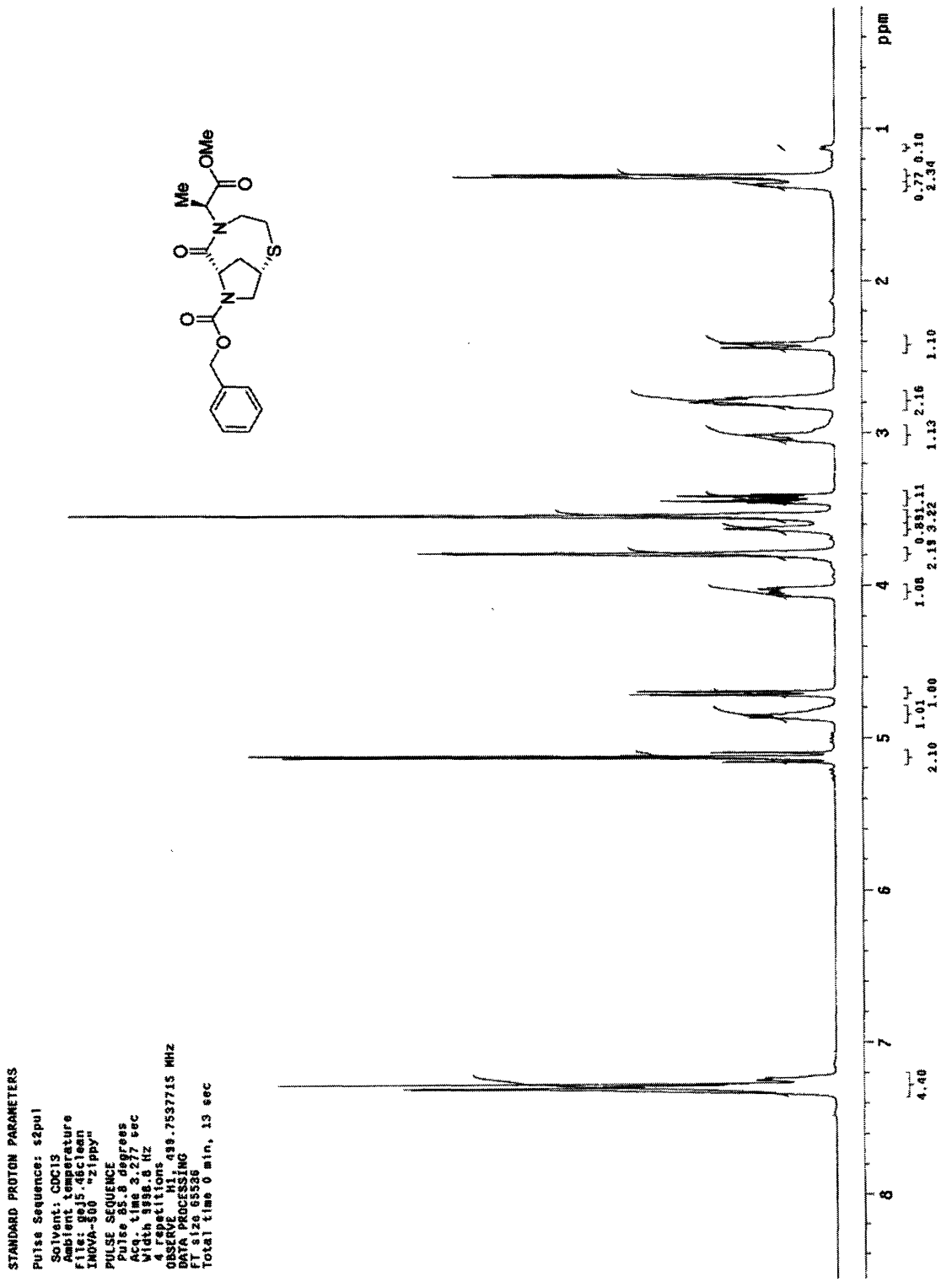
STANDARD PROTON PARAMETERS
Pulse Sequence: s2pul
Solvent: CDCl3
Ambient temperature
File: mj5-46clean
INOVA-500 "zippy"
PULSE SEQUENCE
Pulse 85.8 degrees
Acq. time 3.277 sec
Width 3998.8 Hz
4 repetitions
OBSERVE H1, 499.7537715 MHz
DATA PROCESSING
FT size 65536
Total time 0 min, 13 sec
Me
OMe
O
N
S
ppm
4.48
2.10 1.01 1.00
1.08 0.851.11
2.19 3.22
1.13 2.16
1.10
0.77 0.10
2.34

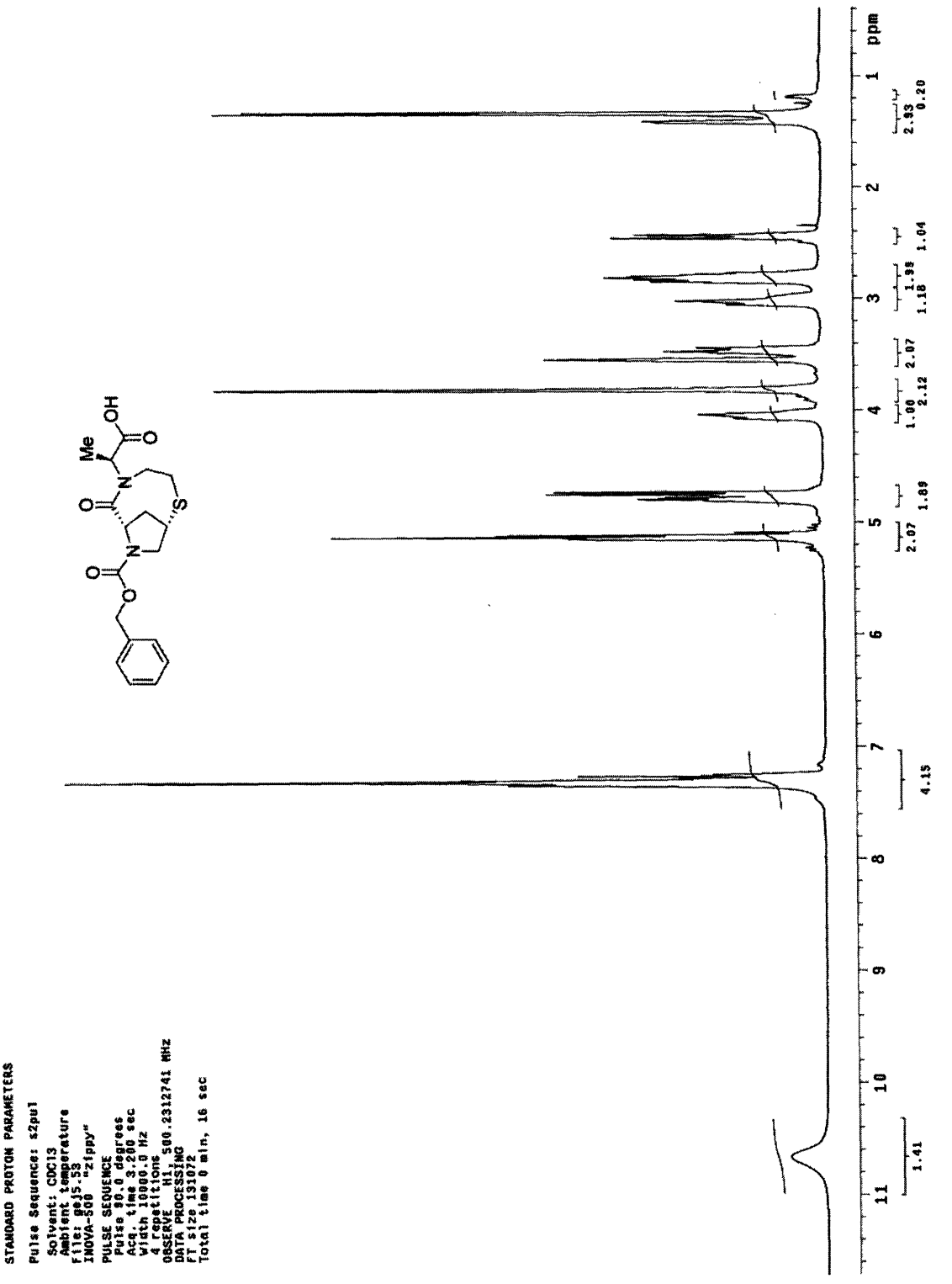
STANDARD PROTON PARAMETERS
Pulse Sequence: s2pul
Solvent: CDCl3
Ambient temperature
File: gdj5-53
INOVA-500 "z1ppy"
PULSE SEQUENCE
Pulse 90.0 degrees
Acq. time 3.200 sec
Width 10000.0 Hz
4 repetitions
OBSERVE H1, 500.2312741 MHz
DATA PROCESSING
FT size 131072
Total time 0 min, 16 sec
Me
OH
O
N
S
ppm
1.41
4.15
2.07
1.89
1.00
2.12
2.07
1.18
1.98
1.04
2.83
0.20

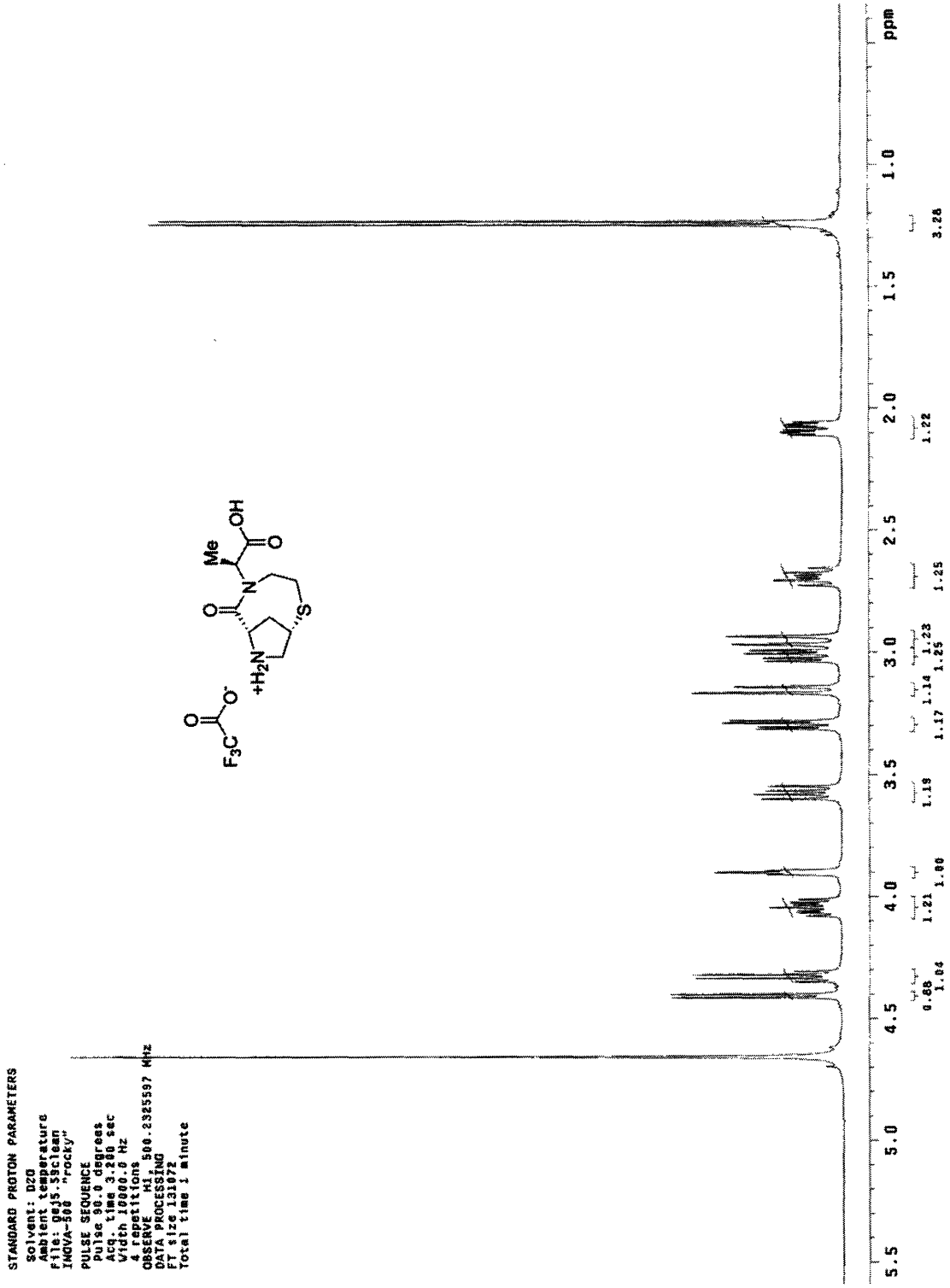
STANDARD PROTON PARAMETERS
Solvent: D20
Ambient temperature
File: gb35.5%clean
INOVA-500 "rocky"
PULSE SEQUENCE
Pulse 90.0 degrees
Acq. time 3.280 sec
Width 10000.0 Hz
4 repetitions
OBSERVE H1, 500.2325597 MHz
DATA PROCESSING
FT size 131072
Total time 1 minute
Me
OH
O
N
O
S
+H2N
O
O-
F3C
ppm
5.5
5.0
4.5
4.0
3.5
3.0
2.5
2.0
1.5
1.0
0.88
1.04
1.21
1.80
1.19
1.17
1.14
1.25
1.23
1.25
1.25
1.22
3.26

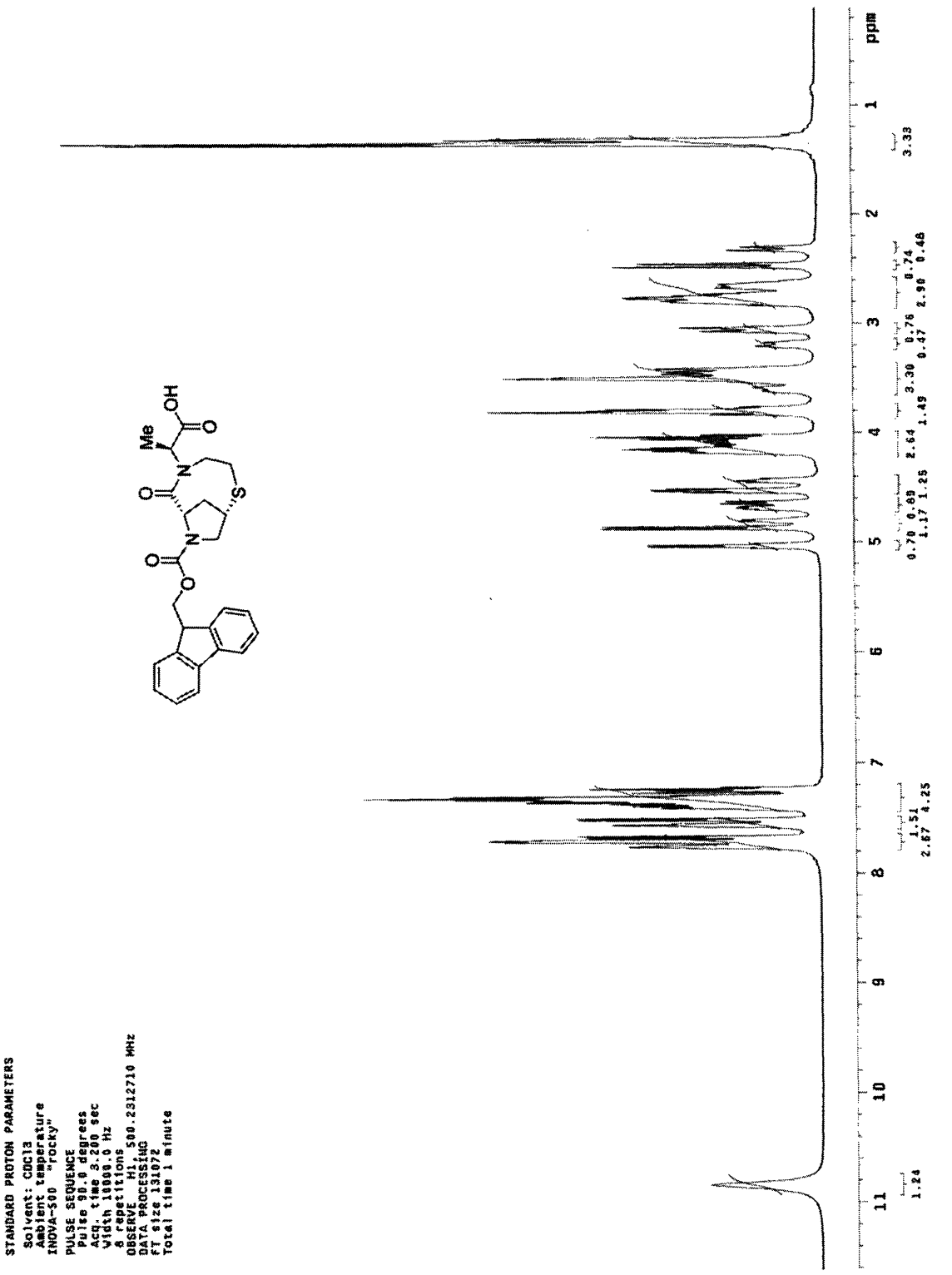
STANDARD PROTON PARAMETERS
Solvent: CDCl3
Ambient temperature
INOVA-500 "rocky"
PULSE SEQUENCE
Pulse 90.0 degrees
Acq. time 3.200 sec
Width 10000.0 Hz
8 repetitions
OBSERVE H1, 500.2312710 MHz
DATA PROCESSING
FT size 131072
Total time 1 minute
Me
OH
O
N
S
ppm
1.24
1.51
2.67 4.25
0.70 0.69
1.17 1.25
2.64
1.49
3.30
0.47
0.76
2.90
0.74
0.48
3.33

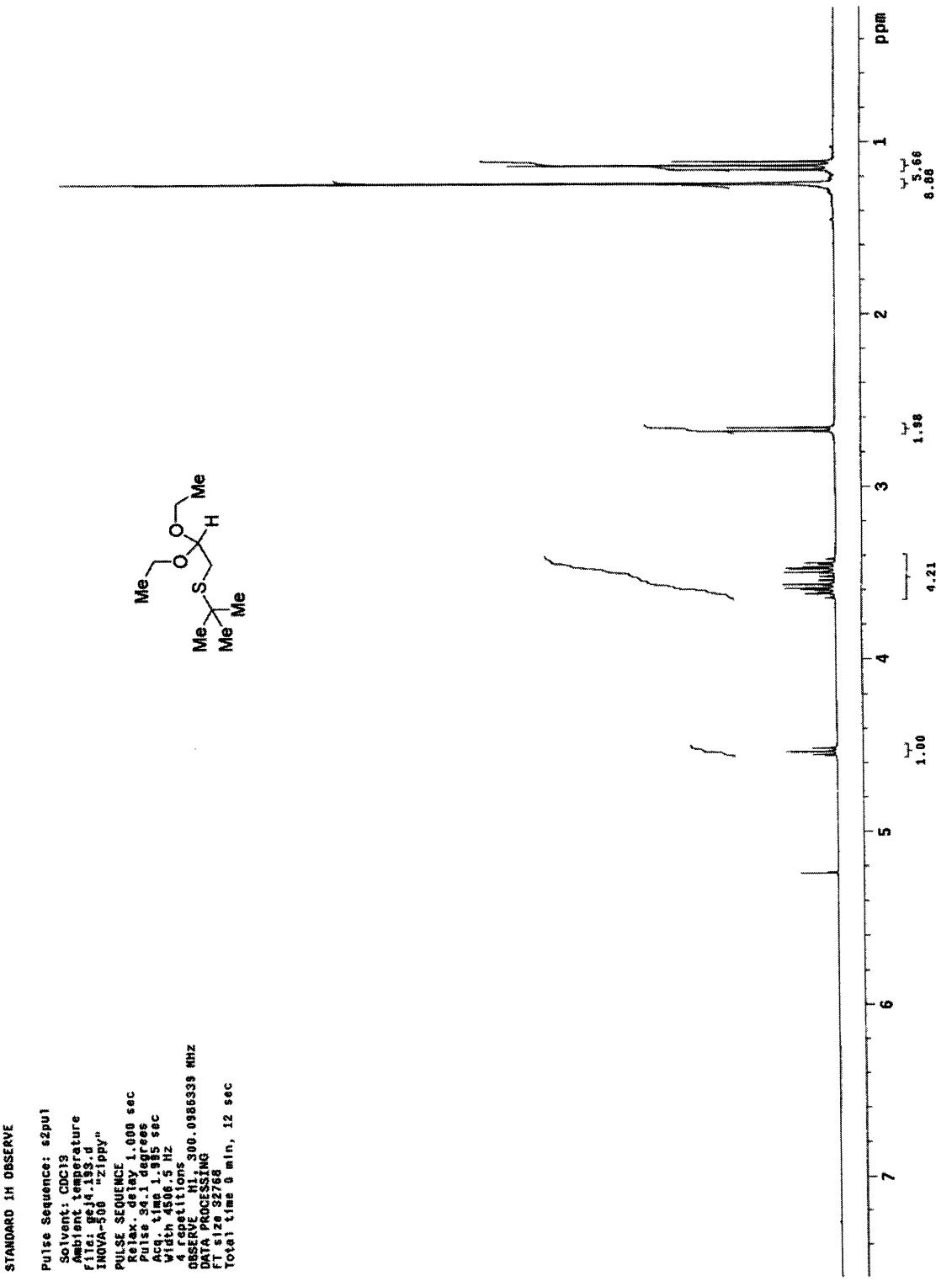
STANDARD 1H OBSERVE
Pulse Sequence: s2pul
Solvent: CDCl3
Ambient temperature
File: gej4.153.d
INOVA-500 "zippy"
PULSE SEQUENCE
Relax. delay 1.000 sec
Pulse 34.1 degrees
Acq. time 1.985 sec
Width 4506.5 Hz
4 repetitions
OBSERVE H1, 300.0986339 MHz
DATA PROCESSING
FT size 32768
Total time 0 min, 12 sec
Me
Me
O
O
H
S
Me
Me
Me
Me
ppm
1
2
3
4
5
6
7
1.00
4.21
1.98
5.66
8.88

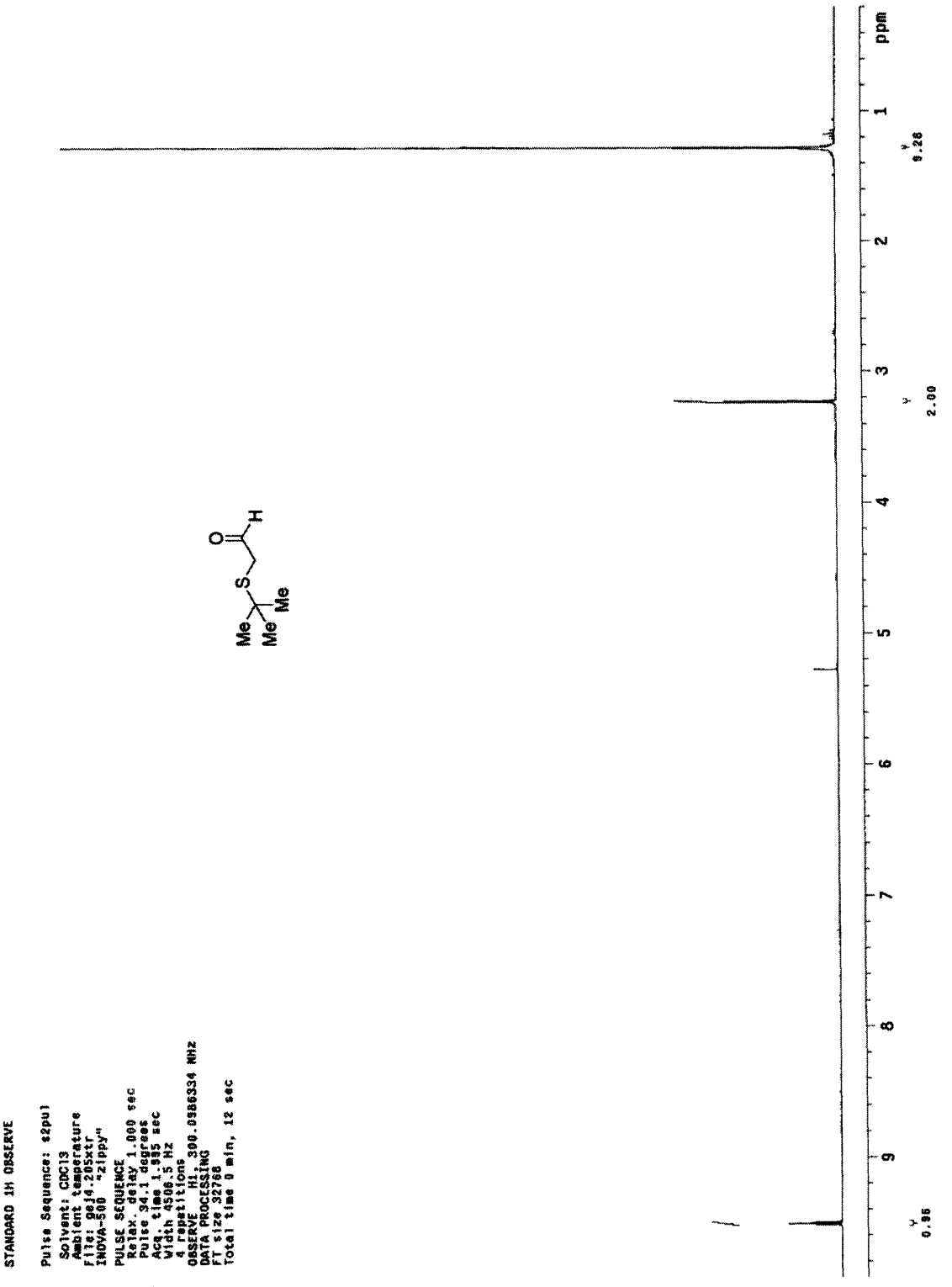
STANDARD 1H OBSERVE
Pulse Sequence: s2pul
Solvent: CDCl3
Ambient temperature
File: gmj4-205xtr
INOVA-500 "zippy"
PULSE SEQUENCE
Relax. delay 1.000 sec
Pulse 34.1 degrees
Acq. time 1.995 sec
Width 4508.5 Hz
4 repetitions
OBSERVE H1, 300.0386334 MHz
DATA PROCESSING
FT size 32768
Total time 0 min, 12 sec
O
H
S
Me
Me
Me
ppm
9.26
2.00
0.96

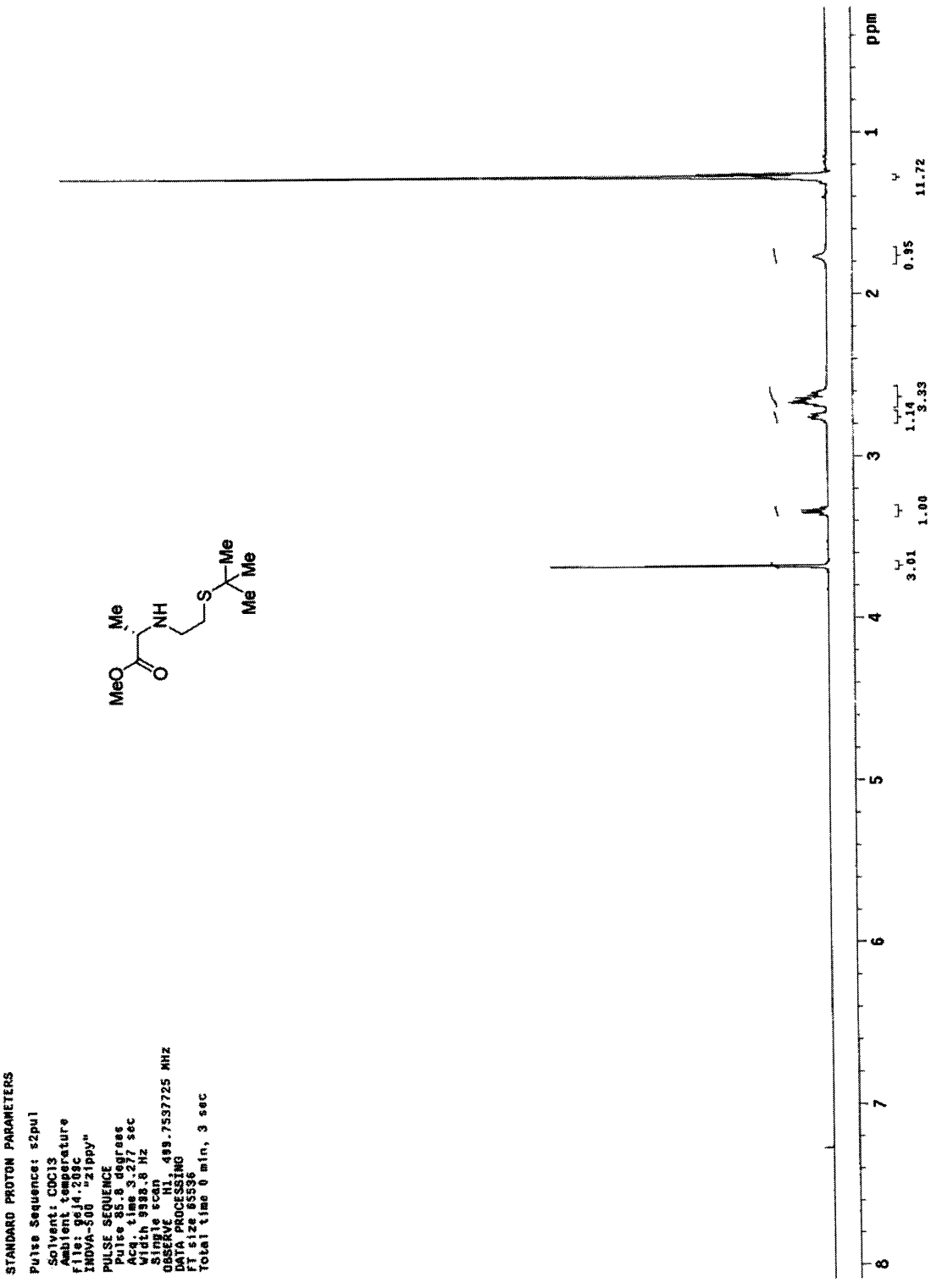
STANDARD PROTON PARAMETERS
Pulse Sequence: s2pul
Solvent: CDCl3
Ambient temperature
File: gsj4.fid
INOVA-500 "21ppy"
PULSE SEQUENCE
Pulse 85.8 degrees
Acq. time 3.277 sec
Width 9938.8 Hz
Single scan
OBSERVE H1, 499.7537725 MHz
DATA PROCESSING
FT size 65536
Total time 0 min, 3 sec
MeO
Me
NH
S
Me
Me
Me
ppm
3.01
1.00
1.14
3.33
0.95
11.72

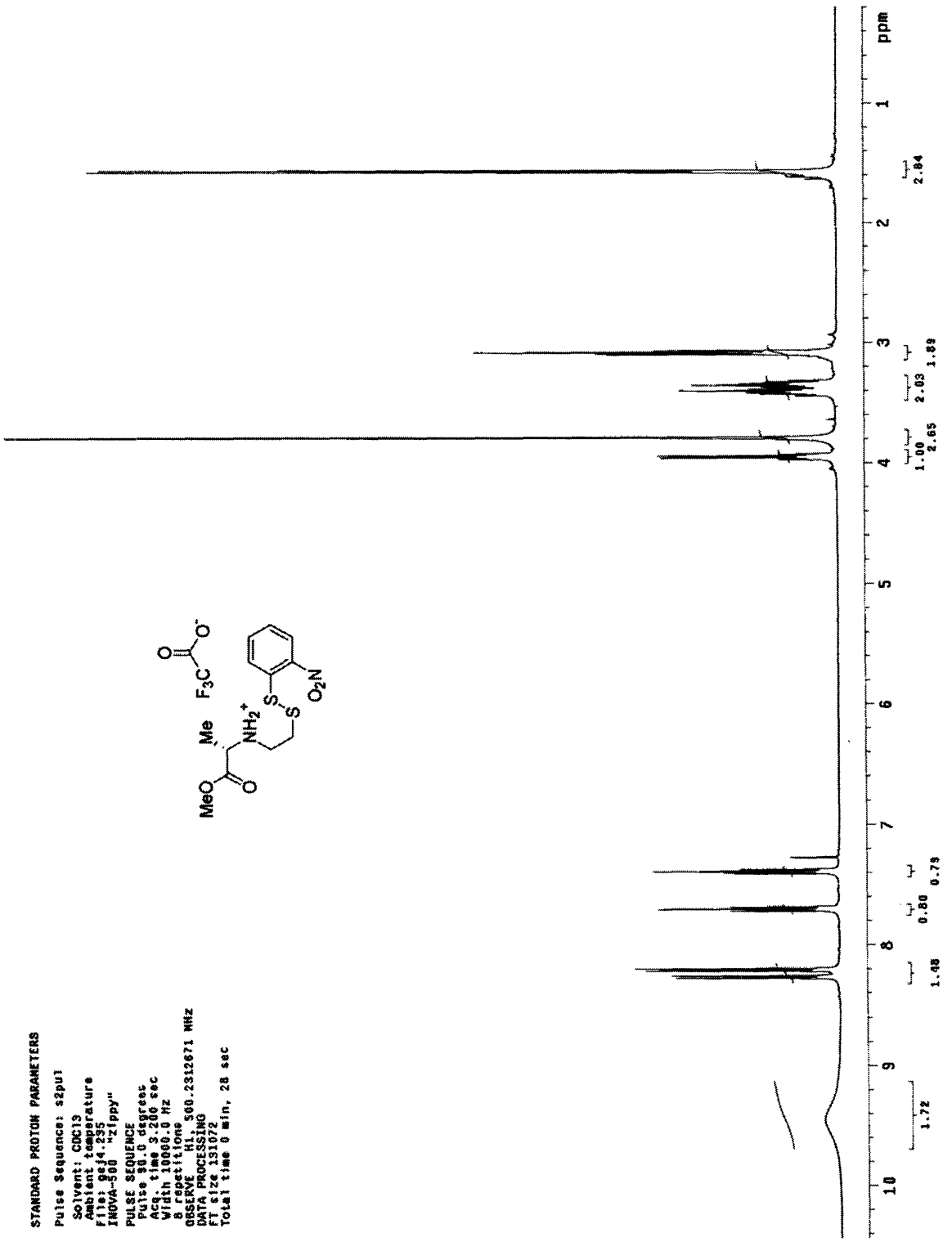
STANDARD PROTON PARAMETERS
Pulse Sequence: s2pul
Solvent: CDCl3
Ambient temperature
File: gaj4.295
INOVA-500 "zippy"
PULSE SEQUENCE
Pulse 30.0 degrees
Acq. time 3.200 sec
Width 10000.0 Hz
8 repetitions
OBSERVE H1, 500.2312671 MHz
DATA PROCESSING
FT size 131072
Total time 0 min, 28 sec
MeO
Me
F3C
NH2+
S
S
O2N
ppm
1.00
2.65
2.03
1.89
2.84
1.48
0.80
0.79
1.72

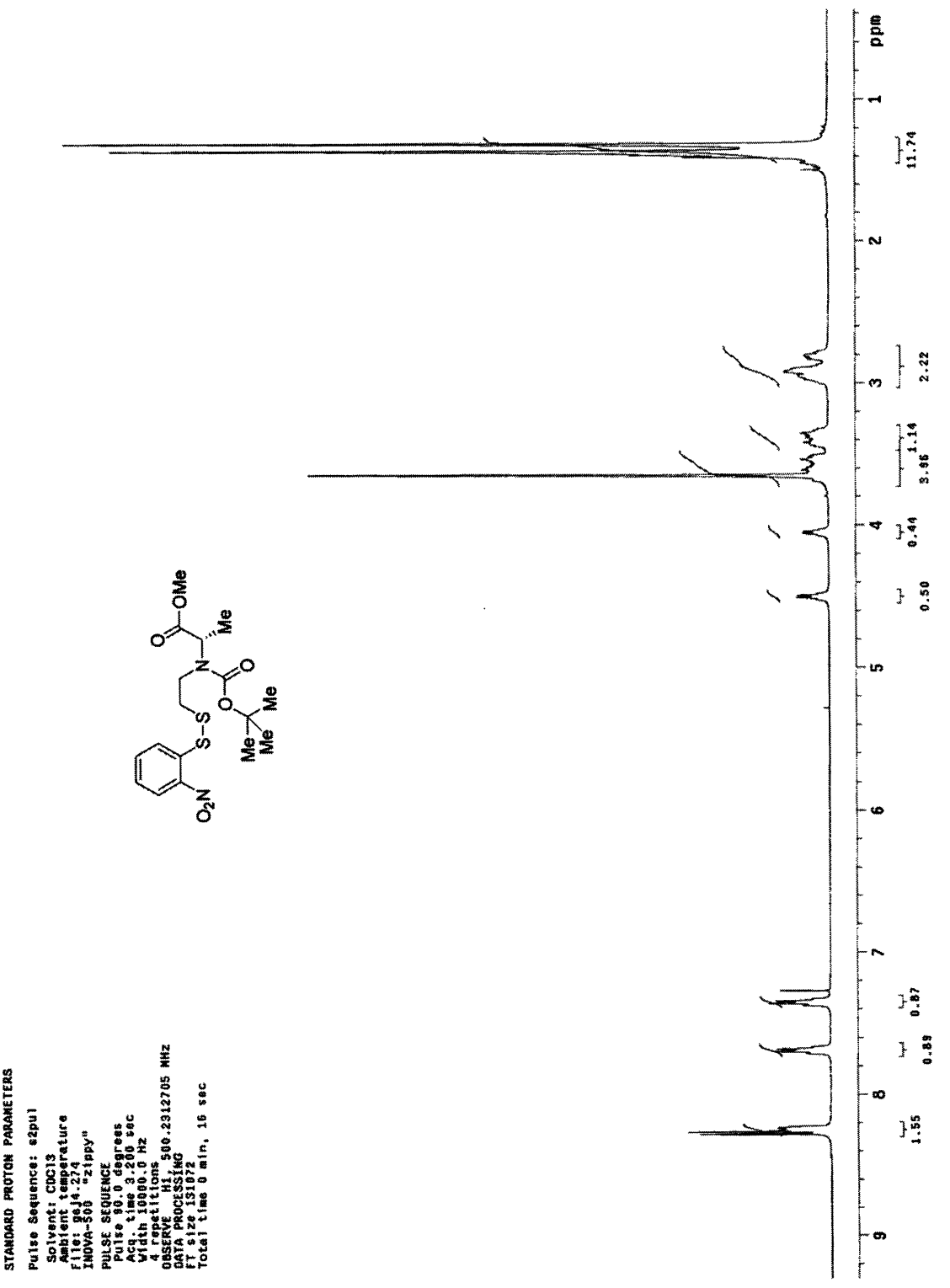
STANDARD PROTON PARAMETERS
Pulse Sequence: s2pul
Solvent: CDCl3
Ambient temperature
File: gaj4.274
INOVA-500 "zippy"
PULSE SEQUENCE
Pulse 90.0 degrees
Acq. time 3.200 sec
Width 10860.6 Hz
4 repetitions
OBSERVE H1, 500.2312705 MHz
DATA PROCESSING
FT size 131072
Total time 0 min, 16 sec
OMe
Me
N
O
O
S
S
Me
Me
Me
O2N
ppm
1.55
0.89
0.87
7
8
9
6
5
0.50
4
0.44
3.96
1.14
3
2.22
2
11.74
1

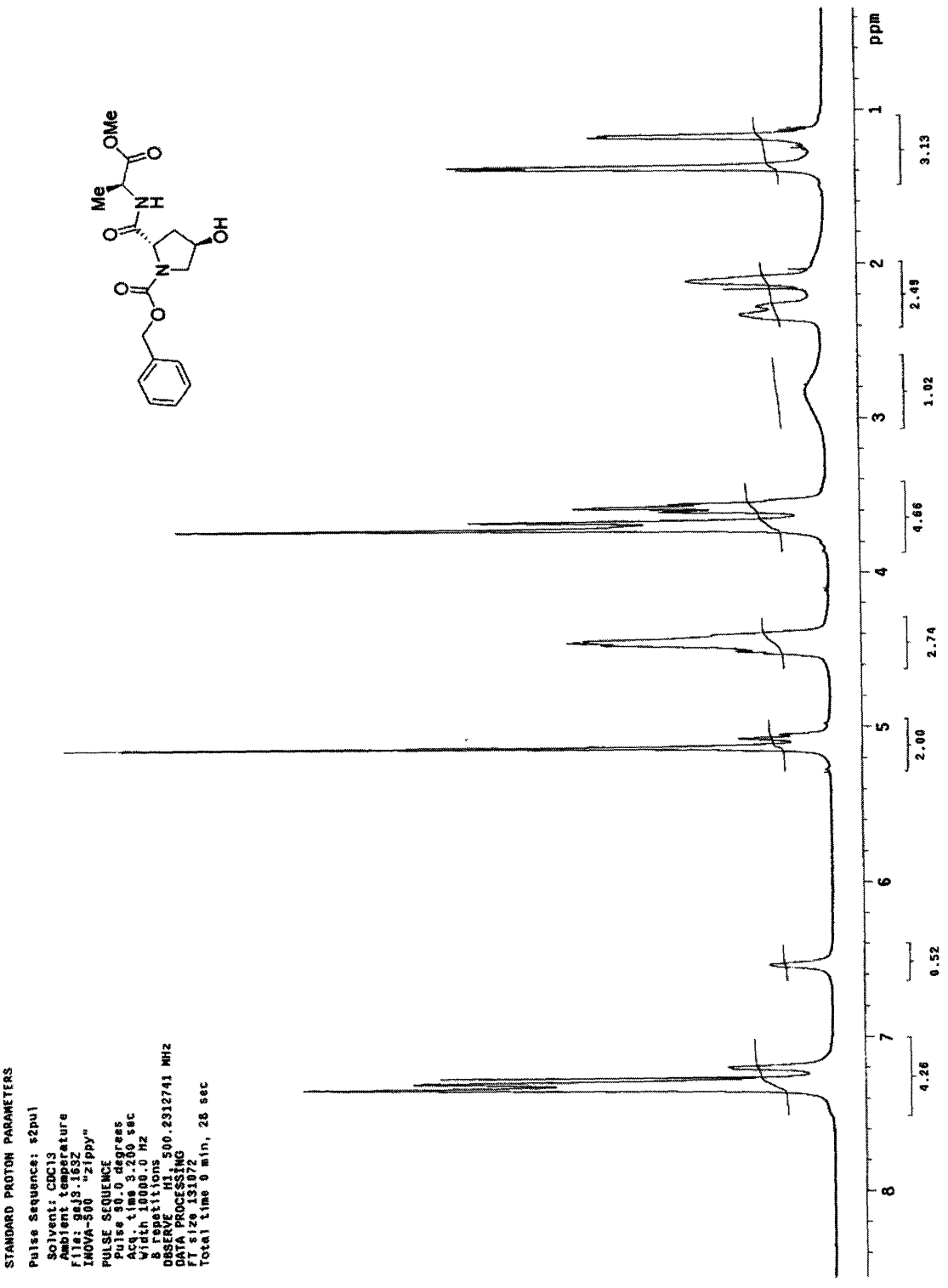
STANDARD PROTON PARAMETERS
Pulse Sequence: s2pul
Solvent: CDCl3
Ambient temperature
File: gdj3.163Z
INOVA-500 "zippy"
PULSE SEQUENCE
Pulse 30.0 degrees
Acq. time 3.200 sec
Width 10000.0 Hz
8 repetitions
OBSERVE H1, 500.2312741 MHz
DATA PROCESSING
FT size 131072
Total time 0 min, 28 sec
Me
OMe
N
H
O
OH
ppm
1
2
3
4
5
6
7
8
3.13
2.49
1.02
4.66
2.74
2.00
0.52
4.26

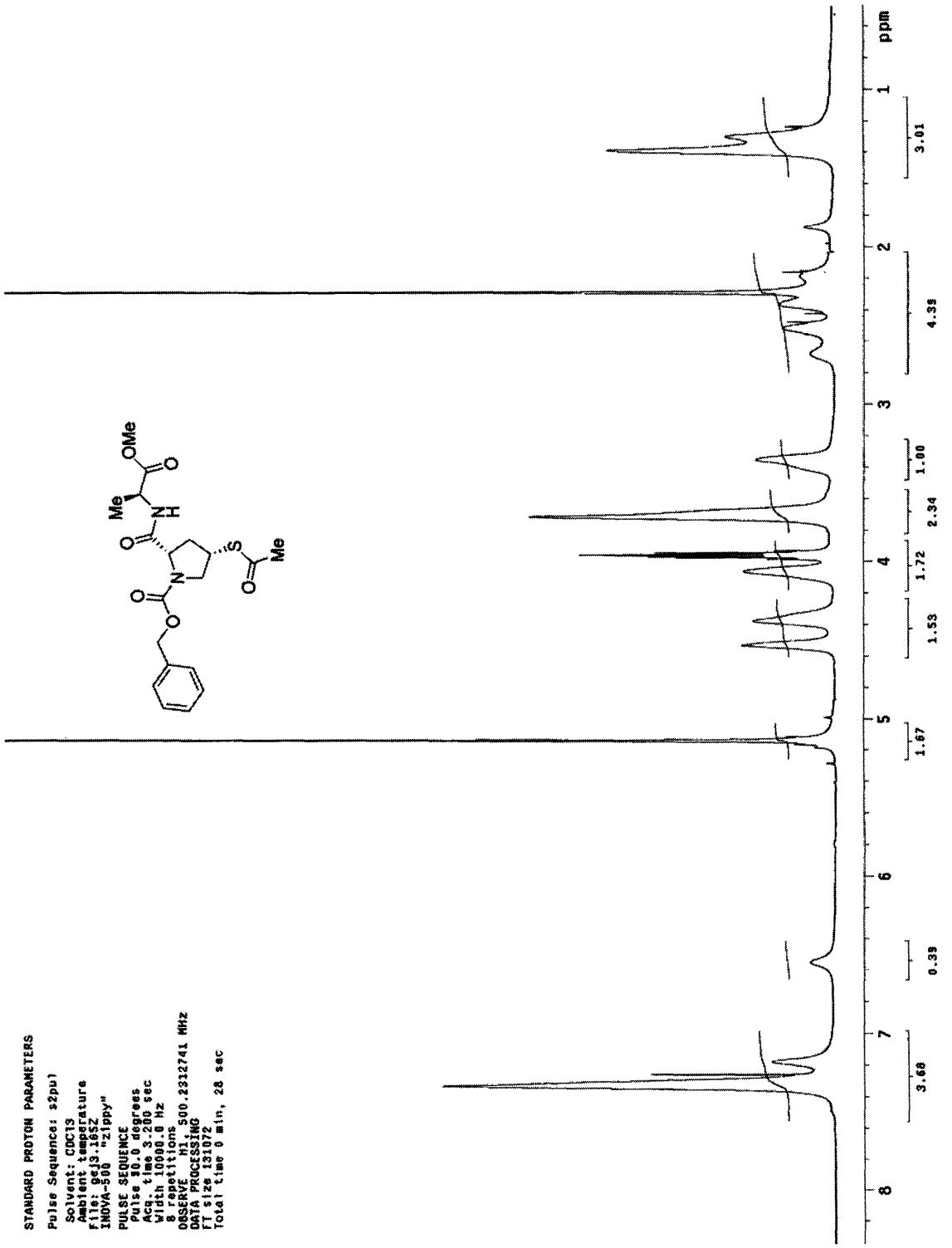
STANDARD PROTON PARAMETERS
Pulse Sequence: s2pul
Solvent: CDCl3
Ambient temperature
File: gej3.1652
INOVA-500 "21ppy"
PULSE SEQUENCE
Pulse 30.0 degrees
Acq. time 3.200 sec
Width 10000.0 Hz
8 repetitions
OBSERVE H1, 500.2312741 MHz
DATA PROCESSING
FT size 131072
Total time 0 min, 28 sec
OMe
Me
N
H
O
O
N
S
Me
O
O
O
O
ppm
8
7
6
5
4
3
2
1
3.68
0.39
1.67
1.53
1.72
2.34
1.00
4.38
3.01

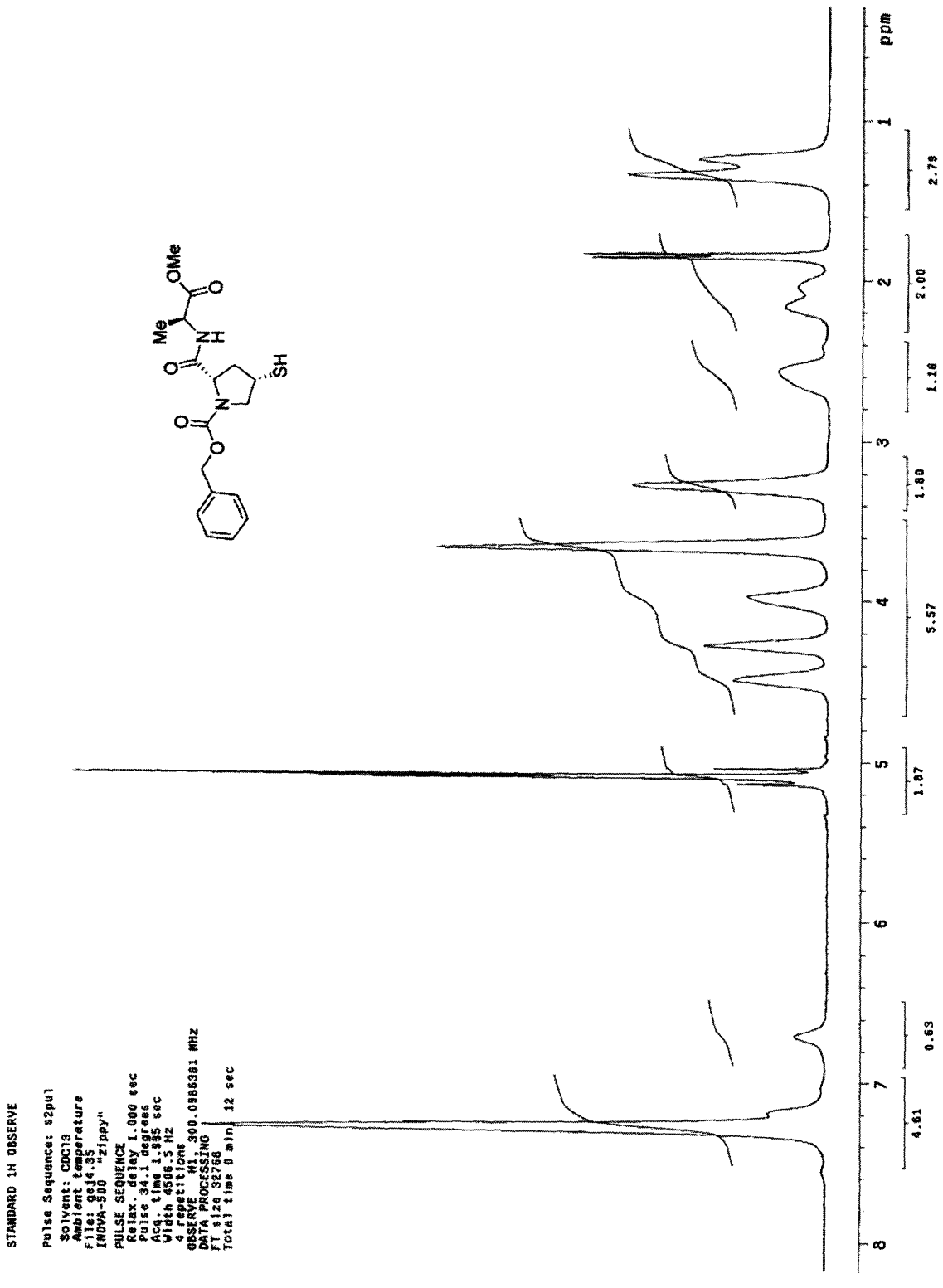
STANDARD 1H OBSERVE
Pulse Sequence: s2pul
Solvent: CDCl3
Ambient temperature
File: gdj4.35
INOVA-500 "zippy"
PULSE SEQUENCE
Relax. delay 1.000 sec
Pulse 34.1 degrees
Acq. time 1.955 sec
Width 4506.5 Hz
4 repetitions
OBSERVE H1, 300.0986361 MHz
DATA PROCESSING
FT size 32768
Total time 0 min 12 sec
Me
OMe
H
N
O
SH
ppm
4.61
0.63
1.87
5.57
1.80
1.16
2.00
2.79

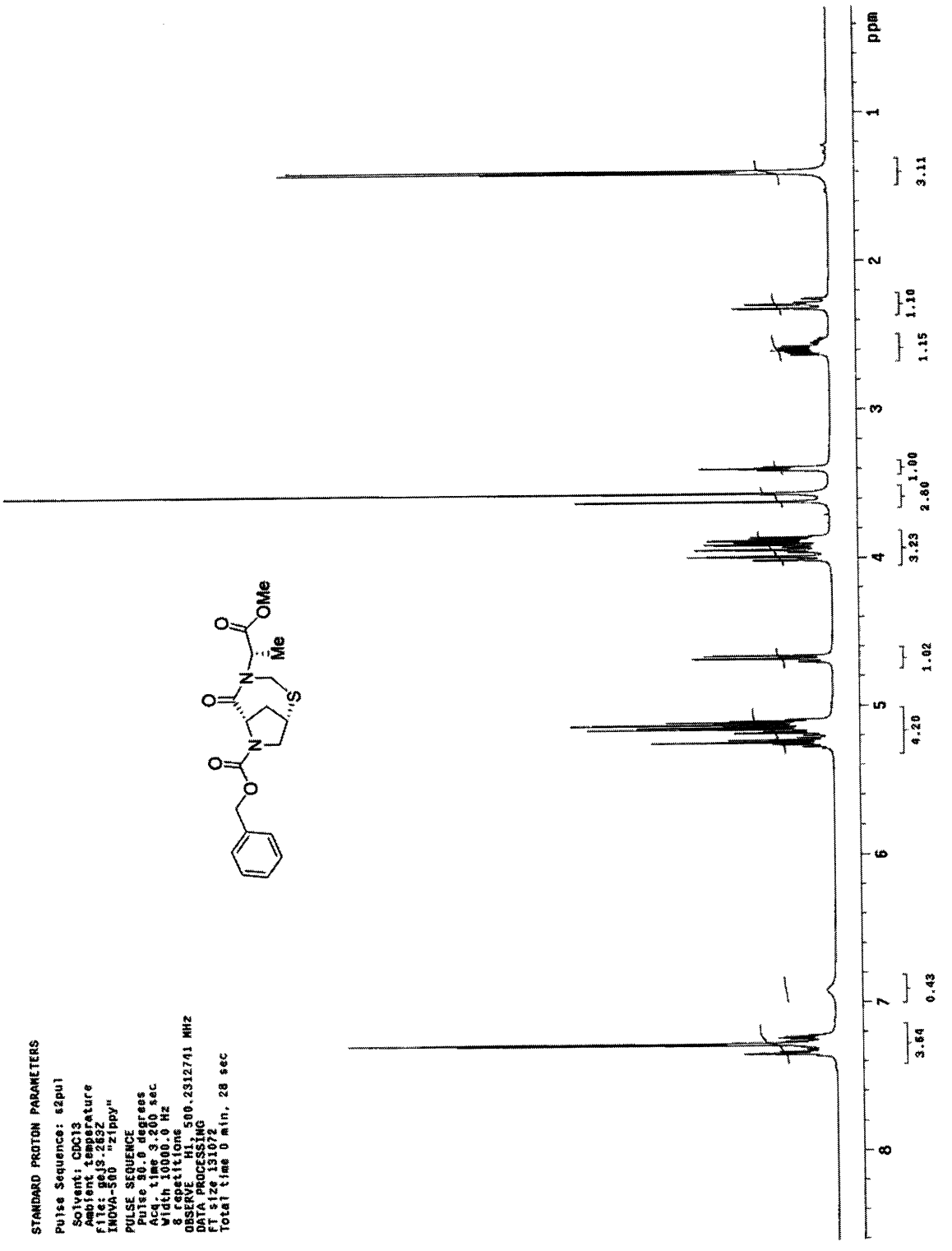
STANDARD PROTON PARAMETERS
Pulse Sequence: s2pul
Solvent: CDCl3
Ambient temperature
File: mej3-2832
INOVA-500 "zippy"
PULSE SEQUENCE
Pulse 30.0 degrees
Acq. time 3.200 sec
Width 10000.0 Hz
8 repetitions
OBSERVE H1, 500.2312741 MHz
DATA PROCESSING
FT size 131072
Total time 0 min, 28 sec
OMe
Me
S
ppm
1
2
3
4
5
6
7
8
3.11
1.10
1.15
1.00
2.80
3.23
1.02
4.20
0.43
3.64

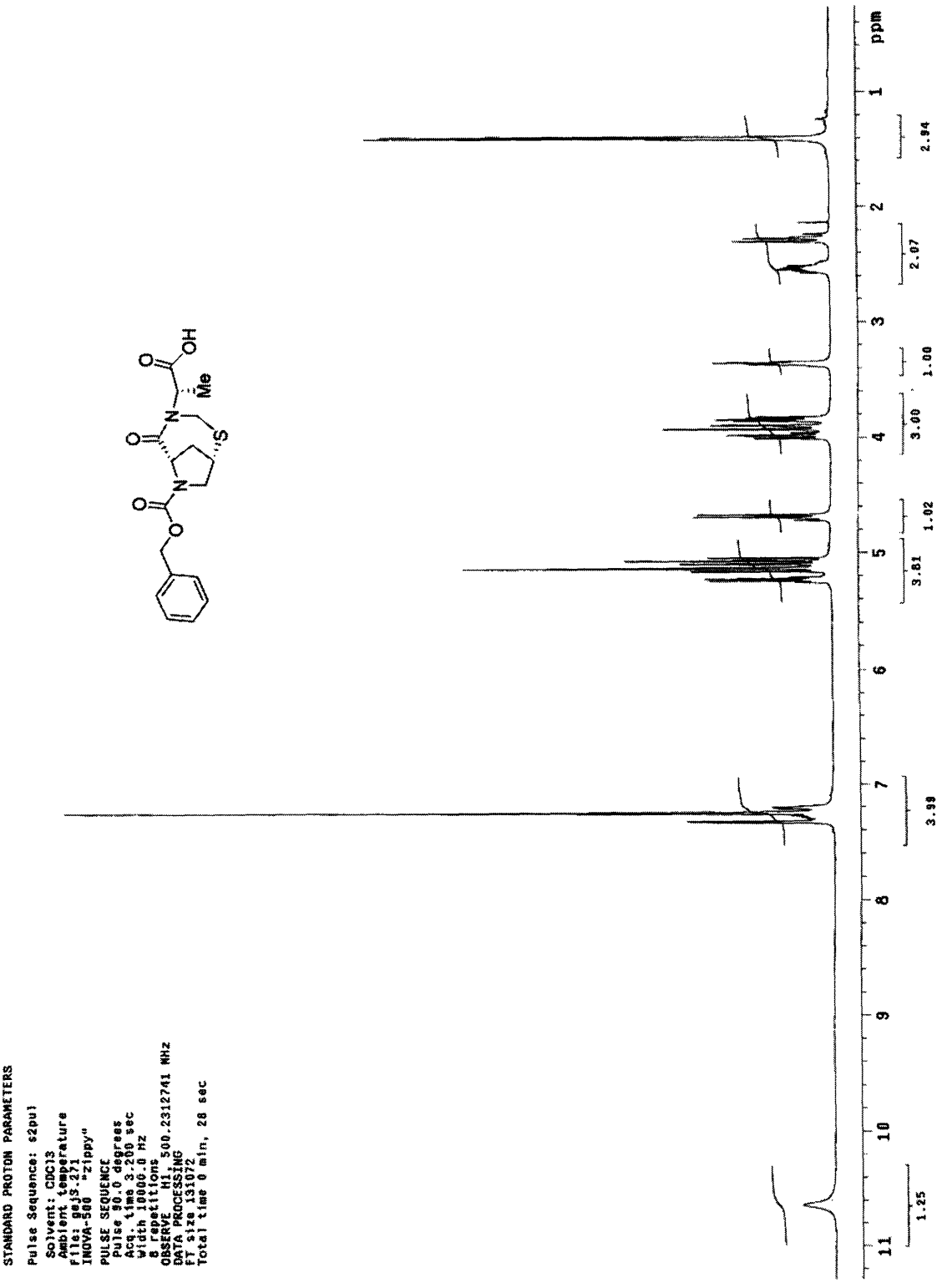
STANDARD PROTON PARAMETERS
Pulse Sequence: s2pul
Solvent: CDCl3
Ambient temperature
File: gejs.271
INOVA-500 "zippy"
PULSE SEQUENCE
Pulse 90.0 degrees
Acq. time 3.200 sec
width 10000.0 Hz
8 repetitions
OBSERVE H1, 500.2312741 MHz
DATA PROCESSING
FT size 131072
Total time 0 min, 28 sec
OH
O
Me
N
S
O
O
N
O
O
ppm
1
2
3
4
5
6
7
8
9
10
11
2.94
2.07
1.00
3.00
1.02
3.81
3.98
1.25

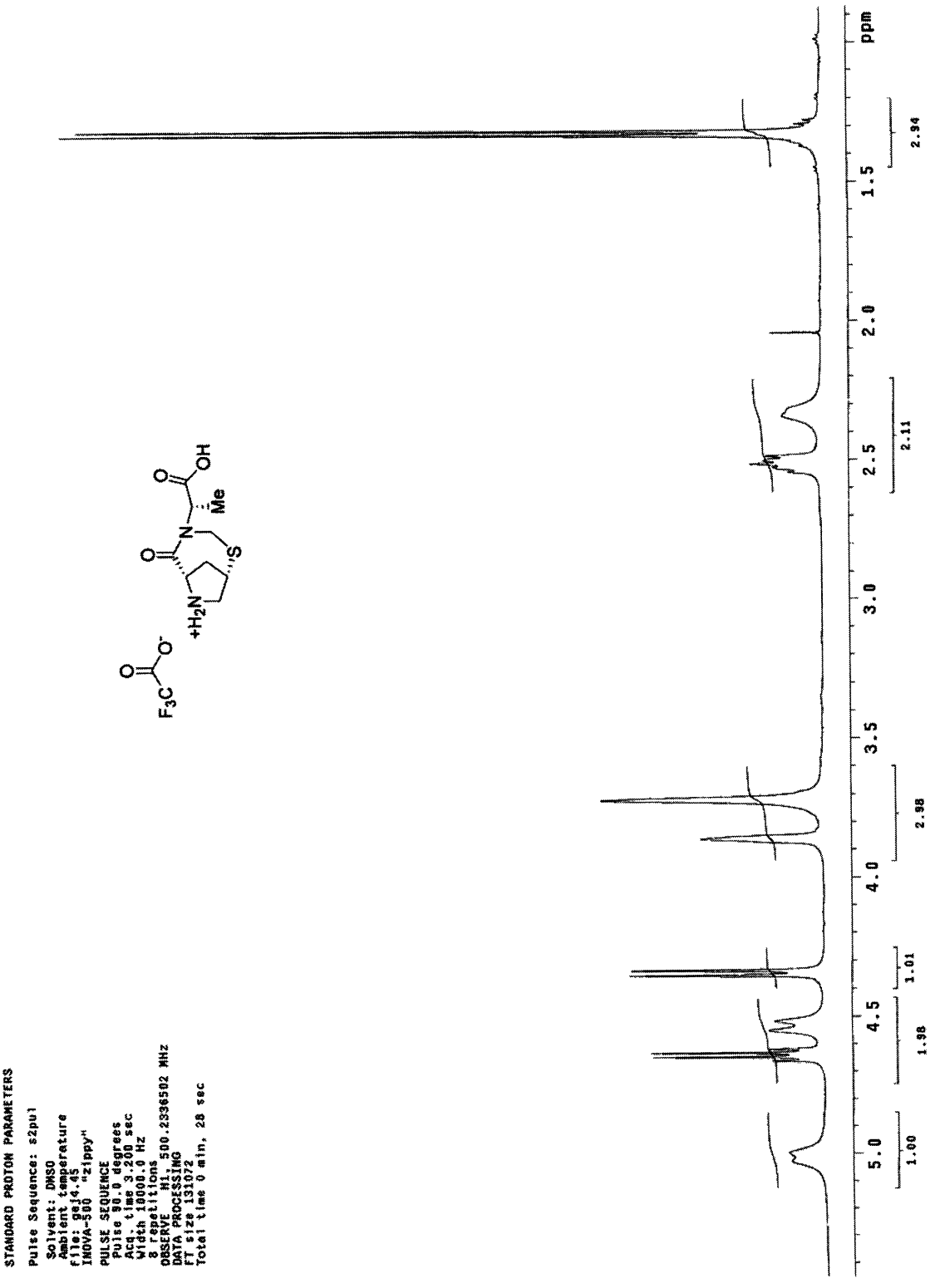
STANDARD PROTON PARAMETERS
Pulse Sequence: s2pul
Solvent: DMSO
Ambient temperature
File: ga14.45
INOVA-500 "zippy"
PULSE SEQUENCE
Pulse 90.0 degrees
Acq. time 3.200 sec
Width 10000.0 Hz
8 repetitions
OBSERVE H1, 500.2336502 MHz
DATA PROCESSING
FT size 131072
Total time 0 min, 28 sec
F3C
O
O-
+H2N
N
S
Me
OH
O
5.0
4.5
4.0
3.5
3.0
2.5
2.0
1.5
ppm
1.00
1.98
1.01
2.98
2.11
2.94

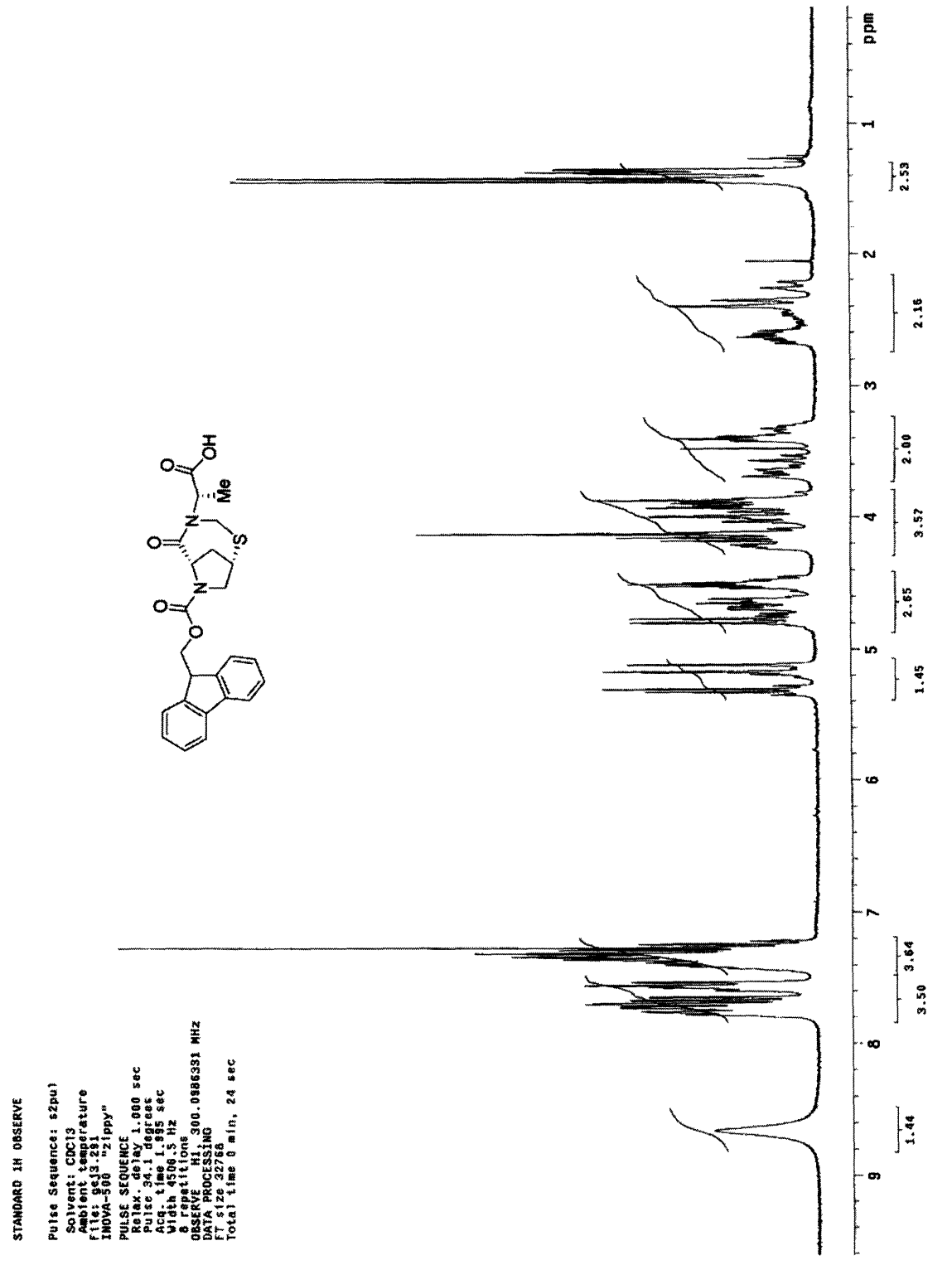
STANDARD 1H OBSERVE
Pulse Sequence: s2pul
Solvent: CDCl3
Ambient temperature
File: gej3.291
INOVA-500 "zippy"
PULSE SEQUENCE
Relax. delay 1.000 sec
Pulse 34.1 degrees
Acq. time 1.995 sec
Width 4506.5 Hz
8 repetitions
OBSERVE H1, 300.0886331 MHz
DATA PROCESSING
FT size 32768
Total time 0 min, 24 sec
OH
Me
S
ppm
1.44
3.50
3.64
1.45
2.65
3.57
2.00
2.16
2.53

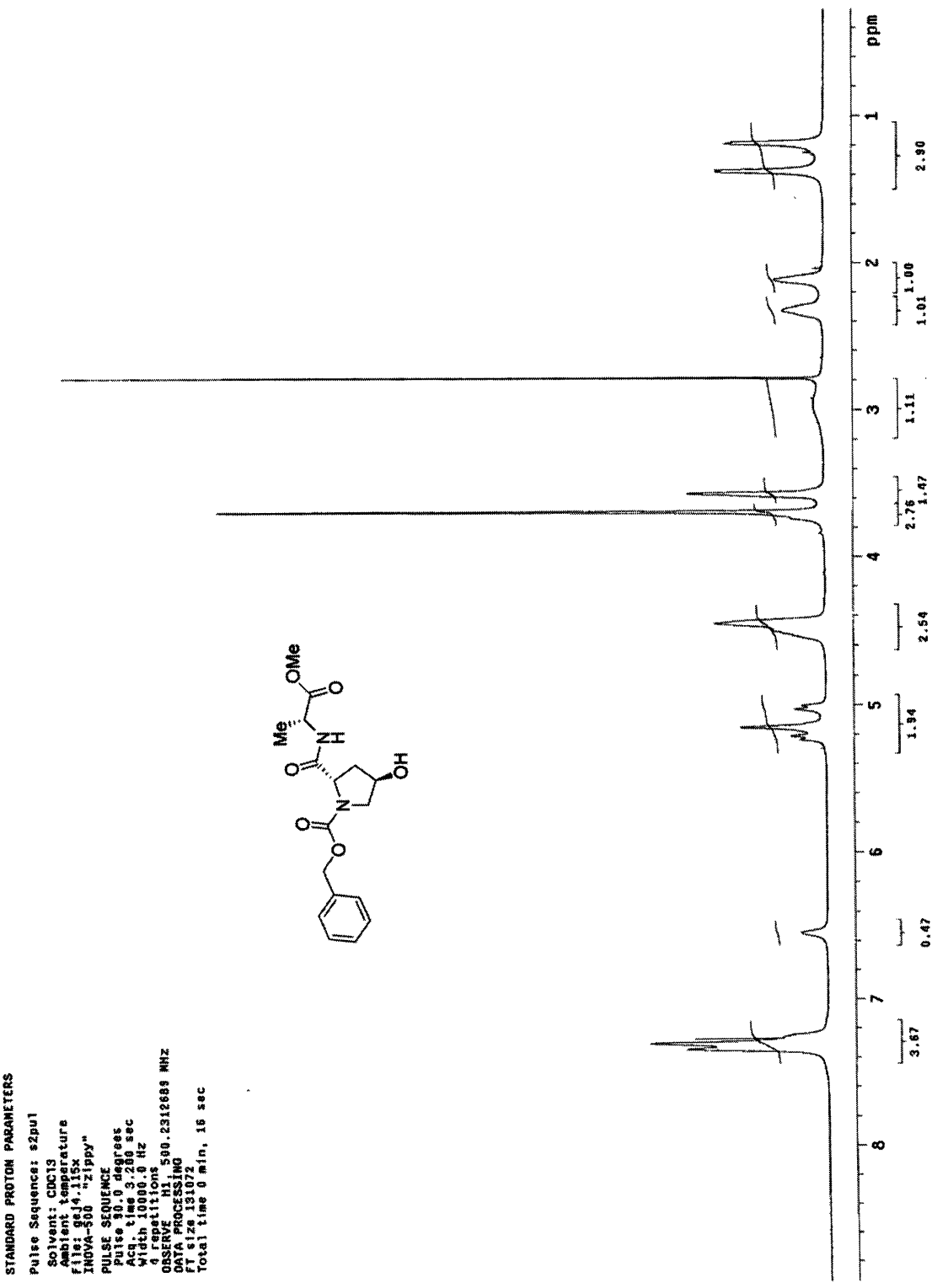
STANDARD PROTON PARAMETERS
Pulse Sequence: s2pul
Solvent: CDCl3
Ambient temperature
File: gej4.115x
INOVA-500 "zippy"
PULSE SEQUENCE
Pulse 90.0 degrees
Acq. time 3.280 sec
Width 10000.0 Hz
4 repetitions
OBSERVE H1, 500.2312689 MHz
DATA PROCESSING
FT size 131072
Total time 0 min, 16 sec
Me
OMe
OH
ppm
3.67
0.47
1.94
2.54
2.76
1.47
1.11
1.01
1.00
2.90

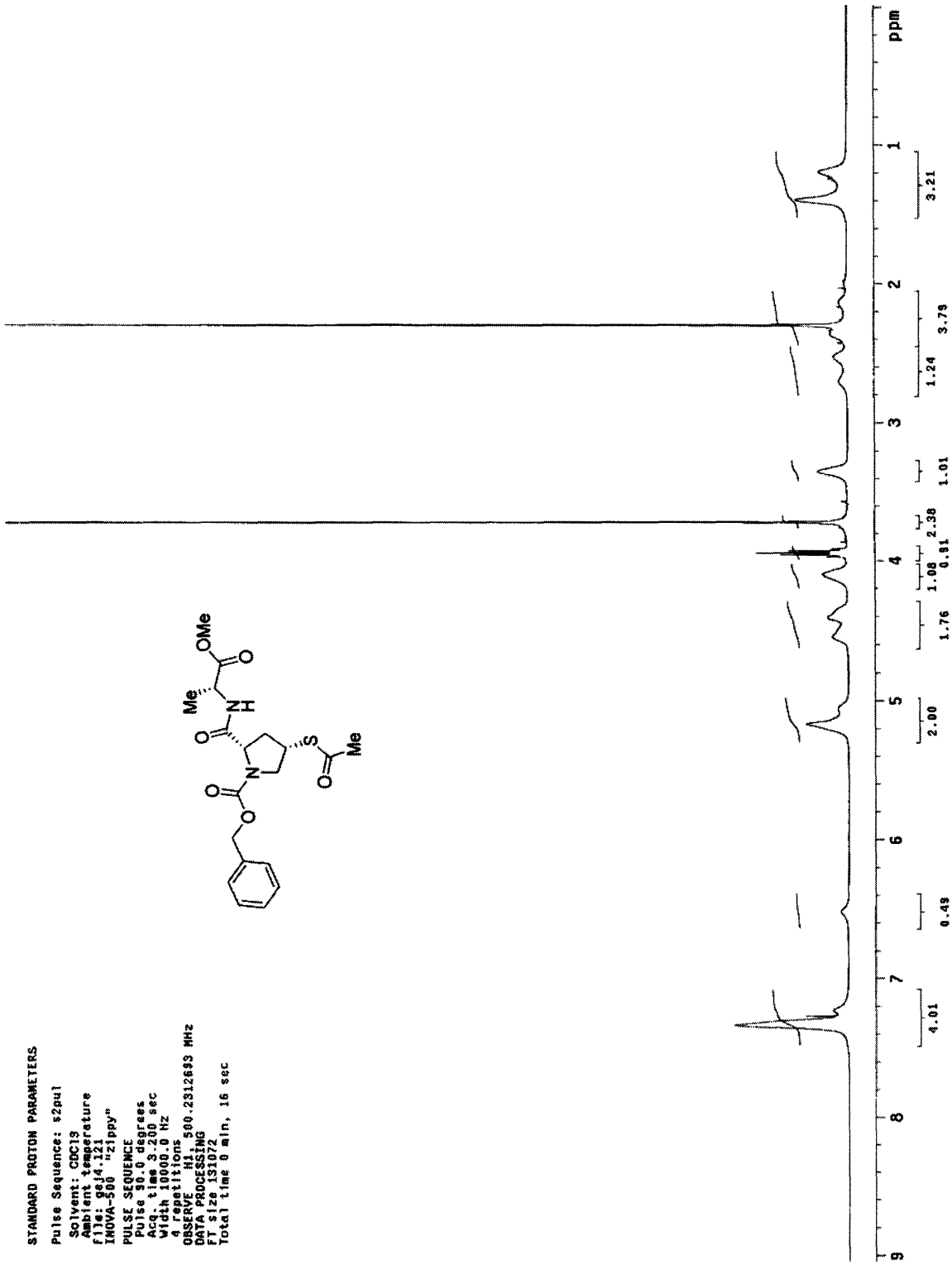
STANDARD PROTON PARAMETERS
Pulse Sequence: s2pul
Solvent: CDCl3
Ambient temperature
File: gd14.121
INOVA-500 "zippy"
PULSE SEQUENCE
Pulse 30.0 degrees
Acq. time 3.200 sec
Width 10000.0 Hz
4 repetitions
OBSERVE H1, 500.2312693 MHz
DATA PROCESSING
FT size 131072
Total time 0 min, 16 sec
Me
OMe
Me
S
Me
ppm
4.01
0.49
2.00
1.76
1.08
0.81
2.38
1.01
1.24
3.79
3.21

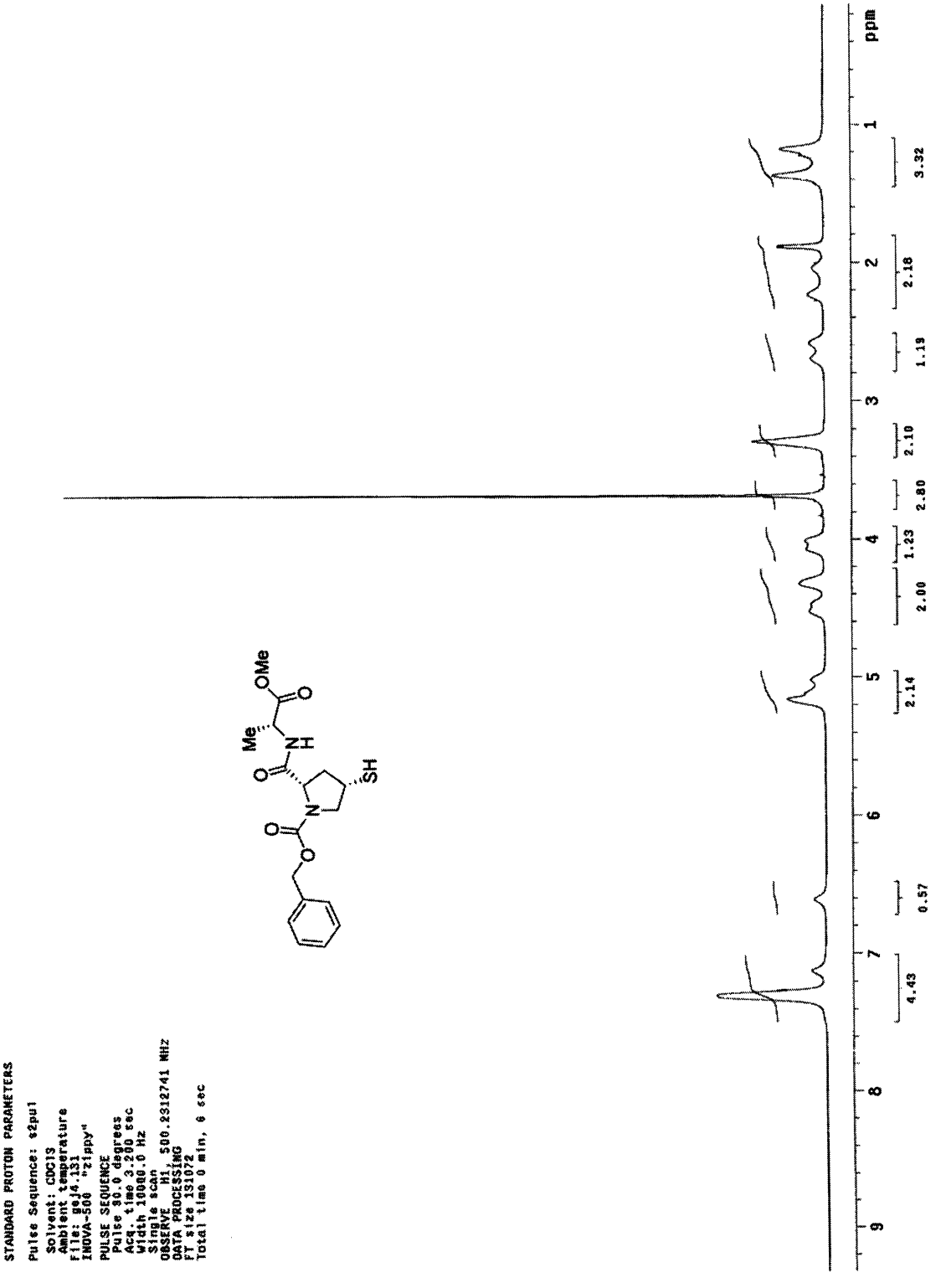
STANDARD PROTON PARAMETERS
Pulse Sequence: s2pul
Solvent: CDCl3
Ambient temperature
File: gaj4.131
INOVA-500 "zippy"
PULSE SEQUENCE
Pulse 90.0 degrees
Acq. time 3.200 sec
Width 10080.0 Hz
Single scan
OBSERVE H1, 500.2312741 MHz
DATA PROCESSING
FT size 131072
Total time 0 min, 6 sec
Me
OMe
O
N
H
O
N
O
O
SH
ppm
9
8
7
6
5
4
3
2
1
4.43
0.57
2.14
2.00
1.23
2.80
2.10
1.19
2.16
3.32

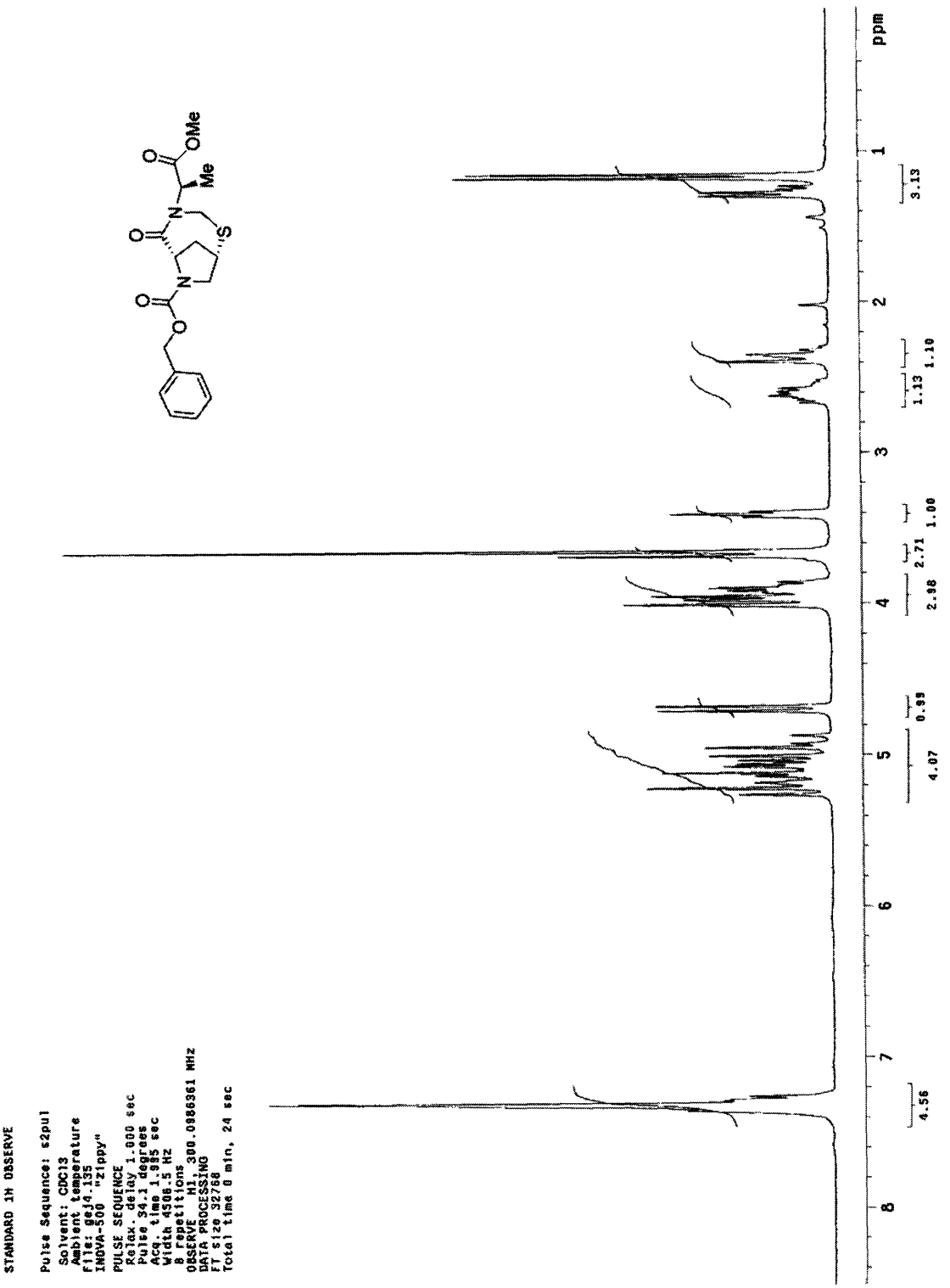
STANDARD 1H OBSERVE
Pulse Sequence: s2pul
Solvent: CDCl3
Ambient temperature
File: gej4.135
INOVA-500 "zippy"
PULSE SEQUENCE
Relax. delay 1.000 sec
Pulse 54.1 degrees
Acq. time 1.985 sec
Width 4508.5 Hz
8 repetitions
OBSERVE H1, 300.0986361 MHz
DATA PROCESSING
FT size 32768
Total time 0 min, 24 sec
OMe
Me
ppm
4.56
4.07
0.99
2.98
2.71
1.00
1.13
1.10
3.13

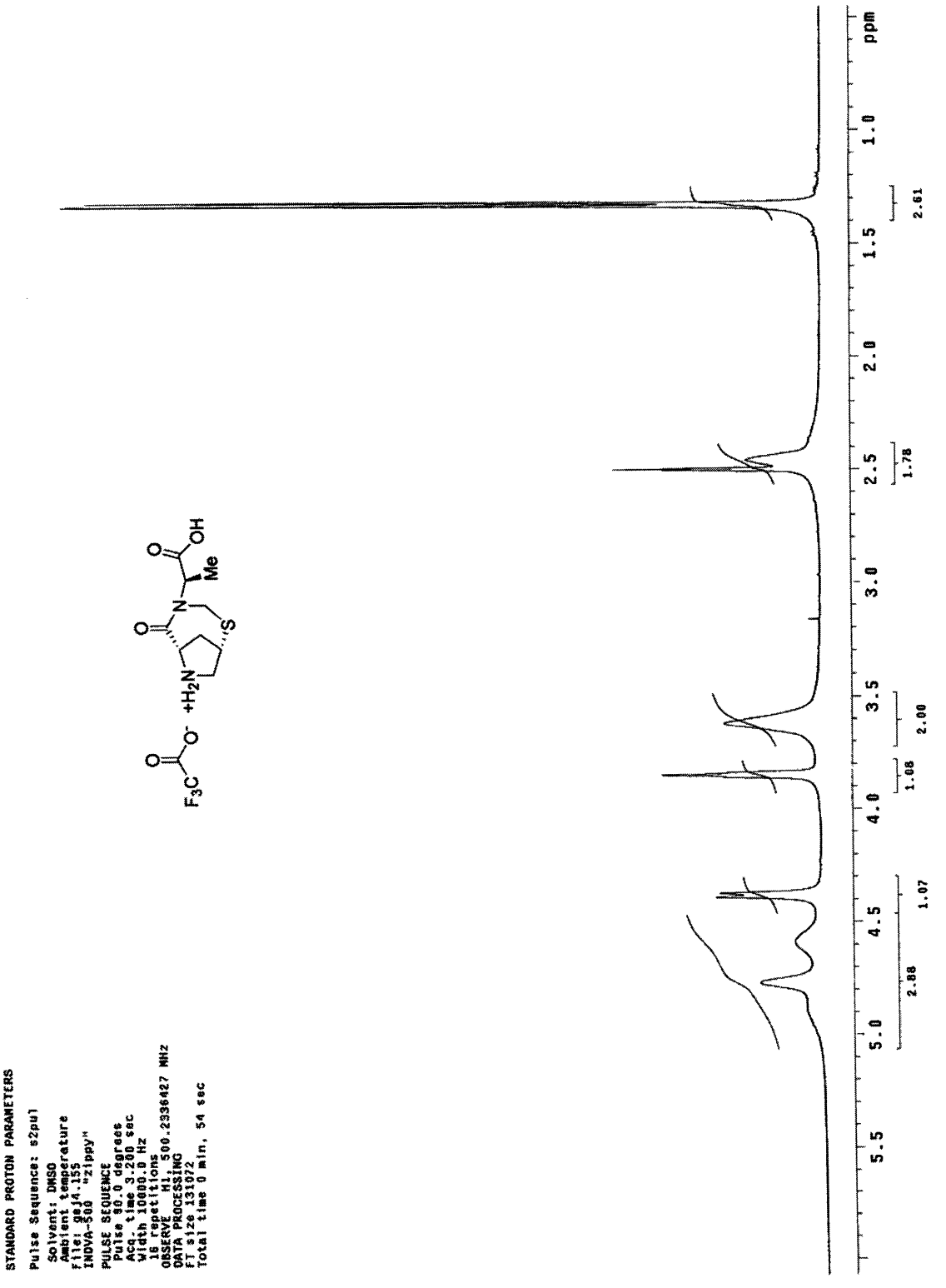
STANDARD PROTON PARAMETERS
Pulse Sequence: s2pul
Solvent: DMSO
Ambient temperature
File: gaj4.155
INOVA-500 "zippy"
PULSE SEQUENCE
Pulse 30.0 degrees
Acq. time 3.280 sec
Width 10000.0 Hz
16 repetitions
OBSERVE H1, 500.2336427 MHz
DATA PROCESSING
FT size 131072
Total time 0 min, 54 sec
F3C
O
O-
+H2N
N
S
O
N
Me
OH
O
5.5
5.0
4.5
4.0
3.5
3.0
2.5
2.0
1.5
1.0
ppm
2.88
1.07
1.08
2.00
1.78
2.61

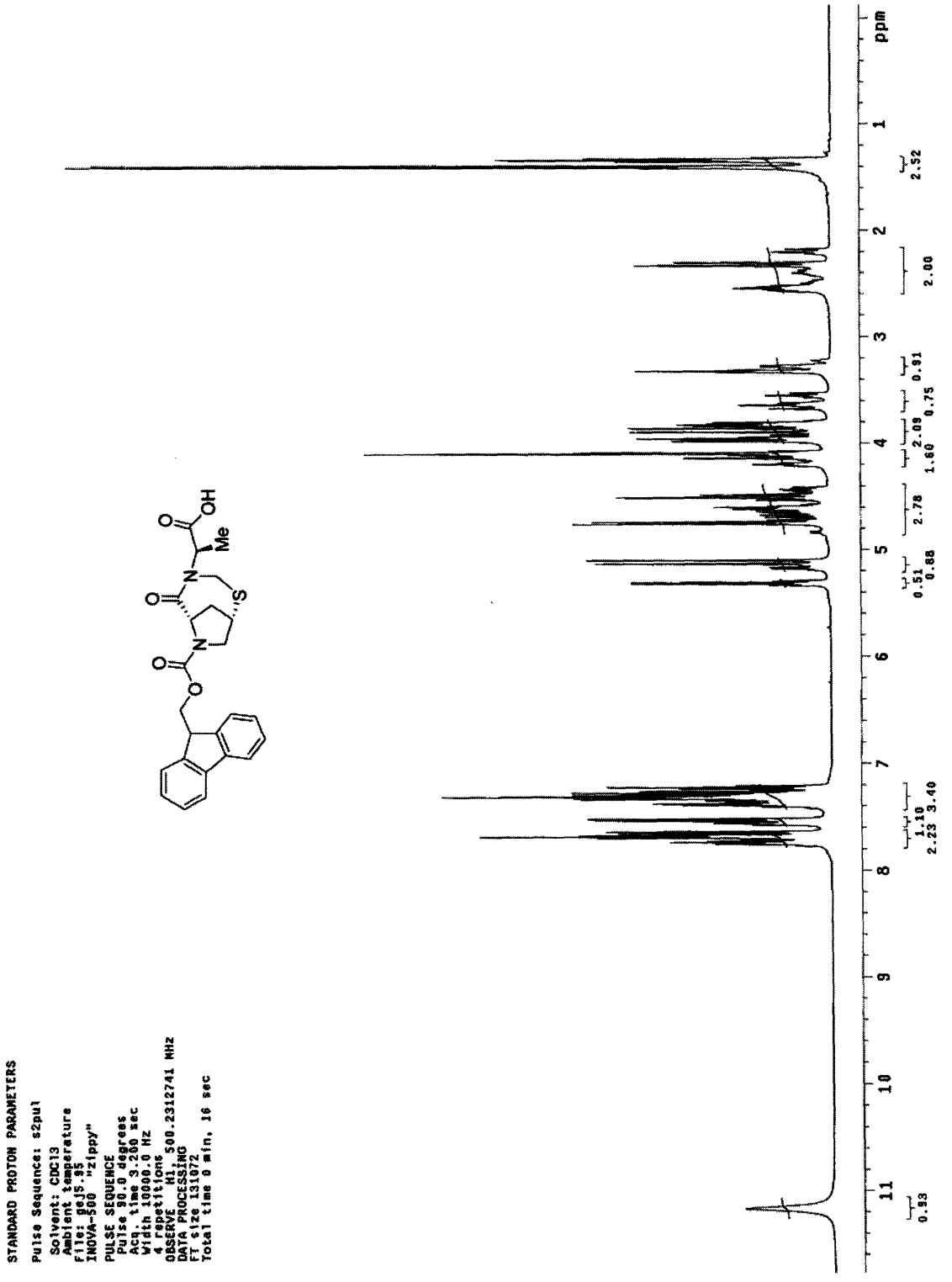
STANDARD PROTON PARAMETERS
Pulse Sequence: s2pul
Solvent: CDCl3
Ambient temperature
File: cdj5.95
INOVA-500 "zippy"
PULSE SEQUENCE
Pulse 90.0 degrees
Acq. time 3.200 sec
Width 10000.0 Hz
4 repetitions
OBSERVE H1, 500.2312741 MHz
DATA PROCESSING
FT size 131072
Total time 9 min, 16 sec
OH
Me
ppm
0.53
1.10
2.23
3.40
0.51
0.88
2.78
1.60
2.08
0.75
0.91
2.52
2.00

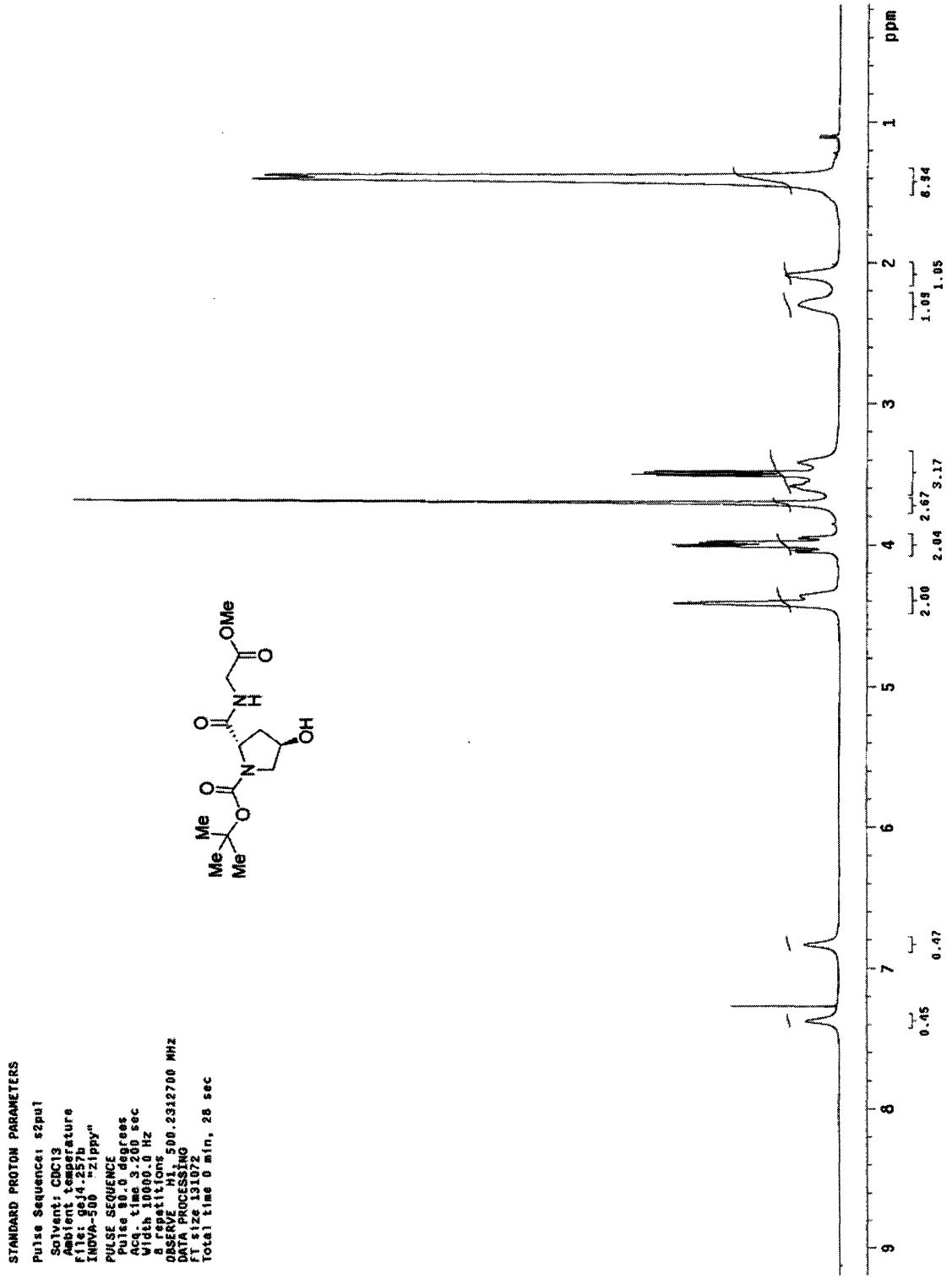
STANDARD PROTON PARAMETERS
Pulse Sequence: s2pul
Solvent: CDCl3
Ambient temperature
File: gd4.257b
INOVA-500 "21ppy"
PULSE SEQUENCE
Pulse 90.0 degrees
Acq. time 3.200 sec
Width 10000.0 Hz
8 repetitions
OBSERVE H1, 500.2312700 MHz
DATA PROCESSING
FT size 131072
Total time 0 min, 28 sec
Me
Me
Me
O
O
O
N
H
O
N
OH
OMe
O
ppm
0.45
0.47
2.00
2.04
2.67
3.17
1.09
1.05
6.34

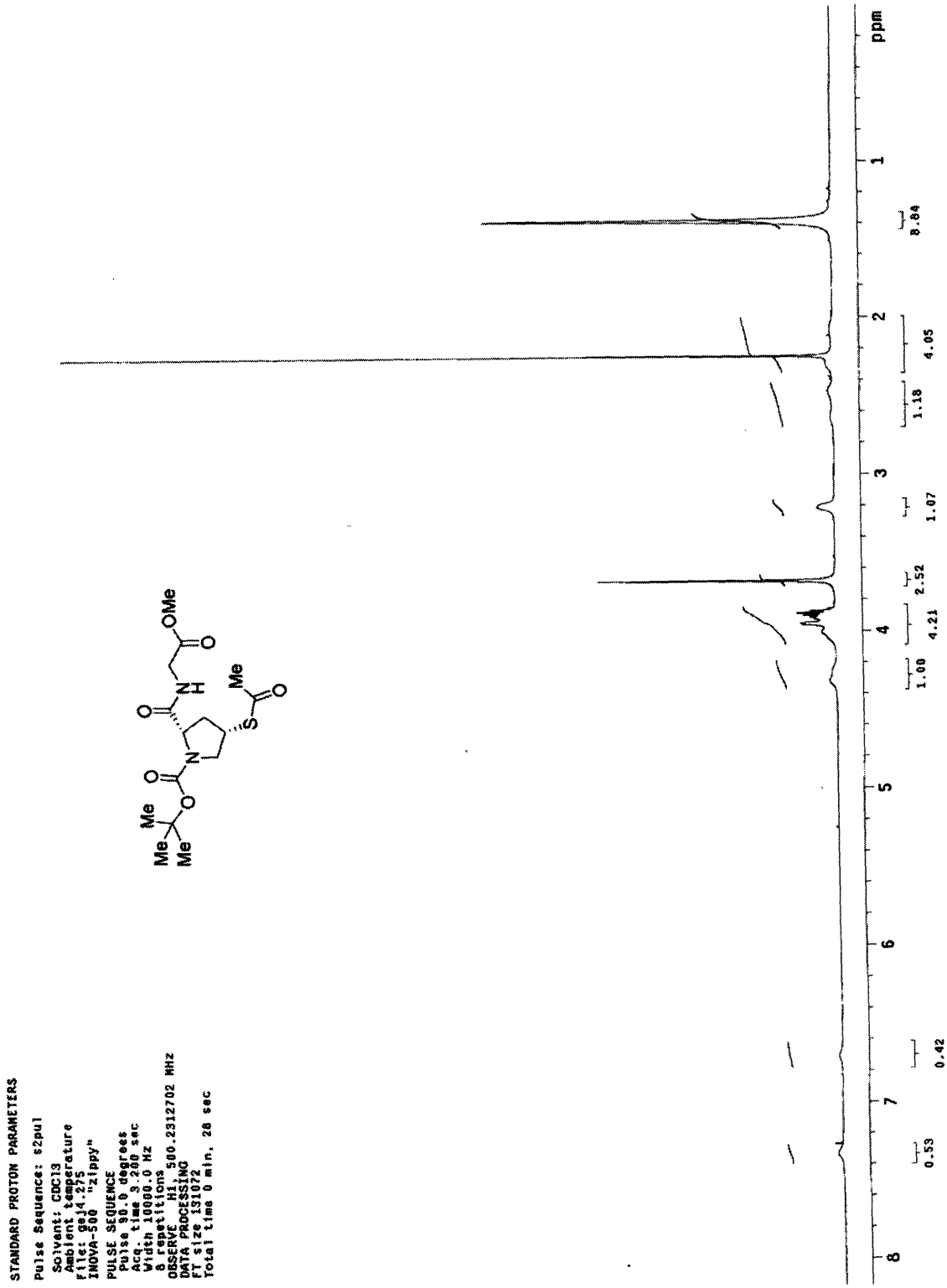
STANDARD PROTON PARAMETERS
Pulse Sequence: s2pul
Solvent: CDCl3
Ambient temperature
File: gd4.fid
INOVA-500 "21ppy"
PULSE SEQUENCE
Pulse 90.0 degrees
Acq. time 3.200 sec
Width 10000.0 Hz
8 repetitions
OBSERVE H1, 500.2312702 MHz
DATA PROCESSING
FT size 131072
Total time 0 min, 28 sec
OMe
Me
Me
Me
Me
ppm
1.00
4.21
2.52
1.07
1.18
4.05
8.04
0.53
0.42

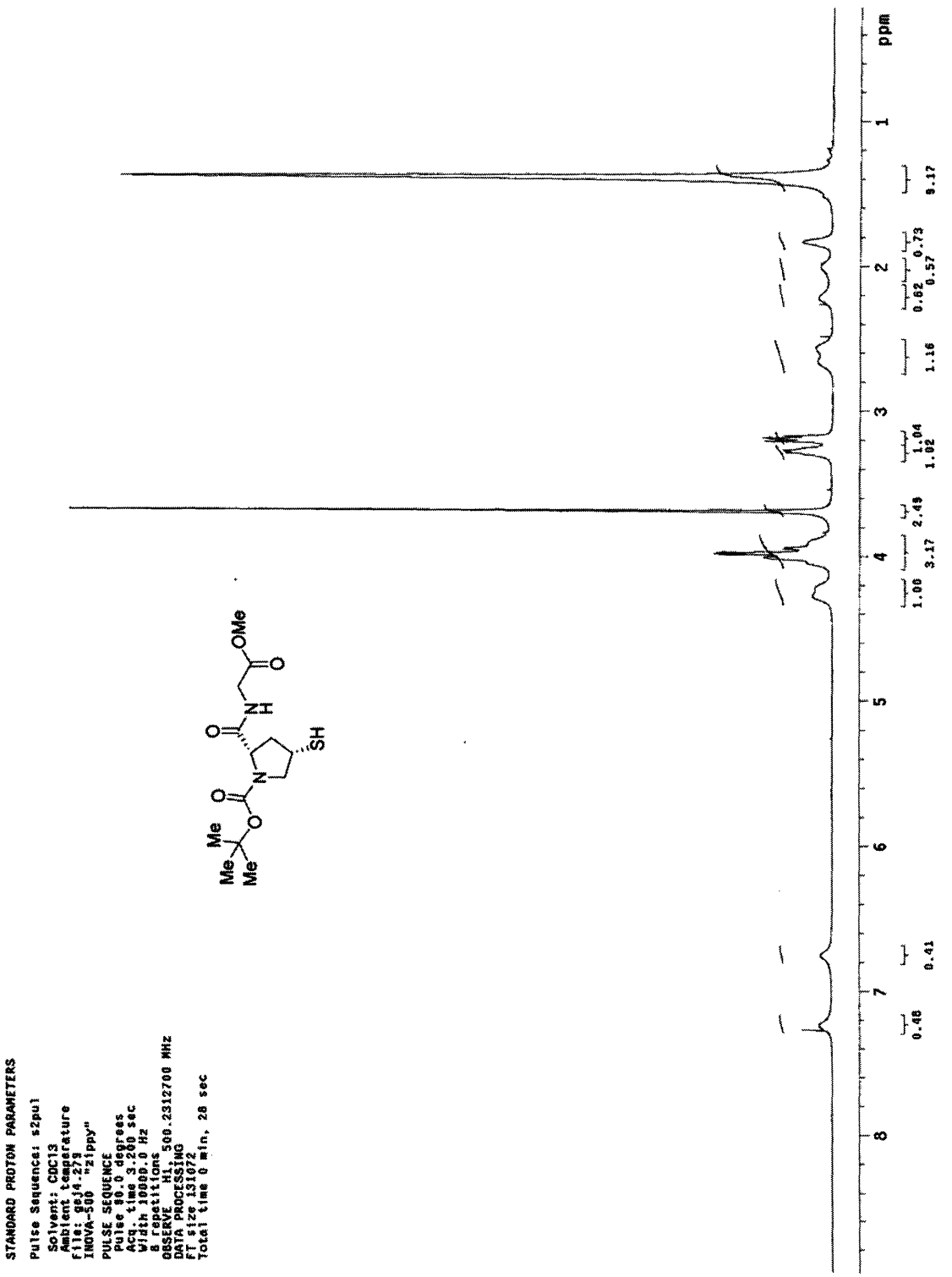
STANDARD PROTON PARAMETERS
Pulse Sequence: s2pul
Solvent: CDCl3
Ambient temperature
File: gej4.27g
INOVA-500 "zippy"
PULSE SEQUENCE
Pulse 90.0 degrees
Acq. time 3.200 sec
Width 10000.0 Hz
8 repetitions
OBSERVE H1, 500.2312700 MHz
DATA PROCESSING
FT size 131072
Total time 0 min, 28 sec
OMe
O
N
H
O
SH
N
O
O
Me
Me
Me
ppm
1.00
3.17
2.49
1.04
1.02
1.16
0.62
0.57
0.73
0.48
0.41
9.17

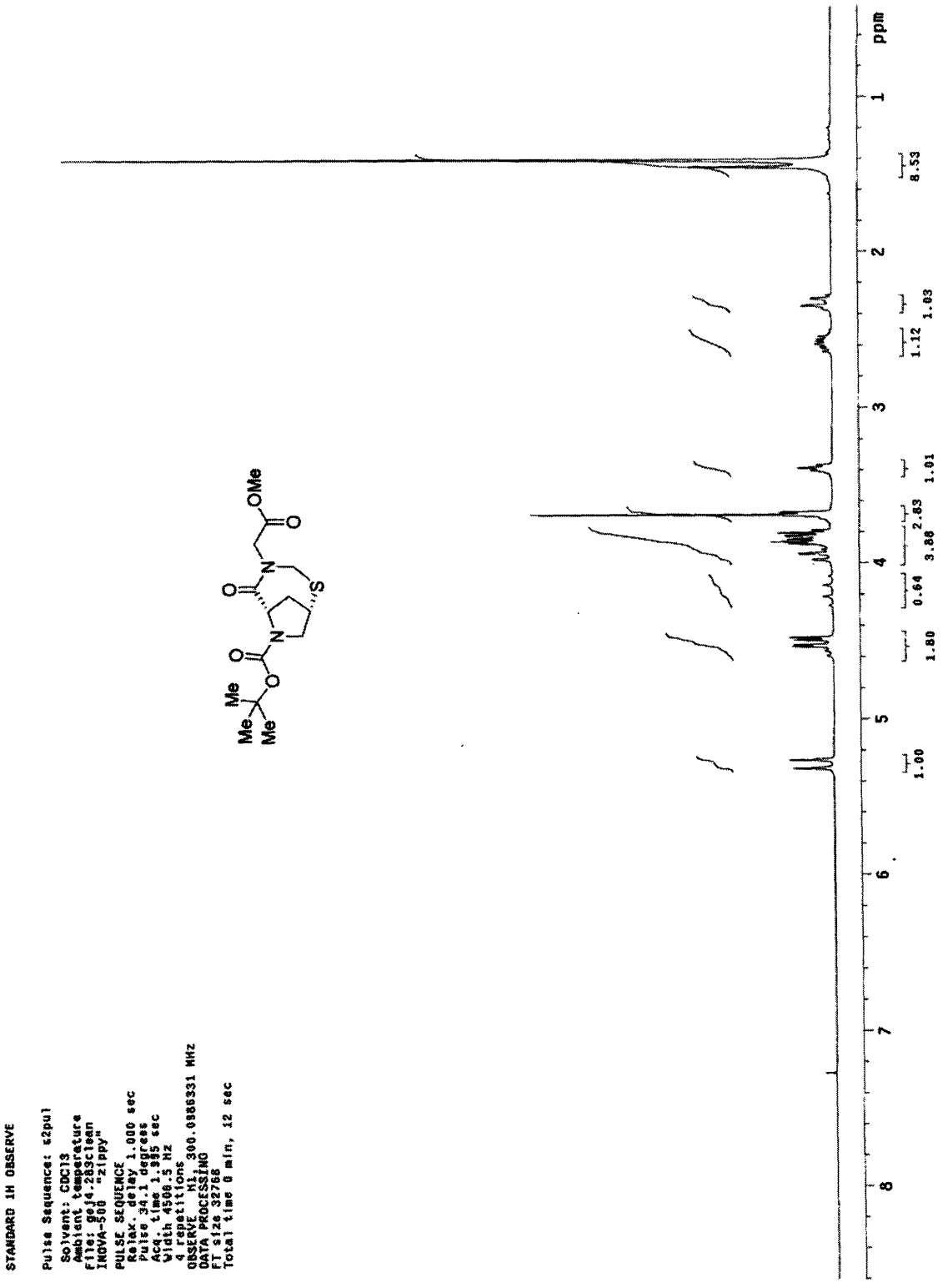
STANDARD 1H OBSERVE
Pulse Sequence: s2pul
Solvent: CDCl3
Ambient temperature
file: gej4.283clean
INOVA-500 "21ppy"
PULSE SEQUENCE
Relax. delay 1.000 sec
Pulse 34.1 degrees
Acq. time 1.995 sec
Width 4506.5 Hz
4 repetitions
OBSERVE H1, 300.0886331 MHz
DATA PROCESSING
FT size 32768
Total time 0 min, 12 sec
OMe
Me
Me
Me
ppm
1.00
1.80
0.64
3.80
2.83
1.01
1.12
1.03
8.53

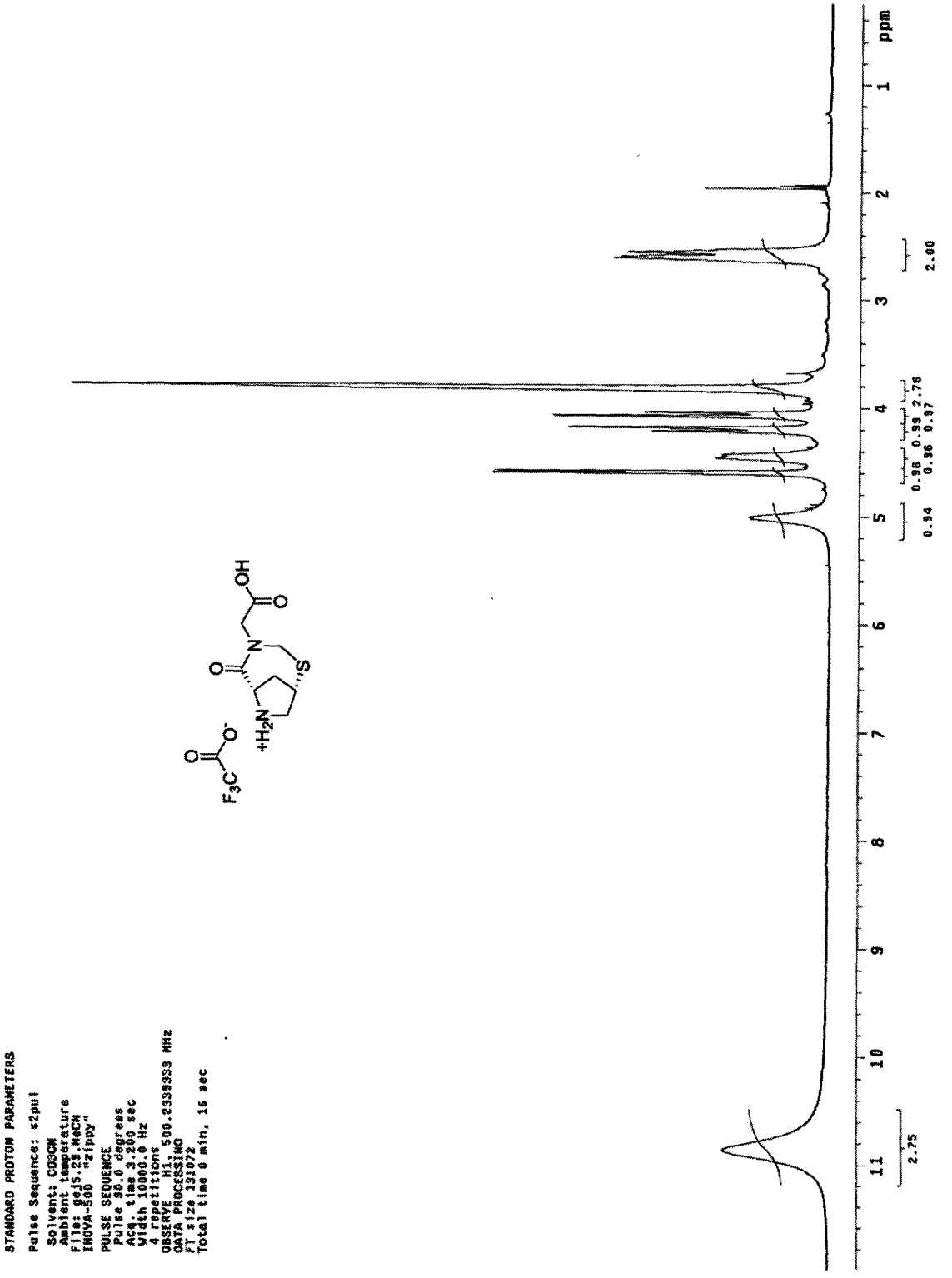
STANDARD PROTON PARAMETERS
Pulse Sequence: s2pul
Solvent: CD3CN
Ambient temperature
File: gej5.29.MeCN
INOVA-500 "zippy"
PULSE SEQUENCE
Pulse 90.0 degrees
Acq. time 3.200 sec
Width 10000.0 Hz
4 repetitions
OBSERVE H1, 500.2339333 MHz
DATA PROCESSING
FT size 131072
Total time 0 min, 16 sec
OH
O
O
N
O
S
+H2N
O
O-
F3C
ppm
1
2
3
4
5
6
7
8
9
10
11
2.00
0.94
0.98
0.96
0.99
0.97
2.76
2.75

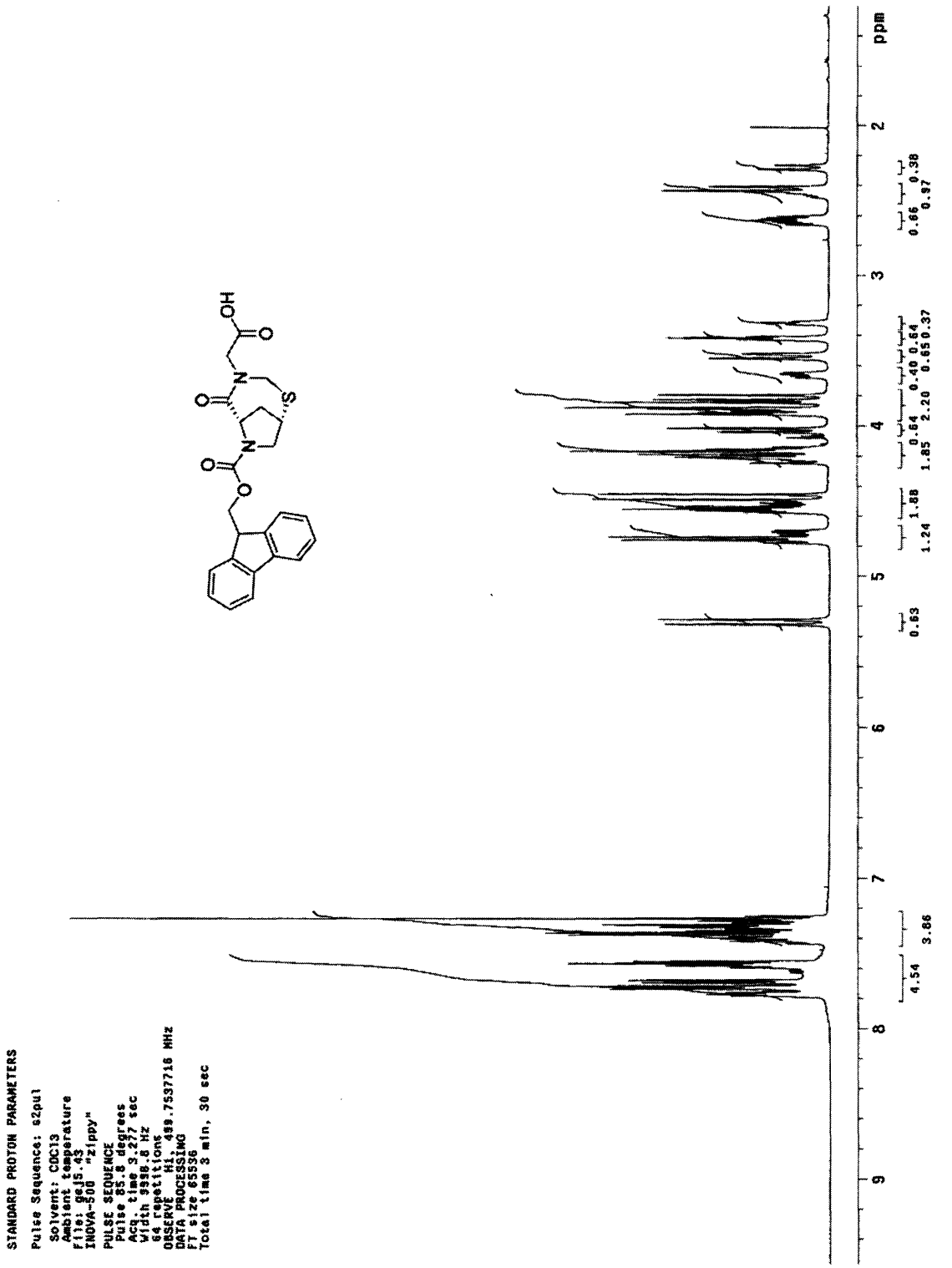
STANDARD PROTON PARAMETERS
Pulse Sequence: s2pul
Solvent: CDCl3
Ambient temperature
File: gej5.43
INOVA-500 "zippy"
PULSE SEQUENCE
Pulse 85.8 degrees
Acq. time 3.277 sec
Width 9398.8 Hz
64 repetitions
OBSERVE H1, 499.7537716 MHz
DATA PROCESSING
FT size 65536
Total time 3 min, 30 sec
OH
O
O
N
S
N
O
O
ppm
9
8
7
6
5
4
3
2
4.54
3.86
0.63
1.24
1.38
0.64
1.85
2.20
0.40
0.64
0.85
0.37
0.66
0.97
0.38

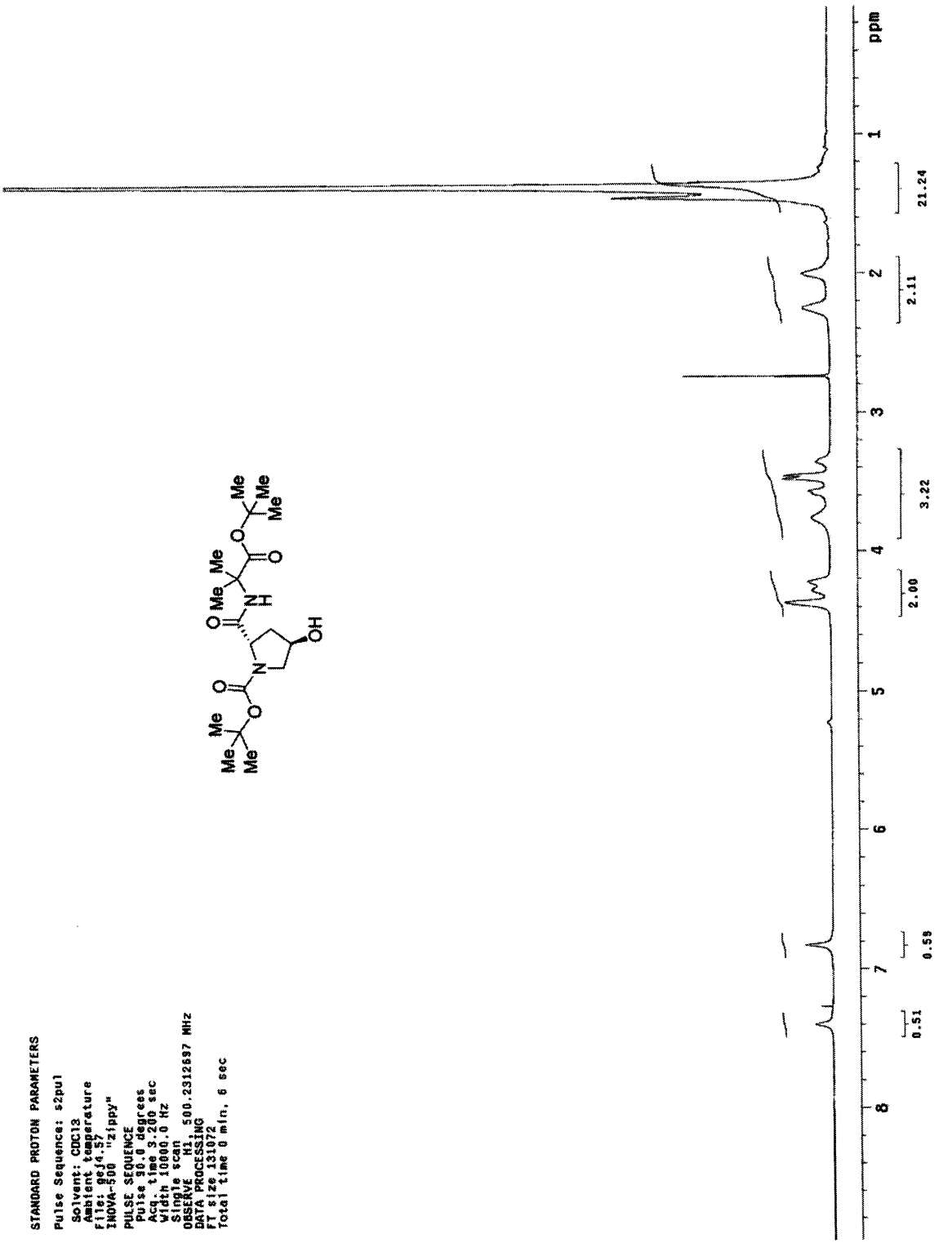
STANDARD PROTON PARAMETERS
Pulse Sequence: s2pul
Solvent: CDCl3
Ambient temperature
File: gej4-57
INOVA-500 "zippy"
PULSE SEQUENCE
Pulse 90.0 degrees
Acq. time 3.200 sec
Width 10000.0 Hz
Single scan
OBSERVE H1, 500.2312697 MHz
DATA PROCESSING
FT size 131072
Total time 0 min, 6 sec
Me
Me
Me
O
O
Me
Me
O
N
H
O
N
O
O
Me
Me
Me
OH
ppm
0.51
0.59
2.00
3.22
2.11
21.24

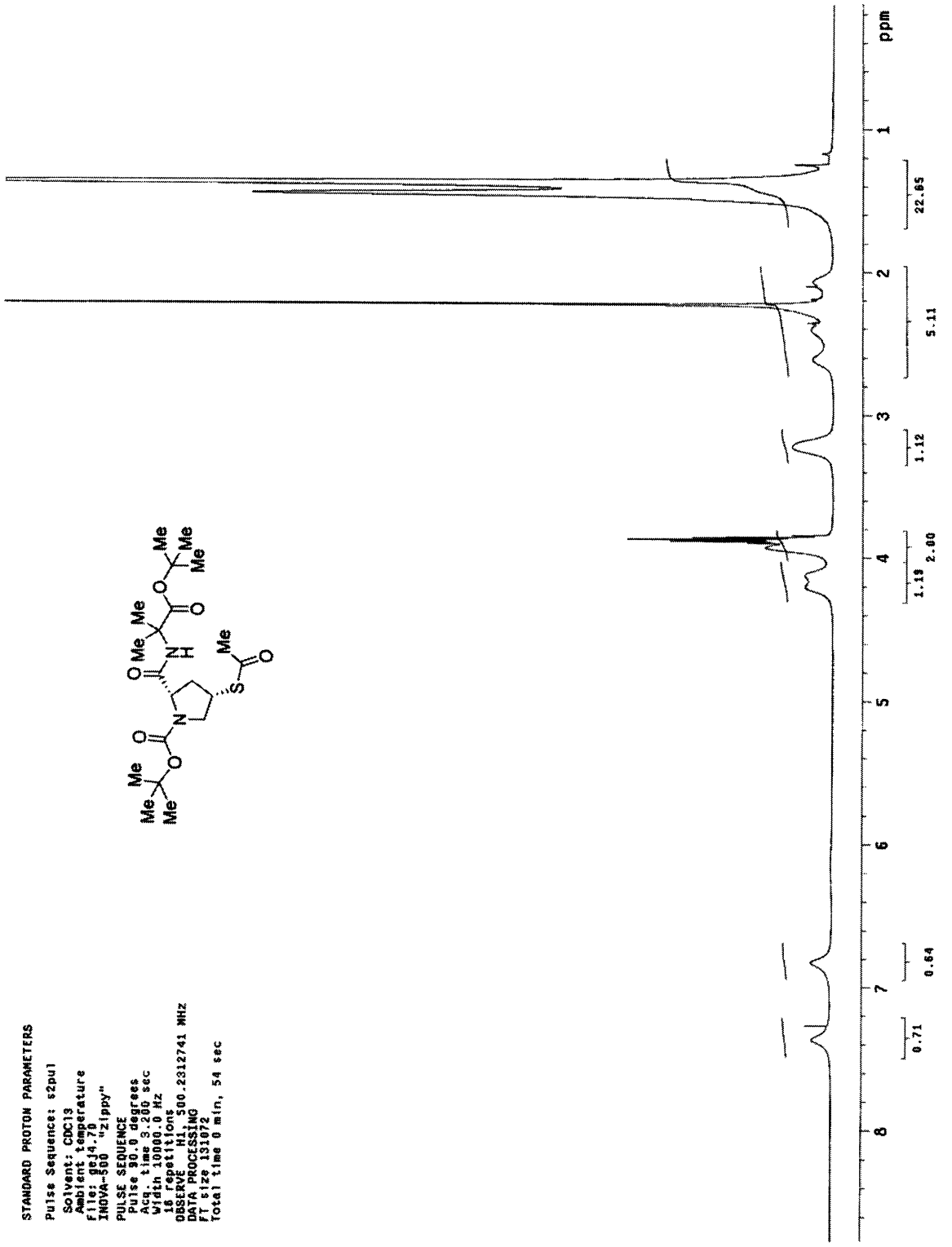
STANDARD PROTON PARAMETERS
Pulse Sequence: s2pul
Solvent: CDCl3
Ambient temperature
File: gdj4.79
INOVA-500 "zippy"
PULSE SEQUENCE
Pulse 90.0 degrees
Acq. time 3.200 sec
Width 10000.0 Hz
16 repetitions
OBSERVE H1, 500.2312741 MHz
DATA PROCESSING
FT size 131072
Total time 0 min, 54 sec
Me
Me
Me
O
Me
Me
O
O
Me
N
H
O
Me
S
O
N
O
O
Me
Me
Me
ppm
1
2
3
4
5
6
7
8
22.65
5.11
1.12
1.18
2.00
0.71
0.64

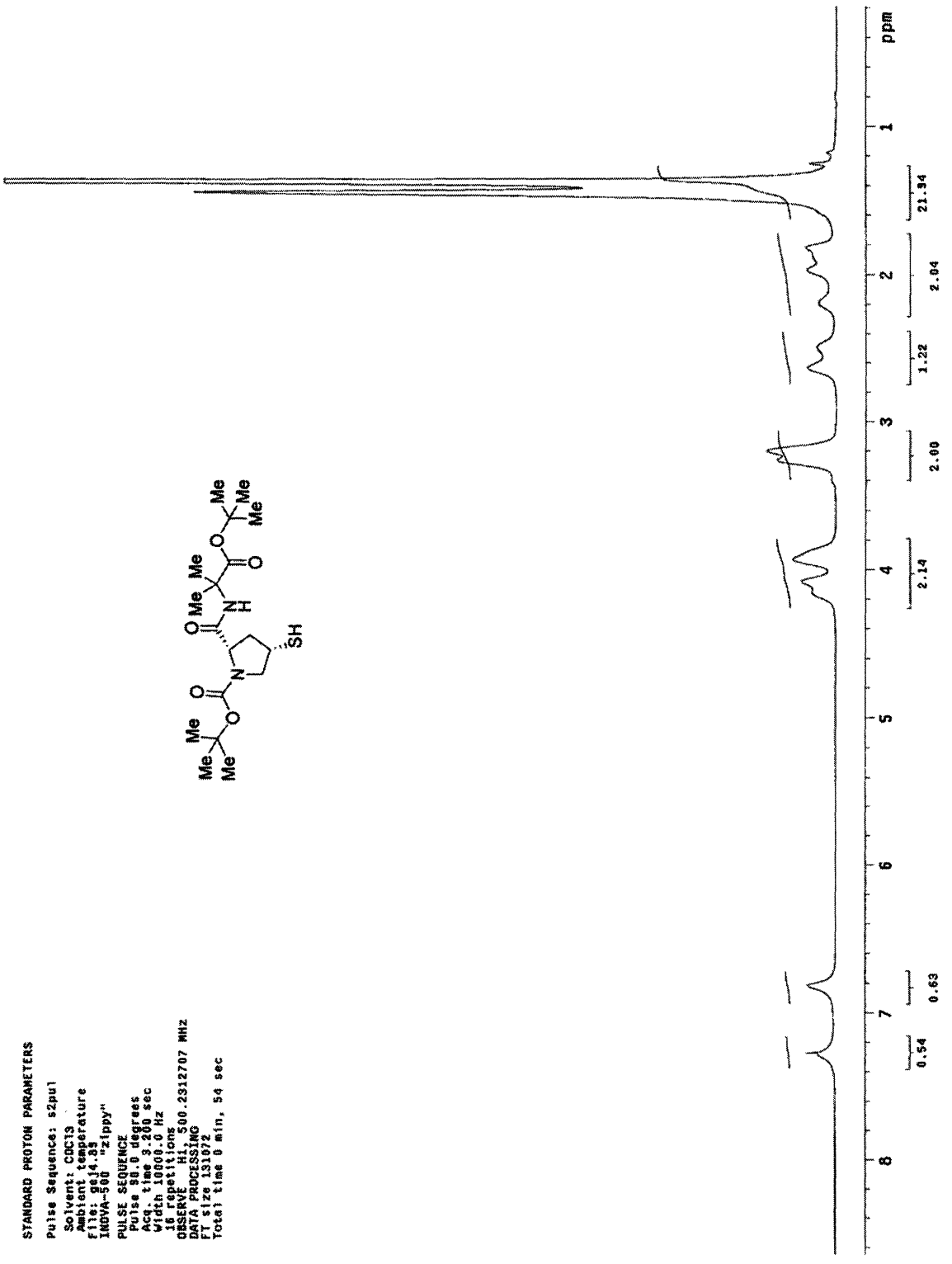
STANDARD PROTON PARAMETERS
Pulse Sequence: s2pul
Solvent: CDCl3
Ambient temperature
File: ge14.03
INOVA-500 "zippy"
PULSE SEQUENCE
Pulse 90.0 degrees
Acq. time 3.200 sec
Width 10000.0 Hz
16 repetitions
OBSERVE H1, 500.2312707 MHz
DATA PROCESSING
FT size 131072
Total time 0 min, 54 sec
Me
Me
Me
O
Me
Me
O
O
N
H
O
N
SH
Me
Me
Me
O
O
ppm
0.54
0.63
2.14
2.00
1.22
2.04
21.34

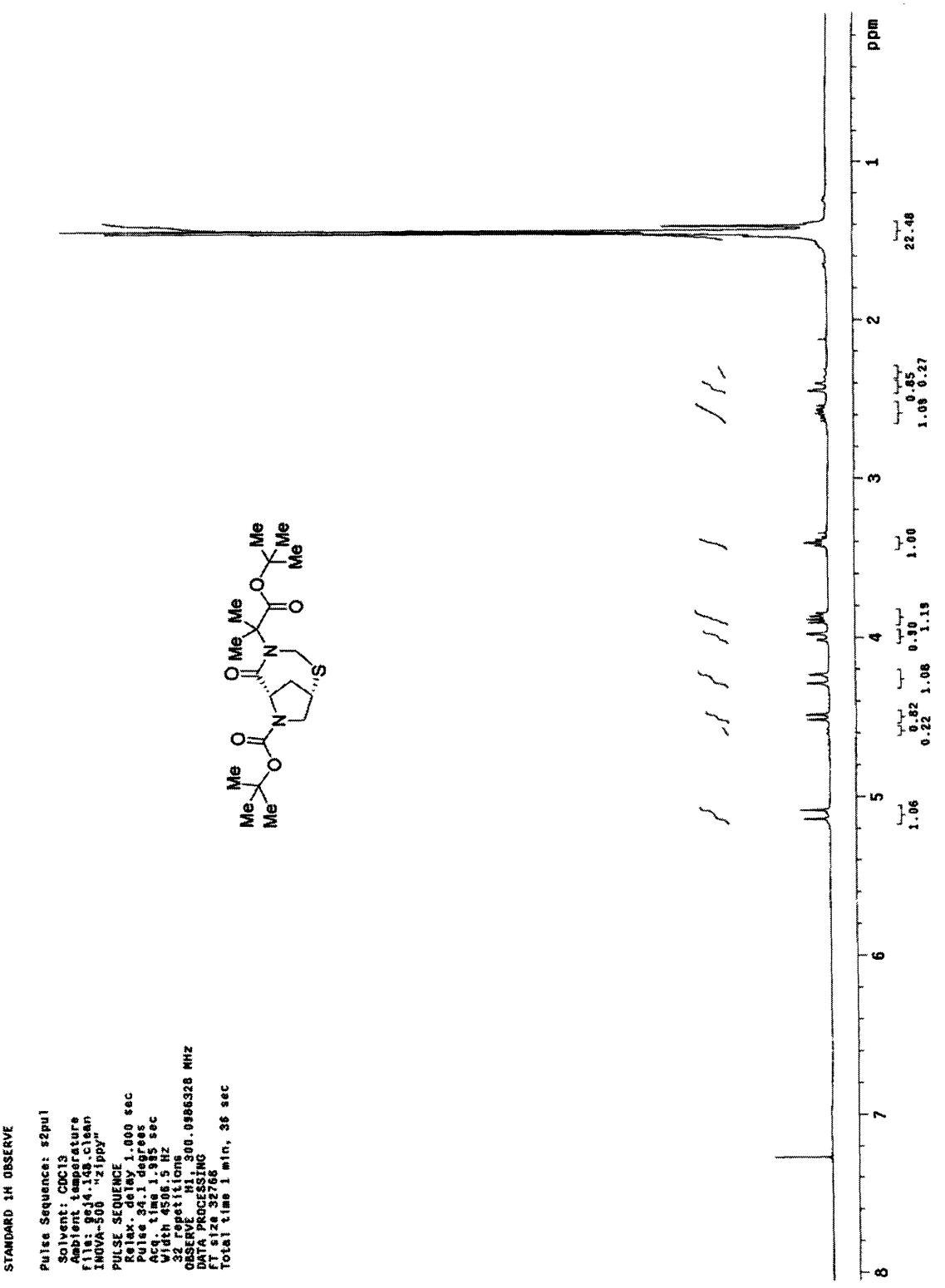
STANDARD 1H OBSERVE
Pulse Sequence: s2pul
Solvent: CDCl3
Ambient temperature
File: gej4.14b.clean
INOVA-500 "zippy"
PULSE SEQUENCE
Relax. delay 1.000 sec
Pulse 34.1 degrees
Acq. time 1.985 sec
Width 4506.5 Hz
32 repetitions
OBSERVE H1, 300.0986328 MHz
DATA PROCESSING
FT size 32768
Total time 1 min, 38 sec
Me
Me
Me
O
Me
Me
O
O
N
S
N
O
O
Me
Me
Me
ppm
1
2
3
4
5
6
7
8
22.48
0.85
1.08
0.27
1.00
0.30
1.19
0.82
1.08
0.22
1.06

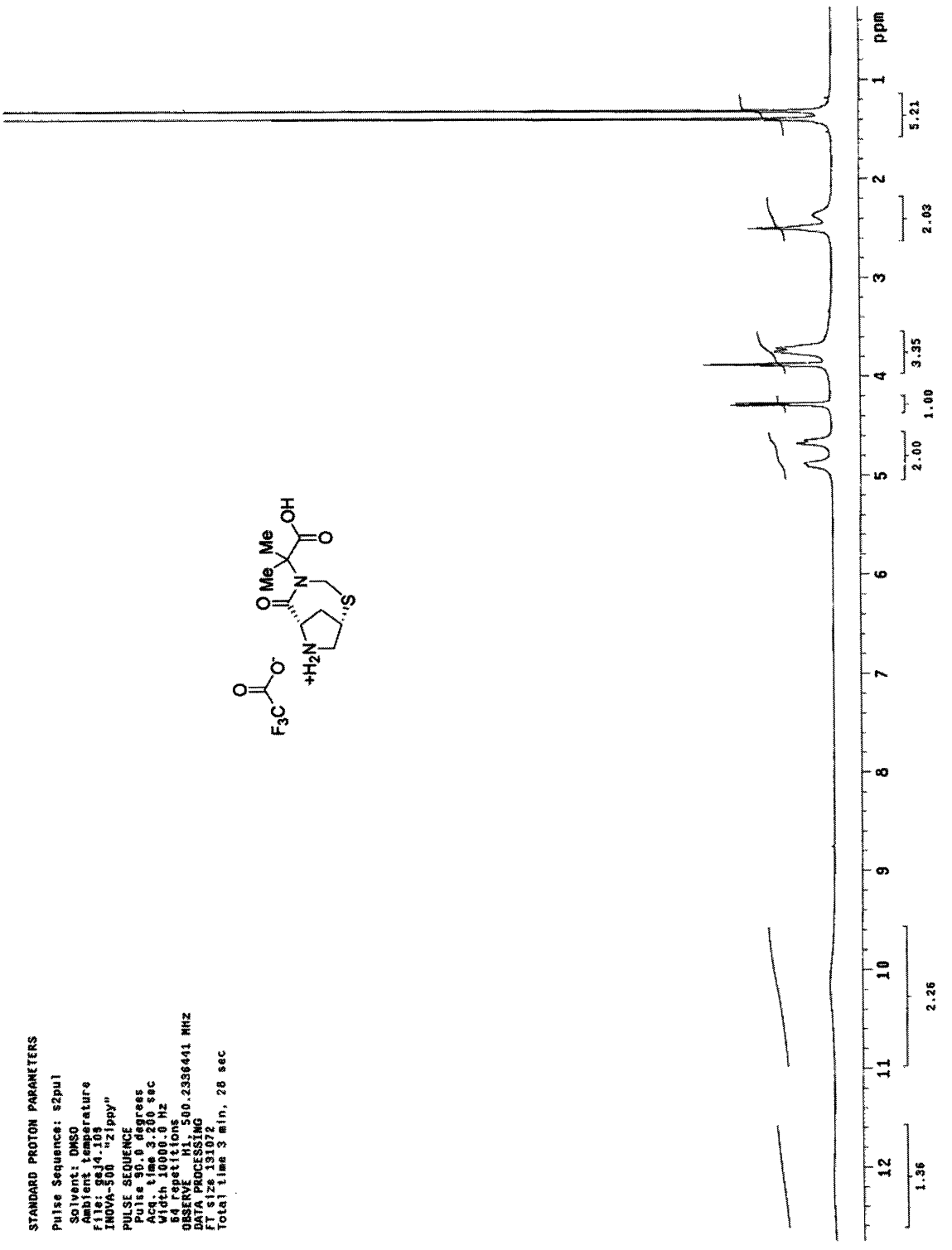
STANDARD PROTON PARAMETERS
Pulse Sequence: s2pul
Solvent: DMSO
Ambient temperature
File: gaj4.109
INOVA-500 "zippy"
PULSE SEQUENCE
Pulse 90.0 degrees
Acq. time 3.200 sec
Width 10000.0 Hz
64 repetitions
OBSERVE H1, 500.2336441 MHz
DATA PROCESSING
FT size 131072
Total time 3 min, 28 sec
Me
Me
OH
O
O
N
S
+H2N
O
O-
F3C
ppm
1
2
3
4
5
6
7
8
9
10
11
12
5.21
2.03
3.35
1.00
2.00
2.26
1.36

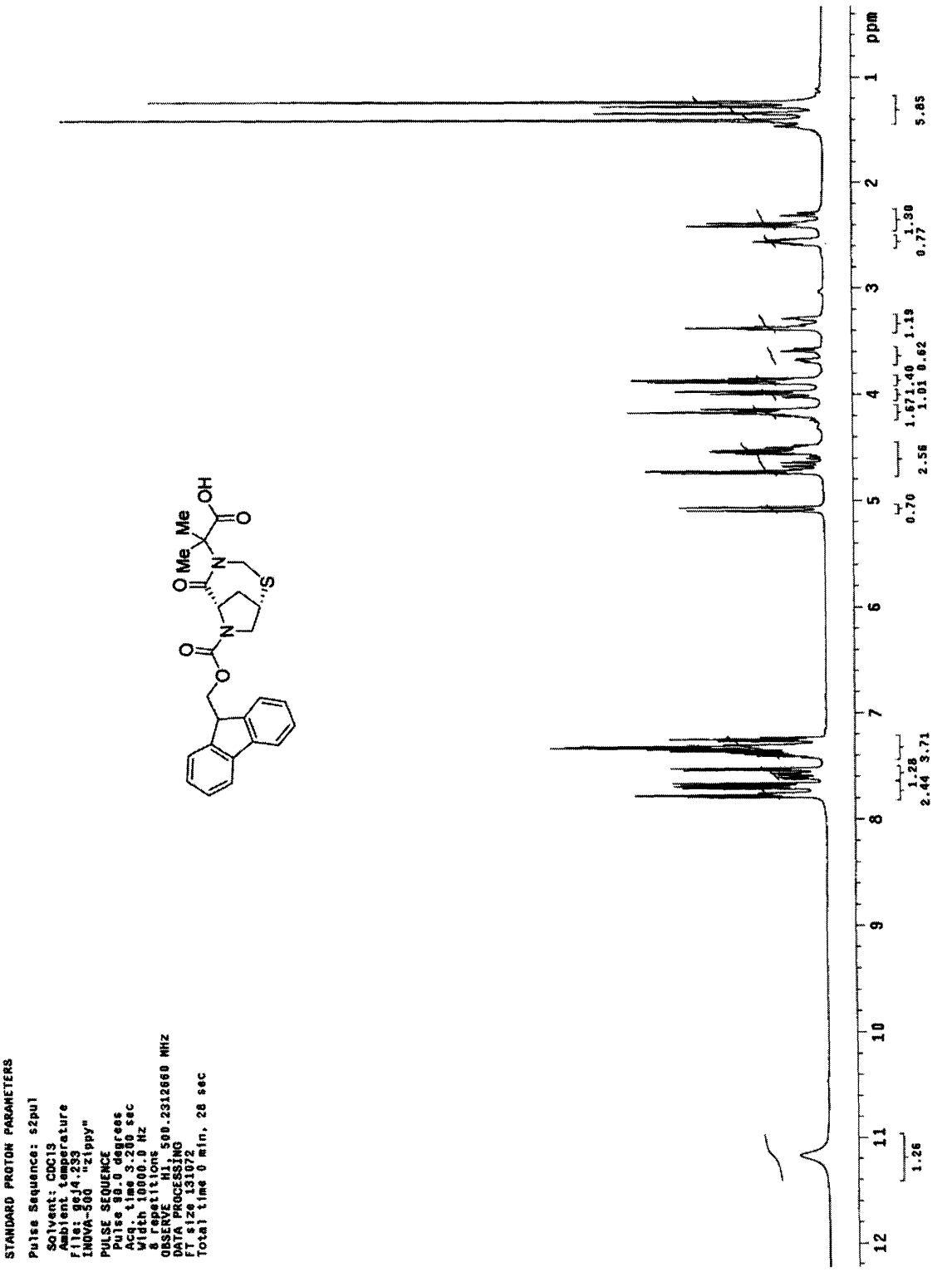
STANDARD PROTON PARAMETERS
Pulse Sequence: s2pul
Solvent: CDCl3
Ambient temperature
File: gej4.233
INOVA-500 "zippy"
PULSE SEQUENCE
Pulse 90.0 degrees
Acq. time 3.200 sec
Width 10000.0 Hz
8 repetitions
OBSERVE H1, 500.2312660 MHz
DATA PROCESSING
FT size 131072
Total time 0 min, 28 sec
Me
Me
OH
O
O
N
S
N
O
O
O
ppm
1.26
1.28
2.44
3.71
0.70
2.56
1.67
1.40
1.01
0.82
1.19
1.30
0.77
5.85

5.12. COSY Spectra

The numbering scheme used for Hel was applied to the new NCaps.

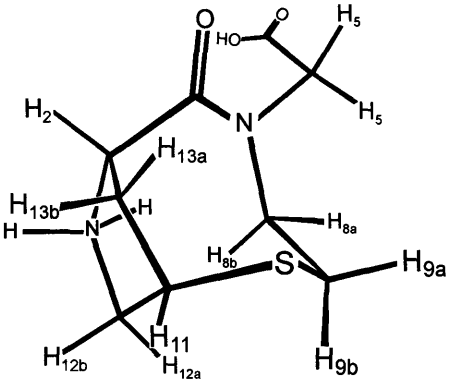

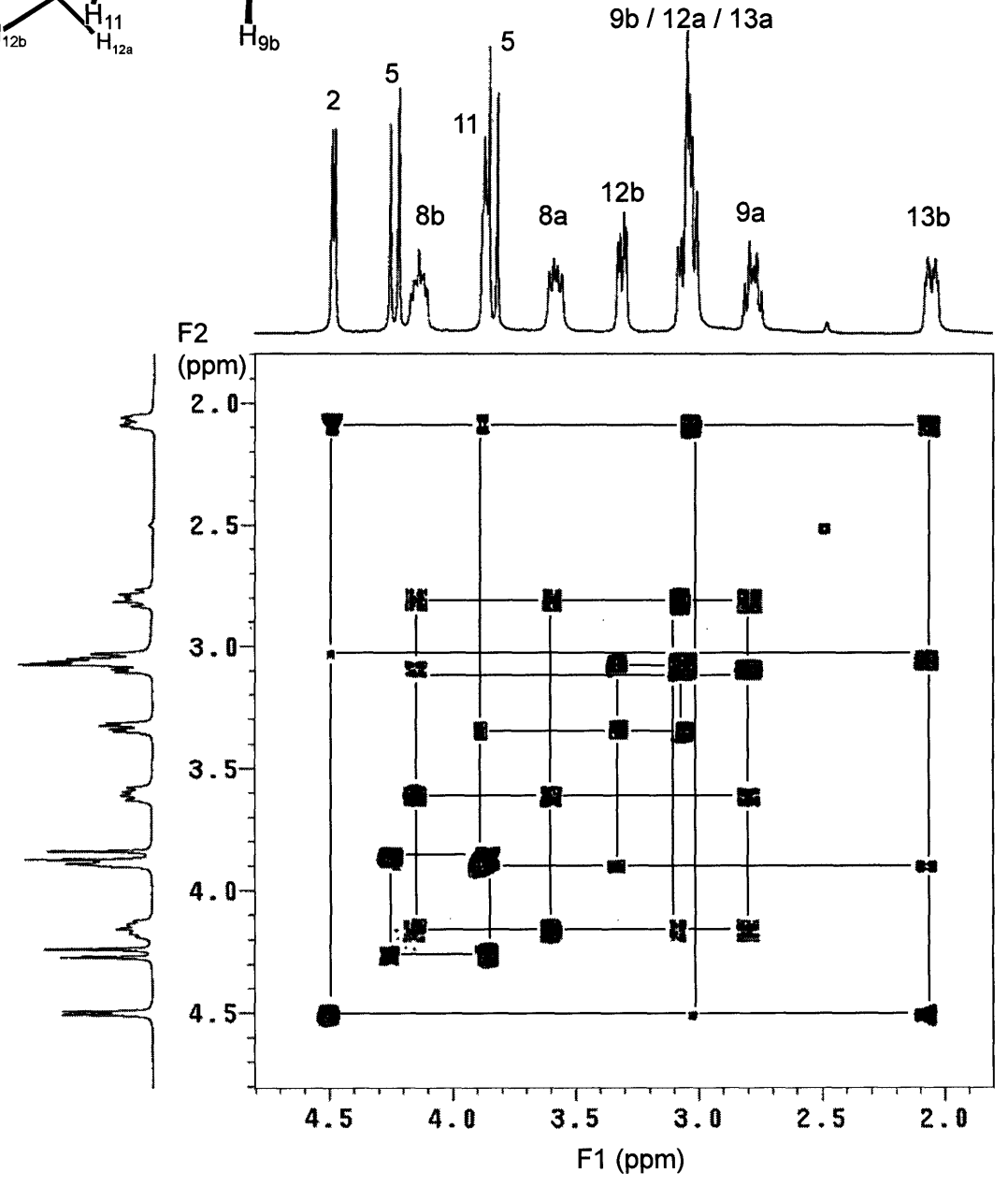

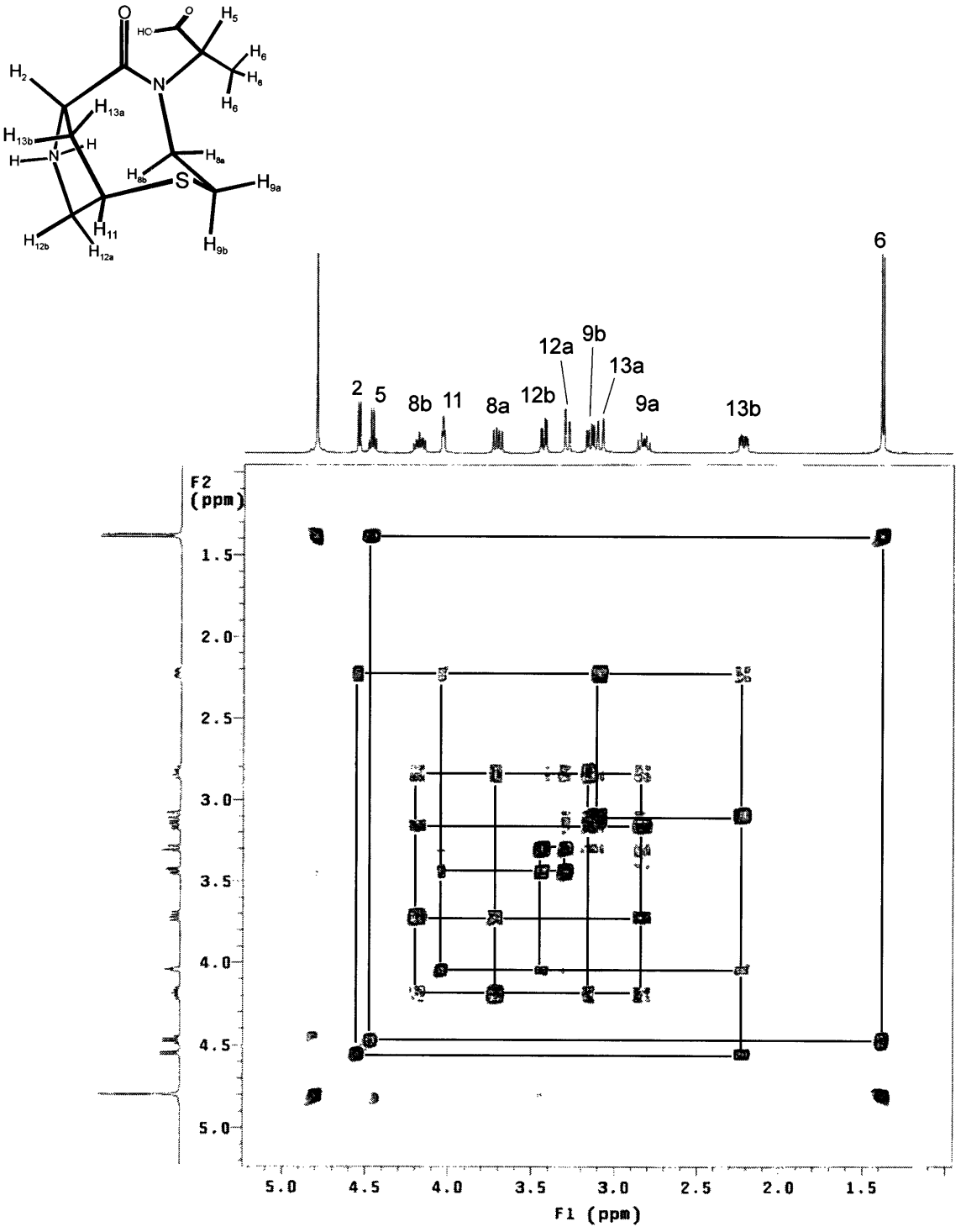
O
HO
O
H5
H6
H6
H6
H2
N
H13a
H13b
H
H
N
H8a
H8b
S
H9a
H11
H12b
H12a
H9b
6
2
5
8b
11
8a
12b
12a
9b
13a
9a
13b
F2 (ppm)
1.5
2.0
2.5
3.0
3.5
4.0
4.5
5.0
5.0
4.5
4.0
3.5
3.0
2.5
2.0
1.5
F1 (ppm)

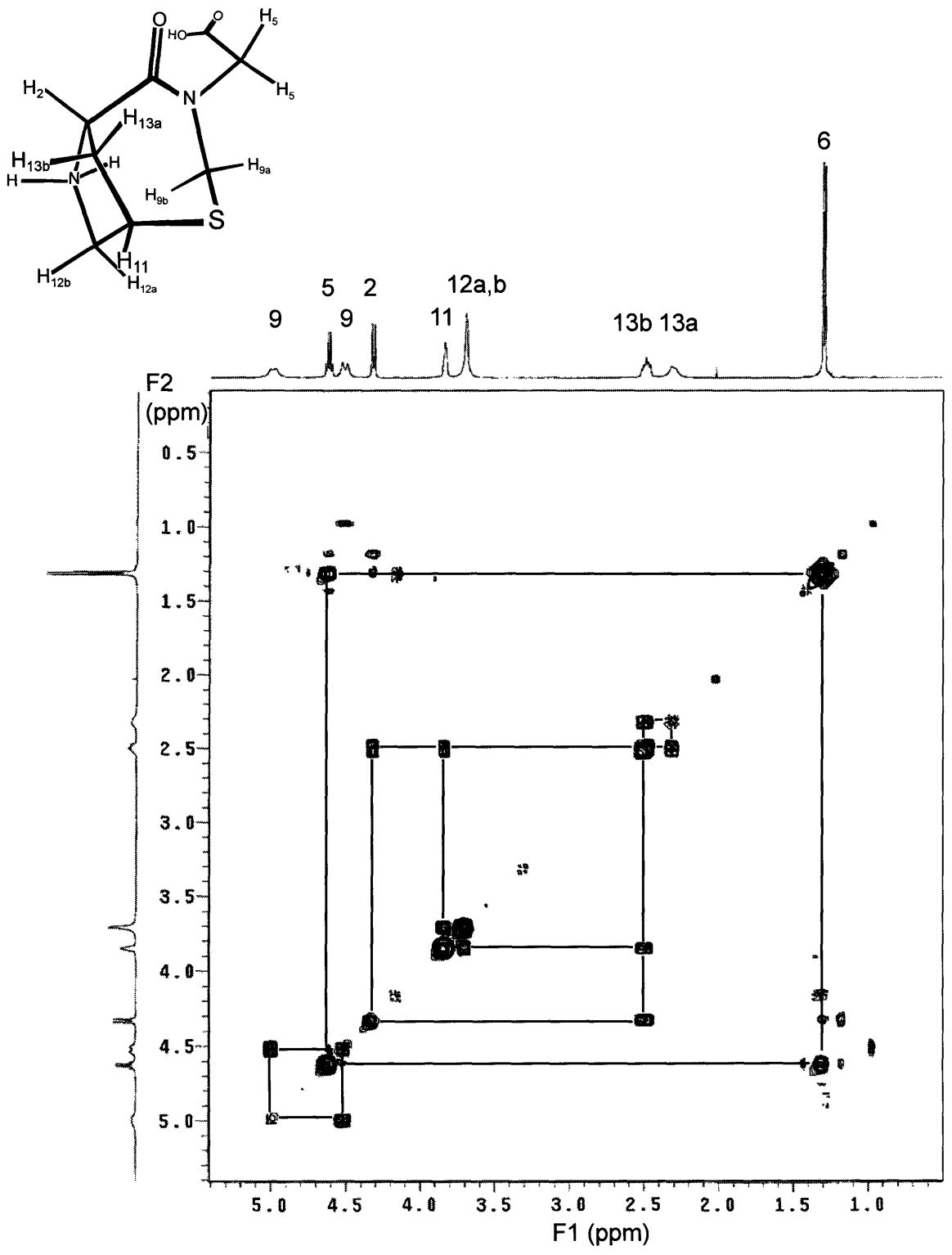
O
HO
O
H5
H5
H2
N
H13a
H13b
H
H
N
H9a
H9b
S
H11
H12b
H12a
6
5
2
12a,b
9
9
11
13b 13a
F2
(ppm)
0.5
1.0
1.5
2.0
2.5
3.0
3.5
4.0
4.5
5.0
5.0
4.5
4.0
3.5
3.0
2.5
2.0
1.5
1.0
F1 (ppm)

Curriculum Vitae

Education

Massachusetts Institute of Technology Cambridge, MA
Ph.D. Chemistry. Anticipated degree date: May, 2005. Thesis: I. Copper-catalyzed Arylation of 1,2-Amino Alcohols II. Synthesis of N-Terminal, Peptide Helix Initiators, and Characterization of Highly Helical, Capped Polyalanine Peptides. Advisors: Stephen Buchwald and Daniel Kemp.

University of Illinois-Champaign, Urbana Urbana, IL
M.S. Chemistry, 2000. Thesis: Effects of Aryl Substituents on the Enantioseparation of Benzhydryl Esters on the Whelk-O1 HPLC Chiral Stationary Phase. Advisor: William Pirkle.

University of Illinois-Champaign, Urbana Urbana, IL
B.S. Chemistry, 1999.

Publications

"NMR and CD Characterization of Fully Helical, Cap-Stabilized, Water-Solubilized Polyalanines." Heitmann, B.; Job, G.E.; Kennedy, R.J.; Walker, S.; Kemp, D.S. *J. Am. Chem. Soc.* **2005**, *127*, 1690–1704.

"The Effects of Aromatic Substituents on the Chromatographic Enantioseparation of Diarylmethyl Esters." Job, G.E.; Shvets, A.; Pirkle, W.H.; Kuwahara, S.; Kosaka, M.; Kasai, Y.; Taji, H.; Fujita, K.; Watanabe, M.; Harada, N. *J. Chromatogr., A* **2004**, *1055*, 41–53.

"Calibrated Calculation of Polyalanine Fractional Helicities from Circular Dichroism (CD) Ellipticities." Job, G.E.; Heitmann, B.; Kennedy, R.J.; Walker, S.; Kemp, D.S. *Angew. Chem., Int. Ed. Engl.* **2004**, *43*, 5649–5651.

"Copper-Catalyzed Coupling of Amides and Carbamates with Vinyl Halides." Jiang, L.; Job, G.E.; Klapars, A.; Buchwald, S.L. *Org. Lett.* **2003**, *5*, 3667–3669.

"Enantioresolution and Absolute Configurations of Chiral meta-Substituted Diphenylmethanols as Determined by X-ray Crystallographic and ^{1}H NMR Anisotropy Methods." Kosaka, M.; Sugito, T.; Kasai, Y.; Kuwahara, S.; Watanabe, M.; Harada, N.; Job, G.E.; Shvets, A.; Pirkle, W.H. *Chirality* **2003**, *15*, 324–328.

"Copper-Catalyzed Arylation of β-Amino Alcohols." Job, G.E.; Buchwald, S.L. *Org. Lett.* **2002**, *4*, 3703–3706.

"Copper-Catalyzed Coupling of Aryl Iodides with Aliphatic Alcohols." Wolter, M.; Nordmann, G.; Job, G.E.; Buchwald, S.L. *Org. Lett.* **2002**, *4*, 973–976.

"Comparison of CD Spectra of (2-methylphenyl)- and (2,6-dimethylphenyl)-phenylmethanols Leads to Erroneous Absolute Configurations." Kosaka, M.; Kuwahara, S.; Watanabe M.; Harada, N.; Job, G.E.; Pirkle, W.H. *Enantiomer* **2002**, *7*, 213–217.

Patent

"Copper-Catalyzed Formation of Carbon–Heteroatom and Carbon–Carbon Bonds by Arylation and Vinylation of Amines, Amides, Hydrazides, Heterocycles, Alcohols, Enolates, and Malonates, Using Aryl, Heteroaryl, and Vinyl Halides and Analogs." Buchwald, S.L.; Klapars, A.; Antilla, J.C.; Job, G.E.; Wolter, M.; Kwong, F.Y.; Nordmann, G.; Hennessy, E.J. 2002, WO02085838.